LHCb-ANA-2017-034
December 21, 2021
Version 5.0

Measurements of the $\psi(2S)$ to J/ψ production ratio and of the $\psi(2S)$ production cross-section in pPb and Pbp collisions at $\sqrt{s_{NN}} = 8.16\,\text{TeV}$

Vladik Balagura[1,a], Francesco Bossù[1], Frédéric Fleuret[1,a], Manuel Guittière[1], Emilie Maurice[1,a], Patrick Robbe[1], Michael Winn[1], Yanxi Zhang[1]

[1] *LAL, Université Paris-Sud, CNRS/IN2P3, Orsay, France*
[a] *Laboratoire Leprince-Ringuet, Palaiseau, France*

Abstract

The measurement of the $\psi(2S)$ over J/ψ production ratio in pPb and Pbp collisions at $\sqrt{s_{NN}} = 8.16\,\text{TeV}$ by LHCb is presented. The measurement comprises the production ratio and its conversion into an absolute $\psi(2S)$ production cross-section and nuclear modification factors using the J/ψ measurements in the same data sample. The measurements are performed as function of the transverse momentum and rapidity of the charmonium states.

VERSION	DATE	COMMENTS
1	06.04.2018	First version: systematic uncertainty for signal extraction and forward-backward and some integrated quantities to be added
2	07.07.2018	2nd version: version for review committee, added model discussion systematic uncertainties for signal extraction still be added
3	02.08.2018	3rd version: addressing most of first iteration of comments from David Ward
4	04.04.2020	4th version: include *pp* reference
5	03.05.2020	5th version: Answer Giacomo's questions

Contents

1 Introduction

The production and suppression of J/ψ and $\psi(2S)$ mesons, and more generally of quarkonium states, have been discussed as a probe sensitive to deconfinement since originally proposed by Matsui and Satz in 1986 [1]. The theory understanding of the bound state dynamics of quarkonium by means of lattice QCD and effective field theory has progressed substiantially in the last 30 years [2]. Experimentally, measurements at the SPS, RHIC and LHC revealed interesting patterns [3]. In particular, at the LHC, a low-p_{T} component can contribute to the J/ψ production [4–8]. This phenomenon has been predicted as sign of charmonium originating from unbound charm quarks generated either during the life-time of the deconfined medium [9] or at the phase boundary [10]. The production of $\psi(2S)$ as well as the ratio $\psi(2S)$ over J/ψ in nucleus-nucleus collisions play a crucial role in the understanding of quarkonium data. The $\psi(2S)$ bound state has a larger spatial extension and a smaller binding energy with respect to the open charm threshold than the J/ψ in vacuum and there is no feed-down contribution from the χ_c-states in constrast to the J/ψ. In addition, phenomenological uncertainties related to the overall charm cross-section cancel in the predictions for the ratio of $\psi(2S)$ over J/ψ production. Its first measurement at the SPS with high precision [11] in heavy-ion collisions triggered the idea presented in Ref. [10]. Presently, the production ratio is discussed as a discriminative tool for models [12] and first initial measurements of this challenging observable at the LHC have been published [7, 13].

Effects that are not related to deconfinement, commonly called Cold Nuclear Matter (CNM) effects, play an important role in the interpretation of the available nucleus-nucleus data and limit precise conclusions based on them. Their size can be measured in proton(deuteron)–nucleus collisions, which have been pursued at various collision energies [3]. At LHC collision energies, the mostly discussed modifications of charmonium production are related to the modification of the gluon flux. It is treated using collinear factorisation with nuclear parton distribution functions (nPDFs) [14–18] or using the colour glass condensate approach to describe the saturation regime of QCD [19, 20]. Furthermore, small angle gluon radiation taking into account interference between initial and final state radiation, called coherent energy loss, was proposed as the dominant nuclear modification of quarkonium production in pA collisions [21]. Calculations based on these approaches [21–26] can describe J/ψ production measurements at the LHC [27–33] reasonably well within their respective uncertainties. These approaches treat the J/ψ and the $\psi(2S)$ on equal footing and differences in the predicted observables of both states due to the slightly different kinematics induced by the mass difference between the two states and due to the feed-down from χ_c states contributing to the J/ψ but not the $\psi(2S)$ production are typically considered to be negligible compared to the uncertainties of the models. In contrast to these phenomenological expectations, a strong relative suppression by about a factor of two, of $\psi(2S)$ meson production with respect to the production of the J/ψ meson has been observed by PHENIX at RHIC [34, 35] and by ALICE [36, 37] and LHCb [38] at the LHC in proton(deuteron)-nucleus collisions in most regions of phase space.

In this analysis, we aim at further clarifying the situation by providing double-differential measurements of the cross-section of $\psi(2S)$ as well as on the production ratio of J/ψ to $\psi(2S)$ in proton-nucleus collisions compared to pp collisions based on larger statistics with the 2016 proton-lead run at the LHC. Thanks to the vertexing capabilities of the LHCb detector, a separation of the prompt component from the $\psi(2S)$-from-b-hadrons component is possible for the whole available phase space. This opportunity allows us to remove an additional uncertainty in modeling the results and to compare the J/ψ-from-b-hadrons and the $\psi(2S)$-from-b-hadrons measurements as a cross check. Comparisons with models invoking factorisation breaking and hadronic or partonic interactions influencing the fate of the $c\bar{c}$ pair after its creation [39–41] are provided.

2 Definition of observables

All observables are cross-sections, ratios of cross-sections or cross-sections derived from other measurements. They require efficiency corrections to event yields obtained from data. The raw event yields are extracted from a combined fit of the di-muon invariant mass and of the pseudo-proper decay time to separate the **prompt** and the **from-b** signal contributions, where the pseudo-proper decay time is defined as

$$t_z = \frac{(z_{J/\psi\,(\psi(2S))} - z_{\rm PV}) \times M_{J/\psi\,(\psi(2S))}}{p_z}, \tag{1}$$

with $z_{J/\psi\,(\psi(2S))}$ the z-coordinate of the J/ψ or $\psi(2S)$ decay vertex and $z_{\rm PV}$ the z-coordinate of the primary vertex.

Prompt here means produced directly at the nucleon-nucleon interaction, or via a decay of a charmonium produced directly at the interaction (such as a $\chi_c \to J/\psi\gamma$ decay). **from-b** means a charmonium coming from a B decay (either directly, or also via a charmonium decay where the charmonium state is produced in a B decay). The observables of the analysis are measured separately for the prompt and from-b production components.

Given the large statistics available, the observables are also computed in bins of $p_{\rm T}$, the transverse momentum with respect to the beam axis and of y^*, the rapidity with respect to the beam axis in the center-of-mass frame, taking the direction of the proton beam to define the polar axis, and neglecting the small angle between the two due to the crossing angle of the two beams at LHCb. The rapidity y^* is related to the rapidity in the lab frame, $y_{\rm lab}$, with $y^* = y_{\rm lab} - 0.465$ for the pPb configuration and with $y^* = -(y_{\rm lab} + 0.465)$ for the Pbp configuration. For pp collisions (used as reference in the various ratios given below), $y^* = y_{\rm lab}$.

2.1 Cross-sections and cross-section ratios

The absolute double differential cross-sections for $\psi(2S)$ or J/ψ production are defined as

$$\frac{{\rm d}^2\sigma}{{\rm d}p_{\rm T}{\rm d}y^*} = \frac{N}{\Delta y^* \Delta p_{\rm T}\, \epsilon^{\rm tot}\, \mathcal{B}_{\mu\mu} L_{int}}, \tag{2}$$

where N represents the raw yield of the J/ψ or $\psi(2S)$ reconstructed in the given rapidity and transverse momentum bin, $\epsilon^{\rm tot}$ the total efficiency, including acceptance, $\mathcal{B}_{\mu\mu}$ the branching ratio of the J/ψ decay or $\psi(2S)$ in two muons and L_{int} the integrated luminosity of the given data sample. The values of the branching fraction used in this measurement is $\mathcal{B}\,(J/\psi \to \mu^+\mu^-) = (5.961 \pm 0.033)\%$ [42]. For the $\psi(2S)$, the branching fraction into two muons has large uncertainties, $\mathcal{B}\,(\psi(2S) \to \mu^+\mu^-) = (8.0 \pm 0.6) \times 10^{-3}$ [42] while the one into two electrons is more precise, $\mathcal{B}\left(\psi(2S) \rightarrow e^{+}e^{-}\right) = (7.93 \pm 0.17) \times 10^{-3}$. Assuming lepton universality, the later is used to compute the cross-section.

For the J/ψ and the $\psi(2S)$ meson, the observable is extracted in the rapidity range $1.5 < y^{*} < 4.0$ ($-5.0 < y^{*} < -2.5$) for pPb (Pbp) in 3 bins, $y^{*} \in [1.5, 2.5]$,$[2.5, 3.25]$, $[3.25, 4.0]$ ($y^{*} \in [-3.25, -2.5], [-4.0, -3.25], [-5.0, -4.0]$), together with the transverse momentum range $0 < p_{\mathrm{T}} < 10\,\mathrm{GeV}/c$ in bins of $1\,\mathrm{GeV}/c$ and one bin from $10 - 14\,\mathrm{GeV}/c$.

In practice, the cross-section for the $\psi(2S)$ is determined in this analysis indirectly via the cross-section ratio using a tight PID selection and the absolute J/ψ cross-section obtained with a looser selection:

$$\frac{\mathrm{d}^{2}\sigma_{\psi(2S)}}{\mathrm{d}p_{\mathrm{T}}\mathrm{d}y^{*}} = \left[\frac{\mathrm{d}^{2}\sigma_{\psi(2S)}/\mathrm{d}p_{\mathrm{T}}\mathrm{d}y^{*}}{\mathrm{d}^{2}\sigma_{J/\psi}/\mathrm{d}p_{\mathrm{T}}\mathrm{d}y^{*}}\right]_{\mathrm{TIGHT}} \cdot \left[\frac{\mathrm{d}^{2}\sigma_{J/\psi}}{\mathrm{d}p_{\mathrm{T}}\mathrm{d}y^{*}}\right]_{\mathrm{LOOSE}}, \tag{3}$$

where

$$\left[\frac{\mathrm{d}^{2}\sigma_{\psi(2S)}/\mathrm{d}p_{\mathrm{T}}\mathrm{d}y^{*}}{\mathrm{d}^{2}\sigma_{J/\psi}/\mathrm{d}p_{\mathrm{T}}\mathrm{d}y^{*}}\right]_{\mathrm{TIGHT}} = \frac{N(\psi(2S))}{N(J/\psi)_{\mathrm{TIGHT}}} \times \frac{\epsilon^{\mathrm{tot}}_{\mathrm{TIGHT}}(J/\psi)}{\epsilon^{\mathrm{tot}}(\psi(2S))} \times \frac{\mathcal{B}\left(J/\psi \rightarrow \mu^{+}\mu^{-}\right)}{\mathcal{B}\left(\psi(2S) \rightarrow e^{+}e^{-}\right)}. \tag{4}$$

Since the $\psi(2S)$ and J/ψ yields are computed for the same dataset, the integrated luminosity cancels in this ratio.

This procedure allows to reduce the statistical uncertainty because the tight PID-selection choice gives a more favorable signal significance for the $\psi(2S)$, with a lower background. The cross-section for the ψ(2S) is not directly computed with the tight selection because of the limited statistics in PID calibration sample in pPb and in Pbp for tight selections, which do not allow for a precise cross check that the usage of the PID calibration samples from pp collisions is justified. For the PID-loose selection, the PID efficiency does vary only very slightly with occupancy, hence this problem can be neglected[1]. The LOOSE selection is identical to the selection used for the measurement of the J/ψ cross-section reported in the LHCb publication [33]. Since the binning used in that analysis is different, the cross-section for the J/ψ production with the LOOSE selection has been recomputed for the binning scheme used in the analysis presented here.

2.2 Nuclear modification factor

The nuclear modification factor of the $\psi(2S)$ is defined as follows,

$$R_{p\mathrm{Pb}}(p_{\mathrm{T}}, y^{*}) = \frac{\left[\frac{\mathrm{d}^{2}\sigma_{\psi(2S)}}{\mathrm{d}p_{\mathrm{T}}\mathrm{d}y^{*}}\right]_{p\mathrm{Pb}}}{208\left[\frac{\mathrm{d}^{2}\sigma_{\psi(2S)}}{\mathrm{d}p_{\mathrm{T}}\mathrm{d}y^{*}}\right]_{pp}}, \tag{5}$$

where 208 is the mass number of the Pb ion. In absence of nuclear effects, the modification factor is expected to be unity.

The pp-reference cross-sections for $\psi(2S)$, $\left[\frac{\mathrm{d}^{2}\sigma_{\psi(2S)}}{\mathrm{d}p_{\mathrm{T}}\mathrm{d}y^{*}}\right]_{pp}$ has to be taken at the same energy than the pPb one, *i.e.* 8.16 TeV. This cross-section is computed from the measurement of the ratio of J/ψ to $\psi(2S)$ cross-section measured at 7 TeV. It is assumed that

[1] Of course, as a cross check the J/ψ cross-section has been compared using the loose and the tight selection.

this ratio is the same at 8.16 TeV. The $\psi(2S)$ cross-section is then obtained multiplying this ratio by the J/ψ cross-section at 8.16 TeV obtained in Ref. [33]. An example for the support of the sufficient precision of this assumption for the purpose of this analysis, we refer to Fig.8 of the following ALICE publication [43].

2.3 Forward-Backward ratio

To investigate nuclear modification in the asymmetric collision system pPb, it is interesting to compare the production in the forward region with the production in the backward region with respect to the direction of the proton beam, *i.e.* compare production measured with the pPb configuration with the measurement in the Pbp configuration, in a common range of absolute values of y^*. This is obtained with the forward-to-backward ratio,

$$R_{\mathrm{FB}}(p_{\mathrm{T}}, y^*) = \frac{\frac{\mathrm{d}^2\sigma}{\mathrm{d}p_{\mathrm{T}}\mathrm{d}y^*}(p_{\mathrm{T}}, y^*)}{\frac{\mathrm{d}^2\sigma}{\mathrm{d}p_{\mathrm{T}}\mathrm{d}y^*}(p_{\mathrm{T}}, -y^*)}. \tag{6}$$

The forward-to-backward ratio is evaluated in the rapidity range $2.5 < |y^*| < 4.0$, which is common to pPb and Pbp.

2.4 J/ψ over ψ(2S) ratios

This is the ratio of the J/ψ and $\psi(2S)$ modification factors defined in Sect. 2.2,

$$R_{\psi(2S)/J/\psi}(p_{\mathrm{T}}, y^*) = \frac{R_{p\mathrm{Pb}}^{\psi(2S)}(p_{\mathrm{T}}, y^*)}{R_{p\mathrm{Pb}}^{J/\psi}(p_{\mathrm{T}}, y^*)} \tag{7}$$

The ratio obtained for the from-b-component is used as a control quantity, since it is expected to be equal to unity: in this case, J/ψ and $\psi(2S)$ mesons come both from decays of b hadrons which have the same nuclear modification factors.

3 Data sets

3.1 Data samples

The data used in this analysis was recorded during the Heavy Ion run of 2016, between Nov. 18th and Nov. 25th for the pPb configuration (p in beam 1, coming from upstream of the VELO) and between Nov. 26th and Dec. 4th for the Pbp configuration (p in beam 2), both at a center-of-mass collision energy of 8.16 TeV. The total recorded luminosity is of $13.6 \pm 0.3\,\mathrm{nb}^{-1}$ for pPb and $20.8 \pm 0.5\,\mathrm{nb}^{-1}$ for Pbp. The magnet polarity was always DOWN (positive polarity) throughout the whole period. The list of selected good runs used in this analysis is given in Table 1 together with the fill number. During the pPb run, one run was flagged bad (186560) because of a misconfiguration in the VELO.

3.2 Monte Carlo samples

The efficiency of the various steps in the analysis chain (acceptance, reconstruction, selection and trigger) is estimated using samples of fully simulated events using the

Table 1: Fill numbers and list of good runs.

Fill	**Good run numbers**
	pPb
5519	186555, 186557, 186558, 186564, 186565
5520	186583, 186584, 186585, 186587, 186588, 186590
5521	186601, 186602, 186603, 186604, 186608, 186609, 186610, 186611, 186612, 186613
5522	186614, 186615, 186616, 186626, 186628, 186629, 186631, 186632, 186633, 186634, 186635, 186636, 186637, 186638, 186639
5523	186647, 186650, 186651, 186652, 186653, 186654, 186655, 186656
5524	186670, 186673
5526	186718, 186721, 186722, 186723, 186724, 186725, 186726, 186727
5527	186735, 186737, 186739, 186740, 186741, 186744, 186745, 186746
5533	186782, 186783, 186785, 186798, 186799, 186802, 186806, 186807
5534	186818, 186819, 186823, 186824
5538	186920, 186915, 186914, 186907, 186903, 186896,186890, 186884, 186879, 186876
	Pbp
5545	186989, 186990, 186991, 186992, 186993
5546	187002, 187005, 187007
5547	187015, 187018, 187019, 187020, 187021, 187023, 187025, 187026
5549	187038, 187040, 187042, 187043, 187044, 187045, 187047, 187048, 187049, 187050, 187051
5550	187058, 187061, 187062, 187063, 187064, 187065
5552	187074, 187078, 187080, 187082, 187083, 187083, 187084, 187085, 187086
5553	187106, 187109, 187110, 187111, 187112, 187113, 187115
5554	187123, 187124, 187127, 187128, 187129
5558	187178, 187182, 187183, 187184
5559	187198, 187199, 187202, 187203, 187204
5562	187229, 187230, 187232, 187233, 187234
5563	187244, 187247, 187248, 187249, 187250, 187251, 187252, 187253, 187254, 187255
5564	187266
5565	187282, 187283, 187289, 187290, 187291, 187292
5568	187325, 187328, 187329, 187330, 187331, 187332, 187333, 187334, 187335, 187336, 187337, 187339, 187340
5569	187348, 187349, 187350, 187351, 187355, 187357, 187358
5570	187372, 187375, 187376, 187377, 187378, 187380, 187381
5571	187389, 187392, 187393, 187394, 187395
5573	187406, 187409, 187410

standard LHCb simulation software, Gauss. The simulated events are then reconstructed and analyzed using the same software tools as the ones used for the data. The simulation is done in two successive steps, first a generation phase based on several external tools such as event generators, and second a simulation phase based on the Geant4 package [44,45]. The simulation phase is the same as the one used for the simulation of pp events within

LHCb and is described in Ref. [46] while the generation phase is specific to the heavy ion analyses. The versions of the software for the simulation is known as Sim09b.

Minimum bias samples of pPb and Pbp collisions are generated using the EPOS event generator, using the LHC model [47]. This generator is interfaced with the GAUSS simulation software via the CRMC (Cosmic Ray Monte Carlo) interface library. All short lived particles are decayed with the EVTGEN decay package [48], similarly to what is done for pp simulation in LHCb. Radiative QED corrections to the decays containing charged particles in the final state are applied with the PHOTOS package [49]. It is particularly important for $J/\psi \to \mu^+\mu^-$ and $\psi(2S) \to \mu^+\mu^-$ decays. Since the instantaneous luminosity of the collisions recorded by the experiment for heavy-ion is low, no pile-up is generated, and events contain only one interaction.

Signal samples of $J/\psi \to \mu^+\mu^-$ and $\psi(2S) \to \mu^+\mu^-$ are generated using an embedding technique: minimum bias events are generated using the PYTHIA (version 8) generator [50], with colliding proton beams having momenta equal to the momenta per nucleon of the heavy ion beams or targets. The J/ψ ($\psi(2S)$) mesons are then extracted from these minimum bias events, discarding all other particles in the events. Their decays are forced to the signal decay modes using the EVTGEN package, and the resulting decay chain is added to a single minimum bias EPOS event generated with beam parameters identical to those seen in data. All the samples are listed in Table 2.

Table 2: Event type, decay and statistics of the simulation samples.

EventType	Decay chain	Number of events
24142001	pPb $J/\psi \to \mu^+\mu^-$	1.5×10^6
24142001	Pbp $J/\psi \to \mu^+\mu^-$	1.0×10^6
28142001	pPb $\psi(2S) \to \mu^+\mu^-$	1.0×10^6
28142001	Pbp $\psi(2S) \to \mu^+\mu^-$	1.0×10^6

3.3 Trigger

The trigger selections applied during the pPb and Pbp runs were close but looser than the selections used during the first month of data taking for Run 2, where the measurement of the J/ψ cross-section at 13 TeV in pp collisions was performed.

3.3.1 L0

A single L0 TCK was used throughout this run, 0x1621. The corresponding configuration is given in Table 3. For this analysis, only reconstructed J/ψ and $\psi(2S)$ with one of their muons satisfying the Muon line criteria are considered (*i.e.* L0Muon TOS candidates). For the lines used in the analysis, no SPD multiplicity cut was applied at L0. The threshold for the muon trigger is also looser than the one used in pp collisions, which is equal to 800 MeV.

Table 3: Definition of L0 TCK 0x1621.

Line name	Condition
SPD	Spd multiplicity > 0
PU	Pile-Up multiplicity > 3
Muon	$p_{\mathrm{T}} > 500\,\mathrm{MeV}$
DiHadron,lowMult	E_{T}(hadron) $> 408\,\mathrm{MeV}$, SPD multiplicity < 20 and Pile-Up multiplicity < 2
Muon,lowMult	SPD multiplicity < 20 and $p_{\mathrm{T}} > 400\,\mathrm{MeV}$
DiMuon,lowMult	SPD multiplicity < 20, $p_{\mathrm{T}1} > 100\,\mathrm{MeV}$ and $p_{\mathrm{T}2} > 100\,\mathrm{MeV}$
Electron,lowMult	SPD multiplicity < 20 and E_{T}(electron) $> 1.2\,\mathrm{GeV}$
Photon,lowMult	SPD multiplicity < 20 and E_{T}(photon) $> 1.2\,\mathrm{GeV}$
DiEM,lowMult	SPD multiplicity < 20, E_{T}(electron) $> 480\,\mathrm{MeV}$ and E_{T}(photon) $> 480\,\mathrm{MeV}$
B1gas	SumEt $> 4992\,\mathrm{MeV}$ on beam-empty crossings
B2gas	Pile-up multiplicity > 9 on empty-beam crossings

3.3.2 HLT1

Two different HLT1 configurations were used: TCK 0x11431621 for runs between 186555 and 187204, and TCK 0x11441621 for the other runs. As far as the analysis presented here is concerned, these two configurations are identical (they differ only for pre-scales of the NoBias line and of dedicated high multiplicity lines). The trigger lines used in the analysis are given in Table 4. All candidates kept for the analysis must be TOS of the DiMuonHighMass line.

Table 4: HLT1 trigger line.

Line name	Conditions
DiMuonHighMass	L0: L0Muon decision Global event cut: number of VELO clusters < 8000 $\mu^{\pm}$: $p_{\mathrm{T}} > 300\,\mathrm{MeV}$, $p > 4\,\mathrm{GeV}$, track $\chi^2 < 4$, IsMuon $\mu^+\mu^-$ combination: $M > 2.5\,\mathrm{GeV}$

3.3.3 HLT2

Three HLT2 configurations were used: TCK 0x21421621, 0x21451621 and 0x21461621. Here also all these TCKs are identical as far as this analysis is concerned. The selections applied in HLT2 are described in Table 5. The lines used in the analysis are saved in the TURBO format and the triggers candidates saved in the data RAW files are taken directly for the final analysis. The offline processing relevant for this analysis was performed using processing pass Turbo03pLead with DaVinci version v41r3.

The analysis makes use of a large NoBias sample recorded at the same time, for cross-checks or computation of trigger efficiency for example. This sample is acquired with a random trigger on bunch crossings, based only on the LHC filling scheme, without any requirement on detector quantities at L0, HLT1 or HLT2, which are pass-through. The NoBias events are stored in a NoBias stream, reconstructed with the same configuration than the triggered events.

Table 5: HLT2 trigger lines.

Line name	Conditions
DiMuonJPsiTurbo	$\mu^{\pm}$: $p_{\mathrm{T}} > 500\,\mathrm{MeV}$
	$\mu^{+}\mu^{-}$ combination: $\lvert M - M(J/\psi)\rvert < 150\,\mathrm{MeV}$ and vertex $\chi^2 < 25$
DiMuonPsi2STurbo	$\mu^{\pm}$: $p_{\mathrm{T}} > 500\,\mathrm{MeV}$
	$\mu^{+}\mu^{-}$ combination: $\lvert M - M(\psi(2S))\rvert < 150\,\mathrm{MeV}$ and vertex $\chi^2 < 25$

4 Selections

4.1 Global Event Selection

Only events with less than 8000 VELO clusters are considered in this analysis, as imposed by the trigger requirements (the standard cut for pp running is 6000 VELO clusters). All events are also required to have at least one reconstructed primary vertex since this information is mandatory to separate the prompt from from-b contributions.

4.2 Candidate Selection

The J/ψ and $\psi(2S)$ candidates are formed from two oppositely charged muons coming from a common vertex. Both decay modes are using very close selection criteria. They are required to be TOS (*Trigger On Signal*) for the L0Muon and Hlt1DiMuonHighMass trigger lines, *i.e.* that the reconstructed candidate or its decay products are associated with a trigger object fulfilling the trigger requirements. Then the candidates used are directly the ones selected by the line Hlt2DiMuonJPsiTurbo and Hlt2DiMuonPsi2STurbo lines respectively, in the TURBO stream, without offline reconstruction. The comparison of reconstructions in TURBO stream and offline has been studied using J/ψ candidates in the 13 TeV early measurement analysis, described in section I in the appendix of the analysis note [51]. The conclusion is that concerning signal yields, the difference is well below 0.1%, and other distributions including invariant mass and t_z are also almost identical. After the early measurement period, improvements have been applied to the TURBO stream, further reducing online-offline differences, see e.g. in Appendix A.2 of the b-hadron analysis in pPb collisions [52].

Finally, additional cuts are applied at the analysis level. Muon tracks have to be in the geometrical acceptance of the spectrometer ($2 < \eta < 5$) and to have $p_{\mathrm{T}} > 750\,\mathrm{MeV}/c$. For the $\psi(2S)$ selection, muons are required to have $p_{\mathrm{T}} > 900\,\mathrm{MeV}/c$ in order to improve the signal over background ratio. Both tracks are required to have a good fit quality, $\chi^2/ndof < 3$ and a ghost probability less than 0.4. They are identified as muons by requiring ProbNN(μ) > 0.5 for the **loose** J/ψ selection. For the **loose** J/ψ selection, the ProbNN(μ) threshold value is chosen to reject a large fraction of background but to be very efficient on signal candidates, as can be seen in Fig. 1. In order to obtain a significant

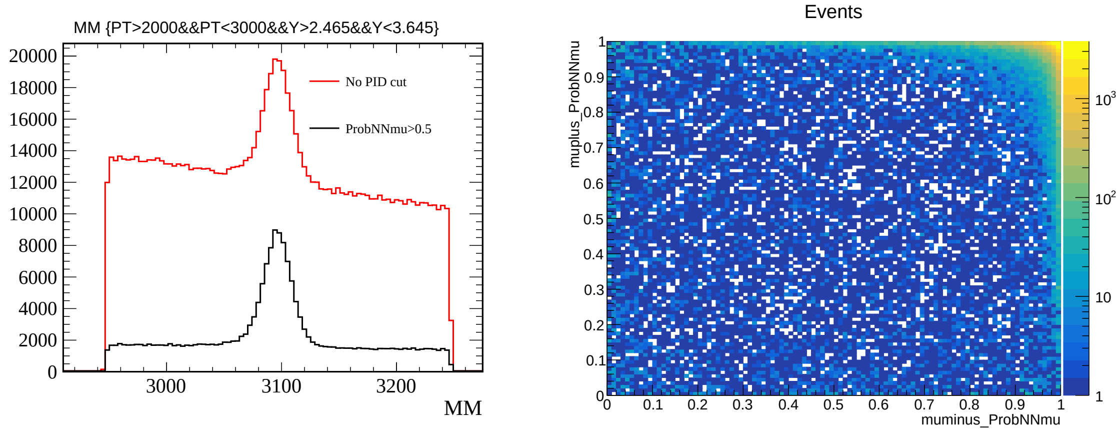

Figure 1: Muon identification cut. Left plot: example of the effect of the ProbNN(μ) > 0.5 cut on J/ψ candidates in pPb for $2 < p_{\mathrm{T}} < 3\mathrm{GeV}/c$ and $2 < y^{*} < 3$ bin. Right plot: two dimensional distribution of ProbNN(μ) for the μ^{+} (y-axis) and the μ^{-} (x-axis) for signal only candidates extracted with the *sPlot* technique.

signal for the $\psi(2\mathrm{S})$ at low p_{T}, a tighter PID selection is required. In terms of significance, all tighter cuts that were checked yield to rather similar significances and hence statistical relative uncertainties. The inclusive $\psi(2\mathrm{S})$ raw yields, the S/B background and the significances are given in Fig. 2 for various cuts on the muon PID. Finally, for the **tight** selection, a selection of ProbNN(μ)> 0.8 was chosen.

In addition, for both J/ψ and $\psi(2S)$, the two muons are required to form a good vertex asking the vertex fit probability Prob(χ^2) $> 0.5\%$. The $\psi(2S)$ and J/ψ candidates are required to have a mass within $120\,\mathrm{MeV}/c^2$ of the PDG value. All selection criteria are specified in Table 6.

Table 6: Offline selection for $\psi(2S)$ and J/ψ candidates.

	Condition
$\mu^{\pm}$	$2 < \eta < 5$
	$p_{\mathrm{T}} > 750$ MeV/c [J/ψ]
	$p_{\mathrm{T}} > 900$ MeV/c [$\psi(2S)$]
	ProbNN(μ) > 0.5 [J/ψ, LOOSE]
	ProbNN(μ) > 0.8 [$\psi(2S)$ and J/ψ TIGHT]
	Track ghost probability < 0.4
	χ^2 per degree of freedom of the track fit < 3
J/ψ or $\psi(2S)$	$\lvert M(\mu^+\mu^-) - M(\psi)\rvert < 120\,\mathrm{MeV}/c^2$
	Vertex χ^2 probability $> 0.5\%$

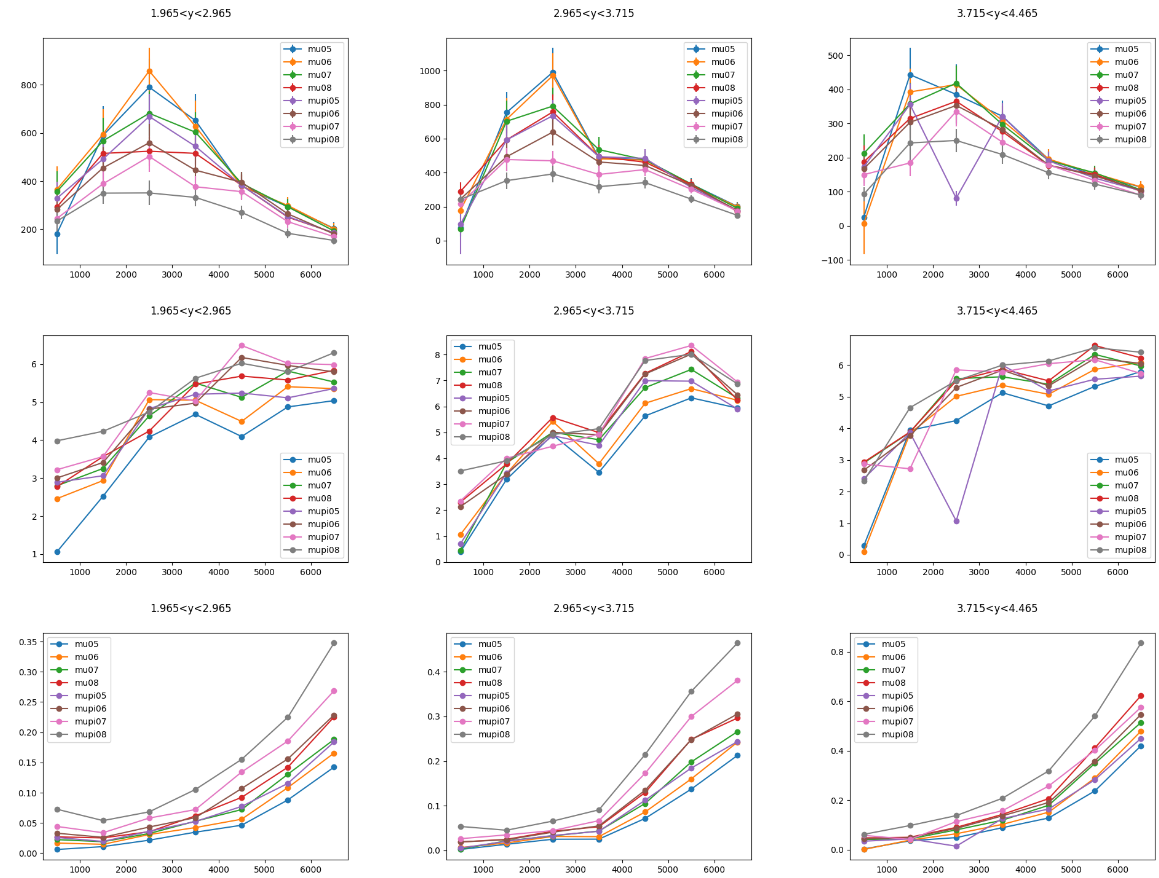

Figure 2: Signal yields (top row), significance (middle row) and signal-to-background (bottom row) ratios as a function of the p_{T} of the $\psi(2S)$, in different y bins, for various cuts on the muon PID. The different colors indicate different PID cuts: mu0x corresponds to ProbNN(μ)$> 0.x$, mupi0x corresponds to ProbNN(μ)$\cdot$(1-ProbNN(π))$> 0.x$. For example, the blue curve, mu05 represents the cut ProbNN(μ)> 0.5.

5 Signal extraction

The numbers of prompt and from-b J/ψ and $\psi(2S)$ signal candidates are extracted from a simultaneous fit to the invariant mass and pseudo-propertime t_z distributions. The pseudo-propertime is defined as (here for J/ψ, the equivalent quantity is defined for the $\psi(2S)$)

$$t_z = \frac{\left(z_{J/\psi} - z_{\mathrm{PV}}\right) \times M_{J/\psi}}{p_z}, \tag{8}$$

where $z_{J/\psi}$ is the z-coordinate of the J/ψ decay vertex, z_{PV} the z-coordinate of the primary vertex, $M_{J/\psi}$ the nominal J/ψ mass and p_z the longitudinal J/ψ momentum. For prompt production, t_z is equal to 0 while for charmonium coming from the decay of a B hadron, t_z is a good approximation of the B hadron propertime and should follow an exponential distribution.

5.1 Mass fit function

The procedure that is described in the following is very close to the one used in previous *pp* analyses, as e.g. [53]. The function describing the invariant mass of the signal candidates is a Crystal Ball function defined as

$$f_{\mathrm{CB}}(x;M,\sigma,\alpha,n)=\begin{cases}\frac{\left(\frac{n}{|\alpha|}\right)^n e^{-\frac{1}{2}\alpha^2}}{\left(\frac{n}{|\alpha|}-|\alpha|-\frac{x-M}{\sigma}\right)^n}, & \text{if } \frac{x-M}{\sigma}<-|\alpha| \\ \exp\left(-\frac{1}{2}\left(\frac{x-M}{\sigma}\right)^2\right), & \text{if } \frac{x-M}{\sigma}\geq-|\alpha|.\end{cases} \tag{9}$$

The value of the parameter n is fixed to 1 following the physics arguments described in [54], while the value of the parameter α is constrained from the values of the resolution parameter σ following

$$\alpha=2.066+0.0085\sigma-0.00011\sigma^2, \tag{10}$$

extracted from toy Monte Carlo studies and where σ is expressed in MeV. The background, which is only combinatorial, is described by an exponential function,

$$f_{\mathrm{bkg}}(x;p)=e^{-px}. \tag{11}$$

Figure 3 shows the results of the mass fits for all reconstructed J/ψ and $\psi(2S)$ candidates for the tight selection, for pPb and Pbp in the full analysis range. The quality of fits is not perfect since the fit parameterisation does not account for the non-negligible variation of signal and background parameters within the phase space considered.

5.2 Pseudo-propertime fit function

The function used to fit the t_z distribution describes three components: the prompt $\psi(2S)$, the $\psi(2S)$-from-b and the combinatorial background. The same method is applied for the J/ψ candidates. The prompt component is described by a Dirac function,

$$f_{\mathrm{prompt}}(x)=\delta(x) \tag{12}$$

and the from-b component by an exponential,

$$f_{\mathrm{from\ b}}(x;\tau)=e^{-\frac{x}{\tau}}. \tag{13}$$

The signal $\psi(2S)$ distributions are then fitted by the sum of these two functions, convoluted with a resolution function which is the sum of three Gaussian functions with a common mean and resolution parameters σ, 2σ and 4σ respectively:

$$f_{\mathrm{resolution}}(x;\sigma,\beta_1,\beta_2,\mu)=\frac{\beta_1}{\sqrt{2\pi}\sigma}e^{-\frac{(x-\mu)^2}{2\sigma^2}}+\frac{\beta_2}{2\sqrt{2\pi}\sigma}e^{-\frac{(x-\mu)^2}{8\sigma^2}}+\frac{1-\beta_1-\beta_2}{4\sqrt{2\pi}\sigma}e^{-\frac{(x-\mu)^2}{32\sigma^2}} \tag{14}$$

The background is described by a function which is the sum of a delta function and five exponentials (three for positive t_z and two for negative t_z, the negative and positive exponentials with the largest lifetimes have their lifetimes fixed to the same value τ_4),

$$\begin{aligned}f_{\mathrm{background}}(x;\tau_1,\tau_2,\tau_3,\tau_4,f_1,f_2,f_3,f_4)=(1-&f_1-f_2-f_3-f_4)\delta(x)+\\ &\theta(x)\left(f_1\frac{e^{-x/\tau_1}}{\tau_1}+f_2\frac{e^{-x/\tau_2}}{\tau_2}\right)+\\ &\theta(-x)\left(f_3\frac{e^{x/\tau_3}}{\tau_3}\right)+f_4\frac{e^{-|x|/\tau_4}}{2\tau_4},\end{aligned} \tag{15}$$

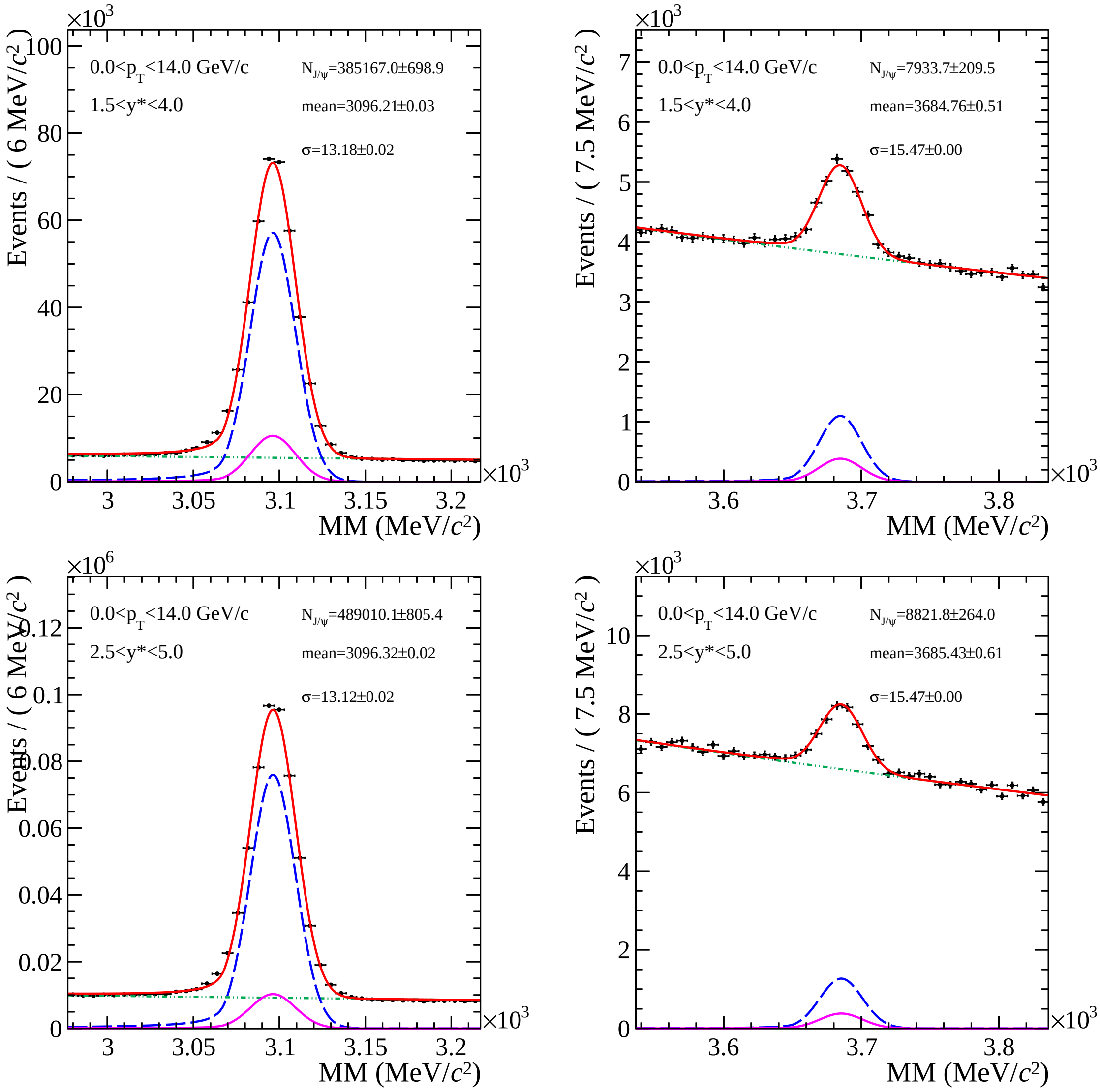

Figure 3: Mass distributions (integrated in $p_{\rm T}$ and y) and fits for the J/ψ (left) and the $\psi(2S)$ (right) in pPb (top) and Pbp (bottom). The black dots are the data points, the red line is the result of the fit described in the text. The blue line is the prompt contribution, the magenta line the contribution from b decays, and the green line the background contribution.

convoluted with the sum of two Gaussian functions. The shape of the background is chosen empirically based on the shape seen in the t_z distribution of the J/ψ mass side-bands. In summary, the fit function has 2 free parameters for the signal, τ and μ, 3 for the resolution function, σ, β_1 and β_2, and 7 for the background, f_1, f_2, f_3, f_4, τ_1, τ_2, τ_3 and τ_4. Figure 4 shows the results of the t_z fits for all reconstructed J/ψ and $\psi(2S)$ candidates.

5.3 Fit results

The measurements shown in this analysis use the number of events for each categories (prompt and from-b) fitted in each of the analysis bin. The fit is performed with the following procedure both for the J/ψ and for the $\psi(2S)$ signal extraction.

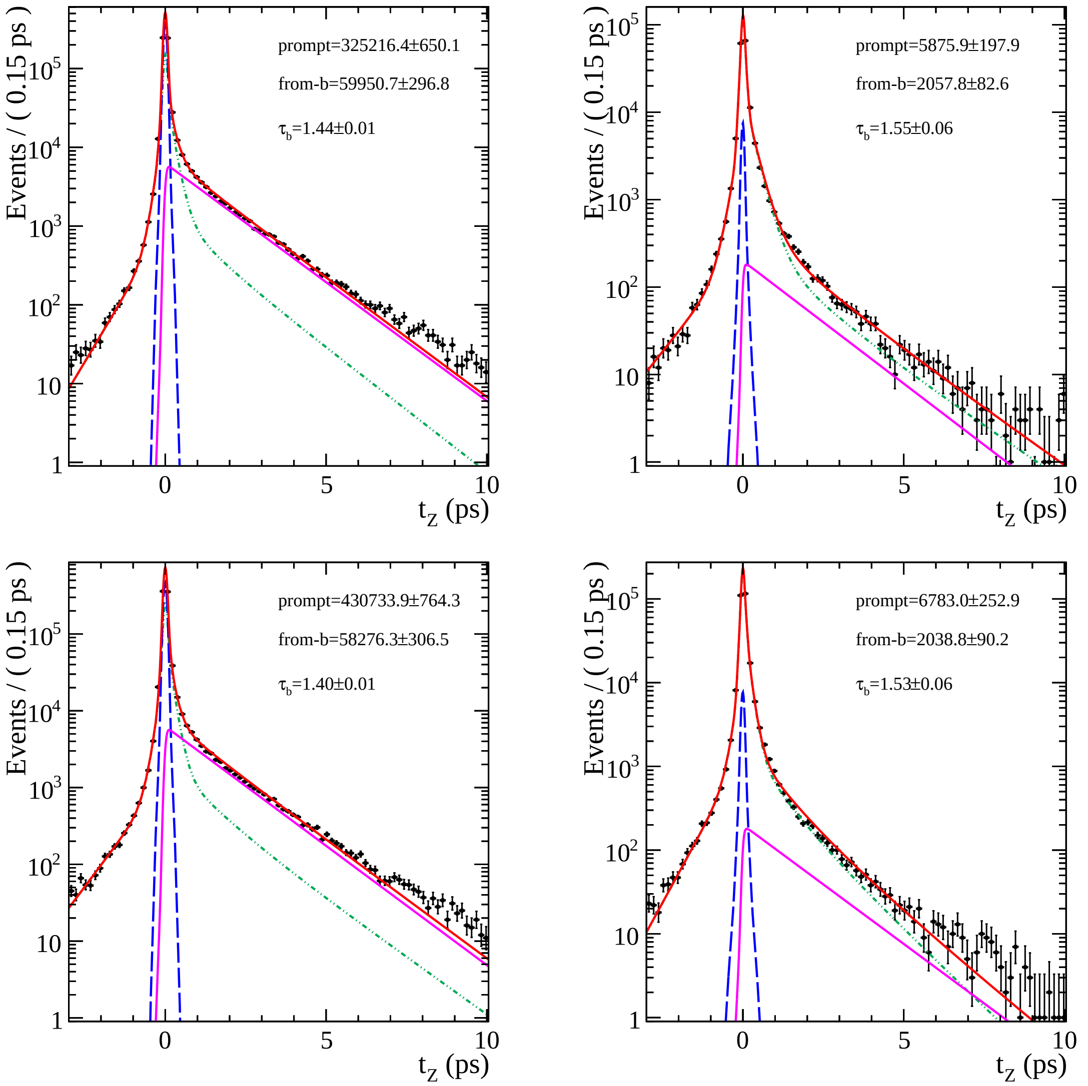

Figure 4: t_z distributions (integrated in p_{T} and y) and fits for the J/ψ (left) and the $\psi(2S)$ (right) in pPb (top) and Pbp (bottom). The black dots are the data points, the red line is the result of the fit described in the text. The blue line is the prompt contribution, the magenta line the contribution from b decays, and the green line the background contribution.

1. First step, the one-dimensional fit to the mass spectrum is performed to estimate the yield and the parameters of inclusive (sum of prompt and from-b) signal candidates, the background yield and of the exponent of the background function. The latter is then kept fixed. For the $\psi(2S)$, the width of the Gaussian part of the Crystal Ball function that describe the signal is fixed to the mass-rescaled value obtained for the J/ψ case in the same analysis bin:

$$\sigma_{\psi(2S)} = \sigma_{J/\psi} \cdot \frac{M^{PDG}_{\psi(2S)}}{M^{PDG}_{J/\psi}}$$

   where the mass values of the particles are taken from the PDG [55].

2. Second step, the high-mass sideband candidates ($M > M^{PDG} + 90\,\mathrm{MeV}/c^2$) are used to fit the t_z distribution for the background. A first fit in the range $0.8 < t_z < 1.2\,\mathrm{ps}$ is used to initialize the mean, the resolution and the τ_1 values. A second fit to the whole range is used to estimate τ_2, τ_3 and τ_4 and the relative contributions. τ_2 and τ_4 are then fixed. For the bins with $p_\mathrm{T} \geq 5\,\mathrm{GeV}/c$, f_4 is forced to zero.

3. Last step, a simultaneous fit to the mass and the pseudo-proper decay time distributions is then performed.

As examples, the J/ψ and $\psi(2S)$ mass and t_z distributions together with the fit results are shown for bin $2 < p_\mathrm{T} < 3\,\mathrm{GeV}/c$ and $2.5 < y^* < 3.25$ in pPb and $-4 < y^* < -3.25$ in Pbp in Fig. 5 and 6.

All other mass and t_z fitted distributions can be found online at

- `http://cern.ch/go/NJL8` for pPb for the p_T bins between 0 and $8\,\mathrm{GeV}/c$,
- `http://cern.ch/go/jm6C` for pPb for the p_T bin between 8 and $10\,\mathrm{GeV}/c$,
- `http://cern.ch/go/97Kt` for pPb for the p_T bin between 10 and $14\,\mathrm{GeV}/c$,
- `http://cern.ch/go/m6HX` for Pbp for the p_T bins between 0 and $8\,\mathrm{GeV}/c$,
- `http://cern.ch/go/9D8G` for Pbp for the p_T bin between 8 and $10\,\mathrm{GeV}/c$,
- `http://cern.ch/go/L8JB` for Pbp for the p_T bin between 10 and $14\,\mathrm{GeV}/c$.

The parameters of the fit function are also given in Fig. 7 and 8 for all bins of the analysis for the loose and tight J/ψ selections, and in Fig. 9 for the $\psi(2S)$. The quality test for the goodness of a fit is based on tests on the pdf parameters: a fit is considered good if $\forall p, \sigma(p)/p > 0.9 \cdot \sqrt{1/|p|}$ and $\sigma(p) < p$, where p is a free parameter of the pdf. The worse mass resolution at high transverse momenta and at high rapidity is a consequence of the worsening of the relative momentum resolution with larger momenta. The better pseudopropertime resolution with increasing p_T can be understood by the larger flight distances from the primary vertex for the same pseudopropertime at a fixed rapidity for larger p_T. For the decay time parameter, at low p_T, approximating the b-meson momentum with the J/ψ momentun in the t_z calculation yields to a small p_T dependence that flattens out at higher p_T. Deviations from this general trend or fluctuations around the nominal mass position are predominantly of statistical nature or small remaining imperfections in the calibration.

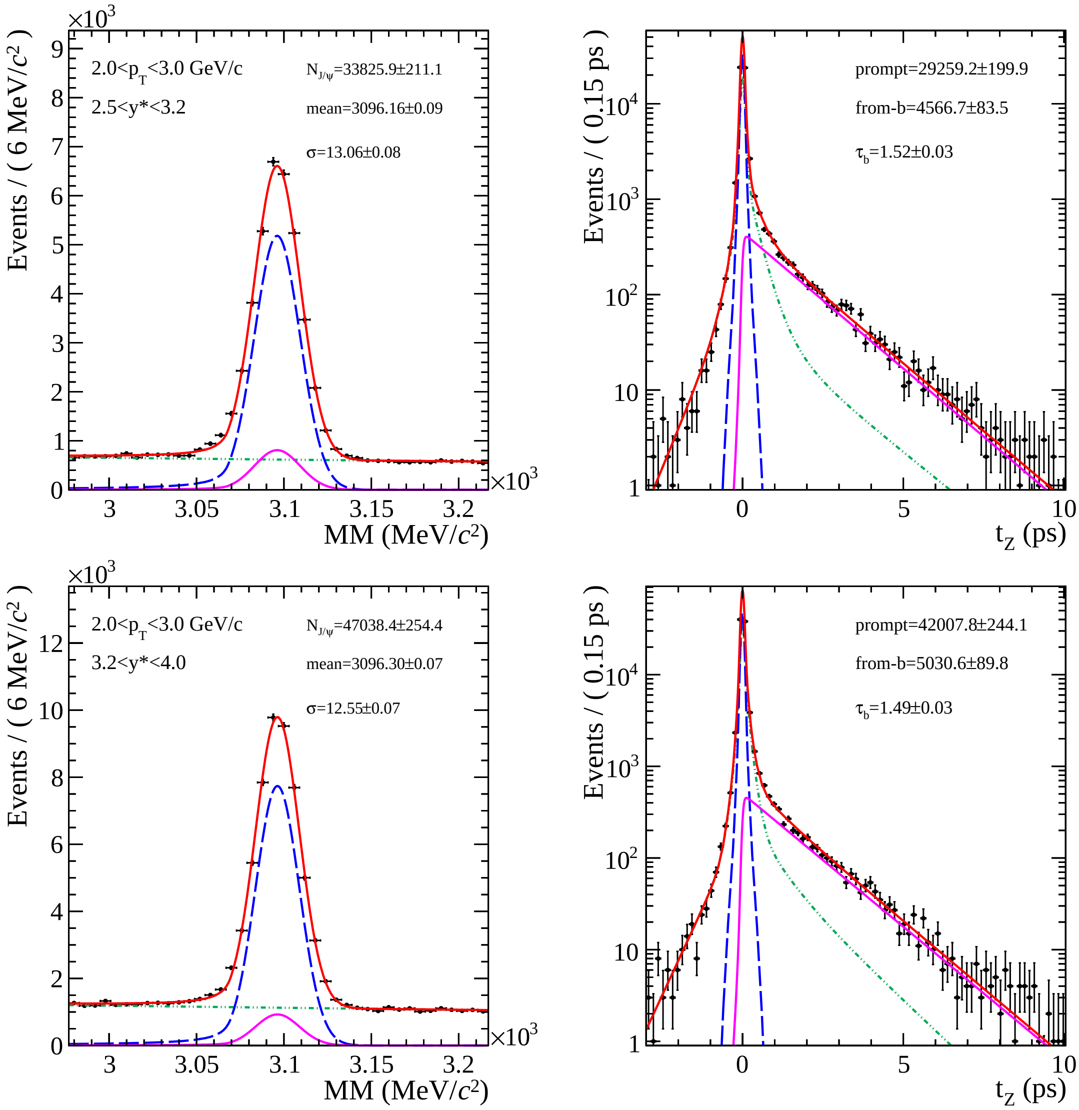

Figure 5: J/ψ mass (left) and t_z (right) distributions for the bin $2 < p_{\mathrm{T}} < 3\,\mathrm{GeV}/c$ and $2.5 < y^* < 3.25$ for pPb (top) and $-3.25 < y^* < 4$ for Pbp (bottom). The black dots with error bars are the data and the red line is the total fit function described in the text. The blue line is the prompt contribution, the magenta line the contribution from b decays, and the green line the background contribution.

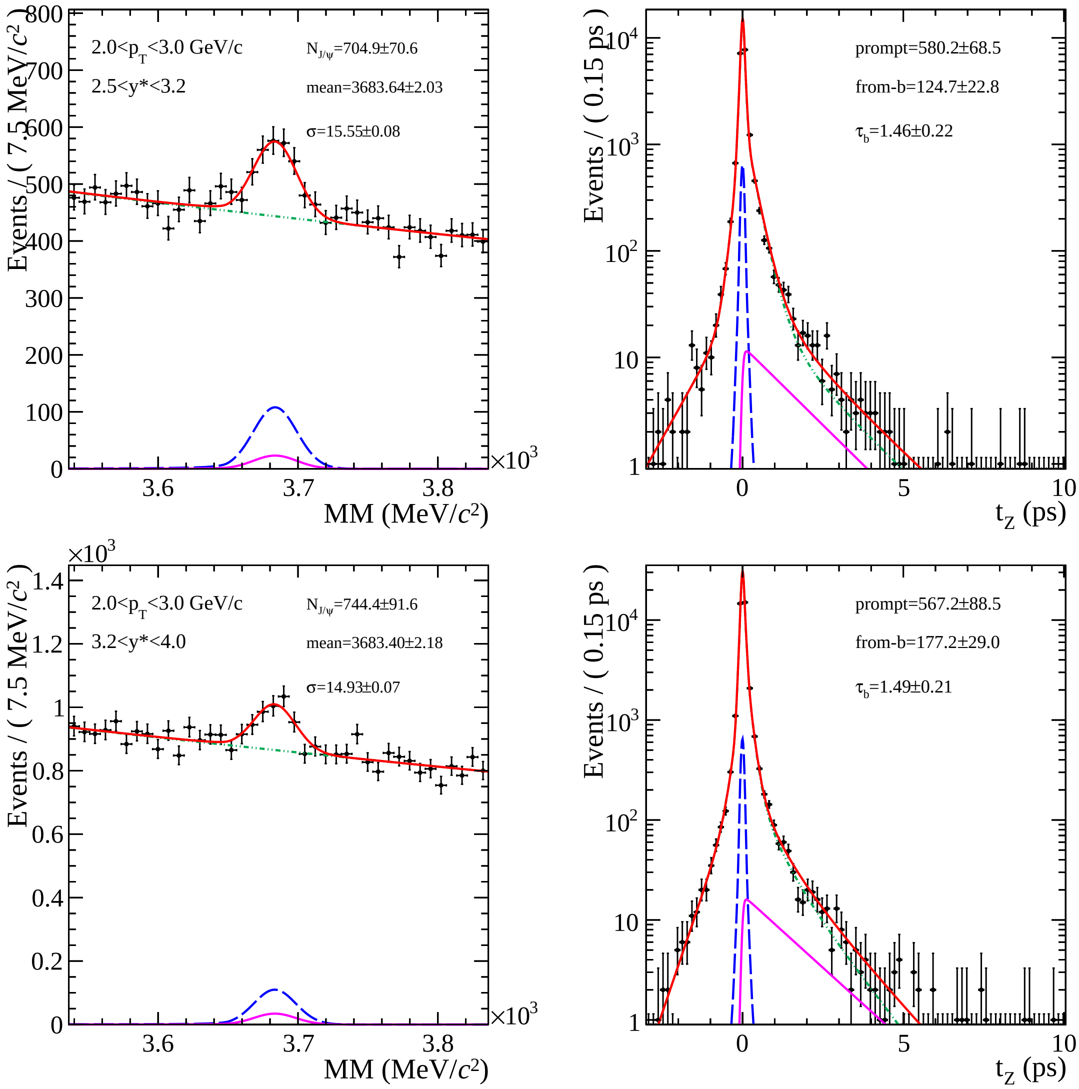

Figure 6: $\psi(2S)$ mass (left) and t_z (right) distributions for the bin $2 < p_{\mathrm{T}} < 3\,\mathrm{GeV}/c$ and $2.5 < y^* < 3.25$ for pPb (top) and $-3.25 < y^* < 4$ for Pbp (bottom). The black dots with error bars are the data and the red line is the total fit function described in the text. The blue line is the prompt contribution, the magenta line the contribution from b decays, and the green line the background contribution.

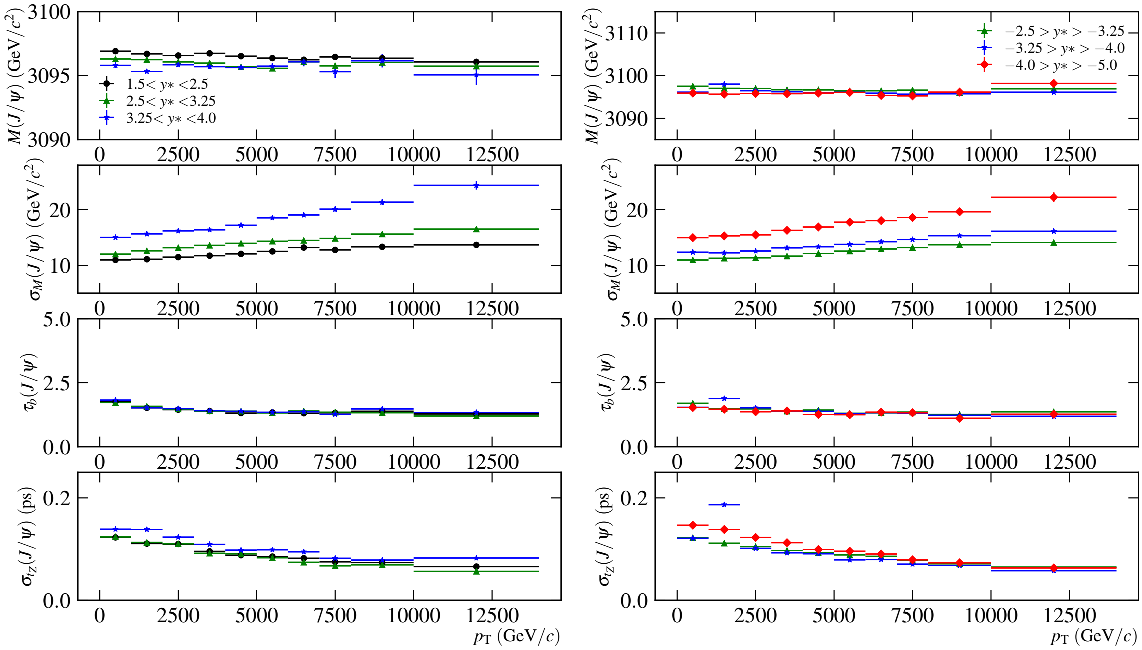

Figure 7: Fit parameters in the analysis bins for the loose J/ψ selection in left: pPb and right: Pbp. From top to bottom: M, σ_M, τ and σ_{t_z}.

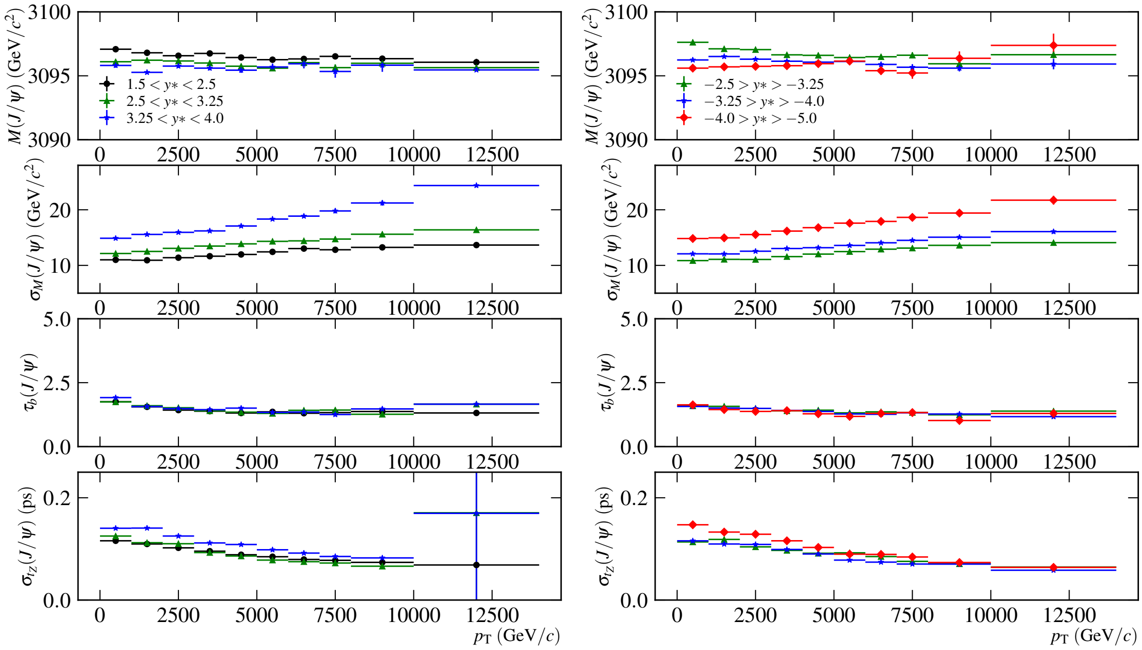

Figure 8: Fit parameters for the tight J/ψ selection in left: pPb and right: Pbp. From top to bottom: M, σ_M, τ and σ_{t_z}.

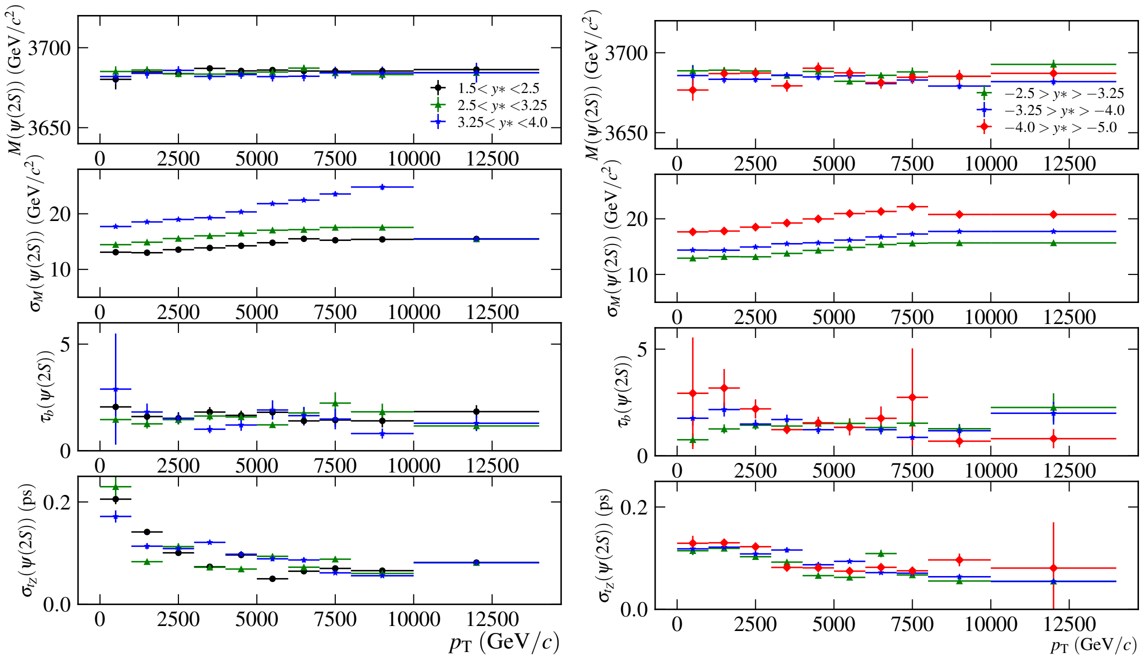

Figure 9: Fit parameters for $\psi(2S)$ in left: pPb and right: Pbp. From top to bottom: M, σ_M, τ and σ_{t_z}.

6 Acceptance and efficiency

The number of signal candidates are corrected, bin by bin, by the total efficiency, $\epsilon(p_{\mathrm{T}}, y^*)$ to obtain the cross-section measurements for J/ψ and $\psi(2S)$. The efficiencies are assumed to be equal for prompt J/ψ ($\psi(2S)$) and J/ψ ($\psi(2S)$) from b as can be seen for example in the measurement of J/ψ cross-section at 13 TeV [51]. The total efficiency is the product of the acceptance efficiency (ϵ_{acc}), the reconstruction efficiency (ϵ_{rec}), the selection efficiency (ϵ_{sel}), the particle identification efficiency (ϵ_{PID}), the trigger efficiency (ϵ_{tri}) and the truth matching efficiency ($\epsilon_{\mathrm{truth}}$):

$$\epsilon_{\mathrm{tot}}(p_{\mathrm{T}}, y^*) = \epsilon_{\mathrm{acc}}(p_{\mathrm{T}}, y^*) \times \epsilon_{\mathrm{rec}}(p_{\mathrm{T}}, y^*) \times \epsilon_{\mathrm{sel}}(p_{\mathrm{T}}, y^*) \times \epsilon_{\mathrm{PID}}(p_{\mathrm{T}}, y^*) \times \epsilon_{\mathrm{tri}}(p_{\mathrm{T}}, y^*) \times \epsilon_{\mathrm{truth}}. \quad (16)$$

All steps are determined from simulation, with truth matched signal decays, except for the tracking efficiency and the particle identification, where data driven methods are used to correct the efficiencies obtained from the simulation. Their exact definitions are given in the following subsections. For the calculation of the cross-section ratio, the ratio of the total efficiencies of the two species is taken.

In the simulation, J/ψ and $\psi(2S)$ mesons are assumed produced without polarization. This assumption affects the efficiencies depending on geometric criteria, mainly the acceptance efficiency and the selection efficiency through transverse momentum selections. For the simulation samples used for this analysis, the truth matching efficiency is equal to $\epsilon_{\mathrm{truth}} = 99.5 \pm 0.1\%$ for both pPb and Pbp samples for J/ψ by comparing the number of simulation J/ψ after all selections compared to the fraction that is truth matched. It is assumed to be independent of p_{T} and y^*.

6.1 Acceptance

The acceptance efficiency is defined as

$$\epsilon_{\mathrm{acc}}(p_{\mathrm{T}}, y^*) = \frac{J/\psi \text{ or } \psi(2S) \text{ in bin } (p_{\mathrm{T}}, y^*) \text{ with both } \mu \text{ in LHCb}}{J/\psi \text{ or } \psi(2S) \text{ generated in bin } (p_{\mathrm{T}}, y^*)}. \quad (17)$$

It is estimated from generator-level only simulations, using the settings described in Sect. 3.2. Both μ in LHCb means here that they have a pseudo-rapidity η between 2 and 5, before the magnet. Figures 10 and 11 give the values of ϵ_{acc} as a function of p_{T} for the different y^* bins of the analysis, for J/ψ and $\psi(2S)$ in pPb and Pbp. The errors are the statistical errors from the generator-level simulations. Tables 7, 8, 9 and 10 give the corresponding numerical values. The ratio between the $\psi(2S)$ and the J/ψ acceptance efficiencies is shown in Fig. 12.

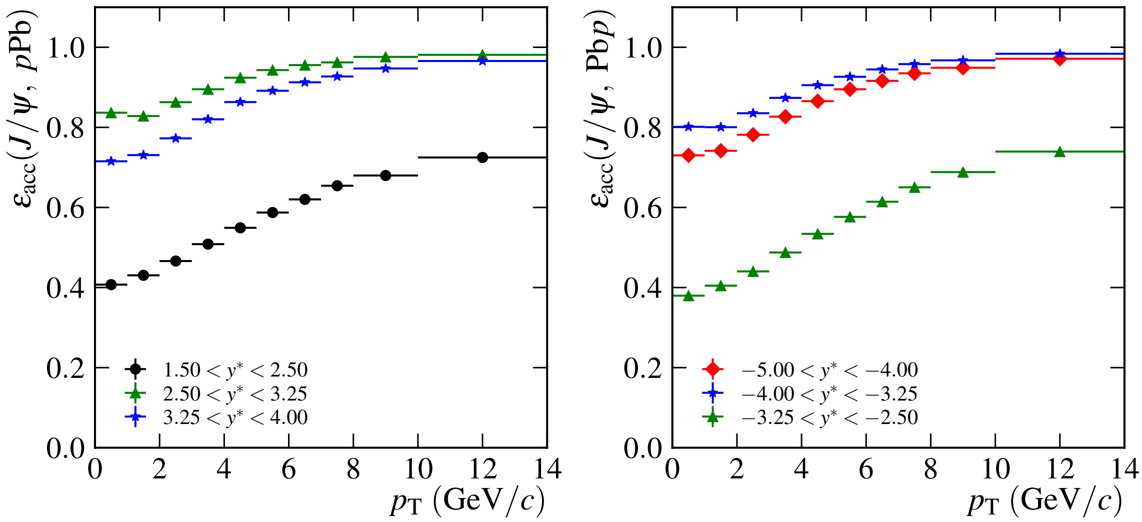

Figure 10: Acceptance efficiency ϵ_{acc} as a function of p_T in different y^* bins for left: J/ψ in pPb, right: J/ψ in Pbp. The displayed uncertainty corresponds to the total uncertainty.

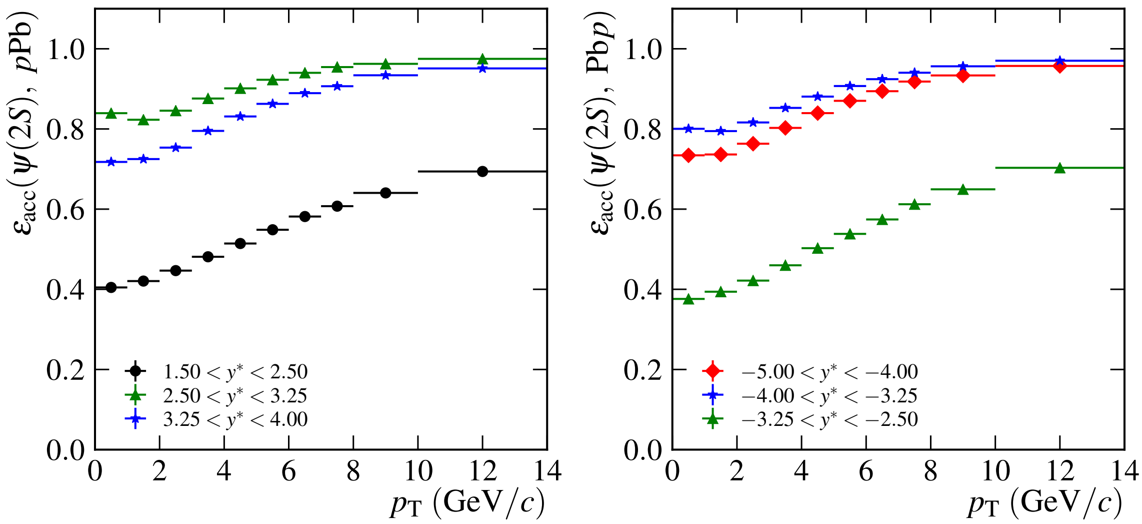

Figure 11: Acceptance efficiency ϵ_{acc} as a fucntion of p_T in different y^* bins for left: $\psi(2S)$ in pPb, right: $\psi(2S)$ in Pbp. The displayed uncertainty corresponds to the total uncertainty.

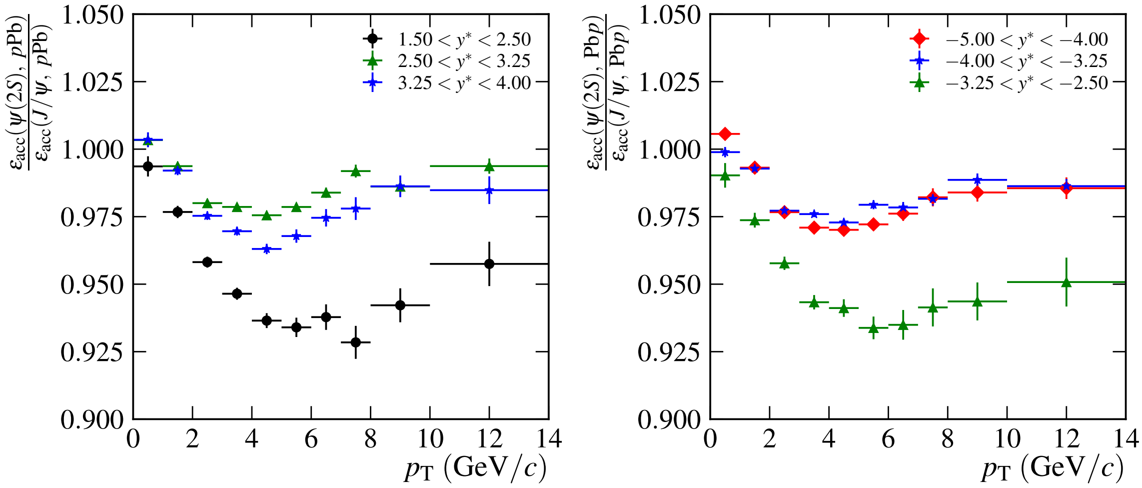

Figure 12: Acceptance efficiency $\epsilon_{\rm acc}^{\psi(2S)}/\epsilon_{\rm acc}^{J/\psi}$ ratio as a function of $p_{\rm T}$ and y^* bins for left: pPb, right: Pbp. The displayed uncertainty corresponds to the total uncertainty.

Table 7: Acceptances for J/ψ in pPb, in bins of p_{T} and y^*. The uncertainties are statistical.

p_{T} bin	y^* bin	ϵ_{acc}
$0 < p_{\mathrm{T}} < 1$	$1.50 < y^* < 2.50$	0.407 ± 0.001
$0 < p_{\mathrm{T}} < 1$	$2.50 < y^* < 3.25$	0.837 ± 0.001
$0 < p_{\mathrm{T}} < 1$	$3.25 < y^* < 4.00$	0.715 ± 0.001
$1 < p_{\mathrm{T}} < 2$	$1.50 < y^* < 2.50$	0.431 ± 0.001
$1 < p_{\mathrm{T}} < 2$	$2.50 < y^* < 3.25$	0.828 ± 0.001
$1 < p_{\mathrm{T}} < 2$	$3.25 < y^* < 4.00$	0.731 ± 0.001
$2 < p_{\mathrm{T}} < 3$	$1.50 < y^* < 2.50$	0.466 ± 0.001
$2 < p_{\mathrm{T}} < 3$	$2.50 < y^* < 3.25$	0.863 ± 0.001
$2 < p_{\mathrm{T}} < 3$	$3.25 < y^* < 4.00$	0.773 ± 0.001
$3 < p_{\mathrm{T}} < 4$	$1.50 < y^* < 2.50$	0.508 ± 0.001
$3 < p_{\mathrm{T}} < 4$	$2.50 < y^* < 3.25$	0.895 ± 0.001
$3 < p_{\mathrm{T}} < 4$	$3.25 < y^* < 4.00$	0.820 ± 0.001
$4 < p_{\mathrm{T}} < 5$	$1.50 < y^* < 2.50$	0.549 ± 0.001
$4 < p_{\mathrm{T}} < 5$	$2.50 < y^* < 3.25$	0.924 ± 0.001
$4 < p_{\mathrm{T}} < 5$	$3.25 < y^* < 4.00$	0.863 ± 0.001
$5 < p_{\mathrm{T}} < 6$	$1.50 < y^* < 2.50$	0.587 ± 0.002
$5 < p_{\mathrm{T}} < 6$	$2.50 < y^* < 3.25$	0.943 ± 0.001
$5 < p_{\mathrm{T}} < 6$	$3.25 < y^* < 4.00$	0.891 ± 0.002
$6 < p_{\mathrm{T}} < 7$	$1.50 < y^* < 2.50$	0.620 ± 0.002
$6 < p_{\mathrm{T}} < 7$	$2.50 < y^* < 3.25$	0.955 ± 0.001
$6 < p_{\mathrm{T}} < 7$	$3.25 < y^* < 4.00$	0.913 ± 0.002
$7 < p_{\mathrm{T}} < 8$	$1.50 < y^* < 2.50$	0.654 ± 0.003
$7 < p_{\mathrm{T}} < 8$	$2.50 < y^* < 3.25$	0.962 ± 0.002
$7 < p_{\mathrm{T}} < 8$	$3.25 < y^* < 4.00$	0.927 ± 0.003
$8 < p_{\mathrm{T}} < 10$	$1.50 < y^* < 2.50$	0.680 ± 0.003
$8 < p_{\mathrm{T}} < 10$	$2.50 < y^* < 3.25$	0.976 ± 0.002
$8 < p_{\mathrm{T}} < 10$	$3.25 < y^* < 4.00$	0.947 ± 0.003
$10 < p_{\mathrm{T}} < 14$	$1.50 < y^* < 2.50$	0.725 ± 0.005
$10 < p_{\mathrm{T}} < 14$	$2.50 < y^* < 3.25$	0.981 ± 0.002
$10 < p_{\mathrm{T}} < 14$	$3.25 < y^* < 4.00$	0.966 ± 0.004

Table 8: Acceptances for J/ψ in Pbp, in bins of p_{T} and y^*. The uncertainties are statistical.

p_{T} bin	y^* bin	ϵ_{acc}
$0 < p_{\mathrm{T}} < 1$	$-3.25 < y^* < -2.50$	0.380 ± 0.001
$0 < p_{\mathrm{T}} < 1$	$-4.00 < y^* < -3.25$	0.801 ± 0.001
$0 < p_{\mathrm{T}} < 1$	$-5.00 < y^* < -4.00$	0.730 ± 0.001
$1 < p_{\mathrm{T}} < 2$	$-3.25 < y^* < -2.50$	0.405 ± 0.001
$1 < p_{\mathrm{T}} < 2$	$-4.00 < y^* < -3.25$	0.800 ± 0.001
$1 < p_{\mathrm{T}} < 2$	$-5.00 < y^* < -4.00$	0.741 ± 0.001
$2 < p_{\mathrm{T}} < 3$	$-3.25 < y^* < -2.50$	0.440 ± 0.001
$2 < p_{\mathrm{T}} < 3$	$-4.00 < y^* < -3.25$	0.835 ± 0.001
$2 < p_{\mathrm{T}} < 3$	$-5.00 < y^* < -4.00$	0.781 ± 0.001
$3 < p_{\mathrm{T}} < 4$	$-3.25 < y^* < -2.50$	0.488 ± 0.001
$3 < p_{\mathrm{T}} < 4$	$-4.00 < y^* < -3.25$	0.874 ± 0.001
$3 < p_{\mathrm{T}} < 4$	$-5.00 < y^* < -4.00$	0.827 ± 0.001
$4 < p_{\mathrm{T}} < 5$	$-3.25 < y^* < -2.50$	0.534 ± 0.001
$4 < p_{\mathrm{T}} < 5$	$-4.00 < y^* < -3.25$	0.905 ± 0.001
$4 < p_{\mathrm{T}} < 5$	$-5.00 < y^* < -4.00$	0.865 ± 0.001
$5 < p_{\mathrm{T}} < 6$	$-3.25 < y^* < -2.50$	0.576 ± 0.002
$5 < p_{\mathrm{T}} < 6$	$-4.00 < y^* < -3.25$	0.926 ± 0.001
$5 < p_{\mathrm{T}} < 6$	$-5.00 < y^* < -4.00$	0.895 ± 0.001
$6 < p_{\mathrm{T}} < 7$	$-3.25 < y^* < -2.50$	0.614 ± 0.003
$6 < p_{\mathrm{T}} < 7$	$-4.00 < y^* < -3.25$	0.945 ± 0.001
$6 < p_{\mathrm{T}} < 7$	$-5.00 < y^* < -4.00$	0.916 ± 0.002
$7 < p_{\mathrm{T}} < 8$	$-3.25 < y^* < -2.50$	0.650 ± 0.004
$7 < p_{\mathrm{T}} < 8$	$-4.00 < y^* < -3.25$	0.958 ± 0.002
$7 < p_{\mathrm{T}} < 8$	$-5.00 < y^* < -4.00$	0.935 ± 0.002
$8 < p_{\mathrm{T}} < 10$	$-3.25 < y^* < -2.50$	0.688 ± 0.004
$8 < p_{\mathrm{T}} < 10$	$-4.00 < y^* < -3.25$	0.967 ± 0.002
$8 < p_{\mathrm{T}} < 10$	$-5.00 < y^* < -4.00$	0.949 ± 0.002
$10 < p_{\mathrm{T}} < 14$	$-3.25 < y^* < -2.50$	0.739 ± 0.005
$10 < p_{\mathrm{T}} < 14$	$-4.00 < y^* < -3.25$	0.984 ± 0.002
$10 < p_{\mathrm{T}} < 14$	$-5.00 < y^* < -4.00$	0.971 ± 0.003

Table 9: Acceptances for $\psi(2S)$ in pPb, in bins of p_T and y^*. The uncertainties are statistical.

p_T bin	y^* bin	ϵ_{acc}
$0 < p_T < 1$	$1.50 < y^* < 2.50$	0.405 ± 0.001
$0 < p_T < 1$	$2.50 < y^* < 3.25$	0.839 ± 0.001
$0 < p_T < 1$	$3.25 < y^* < 4.00$	0.718 ± 0.001
$1 < p_T < 2$	$1.50 < y^* < 2.50$	0.421 ± 0.001
$1 < p_T < 2$	$2.50 < y^* < 3.25$	0.823 ± 0.001
$1 < p_T < 2$	$3.25 < y^* < 4.00$	0.725 ± 0.001
$2 < p_T < 3$	$1.50 < y^* < 2.50$	0.447 ± 0.001
$2 < p_T < 3$	$2.50 < y^* < 3.25$	0.846 ± 0.001
$2 < p_T < 3$	$3.25 < y^* < 4.00$	0.753 ± 0.001
$3 < p_T < 4$	$1.50 < y^* < 2.50$	0.481 ± 0.001
$3 < p_T < 4$	$2.50 < y^* < 3.25$	0.876 ± 0.001
$3 < p_T < 4$	$3.25 < y^* < 4.00$	0.795 ± 0.001
$4 < p_T < 5$	$1.50 < y^* < 2.50$	0.514 ± 0.001
$4 < p_T < 5$	$2.50 < y^* < 3.25$	0.901 ± 0.001
$4 < p_T < 5$	$3.25 < y^* < 4.00$	0.831 ± 0.001
$5 < p_T < 6$	$1.50 < y^* < 2.50$	0.549 ± 0.001
$5 < p_T < 6$	$2.50 < y^* < 3.25$	0.923 ± 0.001
$5 < p_T < 6$	$3.25 < y^* < 4.00$	0.863 ± 0.002
$6 < p_T < 7$	$1.50 < y^* < 2.50$	0.582 ± 0.002
$6 < p_T < 7$	$2.50 < y^* < 3.25$	0.940 ± 0.001
$6 < p_T < 7$	$3.25 < y^* < 4.00$	0.889 ± 0.002
$7 < p_T < 8$	$1.50 < y^* < 2.50$	0.607 ± 0.003
$7 < p_T < 8$	$2.50 < y^* < 3.25$	0.954 ± 0.002
$7 < p_T < 8$	$3.25 < y^* < 4.00$	0.907 ± 0.003
$8 < p_T < 10$	$1.50 < y^* < 2.50$	0.640 ± 0.003
$8 < p_T < 10$	$2.50 < y^* < 3.25$	0.962 ± 0.002
$8 < p_T < 10$	$3.25 < y^* < 4.00$	0.934 ± 0.003
$10 < p_T < 14$	$1.50 < y^* < 2.50$	0.694 ± 0.004
$10 < p_T < 14$	$2.50 < y^* < 3.25$	0.975 ± 0.002
$10 < p_T < 14$	$3.25 < y^* < 4.00$	0.951 ± 0.003

Table 10: Acceptances for $\psi(2S)$ in Pbp, in bins of p_T and y^*. The uncertainties are statistical.

p_T bin	y^* bin	ϵ_{acc}
$0 < p_T < 1$	$-3.25 < y^* < -2.50$	0.376 ± 0.001
$0 < p_T < 1$	$-4.00 < y^* < -3.25$	0.800 ± 0.001
$0 < p_T < 1$	$-5.00 < y^* < -4.00$	0.734 ± 0.001
$1 < p_T < 2$	$-3.25 < y^* < -2.50$	0.394 ± 0.001
$1 < p_T < 2$	$-4.00 < y^* < -3.25$	0.795 ± 0.001
$1 < p_T < 2$	$-5.00 < y^* < -4.00$	0.736 ± 0.001
$2 < p_T < 3$	$-3.25 < y^* < -2.50$	0.422 ± 0.001
$2 < p_T < 3$	$-4.00 < y^* < -3.25$	0.816 ± 0.001
$2 < p_T < 3$	$-5.00 < y^* < -4.00$	0.763 ± 0.001
$3 < p_T < 4$	$-3.25 < y^* < -2.50$	0.460 ± 0.001
$3 < p_T < 4$	$-4.00 < y^* < -3.25$	0.853 ± 0.001
$3 < p_T < 4$	$-5.00 < y^* < -4.00$	0.803 ± 0.001
$4 < p_T < 5$	$-3.25 < y^* < -2.50$	0.503 ± 0.001
$4 < p_T < 5$	$-4.00 < y^* < -3.25$	0.881 ± 0.001
$4 < p_T < 5$	$-5.00 < y^* < -4.00$	0.840 ± 0.001
$5 < p_T < 6$	$-3.25 < y^* < -2.50$	0.538 ± 0.002
$5 < p_T < 6$	$-4.00 < y^* < -3.25$	0.907 ± 0.001
$5 < p_T < 6$	$-5.00 < y^* < -4.00$	0.870 ± 0.001
$6 < p_T < 7$	$-3.25 < y^* < -2.50$	0.574 ± 0.002
$6 < p_T < 7$	$-4.00 < y^* < -3.25$	0.924 ± 0.001
$6 < p_T < 7$	$-5.00 < y^* < -4.00$	0.894 ± 0.002
$7 < p_T < 8$	$-3.25 < y^* < -2.50$	0.612 ± 0.003
$7 < p_T < 8$	$-4.00 < y^* < -3.25$	0.940 ± 0.002
$7 < p_T < 8$	$-5.00 < y^* < -4.00$	0.918 ± 0.002
$8 < p_T < 10$	$-3.25 < y^* < -2.50$	0.649 ± 0.003
$8 < p_T < 10$	$-4.00 < y^* < -3.25$	0.956 ± 0.002
$8 < p_T < 10$	$-5.00 < y^* < -4.00$	0.934 ± 0.002
$10 < p_T < 14$	$-3.25 < y^* < -2.50$	0.703 ± 0.004
$10 < p_T < 14$	$-4.00 < y^* < -3.25$	0.970 ± 0.002
$10 < p_T < 14$	$-5.00 < y^* < -4.00$	0.957 ± 0.003

Table 11: $\psi(2S)$ over J/ψ acceptance efficiency ratios in pPb, in bins of p_{T} and y^* with total uncertainties.

p_{T} bin	y^* bin	$\epsilon_{\mathrm{acc}}^{\psi(2S)}/\epsilon_{\mathrm{acc}}^{J/\psi}$
$0 < p_{\mathrm{T}} < 1$	$1.50 < y^* < 2.50$	0.994 ± 0.004
$0 < p_{\mathrm{T}} < 1$	$2.50 < y^* < 3.25$	1.003 ± 0.002
$0 < p_{\mathrm{T}} < 1$	$3.25 < y^* < 4.00$	1.003 ± 0.003
$1 < p_{\mathrm{T}} < 2$	$1.50 < y^* < 2.50$	0.977 ± 0.002
$1 < p_{\mathrm{T}} < 2$	$2.50 < y^* < 3.25$	0.994 ± 0.001
$1 < p_{\mathrm{T}} < 2$	$3.25 < y^* < 4.00$	0.992 ± 0.002
$2 < p_{\mathrm{T}} < 3$	$1.50 < y^* < 2.50$	0.958 ± 0.002
$2 < p_{\mathrm{T}} < 3$	$2.50 < y^* < 3.25$	0.980 ± 0.001
$2 < p_{\mathrm{T}} < 3$	$3.25 < y^* < 4.00$	0.975 ± 0.002
$3 < p_{\mathrm{T}} < 4$	$1.50 < y^* < 2.50$	0.946 ± 0.002
$3 < p_{\mathrm{T}} < 4$	$2.50 < y^* < 3.25$	0.979 ± 0.001
$3 < p_{\mathrm{T}} < 4$	$3.25 < y^* < 4.00$	0.970 ± 0.002
$4 < p_{\mathrm{T}} < 5$	$1.50 < y^* < 2.50$	0.936 ± 0.003
$4 < p_{\mathrm{T}} < 5$	$2.50 < y^* < 3.25$	0.976 ± 0.001
$4 < p_{\mathrm{T}} < 5$	$3.25 < y^* < 4.00$	0.963 ± 0.002
$5 < p_{\mathrm{T}} < 6$	$1.50 < y^* < 2.50$	0.934 ± 0.004
$5 < p_{\mathrm{T}} < 6$	$2.50 < y^* < 3.25$	0.979 ± 0.001
$5 < p_{\mathrm{T}} < 6$	$3.25 < y^* < 4.00$	0.968 ± 0.002
$6 < p_{\mathrm{T}} < 7$	$1.50 < y^* < 2.50$	0.938 ± 0.005
$6 < p_{\mathrm{T}} < 7$	$2.50 < y^* < 3.25$	0.984 ± 0.002
$6 < p_{\mathrm{T}} < 7$	$3.25 < y^* < 4.00$	0.975 ± 0.003
$7 < p_{\mathrm{T}} < 8$	$1.50 < y^* < 2.50$	0.928 ± 0.006
$7 < p_{\mathrm{T}} < 8$	$2.50 < y^* < 3.25$	0.992 ± 0.002
$7 < p_{\mathrm{T}} < 8$	$3.25 < y^* < 4.00$	0.978 ± 0.004
$8 < p_{\mathrm{T}} < 10$	$1.50 < y^* < 2.50$	0.942 ± 0.006
$8 < p_{\mathrm{T}} < 10$	$2.50 < y^* < 3.25$	0.986 ± 0.002
$8 < p_{\mathrm{T}} < 10$	$3.25 < y^* < 4.00$	0.986 ± 0.004
$10 < p_{\mathrm{T}} < 14$	$1.50 < y^* < 2.50$	0.957 ± 0.008
$10 < p_{\mathrm{T}} < 14$	$2.50 < y^* < 3.25$	0.994 ± 0.003
$10 < p_{\mathrm{T}} < 14$	$3.25 < y^* < 4.00$	0.985 ± 0.005

Table 12: $\psi(2S)$ over J/ψ acceptance efficiency ratios in Pbp, in bins of p_{T} and y^* with total uncertainties.

p_{T} bin	y^* bin	$\epsilon_{\mathrm{acc}}^{\psi(2S)}/\epsilon_{\mathrm{acc}}^{J/\psi}$
$0 < p_{\mathrm{T}} < 1$	$-3.25 < y^* < -2.50$	0.990 ± 0.005
$0 < p_{\mathrm{T}} < 1$	$-4.00 < y^* < -3.25$	0.999 ± 0.002
$0 < p_{\mathrm{T}} < 1$	$-5.00 < y^* < -4.00$	1.006 ± 0.002
$1 < p_{\mathrm{T}} < 2$	$-3.25 < y^* < -2.50$	0.974 ± 0.003
$1 < p_{\mathrm{T}} < 2$	$-4.00 < y^* < -3.25$	0.993 ± 0.001
$1 < p_{\mathrm{T}} < 2$	$-5.00 < y^* < -4.00$	0.993 ± 0.001
$2 < p_{\mathrm{T}} < 3$	$-3.25 < y^* < -2.50$	0.958 ± 0.002
$2 < p_{\mathrm{T}} < 3$	$-4.00 < y^* < -3.25$	0.977 ± 0.001
$2 < p_{\mathrm{T}} < 3$	$-5.00 < y^* < -4.00$	0.977 ± 0.001
$3 < p_{\mathrm{T}} < 4$	$-3.25 < y^* < -2.50$	0.943 ± 0.003
$3 < p_{\mathrm{T}} < 4$	$-4.00 < y^* < -3.25$	0.976 ± 0.001
$3 < p_{\mathrm{T}} < 4$	$-5.00 < y^* < -4.00$	0.971 ± 0.001
$4 < p_{\mathrm{T}} < 5$	$-3.25 < y^* < -2.50$	0.941 ± 0.003
$4 < p_{\mathrm{T}} < 5$	$-4.00 < y^* < -3.25$	0.973 ± 0.001
$4 < p_{\mathrm{T}} < 5$	$-5.00 < y^* < -4.00$	0.970 ± 0.002
$5 < p_{\mathrm{T}} < 6$	$-3.25 < y^* < -2.50$	0.934 ± 0.004
$5 < p_{\mathrm{T}} < 6$	$-4.00 < y^* < -3.25$	0.979 ± 0.002
$5 < p_{\mathrm{T}} < 6$	$-5.00 < y^* < -4.00$	0.972 ± 0.002
$6 < p_{\mathrm{T}} < 7$	$-3.25 < y^* < -2.50$	0.935 ± 0.006
$6 < p_{\mathrm{T}} < 7$	$-4.00 < y^* < -3.25$	0.978 ± 0.002
$6 < p_{\mathrm{T}} < 7$	$-5.00 < y^* < -4.00$	0.976 ± 0.003
$7 < p_{\mathrm{T}} < 8$	$-3.25 < y^* < -2.50$	0.941 ± 0.007
$7 < p_{\mathrm{T}} < 8$	$-4.00 < y^* < -3.25$	0.982 ± 0.003
$7 < p_{\mathrm{T}} < 8$	$-5.00 < y^* < -4.00$	0.982 ± 0.003
$8 < p_{\mathrm{T}} < 10$	$-3.25 < y^* < -2.50$	0.944 ± 0.007
$8 < p_{\mathrm{T}} < 10$	$-4.00 < y^* < -3.25$	0.989 ± 0.002
$8 < p_{\mathrm{T}} < 10$	$-5.00 < y^* < -4.00$	0.984 ± 0.003
$10 < p_{\mathrm{T}} < 14$	$-3.25 < y^* < -2.50$	0.951 ± 0.009
$10 < p_{\mathrm{T}} < 14$	$-4.00 < y^* < -3.25$	0.986 ± 0.003
$10 < p_{\mathrm{T}} < 14$	$-5.00 < y^* < -4.00$	0.986 ± 0.004

6.2 Reconstruction efficiency

The reconstruction or tracking efficiency is defined as the fraction of J/ψ ($\psi(2S)$) in the acceptance, where both muons are reconstructed as long tracks,

$$\epsilon_{\rm rec}(p_{\rm T}, y^*) = \frac{J/\psi \text{ or } \psi(2S) \text{ in bin } (p_{\rm T}, y^*) \text{ with both } \mu \text{ reconstructed as long tracks}}{J/\psi \text{ or } \psi(2S) \text{ with both } \mu \text{ in LHCb}}. \quad (18)$$

The tracking efficiency is computed using the simulation samples, and this efficiency is corrected using the reconstruction efficiency per-track estimated in data. The **long** method with tag-probe strategy for tracking efficiency calibration (more details can be found on the tracking TWiki page [56]) is implemented. In this method, a **probe** track is reconstructed only with hits in the TT and MUON stations. This probe muon track is combined with a standard long muon track to form a J/ψ candidate, and these candidates build a "pre-matched" sample. This standard long track has the same reconstruction algorithm as the signal tracks in our analysis, so they have the same tracking efficiency when they are in the same phase space.

An additional standard long track, identified as a muon and with the same charge as the **probe** track, is combined with the J/ψ in the "pre-matched" sample to form a good vertex. If this third track shares with the **probe** track more than 40% of the hits in both the TT and MUON stations, the probe track is referred to as "matched". The J/ψ candidates in the "pre-match" sample that have the probe track matched, form the "matched" sample.

The tracking efficiency is computed as the matching efficiency, which is the fraction of probe tracks that match standard long tracks. The number of signal probe tracks and those matched to long tracks are estimated from the number of J/ψ signal candidates, measured by fitting to the $\mu^+\mu^-$ invariant mass distribution in the "pre-matched" sample and the "matched" sample, respectively. The reconstruction of the probe tracks, of the J/ψ candidates and the implementation of the matching are done at the trigger (HLT) level, available in both pp and proton-lead data. The relevant trigger lines are called Hlt2TrackEffDiMuonMuonTT(Minus|Plus)* (which selects the "pre-matched" samples), where Plus (Minus) means that the μ^+ (μ^-) is the probe track. These calibration events are processed via the TurboCalib stream. Due to higher multiplicity in proton-lead data, especially in the backward configuration, additional offline selections are applied to the J/ψ candidates out of TurboCalib stream. The tag track of the J/ψ candidates is required to have a good muon-pion separation with PID(μ) > 3, and the probe track is required to have a better fit quality with $\text{Prob}(\chi^2_{\rm trk}) > 0.2$. The effect of these extra selections is studied with the proton-lead forward data sample (pPb), where a better signal purity is obtained.

Simulated J/ψ samples are produced with the same trigger processing as data for the calibration. The reconstruction software is identical to those used to reconstruct the simulated signals used in the analysis.

The signal extraction fits to the mass distributions are implemented in bins of η and p of the probe tracks, allowing to determine the track reconstruction efficiency in the same bins. The bin boundaries are 1.9, 3.2 and 5.0 for η and 6, 10, 20, 40, 100 and 500 GeV/c for p. No binning in detector occupancy is implemented due to limited statistics. However, since for both data and simulation, the occupancy distribution in the analysis samples and the calibration samples are consistent with each other, the binning in detector occupancy is not necessary. Fig. 14 shows the distributions as function of SPDhits for the calibration samples and the data samples, which are consistent with each other.

The μ^+ and μ^- probe tracks are fit separately. Thus for each kinematic bins, there are eight fits: μ^+ or μ^- as the probe track; in the "pre-matched" or "matched" sample; for pPb or Pbp. For the fits, the same signal shape is used for bins of the same (p, η) interval: a Gaussian function plus a Crystal Ball function. The background is described by an exponential function. An example of the fit is shown in Fig. 13.

The procedure performed on data is applied identically to the pPb and Pbp simulation calibration samples. The tracking efficiencies for μ^+ and μ^- are averaged, as for the cross-section measurements charge conjugated states are added together. The track reconstruction efficiency measured in data and in simulation, in bins of the η and p, for pPb and Pbp, are given in Fig. 15.

Finally, we calculate the ratio of single track reconstructions efficiencies between data and simulation. The results are given in Fig. 16. The corresponding uncertainty for each value is also shown, while the details of the studies for the uncertainty is provided in Sect. 7.5.

The reconstruction efficiency $\epsilon_{\rm rec}$ is then computed from the full simulation, and correcting the efficiency using the per-track efficiency ratios detailed above. The result is shown on Fig. 17, where the errors are the statistical errors from the simulation and the errors on the correction factors for the efficiency, added quadratically. Tables 13 and 14 give the corresponding numerical values. Figure 18 shows the same quantity for the $\psi(2S)$ and the numerical values are given in Table 15. The reconstruction efficiency ratio is shown in Fig. 19 and in Table 16.

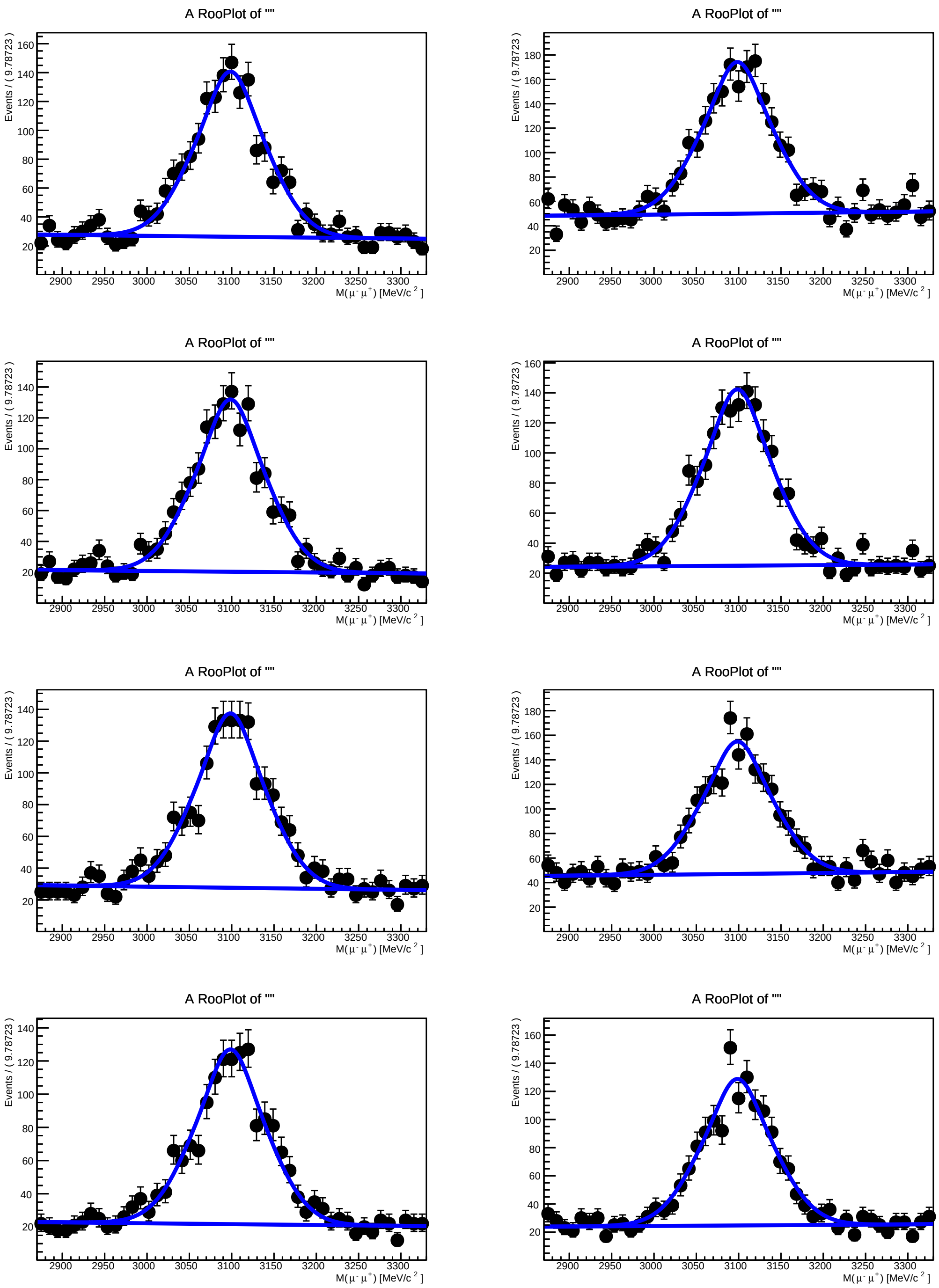

Figure 13: Fit to the invariant mass distribution of J/ψ candidates in the track calibration sample of proton-lead data. The left and right hand side columns correspond to pPb and Pbp data, respectively. The first and third rows correspond to the "pre-matched" samples for μ^+ and μ^- probe tracks, respectively. The second and forth rows correspond to the "matched" samples for μ^+ and μ^- probe tracks, respectively.

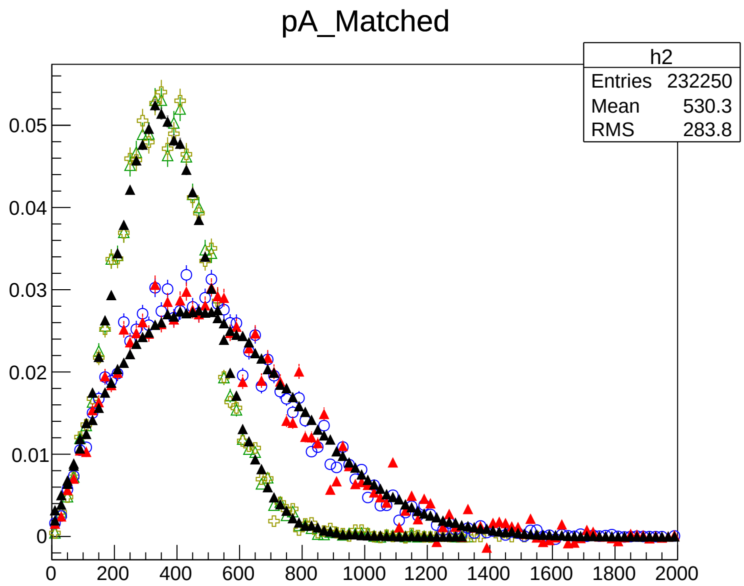

Figure 14: Background subtracted distributions of SPD hits in the pPb calibration sample: olive for all J/ψ and green for the track-matched J/ψ; and in the Pbp calibration sample: red for all J/ψ and bleu for the track matched J/ψ. The black dots represent the same quantity for the inclusive J/ψ of the analysis samples.

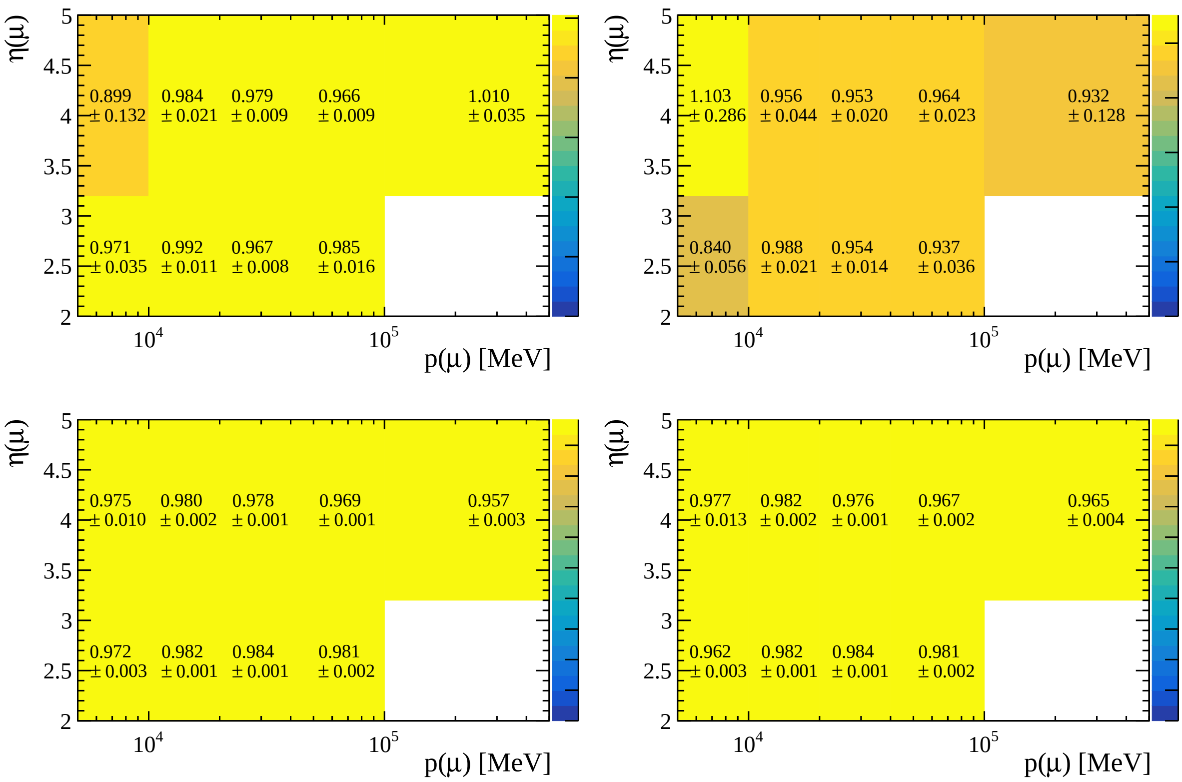

Figure 15: Tracking efficiency in bins of η and p for top left: pPb data, top right: Pbp, bottom left: pPb simulation, bottom right: Pbp simulation.

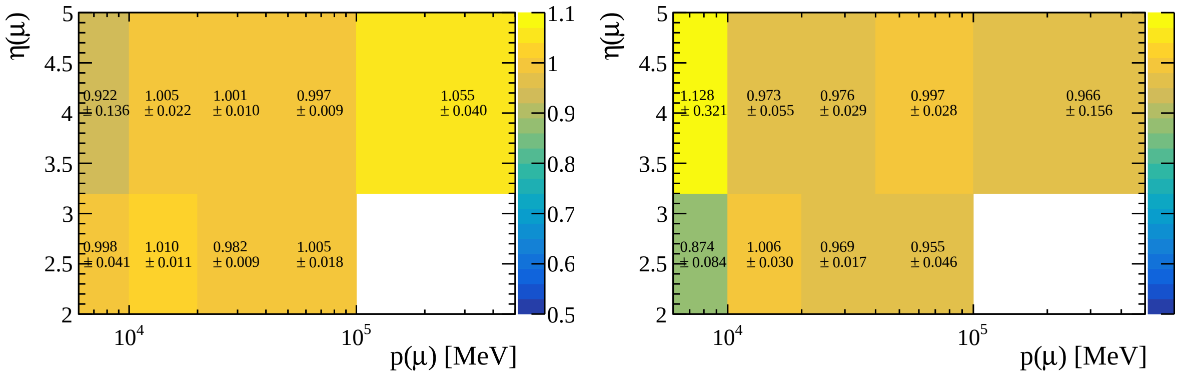

Figure 16: Ratio between data and pPb/Pbp simulation of per-track tracking efficiency in bins of the track η and p. Left: pPb, right: Pbp.

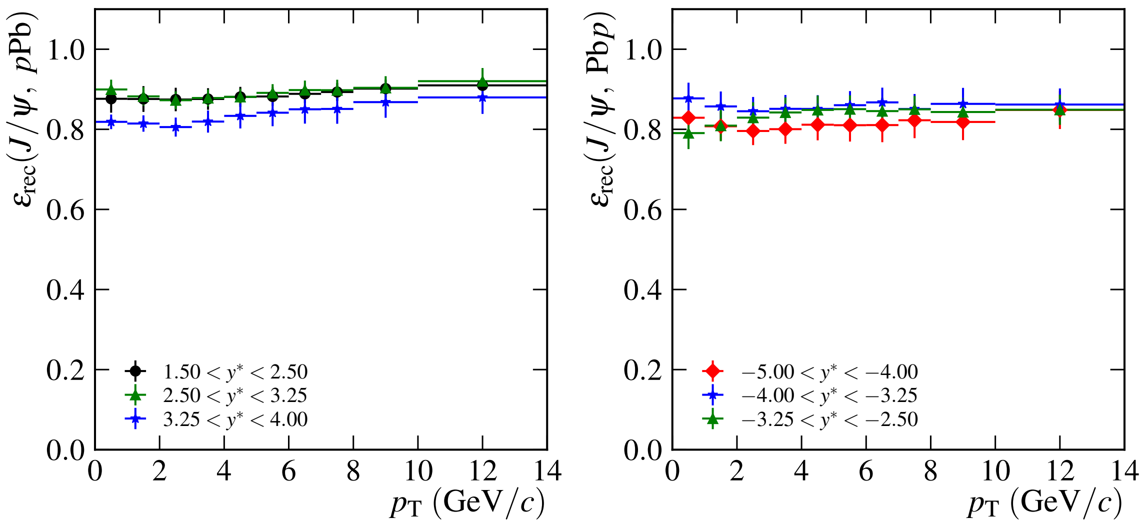

Figure 17: Reconstruction efficiency $\epsilon_{\rm rec}$ as a function of $p_{\rm T}$ in different y^* bins for left: J/ψ in pPb, right: J/ψ in Pbp. The displayed uncertainty corresponds to the uncertainty from the efficiency tables.

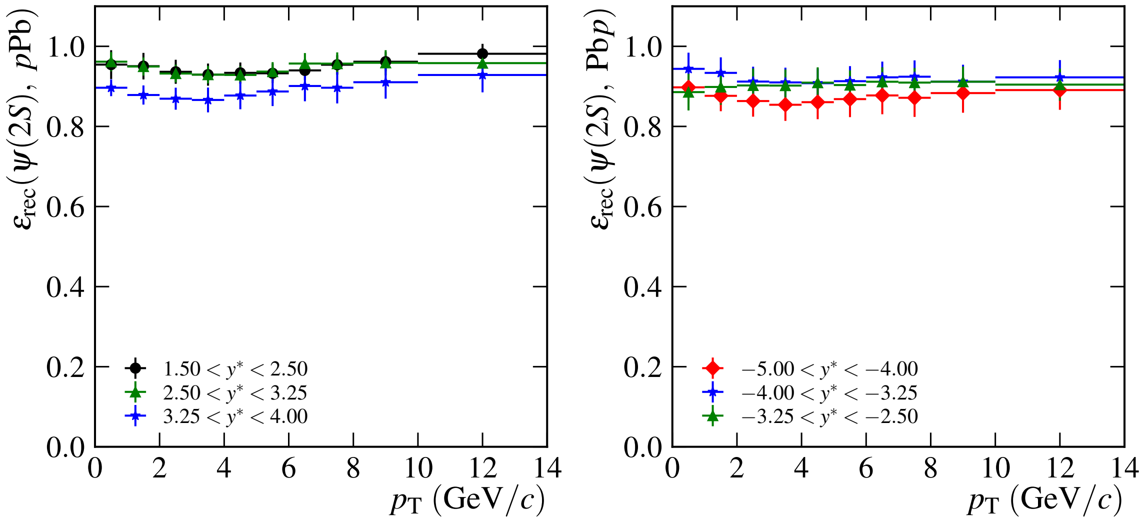

Figure 18: Reconstruction efficiency $\epsilon_{\rm rec}$ as a function of $p_{\rm T}$ in different y^* bins for left: $\psi(2S)$ in pPb, right: $\psi(2S)$ in Pbp. The displayed uncertainty corresponds to the uncertainty from the efficiency tables.

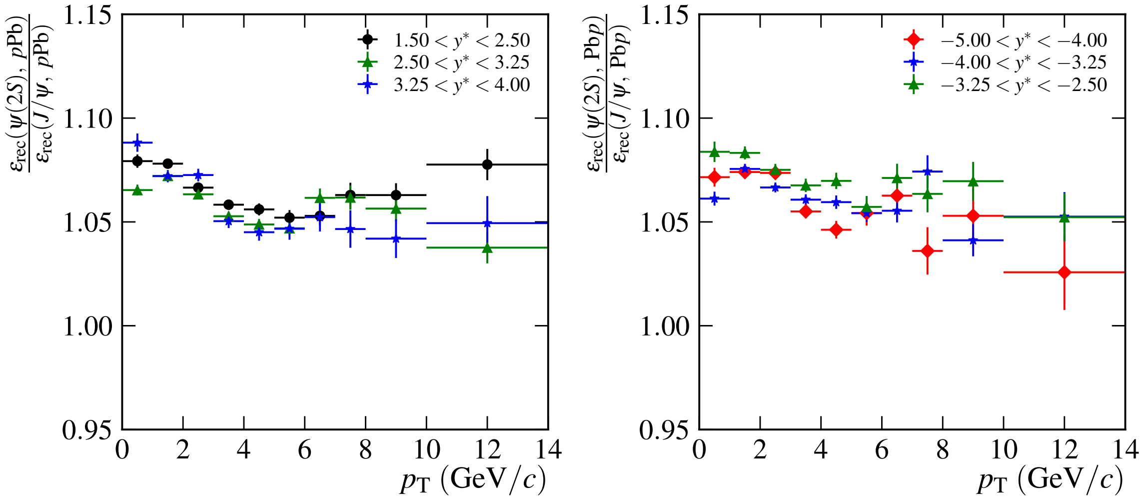

Figure 19: Reconstruction efficiency $\epsilon_{\rm rec}^{\psi(2S)}/\epsilon_{\rm rec}^{J/\psi}$ ratio as a function of $p_{\rm T}$ and y^* bins for left: pPb, right: Pbp. The displayed uncertainty is the total uncertainty including the uncertainty due to the data-driven correction tables, discussed in the following section and the statistical uncertainty due to finite Monte Carlo statistics.

Table 13: Reconstruction efficiencies for J/ψ in pPb, in bins of p_{T} and y^*. The uncertainties are the uncertainties from the correction tables.

p_{T} bin	y^* bin	ϵ_{rec}
$0 < p_{\mathrm{T}} < 1$	$1.50 < y^* < 2.50$	0.876 ± 0.035
$0 < p_{\mathrm{T}} < 1$	$2.50 < y^* < 3.25$	0.900 ± 0.024
$0 < p_{\mathrm{T}} < 1$	$3.25 < y^* < 4.00$	0.819 ± 0.018
$1 < p_{\mathrm{T}} < 2$	$1.50 < y^* < 2.50$	0.876 ± 0.032
$1 < p_{\mathrm{T}} < 2$	$2.50 < y^* < 3.25$	0.882 ± 0.023
$1 < p_{\mathrm{T}} < 2$	$3.25 < y^* < 4.00$	0.814 ± 0.020
$2 < p_{\mathrm{T}} < 3$	$1.50 < y^* < 2.50$	0.874 ± 0.029
$2 < p_{\mathrm{T}} < 3$	$2.50 < y^* < 3.25$	0.873 ± 0.022
$2 < p_{\mathrm{T}} < 3$	$3.25 < y^* < 4.00$	0.806 ± 0.024
$3 < p_{\mathrm{T}} < 4$	$1.50 < y^* < 2.50$	0.876 ± 0.027
$3 < p_{\mathrm{T}} < 4$	$2.50 < y^* < 3.25$	0.878 ± 0.021
$3 < p_{\mathrm{T}} < 4$	$3.25 < y^* < 4.00$	0.819 ± 0.028
$4 < p_{\mathrm{T}} < 5$	$1.50 < y^* < 2.50$	0.881 ± 0.025
$4 < p_{\mathrm{T}} < 5$	$2.50 < y^* < 3.25$	0.881 ± 0.021
$4 < p_{\mathrm{T}} < 5$	$3.25 < y^* < 4.00$	0.834 ± 0.031
$5 < p_{\mathrm{T}} < 6$	$1.50 < y^* < 2.50$	0.882 ± 0.024
$5 < p_{\mathrm{T}} < 6$	$2.50 < y^* < 3.25$	0.891 ± 0.022
$5 < p_{\mathrm{T}} < 6$	$3.25 < y^* < 4.00$	0.841 ± 0.034
$6 < p_{\mathrm{T}} < 7$	$1.50 < y^* < 2.50$	0.889 ± 0.023
$6 < p_{\mathrm{T}} < 7$	$2.50 < y^* < 3.25$	0.898 ± 0.024
$6 < p_{\mathrm{T}} < 7$	$3.25 < y^* < 4.00$	0.850 ± 0.036
$7 < p_{\mathrm{T}} < 8$	$1.50 < y^* < 2.50$	0.893 ± 0.022
$7 < p_{\mathrm{T}} < 8$	$2.50 < y^* < 3.25$	0.898 ± 0.026
$7 < p_{\mathrm{T}} < 8$	$3.25 < y^* < 4.00$	0.851 ± 0.037
$8 < p_{\mathrm{T}} < 10$	$1.50 < y^* < 2.50$	0.902 ± 0.022
$8 < p_{\mathrm{T}} < 10$	$2.50 < y^* < 3.25$	0.904 ± 0.029
$8 < p_{\mathrm{T}} < 10$	$3.25 < y^* < 4.00$	0.868 ± 0.039
$10 < p_{\mathrm{T}} < 14$	$1.50 < y^* < 2.50$	0.910 ± 0.023
$10 < p_{\mathrm{T}} < 14$	$2.50 < y^* < 3.25$	0.920 ± 0.033
$10 < p_{\mathrm{T}} < 14$	$3.25 < y^* < 4.00$	0.880 ± 0.041

Table 14: Reconstruction efficiencies for J/ψ in Pbp, in bins of p_{T} and y^*. The uncertainties are the uncertainties from the correction tables.

p_{T} bin	y^* bin	ϵ_{rec}
$0 < p_{\mathrm{T}} < 1$	$-3.25 < y^* < -2.50$	0.791 ± 0.040
$0 < p_{\mathrm{T}} < 1$	$-4.00 < y^* < -3.25$	0.877 ± 0.039
$0 < p_{\mathrm{T}} < 1$	$-5.00 < y^* < -4.00$	0.829 ± 0.036
$1 < p_{\mathrm{T}} < 2$	$-3.25 < y^* < -2.50$	0.809 ± 0.039
$1 < p_{\mathrm{T}} < 2$	$-4.00 < y^* < -3.25$	0.857 ± 0.037
$1 < p_{\mathrm{T}} < 2$	$-5.00 < y^* < -4.00$	0.808 ± 0.035
$2 < p_{\mathrm{T}} < 3$	$-3.25 < y^* < -2.50$	0.829 ± 0.038
$2 < p_{\mathrm{T}} < 3$	$-4.00 < y^* < -3.25$	0.845 ± 0.036
$2 < p_{\mathrm{T}} < 3$	$-5.00 < y^* < -4.00$	0.796 ± 0.035
$3 < p_{\mathrm{T}} < 4$	$-3.25 < y^* < -2.50$	0.842 ± 0.037
$3 < p_{\mathrm{T}} < 4$	$-4.00 < y^* < -3.25$	0.851 ± 0.035
$3 < p_{\mathrm{T}} < 4$	$-5.00 < y^* < -4.00$	0.800 ± 0.037
$4 < p_{\mathrm{T}} < 5$	$-3.25 < y^* < -2.50$	0.848 ± 0.036
$4 < p_{\mathrm{T}} < 5$	$-4.00 < y^* < -3.25$	0.851 ± 0.034
$4 < p_{\mathrm{T}} < 5$	$-5.00 < y^* < -4.00$	0.811 ± 0.039
$5 < p_{\mathrm{T}} < 6$	$-3.25 < y^* < -2.50$	0.850 ± 0.035
$5 < p_{\mathrm{T}} < 6$	$-4.00 < y^* < -3.25$	0.860 ± 0.035
$5 < p_{\mathrm{T}} < 6$	$-5.00 < y^* < -4.00$	0.810 ± 0.041
$6 < p_{\mathrm{T}} < 7$	$-3.25 < y^* < -2.50$	0.845 ± 0.033
$6 < p_{\mathrm{T}} < 7$	$-4.00 < y^* < -3.25$	0.867 ± 0.037
$6 < p_{\mathrm{T}} < 7$	$-5.00 < y^* < -4.00$	0.811 ± 0.043
$7 < p_{\mathrm{T}} < 8$	$-3.25 < y^* < -2.50$	0.850 ± 0.034
$7 < p_{\mathrm{T}} < 8$	$-4.00 < y^* < -3.25$	0.851 ± 0.037
$7 < p_{\mathrm{T}} < 8$	$-5.00 < y^* < -4.00$	0.823 ± 0.045
$8 < p_{\mathrm{T}} < 10$	$-3.25 < y^* < -2.50$	0.843 ± 0.034
$8 < p_{\mathrm{T}} < 10$	$-4.00 < y^* < -3.25$	0.864 ± 0.040
$8 < p_{\mathrm{T}} < 10$	$-5.00 < y^* < -4.00$	0.818 ± 0.045
$10 < p_{\mathrm{T}} < 14$	$-3.25 < y^* < -2.50$	0.849 ± 0.038
$10 < p_{\mathrm{T}} < 14$	$-4.00 < y^* < -3.25$	0.862 ± 0.040
$10 < p_{\mathrm{T}} < 14$	$-5.00 < y^* < -4.00$	0.848 ± 0.048

Table 15: Reconstruction efficiencies for $\psi(2S)$ in pPb, in bins of p_T and y^*. The uncertainties are the uncertainties from the correction tables.

p_T bin	y^* bin	ϵ_{rec}
$0 < p_T < 1$	$1.50 < y^* < 2.50$	0.954 ± 0.036
$0 < p_T < 1$	$2.50 < y^* < 3.25$	0.962 ± 0.024
$0 < p_T < 1$	$3.25 < y^* < 4.00$	0.897 ± 0.021
$1 < p_T < 2$	$1.50 < y^* < 2.50$	0.950 ± 0.033
$1 < p_T < 2$	$2.50 < y^* < 3.25$	0.950 ± 0.023
$1 < p_T < 2$	$3.25 < y^* < 4.00$	0.878 ± 0.024
$2 < p_T < 3$	$1.50 < y^* < 2.50$	0.936 ± 0.030
$2 < p_T < 3$	$2.50 < y^* < 3.25$	0.932 ± 0.022
$2 < p_T < 3$	$3.25 < y^* < 4.00$	0.869 ± 0.027
$3 < p_T < 4$	$1.50 < y^* < 2.50$	0.929 ± 0.028
$3 < p_T < 4$	$2.50 < y^* < 3.25$	0.929 ± 0.022
$3 < p_T < 4$	$3.25 < y^* < 4.00$	0.866 ± 0.031
$4 < p_T < 5$	$1.50 < y^* < 2.50$	0.934 ± 0.026
$4 < p_T < 5$	$2.50 < y^* < 3.25$	0.929 ± 0.022
$4 < p_T < 5$	$3.25 < y^* < 4.00$	0.877 ± 0.034
$5 < p_T < 6$	$1.50 < y^* < 2.50$	0.933 ± 0.024
$5 < p_T < 6$	$2.50 < y^* < 3.25$	0.937 ± 0.024
$5 < p_T < 6$	$3.25 < y^* < 4.00$	0.887 ± 0.036
$6 < p_T < 7$	$1.50 < y^* < 2.50$	0.940 ± 0.024
$6 < p_T < 7$	$2.50 < y^* < 3.25$	0.957 ± 0.026
$6 < p_T < 7$	$3.25 < y^* < 4.00$	0.901 ± 0.038
$7 < p_T < 8$	$1.50 < y^* < 2.50$	0.954 ± 0.024
$7 < p_T < 8$	$2.50 < y^* < 3.25$	0.957 ± 0.028
$7 < p_T < 8$	$3.25 < y^* < 4.00$	0.897 ± 0.039
$8 < p_T < 10$	$1.50 < y^* < 2.50$	0.962 ± 0.024
$8 < p_T < 10$	$2.50 < y^* < 3.25$	0.959 ± 0.031
$8 < p_T < 10$	$3.25 < y^* < 4.00$	0.910 ± 0.041
$10 < p_T < 14$	$1.50 < y^* < 2.50$	0.981 ± 0.025
$10 < p_T < 14$	$2.50 < y^* < 3.25$	0.958 ± 0.034
$10 < p_T < 14$	$3.25 < y^* < 4.00$	0.928 ± 0.043

Table 16: Reconstruction efficiencies $\psi(2S)$ in Pbp, in bins of p_T and y^*. The uncertainties are the uncertainties from the correction tables.

p_T bin	y^* bin	ϵ_{rec}
$0 < p_T < 1$	$-3.25 < y^* < -2.50$	0.886 ± 0.046
$0 < p_T < 1$	$-4.00 < y^* < -3.25$	0.944 ± 0.040
$0 < p_T < 1$	$-5.00 < y^* < -4.00$	0.898 ± 0.039
$1 < p_T < 2$	$-3.25 < y^* < -2.50$	0.899 ± 0.044
$1 < p_T < 2$	$-4.00 < y^* < -3.25$	0.934 ± 0.039
$1 < p_T < 2$	$-5.00 < y^* < -4.00$	0.876 ± 0.038
$2 < p_T < 3$	$-3.25 < y^* < -2.50$	0.902 ± 0.042
$2 < p_T < 3$	$-4.00 < y^* < -3.25$	0.912 ± 0.037
$2 < p_T < 3$	$-5.00 < y^* < -4.00$	0.863 ± 0.039
$3 < p_T < 4$	$-3.25 < y^* < -2.50$	0.902 ± 0.040
$3 < p_T < 4$	$-4.00 < y^* < -3.25$	0.910 ± 0.037
$3 < p_T < 4$	$-5.00 < y^* < -4.00$	0.854 ± 0.040
$4 < p_T < 5$	$-3.25 < y^* < -2.50$	0.909 ± 0.038
$4 < p_T < 5$	$-4.00 < y^* < -3.25$	0.908 ± 0.037
$4 < p_T < 5$	$-5.00 < y^* < -4.00$	0.861 ± 0.043
$5 < p_T < 6$	$-3.25 < y^* < -2.50$	0.903 ± 0.037
$5 < p_T < 6$	$-4.00 < y^* < -3.25$	0.913 ± 0.038
$5 < p_T < 6$	$-5.00 < y^* < -4.00$	0.868 ± 0.045
$6 < p_T < 7$	$-3.25 < y^* < -2.50$	0.912 ± 0.036
$6 < p_T < 7$	$-4.00 < y^* < -3.25$	0.923 ± 0.039
$6 < p_T < 7$	$-5.00 < y^* < -4.00$	0.877 ± 0.047
$7 < p_T < 8$	$-3.25 < y^* < -2.50$	0.909 ± 0.037
$7 < p_T < 8$	$-4.00 < y^* < -3.25$	0.924 ± 0.041
$7 < p_T < 8$	$-5.00 < y^* < -4.00$	0.871 ± 0.048
$8 < p_T < 10$	$-3.25 < y^* < -2.50$	0.912 ± 0.038
$8 < p_T < 10$	$-4.00 < y^* < -3.25$	0.912 ± 0.042
$8 < p_T < 10$	$-5.00 < y^* < -4.00$	0.883 ± 0.049
$10 < p_T < 14$	$-3.25 < y^* < -2.50$	0.904 ± 0.040
$10 < p_T < 14$	$-4.00 < y^* < -3.25$	0.923 ± 0.043
$10 < p_T < 14$	$-5.00 < y^* < -4.00$	0.891 ± 0.049

Table 17: $\psi(2S)$ over J/ψ reconstruction efficiency ratios in pPb, in bins of p_{T} and y^* with total uncertainties.

p_{T} bin	y^* bin	$\epsilon_{\mathrm{rec}}^{\psi(2S)}/\epsilon_{\mathrm{rec}}^{J/\psi}$
$0 < p_{\mathrm{T}} < 1$	$1.50 < y^* < 2.50$	1.079 ± 0.003
$0 < p_{\mathrm{T}} < 1$	$2.50 < y^* < 3.25$	1.065 ± 0.003
$0 < p_{\mathrm{T}} < 1$	$3.25 < y^* < 4.00$	1.088 ± 0.004
$1 < p_{\mathrm{T}} < 2$	$1.50 < y^* < 2.50$	1.078 ± 0.002
$1 < p_{\mathrm{T}} < 2$	$2.50 < y^* < 3.25$	1.072 ± 0.002
$1 < p_{\mathrm{T}} < 2$	$3.25 < y^* < 4.00$	1.072 ± 0.003
$2 < p_{\mathrm{T}} < 3$	$1.50 < y^* < 2.50$	1.067 ± 0.002
$2 < p_{\mathrm{T}} < 3$	$2.50 < y^* < 3.25$	1.063 ± 0.002
$2 < p_{\mathrm{T}} < 3$	$3.25 < y^* < 4.00$	1.073 ± 0.003
$3 < p_{\mathrm{T}} < 4$	$1.50 < y^* < 2.50$	1.058 ± 0.002
$3 < p_{\mathrm{T}} < 4$	$2.50 < y^* < 3.25$	1.053 ± 0.002
$3 < p_{\mathrm{T}} < 4$	$3.25 < y^* < 4.00$	1.050 ± 0.003
$4 < p_{\mathrm{T}} < 5$	$1.50 < y^* < 2.50$	1.056 ± 0.003
$4 < p_{\mathrm{T}} < 5$	$2.50 < y^* < 3.25$	1.049 ± 0.003
$4 < p_{\mathrm{T}} < 5$	$3.25 < y^* < 4.00$	1.045 ± 0.004
$5 < p_{\mathrm{T}} < 6$	$1.50 < y^* < 2.50$	1.052 ± 0.004
$5 < p_{\mathrm{T}} < 6$	$2.50 < y^* < 3.25$	1.047 ± 0.003
$5 < p_{\mathrm{T}} < 6$	$3.25 < y^* < 4.00$	1.047 ± 0.005
$6 < p_{\mathrm{T}} < 7$	$1.50 < y^* < 2.50$	1.053 ± 0.005
$6 < p_{\mathrm{T}} < 7$	$2.50 < y^* < 3.25$	1.062 ± 0.004
$6 < p_{\mathrm{T}} < 7$	$3.25 < y^* < 4.00$	1.052 ± 0.007
$7 < p_{\mathrm{T}} < 8$	$1.50 < y^* < 2.50$	1.063 ± 0.006
$7 < p_{\mathrm{T}} < 8$	$2.50 < y^* < 3.25$	1.062 ± 0.006
$7 < p_{\mathrm{T}} < 8$	$3.25 < y^* < 4.00$	1.047 ± 0.009
$8 < p_{\mathrm{T}} < 10$	$1.50 < y^* < 2.50$	1.063 ± 0.006
$8 < p_{\mathrm{T}} < 10$	$2.50 < y^* < 3.25$	1.056 ± 0.006
$8 < p_{\mathrm{T}} < 10$	$3.25 < y^* < 4.00$	1.042 ± 0.009
$10 < p_{\mathrm{T}} < 14$	$1.50 < y^* < 2.50$	1.078 ± 0.008
$10 < p_{\mathrm{T}} < 14$	$2.50 < y^* < 3.25$	1.038 ± 0.008
$10 < p_{\mathrm{T}} < 14$	$3.25 < y^* < 4.00$	1.049 ± 0.013

Table 18: $\psi(2S)$ over J/ψ reconstruction efficiency ratios in Pbp, in bins of p_{T} and y^* with total uncertainties.

p_{T} bin	y^* bin	$\epsilon_{\mathrm{rec}}^{\psi(2S)}/\epsilon_{\mathrm{rec}}^{J/\psi}$
$0 < p_{\mathrm{T}} < 1$	$-3.25 < y^* < -2.50$	1.084 ± 0.005
$0 < p_{\mathrm{T}} < 1$	$-4.00 < y^* < -3.25$	1.061 ± 0.003
$0 < p_{\mathrm{T}} < 1$	$-5.00 < y^* < -4.00$	1.072 ± 0.005
$1 < p_{\mathrm{T}} < 2$	$-3.25 < y^* < -2.50$	1.083 ± 0.003
$1 < p_{\mathrm{T}} < 2$	$-4.00 < y^* < -3.25$	1.076 ± 0.002
$1 < p_{\mathrm{T}} < 2$	$-5.00 < y^* < -4.00$	1.074 ± 0.003
$2 < p_{\mathrm{T}} < 3$	$-3.25 < y^* < -2.50$	1.075 ± 0.003
$2 < p_{\mathrm{T}} < 3$	$-4.00 < y^* < -3.25$	1.067 ± 0.002
$2 < p_{\mathrm{T}} < 3$	$-5.00 < y^* < -4.00$	1.074 ± 0.003
$3 < p_{\mathrm{T}} < 4$	$-3.25 < y^* < -2.50$	1.068 ± 0.003
$3 < p_{\mathrm{T}} < 4$	$-4.00 < y^* < -3.25$	1.061 ± 0.003
$3 < p_{\mathrm{T}} < 4$	$-5.00 < y^* < -4.00$	1.055 ± 0.003
$4 < p_{\mathrm{T}} < 5$	$-3.25 < y^* < -2.50$	1.070 ± 0.004
$4 < p_{\mathrm{T}} < 5$	$-4.00 < y^* < -3.25$	1.060 ± 0.003
$4 < p_{\mathrm{T}} < 5$	$-5.00 < y^* < -4.00$	1.046 ± 0.004
$5 < p_{\mathrm{T}} < 6$	$-3.25 < y^* < -2.50$	1.057 ± 0.005
$5 < p_{\mathrm{T}} < 6$	$-4.00 < y^* < -3.25$	1.054 ± 0.004
$5 < p_{\mathrm{T}} < 6$	$-5.00 < y^* < -4.00$	1.054 ± 0.006
$6 < p_{\mathrm{T}} < 7$	$-3.25 < y^* < -2.50$	1.071 ± 0.007
$6 < p_{\mathrm{T}} < 7$	$-4.00 < y^* < -3.25$	1.055 ± 0.006
$6 < p_{\mathrm{T}} < 7$	$-5.00 < y^* < -4.00$	1.063 ± 0.008
$7 < p_{\mathrm{T}} < 8$	$-3.25 < y^* < -2.50$	1.063 ± 0.009
$7 < p_{\mathrm{T}} < 8$	$-4.00 < y^* < -3.25$	1.074 ± 0.008
$7 < p_{\mathrm{T}} < 8$	$-5.00 < y^* < -4.00$	1.036 ± 0.011
$8 < p_{\mathrm{T}} < 10$	$-3.25 < y^* < -2.50$	1.070 ± 0.009
$8 < p_{\mathrm{T}} < 10$	$-4.00 < y^* < -3.25$	1.041 ± 0.008
$8 < p_{\mathrm{T}} < 10$	$-5.00 < y^* < -4.00$	1.053 ± 0.013
$10 < p_{\mathrm{T}} < 14$	$-3.25 < y^* < -2.50$	1.052 ± 0.012
$10 < p_{\mathrm{T}} < 14$	$-4.00 < y^* < -3.25$	1.053 ± 0.012
$10 < p_{\mathrm{T}} < 14$	$-5.00 < y^* < -4.00$	1.026 ± 0.018

6.3 Selection efficiency

The selection efficiency is defined as

$$\epsilon_{\mathrm{sel}}(p_{\mathrm{T}}, y^*) = \frac{J/\psi \text{ or } \psi(2S) \text{ selected in bin } (p_{\mathrm{T}}, y^*)}{J/\psi \text{ or } \psi(2S) \text{ in bin } (p_{\mathrm{T}}, y^*) \text{ with both } \mu \text{ reconstructed as long tracks}}. \tag{19}$$

For the selection efficiency computation, particle identification criteria, the global event cut on the number of VELO clusters and the finding of the primary vertex are excluded since their efficiencies are derived from data as described below and in the next section. The main reduction of the efficiency in the selection is caused by the transverse momentum requirements on the daughter tracks. This loss of efficiency is purely of kinematic nature and can be calculated from the simulation samples (with the assumption that J/ψ mesons are produced unpolarized). Figure 20 shows the selection efficiencies for the J/ψ case, with statistical errors only. Figure 21 shows the same quantity for the $\psi(2S)$. The ratio is shown in Fig. 22. Tables 19, 20, 21 and 22 give the corresponding numerical values.

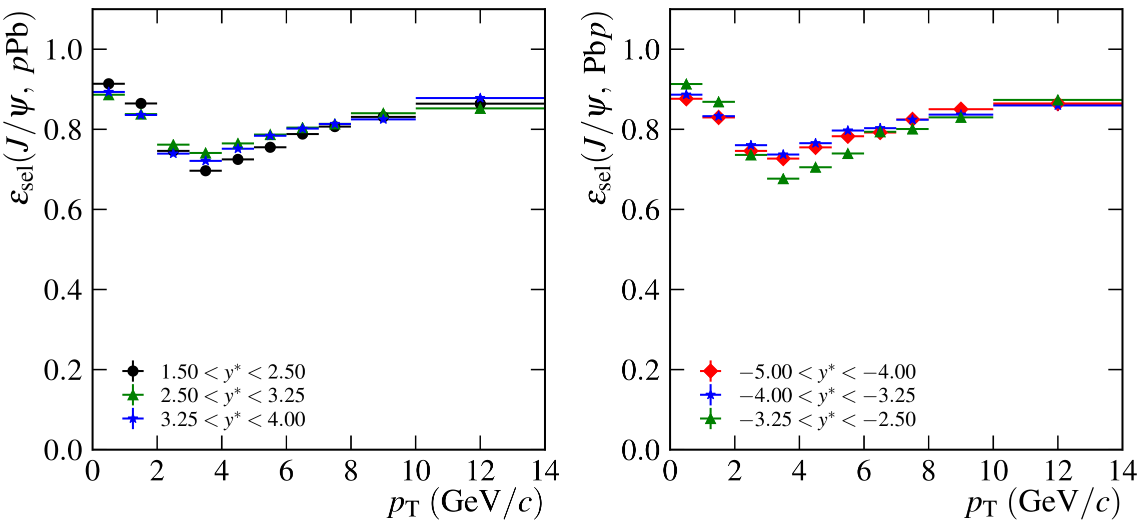

Figure 20: Selection efficiency ϵ_{sel} as a function of p_{T} in different y^* bins for left: J/ψ in pPb, right: J/ψ in Pbp. The displayed uncertainty corresponds to the total uncertainty.

The efficiency of the global event cut on the number of VELO clusters (required to be less than 8000) is computed directly from data, using di-muon candidates triggered by the NoBias line. For this trigger line, the global event cut is not applied, and the cut efficiency is computed by comparing the number of J/ψ candidates for a number of VELO clusters below 8000 to the total number of candidates. These numbers are extracted from a fit of the distributions of VELO clusters for J/ψ signal candidates (after background substraction). Figure 23 shows the fitted distributions and the efficiency is found equal to 1.000 for pPb and 0.998 for Pbp. The efficiency of this global event cut is assumed to be the same for candidates coming from b decays, and also to be independent of the charmonium p_{T} and y^* values. We assume also the same efficiency for the $\psi(2S)$.

The efficiency of the requirement that the number of reconstructed primary vertex is larger or equal to one is computed from J/ψ pp simulations, and found equal to $99.9 \pm 0.1\%$.

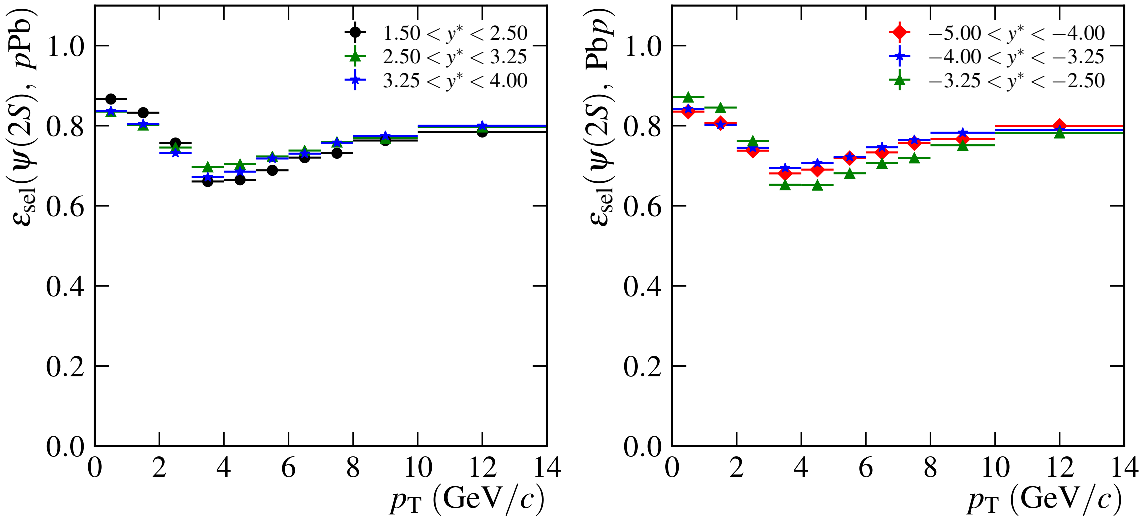

Figure 21: Selection efficiency $\epsilon_{\rm sel}$ as a function of $p_{\rm T}$ in different y^* bins for left: $\psi(2S)$ in pPb, right: $\psi(2S)$ in Pbp. The displayed uncertainty corresponds to the total uncertainty.

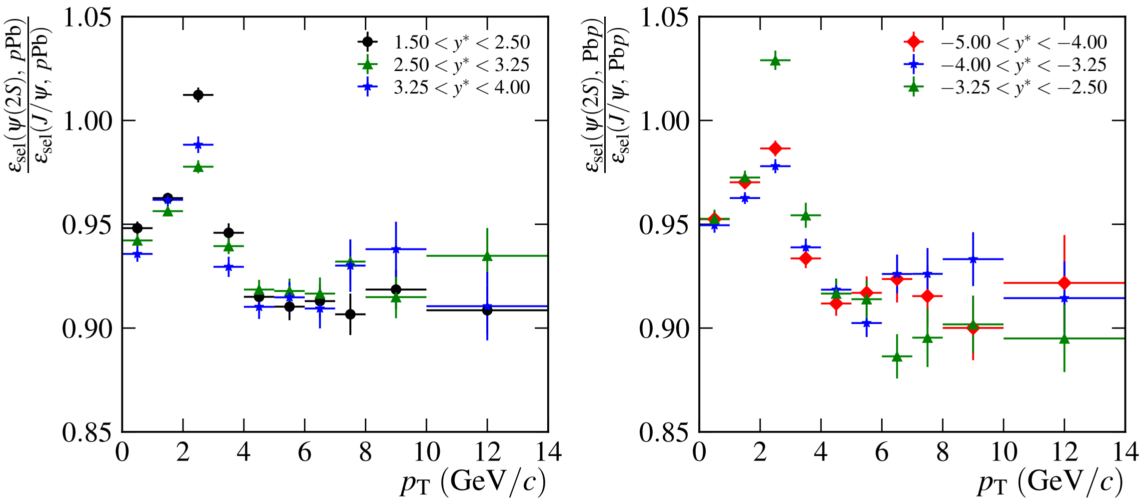

Figure 22: Selection efficiency ratio $\epsilon_{\rm sel}^{\psi(2S)}/\epsilon_{\rm sel}^{J/\psi}$ as a function of $p_{\rm T}$ and y^* bins for left: pPb, right: Pbp. The displayed uncertainty corresponds to the total uncertainty.

It is here also assumed to be identical for pPb and Pbp, for $\psi(2S)$ and for candidates from b decays and not to depend on the kinematics of the signal candidate.

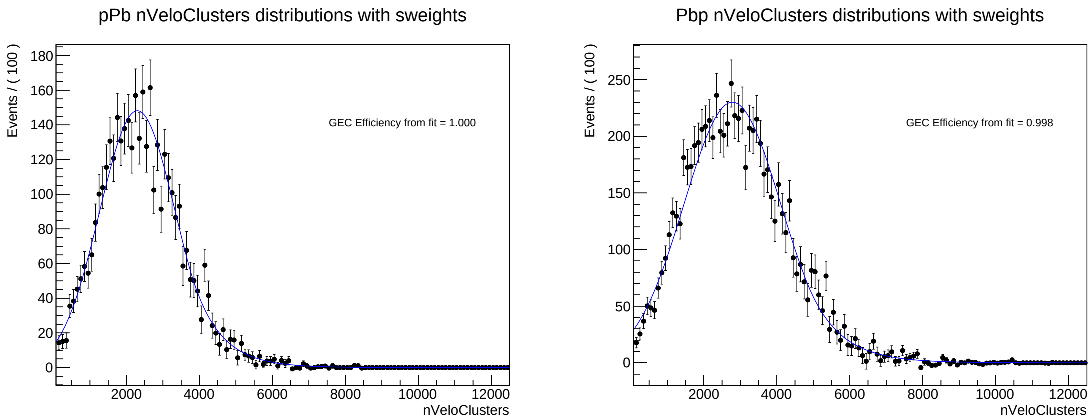

Figure 23: Number of VELO clusters, after background subtraction, for left: J/ψ in pPb and right: J/ψ in Pbp.

Table 19: Selection efficiencies J/ψ in pPb, in bins of p_{T} and y^{*}. The uncertainties are statistical.

p_{T} bin	y^{*} bin	ϵ_{sel}
$0 < p_{\mathrm{T}} < 1$	$1.50 < y^{*} < 2.50$	0.914 ± 0.002
$0 < p_{\mathrm{T}} < 1$	$2.50 < y^{*} < 3.25$	0.886 ± 0.001
$0 < p_{\mathrm{T}} < 1$	$3.25 < y^{*} < 4.00$	0.893 ± 0.002
$1 < p_{\mathrm{T}} < 2$	$1.50 < y^{*} < 2.50$	0.865 ± 0.001
$1 < p_{\mathrm{T}} < 2$	$2.50 < y^{*} < 3.25$	0.838 ± 0.001
$1 < p_{\mathrm{T}} < 2$	$3.25 < y^{*} < 4.00$	0.836 ± 0.002
$2 < p_{\mathrm{T}} < 3$	$1.50 < y^{*} < 2.50$	0.746 ± 0.002
$2 < p_{\mathrm{T}} < 3$	$2.50 < y^{*} < 3.25$	0.762 ± 0.002
$2 < p_{\mathrm{T}} < 3$	$3.25 < y^{*} < 4.00$	0.739 ± 0.002
$3 < p_{\mathrm{T}} < 4$	$1.50 < y^{*} < 2.50$	0.697 ± 0.002
$3 < p_{\mathrm{T}} < 4$	$2.50 < y^{*} < 3.25$	0.741 ± 0.002
$3 < p_{\mathrm{T}} < 4$	$3.25 < y^{*} < 4.00$	0.721 ± 0.002
$4 < p_{\mathrm{T}} < 5$	$1.50 < y^{*} < 2.50$	0.725 ± 0.003
$4 < p_{\mathrm{T}} < 5$	$2.50 < y^{*} < 3.25$	0.765 ± 0.002
$4 < p_{\mathrm{T}} < 5$	$3.25 < y^{*} < 4.00$	0.752 ± 0.003
$5 < p_{\mathrm{T}} < 6$	$1.50 < y^{*} < 2.50$	0.755 ± 0.003
$5 < p_{\mathrm{T}} < 6$	$2.50 < y^{*} < 3.25$	0.787 ± 0.003
$5 < p_{\mathrm{T}} < 6$	$3.25 < y^{*} < 4.00$	0.784 ± 0.004
$6 < p_{\mathrm{T}} < 7$	$1.50 < y^{*} < 2.50$	0.788 ± 0.004
$6 < p_{\mathrm{T}} < 7$	$2.50 < y^{*} < 3.25$	0.804 ± 0.004
$6 < p_{\mathrm{T}} < 7$	$3.25 < y^{*} < 4.00$	0.802 ± 0.005
$7 < p_{\mathrm{T}} < 8$	$1.50 < y^{*} < 2.50$	0.807 ± 0.005
$7 < p_{\mathrm{T}} < 8$	$2.50 < y^{*} < 3.25$	0.814 ± 0.005
$7 < p_{\mathrm{T}} < 8$	$3.25 < y^{*} < 4.00$	0.813 ± 0.006
$8 < p_{\mathrm{T}} < 10$	$1.50 < y^{*} < 2.50$	0.831 ± 0.005
$8 < p_{\mathrm{T}} < 10$	$2.50 < y^{*} < 3.25$	0.840 ± 0.005
$8 < p_{\mathrm{T}} < 10$	$3.25 < y^{*} < 4.00$	0.825 ± 0.007
$10 < p_{\mathrm{T}} < 14$	$1.50 < y^{*} < 2.50$	0.864 ± 0.006
$10 < p_{\mathrm{T}} < 14$	$2.50 < y^{*} < 3.25$	0.852 ± 0.007
$10 < p_{\mathrm{T}} < 14$	$3.25 < y^{*} < 4.00$	0.878 ± 0.008

Table 20: Selection efficiencies J/ψ in Pbp, in bins of p_{T} and y^{*}. The uncertainties are statistical.

p_{T} bin	y^{*} bin	ϵ_{sel}
$0 < p_{\mathrm{T}} < 1$	$-3.25 < y^{*} < -2.50$	0.913 ± 0.003
$0 < p_{\mathrm{T}} < 1$	$-4.00 < y^{*} < -3.25$	0.886 ± 0.002
$0 < p_{\mathrm{T}} < 1$	$-5.00 < y^{*} < -4.00$	0.876 ± 0.003
$1 < p_{\mathrm{T}} < 2$	$-3.25 < y^{*} < -2.50$	0.869 ± 0.002
$1 < p_{\mathrm{T}} < 2$	$-4.00 < y^{*} < -3.25$	0.833 ± 0.002
$1 < p_{\mathrm{T}} < 2$	$-5.00 < y^{*} < -4.00$	0.830 ± 0.002
$2 < p_{\mathrm{T}} < 3$	$-3.25 < y^{*} < -2.50$	0.736 ± 0.003
$2 < p_{\mathrm{T}} < 3$	$-4.00 < y^{*} < -3.25$	0.760 ± 0.002
$2 < p_{\mathrm{T}} < 3$	$-5.00 < y^{*} < -4.00$	0.746 ± 0.002
$3 < p_{\mathrm{T}} < 4$	$-3.25 < y^{*} < -2.50$	0.677 ± 0.003
$3 < p_{\mathrm{T}} < 4$	$-4.00 < y^{*} < -3.25$	0.737 ± 0.002
$3 < p_{\mathrm{T}} < 4$	$-5.00 < y^{*} < -4.00$	0.727 ± 0.003
$4 < p_{\mathrm{T}} < 5$	$-3.25 < y^{*} < -2.50$	0.705 ± 0.004
$4 < p_{\mathrm{T}} < 5$	$-4.00 < y^{*} < -3.25$	0.765 ± 0.003
$4 < p_{\mathrm{T}} < 5$	$-5.00 < y^{*} < -4.00$	0.755 ± 0.004
$5 < p_{\mathrm{T}} < 6$	$-3.25 < y^{*} < -2.50$	0.740 ± 0.006
$5 < p_{\mathrm{T}} < 6$	$-4.00 < y^{*} < -3.25$	0.797 ± 0.004
$5 < p_{\mathrm{T}} < 6$	$-5.00 < y^{*} < -4.00$	0.783 ± 0.005
$6 < p_{\mathrm{T}} < 7$	$-3.25 < y^{*} < -2.50$	0.794 ± 0.007
$6 < p_{\mathrm{T}} < 7$	$-4.00 < y^{*} < -3.25$	0.803 ± 0.006
$6 < p_{\mathrm{T}} < 7$	$-5.00 < y^{*} < -4.00$	0.792 ± 0.008
$7 < p_{\mathrm{T}} < 8$	$-3.25 < y^{*} < -2.50$	0.801 ± 0.009
$7 < p_{\mathrm{T}} < 8$	$-4.00 < y^{*} < -3.25$	0.824 ± 0.009
$7 < p_{\mathrm{T}} < 8$	$-5.00 < y^{*} < -4.00$	0.825 ± 0.011
$8 < p_{\mathrm{T}} < 10$	$-3.25 < y^{*} < -2.50$	0.830 ± 0.010
$8 < p_{\mathrm{T}} < 10$	$-4.00 < y^{*} < -3.25$	0.837 ± 0.009
$8 < p_{\mathrm{T}} < 10$	$-5.00 < y^{*} < -4.00$	0.850 ± 0.012
$10 < p_{\mathrm{T}} < 14$	$-3.25 < y^{*} < -2.50$	0.873 ± 0.012
$10 < p_{\mathrm{T}} < 14$	$-4.00 < y^{*} < -3.25$	0.860 ± 0.014
$10 < p_{\mathrm{T}} < 14$	$-5.00 < y^{*} < -4.00$	0.865 ± 0.019

Table 21: Selection efficiencies $\psi(2S)$ in pPb, in bins of p_T and y^*. The uncertainties are statistical.

p_T bin	y^* bin	ϵ_{sel}
$0 < p_T < 1$	$1.50 < y^* < 2.50$	0.867 ± 0.003
$0 < p_T < 1$	$2.50 < y^* < 3.25$	0.835 ± 0.002
$0 < p_T < 1$	$3.25 < y^* < 4.00$	0.836 ± 0.003
$1 < p_T < 2$	$1.50 < y^* < 2.50$	0.833 ± 0.002
$1 < p_T < 2$	$2.50 < y^* < 3.25$	0.802 ± 0.002
$1 < p_T < 2$	$3.25 < y^* < 4.00$	0.805 ± 0.002
$2 < p_T < 3$	$1.50 < y^* < 2.50$	0.757 ± 0.002
$2 < p_T < 3$	$2.50 < y^* < 3.25$	0.746 ± 0.002
$2 < p_T < 3$	$3.25 < y^* < 4.00$	0.732 ± 0.002
$3 < p_T < 4$	$1.50 < y^* < 2.50$	0.661 ± 0.002
$3 < p_T < 4$	$2.50 < y^* < 3.25$	0.697 ± 0.002
$3 < p_T < 4$	$3.25 < y^* < 4.00$	0.672 ± 0.003
$4 < p_T < 5$	$1.50 < y^* < 2.50$	0.665 ± 0.003
$4 < p_T < 5$	$2.50 < y^* < 3.25$	0.704 ± 0.003
$4 < p_T < 5$	$3.25 < y^* < 4.00$	0.685 ± 0.003
$5 < p_T < 6$	$1.50 < y^* < 2.50$	0.689 ± 0.004
$5 < p_T < 6$	$2.50 < y^* < 3.25$	0.723 ± 0.004
$5 < p_T < 6$	$3.25 < y^* < 4.00$	0.718 ± 0.005
$6 < p_T < 7$	$1.50 < y^* < 2.50$	0.720 ± 0.005
$6 < p_T < 7$	$2.50 < y^* < 3.25$	0.738 ± 0.005
$6 < p_T < 7$	$3.25 < y^* < 4.00$	0.730 ± 0.006
$7 < p_T < 8$	$1.50 < y^* < 2.50$	0.731 ± 0.007
$7 < p_T < 8$	$2.50 < y^* < 3.25$	0.759 ± 0.007
$7 < p_T < 8$	$3.25 < y^* < 4.00$	0.758 ± 0.008
$8 < p_T < 10$	$1.50 < y^* < 2.50$	0.763 ± 0.007
$8 < p_T < 10$	$2.50 < y^* < 3.25$	0.769 ± 0.007
$8 < p_T < 10$	$3.25 < y^* < 4.00$	0.775 ± 0.009
$10 < p_T < 14$	$1.50 < y^* < 2.50$	0.784 ± 0.008
$10 < p_T < 14$	$2.50 < y^* < 3.25$	0.797 ± 0.009
$10 < p_T < 14$	$3.25 < y^* < 4.00$	0.800 ± 0.012

Table 22: Selection efficiencies $\psi(2S)$ in Pbp, in bins of p_T and y^*. The uncertainties are statistical.

p_T bin	y^* bin	ϵ_{sel}
$0 < p_T < 1$	$-3.25 < y^* < -2.50$	0.872 ± 0.003
$0 < p_T < 1$	$-4.00 < y^* < -3.25$	0.842 ± 0.002
$0 < p_T < 1$	$-5.00 < y^* < -4.00$	0.835 ± 0.003
$1 < p_T < 2$	$-3.25 < y^* < -2.50$	0.845 ± 0.002
$1 < p_T < 2$	$-4.00 < y^* < -3.25$	0.802 ± 0.002
$1 < p_T < 2$	$-5.00 < y^* < -4.00$	0.806 ± 0.002
$2 < p_T < 3$	$-3.25 < y^* < -2.50$	0.762 ± 0.002
$2 < p_T < 3$	$-4.00 < y^* < -3.25$	0.745 ± 0.002
$2 < p_T < 3$	$-5.00 < y^* < -4.00$	0.738 ± 0.002
$3 < p_T < 4$	$-3.25 < y^* < -2.50$	0.653 ± 0.003
$3 < p_T < 4$	$-4.00 < y^* < -3.25$	0.695 ± 0.002
$3 < p_T < 4$	$-5.00 < y^* < -4.00$	0.681 ± 0.002
$4 < p_T < 5$	$-3.25 < y^* < -2.50$	0.652 ± 0.004
$4 < p_T < 5$	$-4.00 < y^* < -3.25$	0.707 ± 0.003
$4 < p_T < 5$	$-5.00 < y^* < -4.00$	0.690 ± 0.003
$5 < p_T < 6$	$-3.25 < y^* < -2.50$	0.681 ± 0.005
$5 < p_T < 6$	$-4.00 < y^* < -3.25$	0.722 ± 0.004
$5 < p_T < 6$	$-5.00 < y^* < -4.00$	0.719 ± 0.004
$6 < p_T < 7$	$-3.25 < y^* < -2.50$	0.706 ± 0.006
$6 < p_T < 7$	$-4.00 < y^* < -3.25$	0.746 ± 0.005
$6 < p_T < 7$	$-5.00 < y^* < -4.00$	0.733 ± 0.005
$7 < p_T < 8$	$-3.25 < y^* < -2.50$	0.720 ± 0.008
$7 < p_T < 8$	$-4.00 < y^* < -3.25$	0.765 ± 0.007
$7 < p_T < 8$	$-5.00 < y^* < -4.00$	0.756 ± 0.007
$8 < p_T < 10$	$-3.25 < y^* < -2.50$	0.751 ± 0.008
$8 < p_T < 10$	$-4.00 < y^* < -3.25$	0.783 ± 0.007
$8 < p_T < 10$	$-5.00 < y^* < -4.00$	0.767 ± 0.008
$10 < p_T < 14$	$-3.25 < y^* < -2.50$	0.782 ± 0.010
$10 < p_T < 14$	$-4.00 < y^* < -3.25$	0.789 ± 0.009
$10 < p_T < 14$	$-5.00 < y^* < -4.00$	0.800 ± 0.010

Table 23: $\psi(2S)$ over J/ψ selection efficiency ratios in pPb, in bins of p_{T} and y^* with total uncertainties.

p_{T} bin	y^* bin	$\epsilon_{\mathrm{sel}}^{\psi(2S)}/\epsilon_{\mathrm{sel}}^{J/\psi}$
$0 < p_{\mathrm{T}} < 1$	$1.50 < y^* < 2.50$	0.948 ± 0.003
$0 < p_{\mathrm{T}} < 1$	$2.50 < y^* < 3.25$	0.942 ± 0.003
$0 < p_{\mathrm{T}} < 1$	$3.25 < y^* < 4.00$	0.936 ± 0.004
$1 < p_{\mathrm{T}} < 2$	$1.50 < y^* < 2.50$	0.963 ± 0.003
$1 < p_{\mathrm{T}} < 2$	$2.50 < y^* < 3.25$	0.956 ± 0.002
$1 < p_{\mathrm{T}} < 2$	$3.25 < y^* < 4.00$	0.962 ± 0.003
$2 < p_{\mathrm{T}} < 3$	$1.50 < y^* < 2.50$	1.012 ± 0.004
$2 < p_{\mathrm{T}} < 3$	$2.50 < y^* < 3.25$	0.978 ± 0.003
$2 < p_{\mathrm{T}} < 3$	$3.25 < y^* < 4.00$	0.988 ± 0.004
$3 < p_{\mathrm{T}} < 4$	$1.50 < y^* < 2.50$	0.946 ± 0.005
$3 < p_{\mathrm{T}} < 4$	$2.50 < y^* < 3.25$	0.939 ± 0.004
$3 < p_{\mathrm{T}} < 4$	$3.25 < y^* < 4.00$	0.929 ± 0.005
$4 < p_{\mathrm{T}} < 5$	$1.50 < y^* < 2.50$	0.915 ± 0.005
$4 < p_{\mathrm{T}} < 5$	$2.50 < y^* < 3.25$	0.919 ± 0.005
$4 < p_{\mathrm{T}} < 5$	$3.25 < y^* < 4.00$	0.910 ± 0.006
$5 < p_{\mathrm{T}} < 6$	$1.50 < y^* < 2.50$	0.910 ± 0.007
$5 < p_{\mathrm{T}} < 6$	$2.50 < y^* < 3.25$	0.918 ± 0.006
$5 < p_{\mathrm{T}} < 6$	$3.25 < y^* < 4.00$	0.915 ± 0.007
$6 < p_{\mathrm{T}} < 7$	$1.50 < y^* < 2.50$	0.913 ± 0.008
$6 < p_{\mathrm{T}} < 7$	$2.50 < y^* < 3.25$	0.917 ± 0.008
$6 < p_{\mathrm{T}} < 7$	$3.25 < y^* < 4.00$	0.909 ± 0.010
$7 < p_{\mathrm{T}} < 8$	$1.50 < y^* < 2.50$	0.907 ± 0.010
$7 < p_{\mathrm{T}} < 8$	$2.50 < y^* < 3.25$	0.932 ± 0.010
$7 < p_{\mathrm{T}} < 8$	$3.25 < y^* < 4.00$	0.930 ± 0.013
$8 < p_{\mathrm{T}} < 10$	$1.50 < y^* < 2.50$	0.919 ± 0.009
$8 < p_{\mathrm{T}} < 10$	$2.50 < y^* < 3.25$	0.915 ± 0.010
$8 < p_{\mathrm{T}} < 10$	$3.25 < y^* < 4.00$	0.938 ± 0.013
$10 < p_{\mathrm{T}} < 14$	$1.50 < y^* < 2.50$	0.909 ± 0.012
$10 < p_{\mathrm{T}} < 14$	$2.50 < y^* < 3.25$	0.935 ± 0.013
$10 < p_{\mathrm{T}} < 14$	$3.25 < y^* < 4.00$	0.911 ± 0.016

Table 24: $\psi(2S)$ over J/ψ selection efficiency ratios in Pbp, in bins of p_{T} and y^* with total uncertainties.

p_{T} bin	y^* bin	$\epsilon_{\mathrm{sel}}^{\psi(2S)}/\epsilon_{\mathrm{sel}}^{J/\psi}$
$0 < p_{\mathrm{T}} < 1$	$-3.25 < y^* < -2.50$	0.953 ± 0.004
$0 < p_{\mathrm{T}} < 1$	$-4.00 < y^* < -3.25$	0.950 ± 0.004
$0 < p_{\mathrm{T}} < 1$	$-5.00 < y^* < -4.00$	0.952 ± 0.004
$1 < p_{\mathrm{T}} < 2$	$-3.25 < y^* < -2.50$	0.973 ± 0.003
$1 < p_{\mathrm{T}} < 2$	$-4.00 < y^* < -3.25$	0.963 ± 0.003
$1 < p_{\mathrm{T}} < 2$	$-5.00 < y^* < -4.00$	0.970 ± 0.003
$2 < p_{\mathrm{T}} < 3$	$-3.25 < y^* < -2.50$	1.029 ± 0.005
$2 < p_{\mathrm{T}} < 3$	$-4.00 < y^* < -3.25$	0.978 ± 0.003
$2 < p_{\mathrm{T}} < 3$	$-5.00 < y^* < -4.00$	0.987 ± 0.004
$3 < p_{\mathrm{T}} < 4$	$-3.25 < y^* < -2.50$	0.954 ± 0.006
$3 < p_{\mathrm{T}} < 4$	$-4.00 < y^* < -3.25$	0.939 ± 0.004
$3 < p_{\mathrm{T}} < 4$	$-5.00 < y^* < -4.00$	0.934 ± 0.005
$4 < p_{\mathrm{T}} < 5$	$-3.25 < y^* < -2.50$	0.917 ± 0.007
$4 < p_{\mathrm{T}} < 5$	$-4.00 < y^* < -3.25$	0.918 ± 0.005
$4 < p_{\mathrm{T}} < 5$	$-5.00 < y^* < -4.00$	0.912 ± 0.006
$5 < p_{\mathrm{T}} < 6$	$-3.25 < y^* < -2.50$	0.914 ± 0.009
$5 < p_{\mathrm{T}} < 6$	$-4.00 < y^* < -3.25$	0.902 ± 0.007
$5 < p_{\mathrm{T}} < 6$	$-5.00 < y^* < -4.00$	0.917 ± 0.008
$6 < p_{\mathrm{T}} < 7$	$-3.25 < y^* < -2.50$	0.886 ± 0.011
$6 < p_{\mathrm{T}} < 7$	$-4.00 < y^* < -3.25$	0.926 ± 0.009
$6 < p_{\mathrm{T}} < 7$	$-5.00 < y^* < -4.00$	0.924 ± 0.011
$7 < p_{\mathrm{T}} < 8$	$-3.25 < y^* < -2.50$	0.895 ± 0.014
$7 < p_{\mathrm{T}} < 8$	$-4.00 < y^* < -3.25$	0.926 ± 0.012
$7 < p_{\mathrm{T}} < 8$	$-5.00 < y^* < -4.00$	0.915 ± 0.015
$8 < p_{\mathrm{T}} < 10$	$-3.25 < y^* < -2.50$	0.902 ± 0.014
$8 < p_{\mathrm{T}} < 10$	$-4.00 < y^* < -3.25$	0.933 ± 0.013
$8 < p_{\mathrm{T}} < 10$	$-5.00 < y^* < -4.00$	0.900 ± 0.016
$10 < p_{\mathrm{T}} < 14$	$-3.25 < y^* < -2.50$	0.895 ± 0.016
$10 < p_{\mathrm{T}} < 14$	$-4.00 < y^* < -3.25$	0.914 ± 0.018
$10 < p_{\mathrm{T}} < 14$	$-5.00 < y^* < -4.00$	0.922 ± 0.023

6.4 PID efficiency

The PID efficiency is defined as

$$\epsilon_{\rm PID}(p_{\rm T}, y^*) = \frac{J/\psi \text{or } \psi(2S) \text{ satisfying the PID selection in bin } (p_{\rm T}, y^*)}{J/\psi \text{ or } \psi(2S) \text{ selected in bin } (p_{\rm T}, y^*)}. \tag{20}$$

The PID efficiency for muons is taken from data using calibration tables (PIDCalib tables) obtained from control samples, namely J/ψ candidates with one of the two muon identified with tight criteria and the other one not identified. These calibration tables give the efficiency of the PID selections as a function of the pseudo-rapidity, of the total momentum of the muon tracks and of the track multiplicity of the event estimated from the number of hits in the SPD. They are available for the pp, pPb and Pbp data taking, however the pPb and Pbp tables have large statistical uncertainties. In this analysis, the pp tables are used, but re-weighted as a function of the SPD multiplicity to take into account the differences in multiplicities between pp, pPb and Pbp. The efficiencies obtained this way are more precise and compatible with the efficiencies measured with the calibration samples in pPb and Pbp as can be seen in Figs. 24 (25) for the loose (tight) selection and in Fig. 26 which gives the efficiencies as a function of the momentum and pseudo-rapidity of the muon of the IsMuon and of the ProbNN(μ) > 0.5 (ProbNN(μ) > 0.8) requirements.

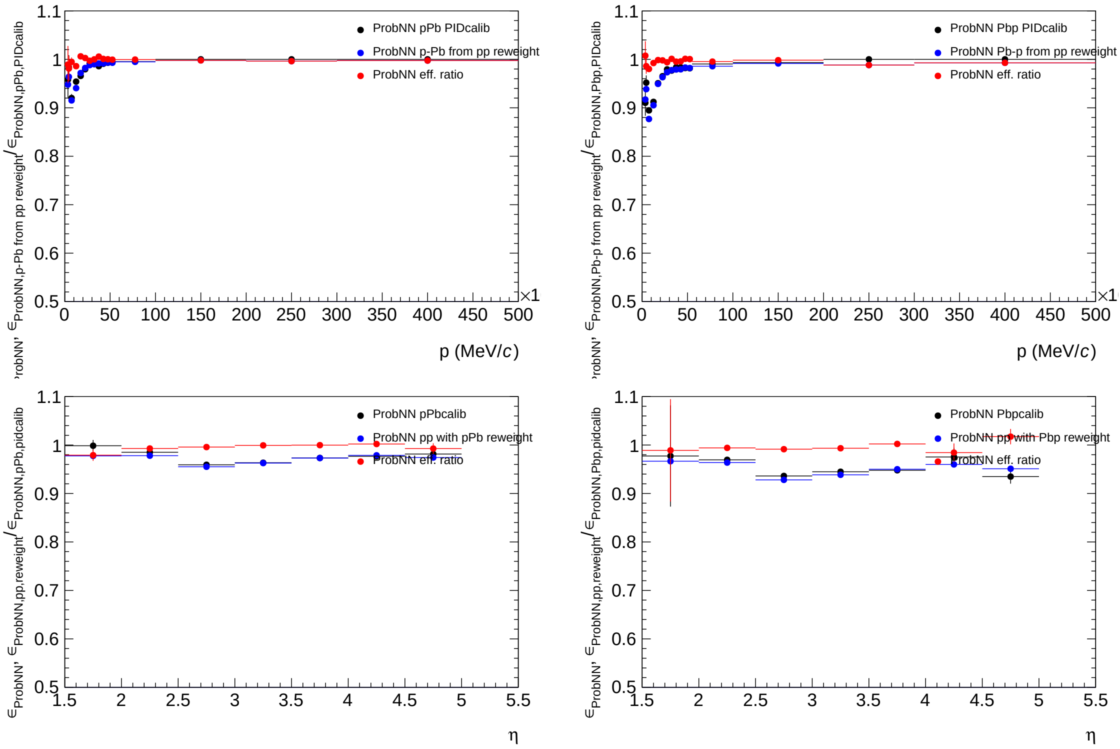

Figure 24: Muon PID efficiency obtained from the pp calibration tables reweighted with the pPb/Pbp multiplicity (blue), from the pPb/Pbp calibration tables (black) and their ratios (red), for the ProbNN(μ) > 0.5 selection as a function of the muon momentum top left: pPb, top right Pbp, as a function of the muon η bottom left: pPb, bottom right: Pbp.

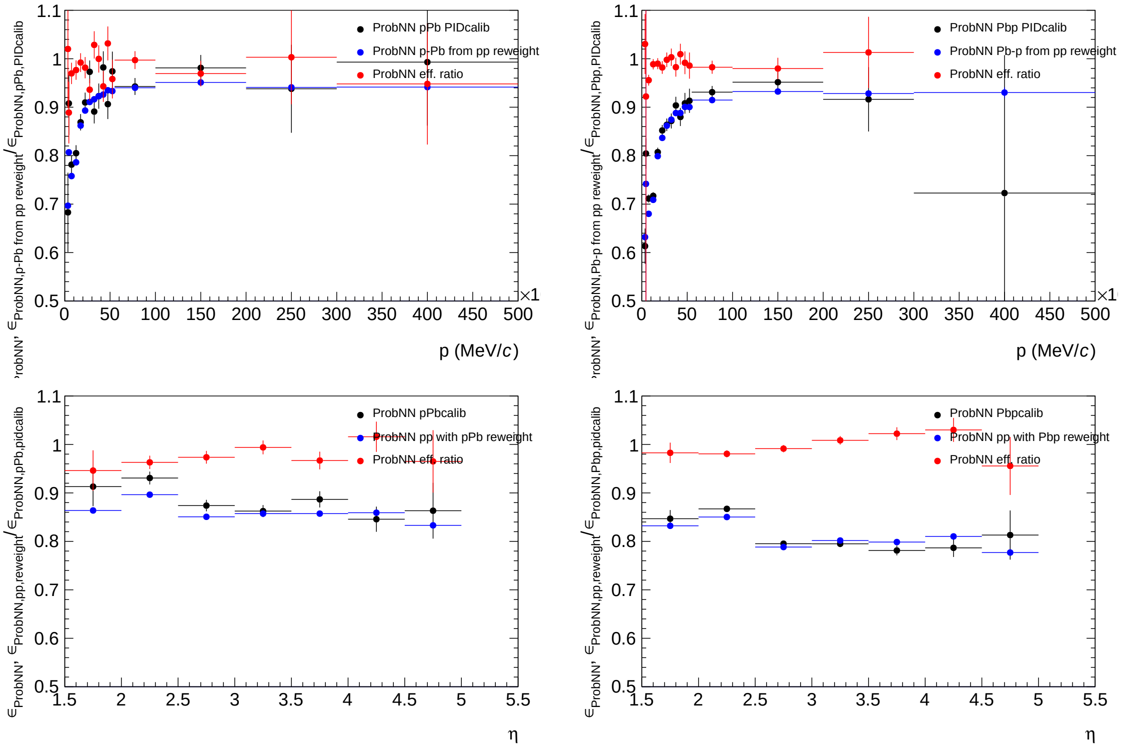

Figure 25: Muon PID efficiency obtained from the pp calibration tables reweighted with the pPb/Pbp multiplicity (blue), from the pPb/Pbp calibration tables (black) and their ratios (red), for the ProbNN(μ) > 0.8 selection as a function of the muon momentum top left: pPb, top right Pbp, as a function of the muon η bottom left: pPb, bottom right: Pbp.

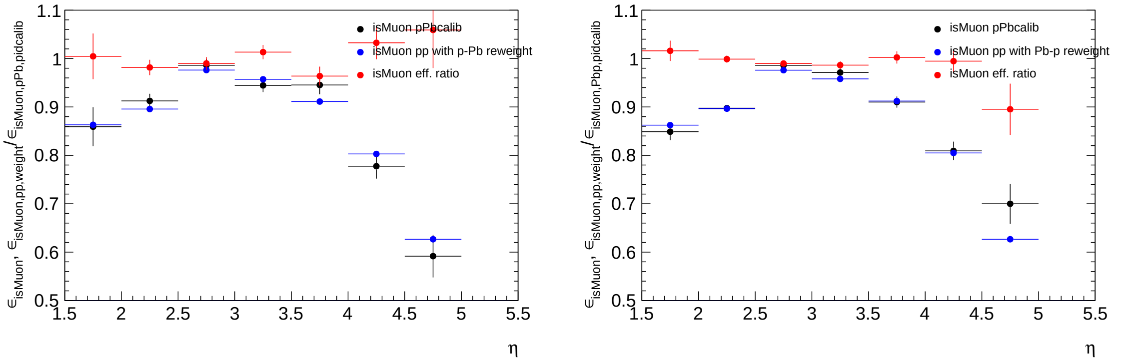

Figure 26: Muon PID efficiency obtained from the pp calibration tables re-weighted with the pPb/Pbp multiplicity (blue), from the pPb/Pbp calibration tables (black) and their ratios (red), for the isMuon selection as a function of the muon η in left: pPb, right Pbp.

The SPD multiplicity in Pbp events can be larger than the maximum seen in pp collisions, and can exceed the maximum multiplicity of the pp tables. This can be seen in Fig. 27 where the muon ID efficiency from the pp, pPb and Pbp tables is shown as a function of the SPD multiplicity, integrated over p and η. In the bins $1000 < \text{SPD} < 1200$

and $1200 < \mathrm{SPD} < 1400$, where there is no measurement of the PID efficiency in pp, the pp efficiencies of the bin $800 < \mathrm{SPD} < 1000$ are used, scaled by the ratio of the efficiencies obtained in Pbp in these bins.

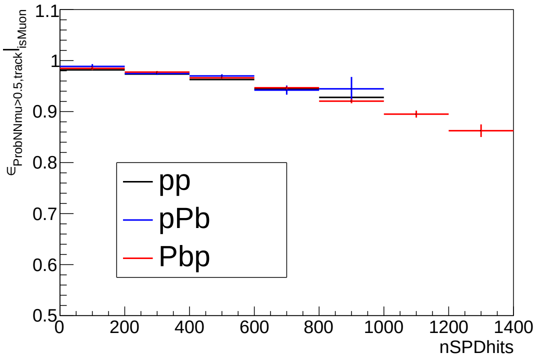

Figure 27: Particle identification efficiency measured in data for black: pp, blue: pPb and red: Pbp for muons, as a function of the SPD multiplicity, integrated over p and η.

The efficiencies ϵ_{PID} as a function of the J/ψ kinematic variables are obtained re-weighting the simulation samples with weights equal to the efficiencies measured in data for each muon track, as a function of its kinematic variables. These efficiencies are shown in Fig. 28 for the loose selection and in Fig. 29 for the tight selection for the J/ψ. The efficiency for the tight selection for the $\psi(2S)$ is shown in Fig. 30. The error bars in these figures are the total uncertainties, described in detail in Sect. 7.7. The ratio of the efficiencies between J/ψ and $\psi(2S)$ for the tight selection is shown in Fig. 31. The uncertainty on the efficiency ratio does include all uncertainties except of the statistical uncertainty due to the finite simulation sample. Tables 25 and 26 for the tight selection and J/ψ, 29 and 30 for the loose selection, 27 and 28 for the tight selection and $\psi(2S)$ give the corresponding numerical values.

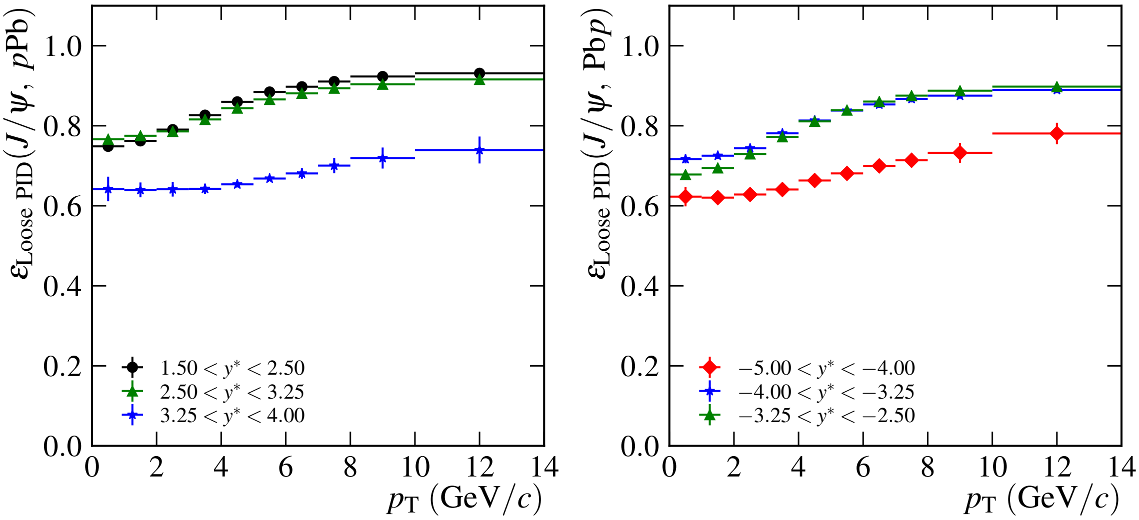

Figure 28: Particle identification efficiency $\epsilon_{\text{loosePID}}$ as a function of p_{T} in different y^* bins for left: J/ψ in pPb, right: J/ψ in Pbp. The displayed uncertainty corresponds to the total uncertainty.

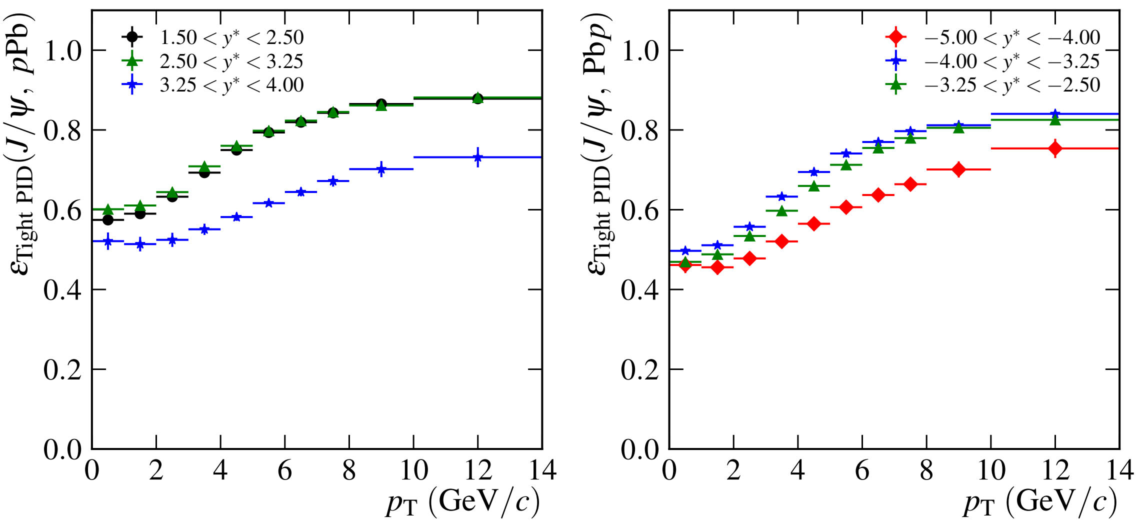

Figure 29: Particle identification efficiency $\epsilon_{\text{tightPID}}$ as a function of p_{T} in different y^* bins for left: J/ψ in pPb, right: J/ψ in Pbp. The displayed uncertainty corresponds to the total uncertainty.

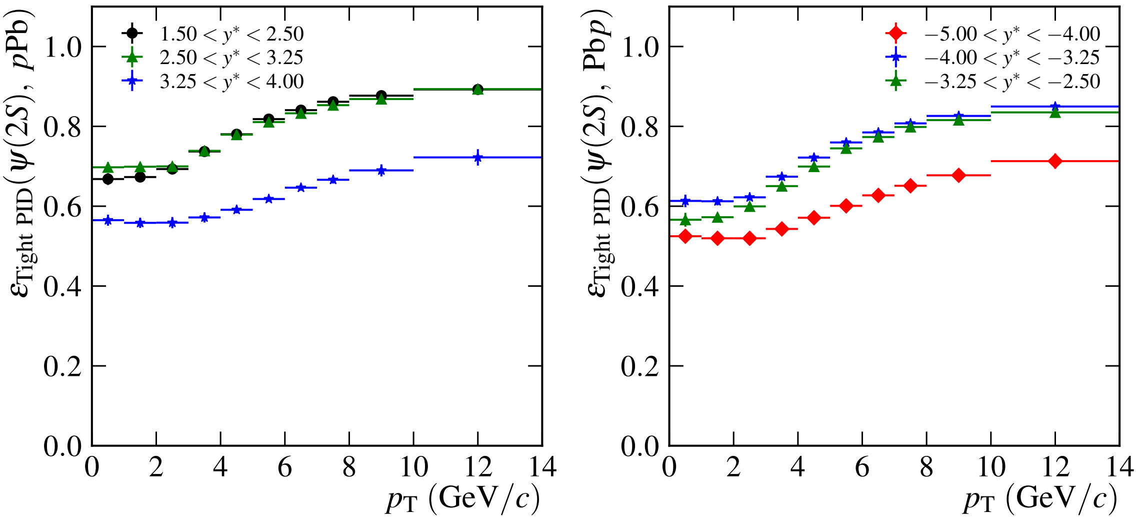

Figure 30: Particle identification efficiency ϵ_{PID} as a function of p_{T} in different y^* bins for left: $\psi(2S)$ in pPb, right: $\psi(2S)$ in Pbp. The displayed uncertainty corresponds to the total uncertainty.

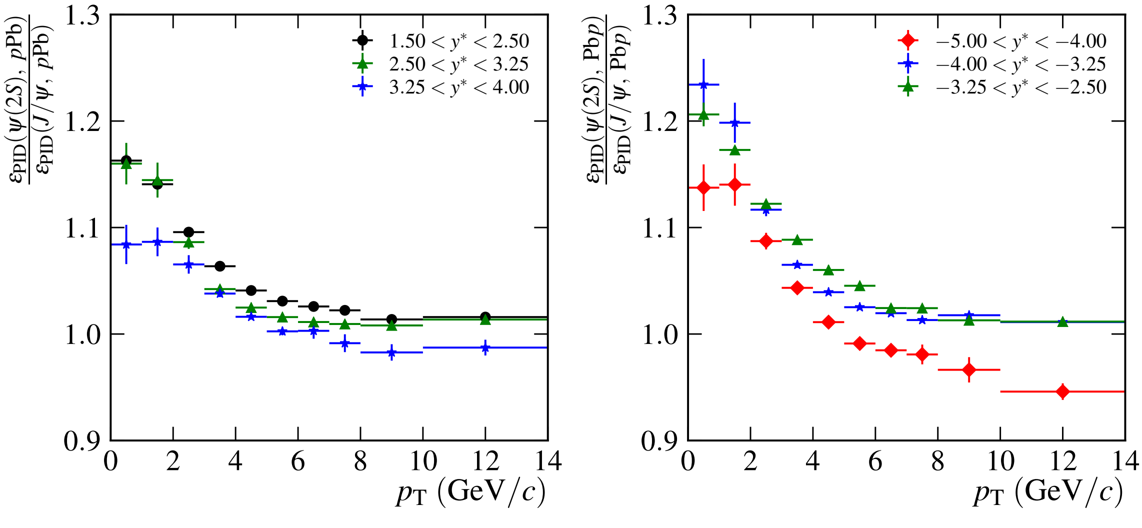

Figure 31: Particle identification efficiency ratio $\epsilon_{\text{PID}}^{\psi(2S)}/\epsilon_{\text{PID}}^{J/\psi}$ as a function of p_{T} and y^* bins for left: pPb, right: Pbp. The displayed uncertainty corresponds to the total uncertainty.

Table 25: PID efficiencies J/ψ in pPb, in bins of p_{T} and y^* for the tight selection. The uncertainties are the total uncertainties for PID.

p_{T} bin	y^* bin	ϵ_{PID}
$0 < p_{\mathrm{T}} < 1$	$1.50 < y^* < 2.50$	0.574 ± 0.010
$0 < p_{\mathrm{T}} < 1$	$2.50 < y^* < 3.25$	0.601 ± 0.004
$0 < p_{\mathrm{T}} < 1$	$3.25 < y^* < 4.00$	0.521 ± 0.022
$1 < p_{\mathrm{T}} < 2$	$1.50 < y^* < 2.50$	0.590 ± 0.007
$1 < p_{\mathrm{T}} < 2$	$2.50 < y^* < 3.25$	0.611 ± 0.005
$1 < p_{\mathrm{T}} < 2$	$3.25 < y^* < 4.00$	0.514 ± 0.018
$2 < p_{\mathrm{T}} < 3$	$1.50 < y^* < 2.50$	0.633 ± 0.004
$2 < p_{\mathrm{T}} < 3$	$2.50 < y^* < 3.25$	0.644 ± 0.005
$2 < p_{\mathrm{T}} < 3$	$3.25 < y^* < 4.00$	0.524 ± 0.018
$3 < p_{\mathrm{T}} < 4$	$1.50 < y^* < 2.50$	0.693 ± 0.003
$3 < p_{\mathrm{T}} < 4$	$2.50 < y^* < 3.25$	0.709 ± 0.006
$3 < p_{\mathrm{T}} < 4$	$3.25 < y^* < 4.00$	0.551 ± 0.014
$4 < p_{\mathrm{T}} < 5$	$1.50 < y^* < 2.50$	0.750 ± 0.003
$4 < p_{\mathrm{T}} < 5$	$2.50 < y^* < 3.25$	0.760 ± 0.007
$4 < p_{\mathrm{T}} < 5$	$3.25 < y^* < 4.00$	0.582 ± 0.009
$5 < p_{\mathrm{T}} < 6$	$1.50 < y^* < 2.50$	0.794 ± 0.003
$5 < p_{\mathrm{T}} < 6$	$2.50 < y^* < 3.25$	0.798 ± 0.007
$5 < p_{\mathrm{T}} < 6$	$3.25 < y^* < 4.00$	0.616 ± 0.005
$6 < p_{\mathrm{T}} < 7$	$1.50 < y^* < 2.50$	0.819 ± 0.004
$6 < p_{\mathrm{T}} < 7$	$2.50 < y^* < 3.25$	0.823 ± 0.007
$6 < p_{\mathrm{T}} < 7$	$3.25 < y^* < 4.00$	0.644 ± 0.011
$7 < p_{\mathrm{T}} < 8$	$1.50 < y^* < 2.50$	0.843 ± 0.004
$7 < p_{\mathrm{T}} < 8$	$2.50 < y^* < 3.25$	0.845 ± 0.007
$7 < p_{\mathrm{T}} < 8$	$3.25 < y^* < 4.00$	0.672 ± 0.014
$8 < p_{\mathrm{T}} < 10$	$1.50 < y^* < 2.50$	0.865 ± 0.004
$8 < p_{\mathrm{T}} < 10$	$2.50 < y^* < 3.25$	0.861 ± 0.007
$8 < p_{\mathrm{T}} < 10$	$3.25 < y^* < 4.00$	0.702 ± 0.020
$10 < p_{\mathrm{T}} < 14$	$1.50 < y^* < 2.50$	0.878 ± 0.005
$10 < p_{\mathrm{T}} < 14$	$2.50 < y^* < 3.25$	0.881 ± 0.006
$10 < p_{\mathrm{T}} < 14$	$3.25 < y^* < 4.00$	0.732 ± 0.025

Table 26: PID efficiencies J/ψ in Pbp, in bins of p_{T} and y^* for the tight selection. The uncertainties are the total uncertainties.

p_{T} bin	y^* bin	ϵ_{PID}
$0 < p_{\mathrm{T}} < 1$	$-3.25 < y^* < -2.50$	0.469 ± 0.010
$0 < p_{\mathrm{T}} < 1$	$-4.00 < y^* < -3.25$	0.497 ± 0.006
$0 < p_{\mathrm{T}} < 1$	$-5.00 < y^* < -4.00$	0.461 ± 0.020
$1 < p_{\mathrm{T}} < 2$	$-3.25 < y^* < -2.50$	0.488 ± 0.009
$1 < p_{\mathrm{T}} < 2$	$-4.00 < y^* < -3.25$	0.511 ± 0.006
$1 < p_{\mathrm{T}} < 2$	$-5.00 < y^* < -4.00$	0.456 ± 0.019
$2 < p_{\mathrm{T}} < 3$	$-3.25 < y^* < -2.50$	0.534 ± 0.006
$2 < p_{\mathrm{T}} < 3$	$-4.00 < y^* < -3.25$	0.557 ± 0.007
$2 < p_{\mathrm{T}} < 3$	$-5.00 < y^* < -4.00$	0.478 ± 0.016
$3 < p_{\mathrm{T}} < 4$	$-3.25 < y^* < -2.50$	0.597 ± 0.005
$3 < p_{\mathrm{T}} < 4$	$-4.00 < y^* < -3.25$	0.633 ± 0.008
$3 < p_{\mathrm{T}} < 4$	$-5.00 < y^* < -4.00$	0.520 ± 0.013
$4 < p_{\mathrm{T}} < 5$	$-3.25 < y^* < -2.50$	0.660 ± 0.005
$4 < p_{\mathrm{T}} < 5$	$-4.00 < y^* < -3.25$	0.695 ± 0.010
$4 < p_{\mathrm{T}} < 5$	$-5.00 < y^* < -4.00$	0.565 ± 0.010
$5 < p_{\mathrm{T}} < 6$	$-3.25 < y^* < -2.50$	0.713 ± 0.005
$5 < p_{\mathrm{T}} < 6$	$-4.00 < y^* < -3.25$	0.741 ± 0.010
$5 < p_{\mathrm{T}} < 6$	$-5.00 < y^* < -4.00$	0.606 ± 0.008
$6 < p_{\mathrm{T}} < 7$	$-3.25 < y^* < -2.50$	0.755 ± 0.006
$6 < p_{\mathrm{T}} < 7$	$-4.00 < y^* < -3.25$	0.770 ± 0.010
$6 < p_{\mathrm{T}} < 7$	$-5.00 < y^* < -4.00$	0.637 ± 0.009
$7 < p_{\mathrm{T}} < 8$	$-3.25 < y^* < -2.50$	0.779 ± 0.007
$7 < p_{\mathrm{T}} < 8$	$-4.00 < y^* < -3.25$	0.797 ± 0.009
$7 < p_{\mathrm{T}} < 8$	$-5.00 < y^* < -4.00$	0.664 ± 0.014
$8 < p_{\mathrm{T}} < 10$	$-3.25 < y^* < -2.50$	0.805 ± 0.008
$8 < p_{\mathrm{T}} < 10$	$-4.00 < y^* < -3.25$	0.812 ± 0.009
$8 < p_{\mathrm{T}} < 10$	$-5.00 < y^* < -4.00$	0.701 ± 0.020
$10 < p_{\mathrm{T}} < 14$	$-3.25 < y^* < -2.50$	0.825 ± 0.010
$10 < p_{\mathrm{T}} < 14$	$-4.00 < y^* < -3.25$	0.840 ± 0.009
$10 < p_{\mathrm{T}} < 14$	$-5.00 < y^* < -4.00$	0.754 ± 0.024

Table 27: PID efficiencies $\psi(2S)$ in pPb, in bins of p_T and y^* for the tight selection. The uncertainties are the total uncertainties.

p_T bin	y^* bin	ϵ_{PID}
$0 < p_T < 1$	$1.50 < y^* < 2.50$	0.668 ± 0.015
$0 < p_T < 1$	$2.50 < y^* < 3.25$	0.697 ± 0.013
$0 < p_T < 1$	$3.25 < y^* < 4.00$	0.565 ± 0.014
$1 < p_T < 2$	$1.50 < y^* < 2.50$	0.673 ± 0.008
$1 < p_T < 2$	$2.50 < y^* < 3.25$	0.699 ± 0.008
$1 < p_T < 2$	$3.25 < y^* < 4.00$	0.558 ± 0.013
$2 < p_T < 3$	$1.50 < y^* < 2.50$	0.693 ± 0.004
$2 < p_T < 3$	$2.50 < y^* < 3.25$	0.700 ± 0.005
$2 < p_T < 3$	$3.25 < y^* < 4.00$	0.559 ± 0.014
$3 < p_T < 4$	$1.50 < y^* < 2.50$	0.737 ± 0.003
$3 < p_T < 4$	$2.50 < y^* < 3.25$	0.739 ± 0.007
$3 < p_T < 4$	$3.25 < y^* < 4.00$	0.572 ± 0.013
$4 < p_T < 5$	$1.50 < y^* < 2.50$	0.780 ± 0.004
$4 < p_T < 5$	$2.50 < y^* < 3.25$	0.779 ± 0.009
$4 < p_T < 5$	$3.25 < y^* < 4.00$	0.591 ± 0.009
$5 < p_T < 6$	$1.50 < y^* < 2.50$	0.818 ± 0.003
$5 < p_T < 6$	$2.50 < y^* < 3.25$	0.811 ± 0.009
$5 < p_T < 6$	$3.25 < y^* < 4.00$	0.618 ± 0.005
$6 < p_T < 7$	$1.50 < y^* < 2.50$	0.841 ± 0.004
$6 < p_T < 7$	$2.50 < y^* < 3.25$	0.833 ± 0.009
$6 < p_T < 7$	$3.25 < y^* < 4.00$	0.646 ± 0.007
$7 < p_T < 8$	$1.50 < y^* < 2.50$	0.862 ± 0.004
$7 < p_T < 8$	$2.50 < y^* < 3.25$	0.853 ± 0.008
$7 < p_T < 8$	$3.25 < y^* < 4.00$	0.666 ± 0.009
$8 < p_T < 10$	$1.50 < y^* < 2.50$	0.877 ± 0.004
$8 < p_T < 10$	$2.50 < y^* < 3.25$	0.868 ± 0.008
$8 < p_T < 10$	$3.25 < y^* < 4.00$	0.690 ± 0.015
$10 < p_T < 14$	$1.50 < y^* < 2.50$	0.892 ± 0.005
$10 < p_T < 14$	$2.50 < y^* < 3.25$	0.893 ± 0.009
$10 < p_T < 14$	$3.25 < y^* < 4.00$	0.722 ± 0.021

Table 28: PID efficiencies $\psi(2S)$ in Pbp, in bins of p_T and y^* for the tight selection. The uncertainties are the total uncertainties.

p_T bin	y^* bin	ϵ_{PID}
$0 < p_T < 1$	$-3.25 < y^* < -2.50$	0.566 ± 0.017
$0 < p_T < 1$	$-4.00 < y^* < -3.25$	0.613 ± 0.016
$0 < p_T < 1$	$-5.00 < y^* < -4.00$	0.525 ± 0.013
$1 < p_T < 2$	$-3.25 < y^* < -2.50$	0.572 ± 0.009
$1 < p_T < 2$	$-4.00 < y^* < -3.25$	0.612 ± 0.010
$1 < p_T < 2$	$-5.00 < y^* < -4.00$	0.520 ± 0.013
$2 < p_T < 3$	$-3.25 < y^* < -2.50$	0.599 ± 0.006
$2 < p_T < 3$	$-4.00 < y^* < -3.25$	0.622 ± 0.008
$2 < p_T < 3$	$-5.00 < y^* < -4.00$	0.520 ± 0.014
$3 < p_T < 4$	$-3.25 < y^* < -2.50$	0.650 ± 0.005
$3 < p_T < 4$	$-4.00 < y^* < -3.25$	0.674 ± 0.009
$3 < p_T < 4$	$-5.00 < y^* < -4.00$	0.543 ± 0.012
$4 < p_T < 5$	$-3.25 < y^* < -2.50$	0.699 ± 0.005
$4 < p_T < 5$	$-4.00 < y^* < -3.25$	0.722 ± 0.010
$4 < p_T < 5$	$-5.00 < y^* < -4.00$	0.571 ± 0.010
$5 < p_T < 6$	$-3.25 < y^* < -2.50$	0.745 ± 0.005
$5 < p_T < 6$	$-4.00 < y^* < -3.25$	0.760 ± 0.010
$5 < p_T < 6$	$-5.00 < y^* < -4.00$	0.601 ± 0.008
$6 < p_T < 7$	$-3.25 < y^* < -2.50$	0.773 ± 0.006
$6 < p_T < 7$	$-4.00 < y^* < -3.25$	0.785 ± 0.010
$6 < p_T < 7$	$-5.00 < y^* < -4.00$	0.627 ± 0.009
$7 < p_T < 8$	$-3.25 < y^* < -2.50$	0.798 ± 0.007
$7 < p_T < 8$	$-4.00 < y^* < -3.25$	0.807 ± 0.009
$7 < p_T < 8$	$-5.00 < y^* < -4.00$	0.651 ± 0.010
$8 < p_T < 10$	$-3.25 < y^* < -2.50$	0.816 ± 0.008
$8 < p_T < 10$	$-4.00 < y^* < -3.25$	0.826 ± 0.009
$8 < p_T < 10$	$-5.00 < y^* < -4.00$	0.677 ± 0.014
$10 < p_T < 14$	$-3.25 < y^* < -2.50$	0.835 ± 0.009
$10 < p_T < 14$	$-4.00 < y^* < -3.25$	0.850 ± 0.009
$10 < p_T < 14$	$-5.00 < y^* < -4.00$	0.713 ± 0.019

Table 29: PID efficiencies J/ψ in pPb, in bins of p_{T} and y^* for the loose selection. The uncertainties are the total uncertainties.

p_{T} bin	y^* bin	$\epsilon_{\text{Loose PID}}$
$0 < p_{\mathrm{T}} < 1$	$1.50 < y^* < 2.50$	0.748 ± 0.008
$0 < p_{\mathrm{T}} < 1$	$2.50 < y^* < 3.25$	0.766 ± 0.004
$0 < p_{\mathrm{T}} < 1$	$3.25 < y^* < 4.00$	0.642 ± 0.031
$1 < p_{\mathrm{T}} < 2$	$1.50 < y^* < 2.50$	0.762 ± 0.006
$1 < p_{\mathrm{T}} < 2$	$2.50 < y^* < 3.25$	0.775 ± 0.004
$1 < p_{\mathrm{T}} < 2$	$3.25 < y^* < 4.00$	0.640 ± 0.019
$2 < p_{\mathrm{T}} < 3$	$1.50 < y^* < 2.50$	0.790 ± 0.004
$2 < p_{\mathrm{T}} < 3$	$2.50 < y^* < 3.25$	0.786 ± 0.004
$2 < p_{\mathrm{T}} < 3$	$3.25 < y^* < 4.00$	0.641 ± 0.018
$3 < p_{\mathrm{T}} < 4$	$1.50 < y^* < 2.50$	0.827 ± 0.005
$3 < p_{\mathrm{T}} < 4$	$2.50 < y^* < 3.25$	0.816 ± 0.006
$3 < p_{\mathrm{T}} < 4$	$3.25 < y^* < 4.00$	0.643 ± 0.013
$4 < p_{\mathrm{T}} < 5$	$1.50 < y^* < 2.50$	0.860 ± 0.006
$4 < p_{\mathrm{T}} < 5$	$2.50 < y^* < 3.25$	0.844 ± 0.007
$4 < p_{\mathrm{T}} < 5$	$3.25 < y^* < 4.00$	0.654 ± 0.008
$5 < p_{\mathrm{T}} < 6$	$1.50 < y^* < 2.50$	0.884 ± 0.005
$5 < p_{\mathrm{T}} < 6$	$2.50 < y^* < 3.25$	0.866 ± 0.007
$5 < p_{\mathrm{T}} < 6$	$3.25 < y^* < 4.00$	0.668 ± 0.005
$6 < p_{\mathrm{T}} < 7$	$1.50 < y^* < 2.50$	0.898 ± 0.004
$6 < p_{\mathrm{T}} < 7$	$2.50 < y^* < 3.25$	0.881 ± 0.007
$6 < p_{\mathrm{T}} < 7$	$3.25 < y^* < 4.00$	0.681 ± 0.013
$7 < p_{\mathrm{T}} < 8$	$1.50 < y^* < 2.50$	0.911 ± 0.004
$7 < p_{\mathrm{T}} < 8$	$2.50 < y^* < 3.25$	0.894 ± 0.006
$7 < p_{\mathrm{T}} < 8$	$3.25 < y^* < 4.00$	0.700 ± 0.019
$8 < p_{\mathrm{T}} < 10$	$1.50 < y^* < 2.50$	0.923 ± 0.004
$8 < p_{\mathrm{T}} < 10$	$2.50 < y^* < 3.25$	0.904 ± 0.006
$8 < p_{\mathrm{T}} < 10$	$3.25 < y^* < 4.00$	0.719 ± 0.026
$10 < p_{\mathrm{T}} < 14$	$1.50 < y^* < 2.50$	0.931 ± 0.004
$10 < p_{\mathrm{T}} < 14$	$2.50 < y^* < 3.25$	0.916 ± 0.005
$10 < p_{\mathrm{T}} < 14$	$3.25 < y^* < 4.00$	0.739 ± 0.034

Table 30: PID efficiencies J/ψ in Pbp, in bins of $p_{\rm T}$ and y^* for the loose selection. The uncertainties are the total uncertainties.

$p_{\rm T}$ bin	y^* bin	$\epsilon_{\rm Loose\ PID}$
$0 < p_{\rm T} < 1$	$-3.25 < y^* < -2.50$	0.678 ± 0.010
$0 < p_{\rm T} < 1$	$-4.00 < y^* < -3.25$	0.717 ± 0.011
$0 < p_{\rm T} < 1$	$-5.00 < y^* < -4.00$	0.623 ± 0.024
$1 < p_{\rm T} < 2$	$-3.25 < y^* < -2.50$	0.695 ± 0.009
$1 < p_{\rm T} < 2$	$-4.00 < y^* < -3.25$	0.725 ± 0.008
$1 < p_{\rm T} < 2$	$-5.00 < y^* < -4.00$	0.620 ± 0.015
$2 < p_{\rm T} < 3$	$-3.25 < y^* < -2.50$	0.730 ± 0.005
$2 < p_{\rm T} < 3$	$-4.00 < y^* < -3.25$	0.744 ± 0.008
$2 < p_{\rm T} < 3$	$-5.00 < y^* < -4.00$	0.628 ± 0.014
$3 < p_{\rm T} < 4$	$-3.25 < y^* < -2.50$	0.772 ± 0.005
$3 < p_{\rm T} < 4$	$-4.00 < y^* < -3.25$	0.781 ± 0.009
$3 < p_{\rm T} < 4$	$-5.00 < y^* < -4.00$	0.641 ± 0.010
$4 < p_{\rm T} < 5$	$-3.25 < y^* < -2.50$	0.811 ± 0.007
$4 < p_{\rm T} < 5$	$-4.00 < y^* < -3.25$	0.813 ± 0.010
$4 < p_{\rm T} < 5$	$-5.00 < y^* < -4.00$	0.663 ± 0.007
$5 < p_{\rm T} < 6$	$-3.25 < y^* < -2.50$	0.839 ± 0.006
$5 < p_{\rm T} < 6$	$-4.00 < y^* < -3.25$	0.838 ± 0.010
$5 < p_{\rm T} < 6$	$-5.00 < y^* < -4.00$	0.681 ± 0.008
$6 < p_{\rm T} < 7$	$-3.25 < y^* < -2.50$	0.860 ± 0.005
$6 < p_{\rm T} < 7$	$-4.00 < y^* < -3.25$	0.853 ± 0.009
$6 < p_{\rm T} < 7$	$-5.00 < y^* < -4.00$	0.700 ± 0.011
$7 < p_{\rm T} < 8$	$-3.25 < y^* < -2.50$	0.875 ± 0.005
$7 < p_{\rm T} < 8$	$-4.00 < y^* < -3.25$	0.867 ± 0.009
$7 < p_{\rm T} < 8$	$-5.00 < y^* < -4.00$	0.714 ± 0.018
$8 < p_{\rm T} < 10$	$-3.25 < y^* < -2.50$	0.888 ± 0.006
$8 < p_{\rm T} < 10$	$-4.00 < y^* < -3.25$	0.875 ± 0.007
$8 < p_{\rm T} < 10$	$-5.00 < y^* < -4.00$	0.732 ± 0.025
$10 < p_{\rm T} < 14$	$-3.25 < y^* < -2.50$	0.898 ± 0.007
$10 < p_{\rm T} < 14$	$-4.00 < y^* < -3.25$	0.890 ± 0.008
$10 < p_{\rm T} < 14$	$-5.00 < y^* < -4.00$	0.781 ± 0.027

Table 31: $\psi(2S)$ over J/ψ tight PID efficiency ratios in pPb, in bins of p_{T} and y^* with total uncertainties.

p_{T} bin	y^* bin	$\epsilon_{\mathrm{PID}}^{\psi(2S)}/\epsilon_{\mathrm{PID}}^{J/\psi}$
$0 < p_{\mathrm{T}} < 1$	$1.50 < y^* < 2.50$	1.163 ± 0.006
$0 < p_{\mathrm{T}} < 1$	$2.50 < y^* < 3.25$	1.160 ± 0.019
$0 < p_{\mathrm{T}} < 1$	$3.25 < y^* < 4.00$	1.084 ± 0.018
$1 < p_{\mathrm{T}} < 2$	$1.50 < y^* < 2.50$	1.141 ± 0.003
$1 < p_{\mathrm{T}} < 2$	$2.50 < y^* < 3.25$	1.145 ± 0.016
$1 < p_{\mathrm{T}} < 2$	$3.25 < y^* < 4.00$	1.087 ± 0.014
$2 < p_{\mathrm{T}} < 3$	$1.50 < y^* < 2.50$	1.096 ± 0.004
$2 < p_{\mathrm{T}} < 3$	$2.50 < y^* < 3.25$	1.086 ± 0.006
$2 < p_{\mathrm{T}} < 3$	$3.25 < y^* < 4.00$	1.065 ± 0.009
$3 < p_{\mathrm{T}} < 4$	$1.50 < y^* < 2.50$	1.064 ± 0.001
$3 < p_{\mathrm{T}} < 4$	$2.50 < y^* < 3.25$	1.042 ± 0.003
$3 < p_{\mathrm{T}} < 4$	$3.25 < y^* < 4.00$	1.038 ± 0.003
$4 < p_{\mathrm{T}} < 5$	$1.50 < y^* < 2.50$	1.041 ± 0.002
$4 < p_{\mathrm{T}} < 5$	$2.50 < y^* < 3.25$	1.025 ± 0.003
$4 < p_{\mathrm{T}} < 5$	$3.25 < y^* < 4.00$	1.016 ± 0.001
$5 < p_{\mathrm{T}} < 6$	$1.50 < y^* < 2.50$	1.031 ± 0.002
$5 < p_{\mathrm{T}} < 6$	$2.50 < y^* < 3.25$	1.016 ± 0.004
$5 < p_{\mathrm{T}} < 6$	$3.25 < y^* < 4.00$	1.003 ± 0.004
$6 < p_{\mathrm{T}} < 7$	$1.50 < y^* < 2.50$	1.026 ± 0.002
$6 < p_{\mathrm{T}} < 7$	$2.50 < y^* < 3.25$	1.011 ± 0.003
$6 < p_{\mathrm{T}} < 7$	$3.25 < y^* < 4.00$	1.003 ± 0.007
$7 < p_{\mathrm{T}} < 8$	$1.50 < y^* < 2.50$	1.022 ± 0.001
$7 < p_{\mathrm{T}} < 8$	$2.50 < y^* < 3.25$	1.009 ± 0.002
$7 < p_{\mathrm{T}} < 8$	$3.25 < y^* < 4.00$	0.991 ± 0.008
$8 < p_{\mathrm{T}} < 10$	$1.50 < y^* < 2.50$	1.014 ± 0.001
$8 < p_{\mathrm{T}} < 10$	$2.50 < y^* < 3.25$	1.008 ± 0.002
$8 < p_{\mathrm{T}} < 10$	$3.25 < y^* < 4.00$	0.983 ± 0.008
$10 < p_{\mathrm{T}} < 14$	$1.50 < y^* < 2.50$	1.016 ± 0.000
$10 < p_{\mathrm{T}} < 14$	$2.50 < y^* < 3.25$	1.014 ± 0.003
$10 < p_{\mathrm{T}} < 14$	$3.25 < y^* < 4.00$	0.987 ± 0.007

Table 32: $\psi(2S)$ over J/ψ tight PID efficiency ratios in Pbp, in bins of p_{T} and y^* with total uncertainties.

p_{T} bin	y^* bin	$\epsilon_{\mathrm{PID}}^{\psi(2S)}/\epsilon_{\mathrm{PID}}^{J/\psi}$
$0 < p_{\mathrm{T}} < 1$	$-3.25 < y^* < -2.50$	1.206 ± 0.011
$0 < p_{\mathrm{T}} < 1$	$-4.00 < y^* < -3.25$	1.234 ± 0.024
$0 < p_{\mathrm{T}} < 1$	$-5.00 < y^* < -4.00$	1.137 ± 0.022
$1 < p_{\mathrm{T}} < 2$	$-3.25 < y^* < -2.50$	1.173 ± 0.003
$1 < p_{\mathrm{T}} < 2$	$-4.00 < y^* < -3.25$	1.198 ± 0.019
$1 < p_{\mathrm{T}} < 2$	$-5.00 < y^* < -4.00$	1.140 ± 0.020
$2 < p_{\mathrm{T}} < 3$	$-3.25 < y^* < -2.50$	1.122 ± 0.003
$2 < p_{\mathrm{T}} < 3$	$-4.00 < y^* < -3.25$	1.117 ± 0.006
$2 < p_{\mathrm{T}} < 3$	$-5.00 < y^* < -4.00$	1.087 ± 0.008
$3 < p_{\mathrm{T}} < 4$	$-3.25 < y^* < -2.50$	1.089 ± 0.002
$3 < p_{\mathrm{T}} < 4$	$-4.00 < y^* < -3.25$	1.065 ± 0.003
$3 < p_{\mathrm{T}} < 4$	$-5.00 < y^* < -4.00$	1.043 ± 0.002
$4 < p_{\mathrm{T}} < 5$	$-3.25 < y^* < -2.50$	1.060 ± 0.004
$4 < p_{\mathrm{T}} < 5$	$-4.00 < y^* < -3.25$	1.039 ± 0.001
$4 < p_{\mathrm{T}} < 5$	$-5.00 < y^* < -4.00$	1.011 ± 0.001
$5 < p_{\mathrm{T}} < 6$	$-3.25 < y^* < -2.50$	1.045 ± 0.001
$5 < p_{\mathrm{T}} < 6$	$-4.00 < y^* < -3.25$	1.025 ± 0.001
$5 < p_{\mathrm{T}} < 6$	$-5.00 < y^* < -4.00$	0.991 ± 0.002
$6 < p_{\mathrm{T}} < 7$	$-3.25 < y^* < -2.50$	1.024 ± 0.001
$6 < p_{\mathrm{T}} < 7$	$-4.00 < y^* < -3.25$	1.020 ± 0.002
$6 < p_{\mathrm{T}} < 7$	$-5.00 < y^* < -4.00$	0.985 ± 0.001
$7 < p_{\mathrm{T}} < 8$	$-3.25 < y^* < -2.50$	1.024 ± 0.001
$7 < p_{\mathrm{T}} < 8$	$-4.00 < y^* < -3.25$	1.013 ± 0.001
$7 < p_{\mathrm{T}} < 8$	$-5.00 < y^* < -4.00$	0.981 ± 0.009
$8 < p_{\mathrm{T}} < 10$	$-3.25 < y^* < -2.50$	1.013 ± 0.001
$8 < p_{\mathrm{T}} < 10$	$-4.00 < y^* < -3.25$	1.018 ± 0.002
$8 < p_{\mathrm{T}} < 10$	$-5.00 < y^* < -4.00$	0.966 ± 0.012
$10 < p_{\mathrm{T}} < 14$	$-3.25 < y^* < -2.50$	1.012 ± 0.002
$10 < p_{\mathrm{T}} < 14$	$-4.00 < y^* < -3.25$	1.011 ± 0.001
$10 < p_{\mathrm{T}} < 14$	$-5.00 < y^* < -4.00$	0.946 ± 0.008

6.5 Trigger efficiency

The trigger efficiency is defined as follows

$$\epsilon_{\mathrm{tri}}(p_{\mathrm{T}}, y^*) = \frac{J/\psi \text{ or } \psi(2S) \text{ TOS of L0 and HLT1 in bin } (p_{\mathrm{T}}, y^*)}{J/\psi \text{ or } \psi(2S) \text{ selected in bin } (p_{\mathrm{T}}, y^*)}, \tag{21}$$

where the selection includes here the PID requirements. The efficiencies are computed with the simulated samples, applying on them the simulation of the PID. Note that since the analysis is done on the TURBO candidates, the efficiency of the HLT2 is included in the reconstruction, PID and selection efficiencies. Since the trigger efficiency is defined as a conditional efficiency after the particle identification selection, it has to be evaluated separately for the tight and the loose PID selection. The trigger efficiency as a function of the candidate p_{T} in different y^* bins is shown in Fig. 32 for J/ψ for the tight selection, where the error bars are the statistical uncertainties of the statistics of the simulation samples. The same quantity for the loose selection is shown in Fig. 33. The ratio of the trigger efficiencies, for the tight selection, between $\psi(2S)$ and J/ψ is shown in Fig. 35. It becomes evident that the tighter PID selection does not affect the trigger efficiency to first approximation. The corresponding quantity for the $\psi(2S)$ for the tight selection is shown in Fig. 34. The systematic uncertainty of the trigger efficiency ratio is discussed in the following section. Tables 33 (J/ψ tight PID selection pPb), 34 (J/ψ tight PID selection Pbp), 37 (J/ψ loose PID selection pPb), 38 (J/ψ loose PID selection Pbp), 35 ($\psi(2S)$ tight selection pPb) and 36 ($\psi(2S)$ tight selection Pbp) give the corresponding numerical values.

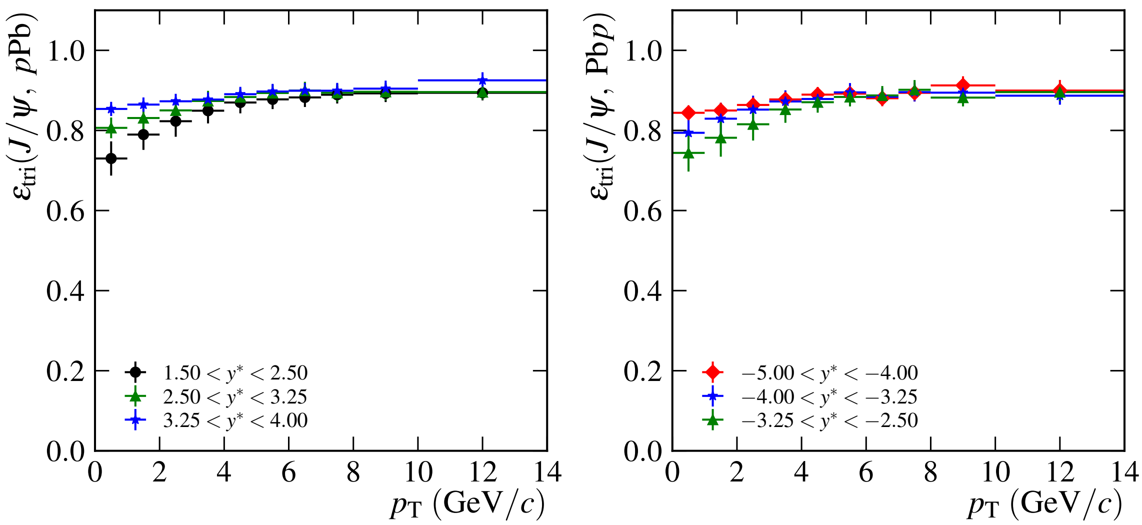

Figure 32: Trigger (L0 and HLT1) efficiency ϵ_{tri} as a function of p_{T} in different y^* bins for the tight PID selection for left: J/ψ in pPb, right: J/ψ in Pbp. The displayed uncertainty corresponds to the total uncertainty.

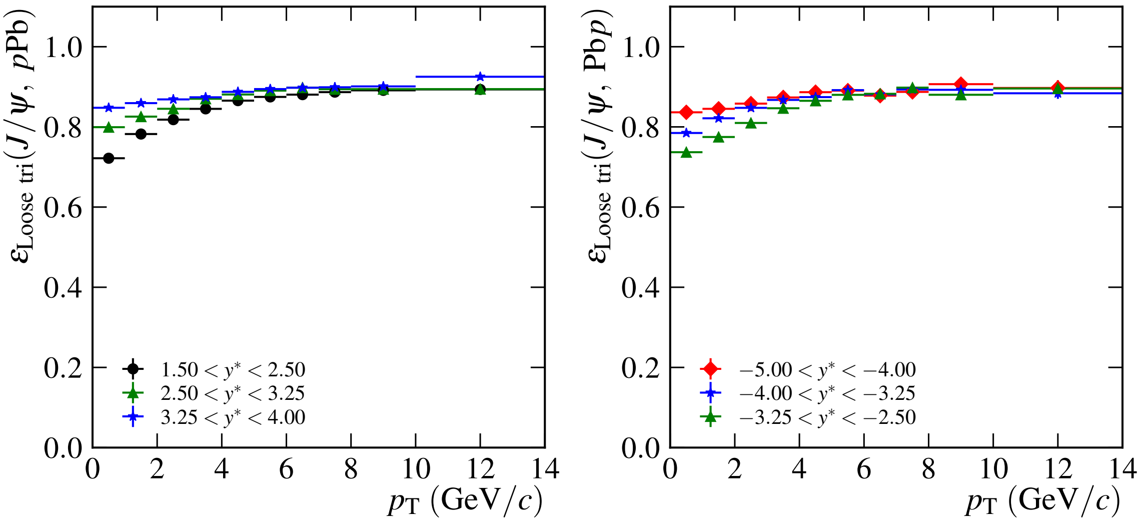

Figure 33: Trigger (L0 and HLT1) efficiency ϵ_{tri} as a function of p_T in different y^* bins for the loose PID selection for left: J/ψ in pPb, right: J/ψ in Pbp. The displayed uncertainty corresponds only to the MC statistical uncertainty.

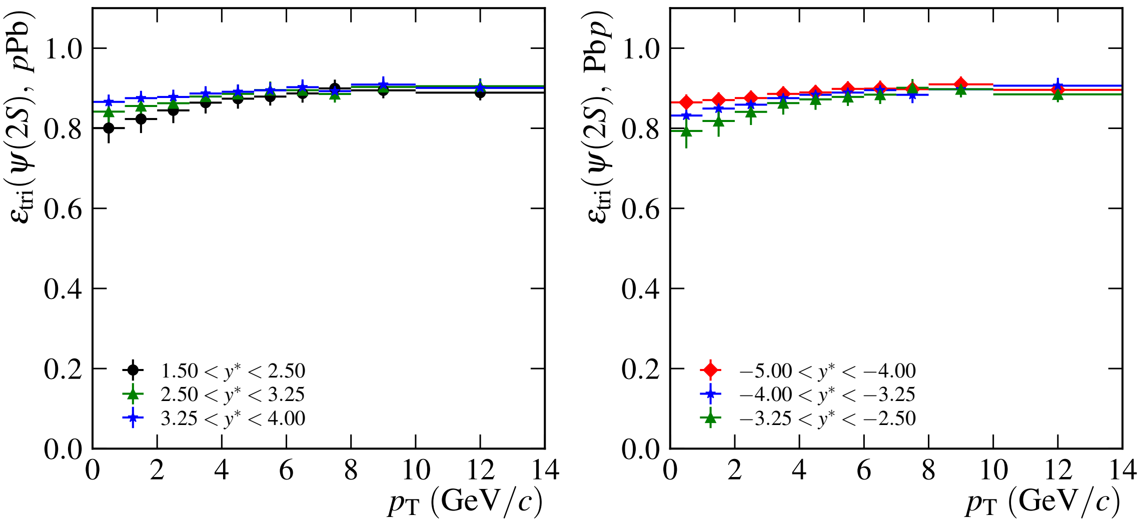

Figure 34: Trigger (L0 and HLT1) efficiency ϵ_{tri} as a function of p_T in different y^* bins for left: $\psi(2S)$ in pPb, right: $\psi(2S)$ in Pbp. The displayed uncertainty corresponds to the total uncertainty.

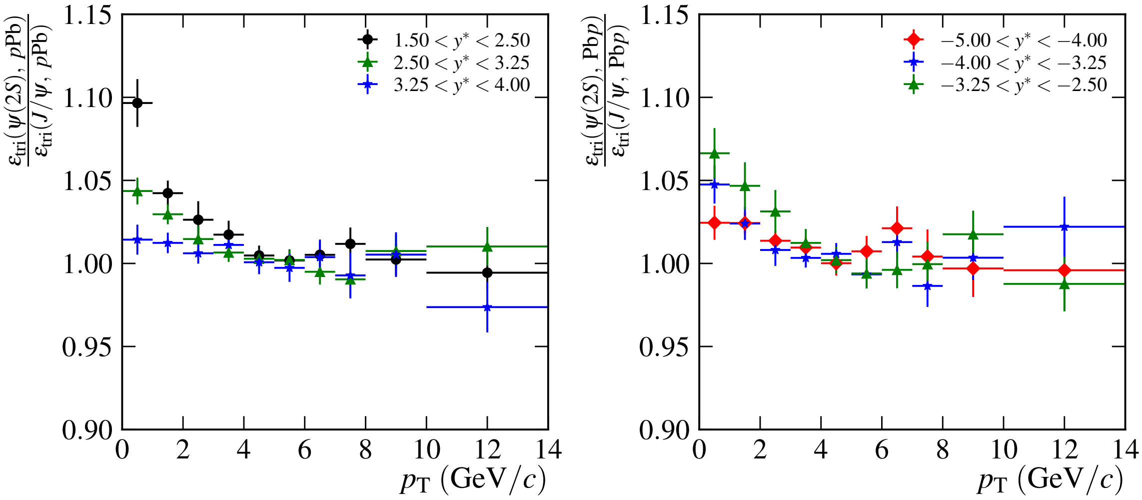

Figure 35: Trigger efficiency ratio $\epsilon_{\mathrm{tri}}^{\psi(2S)}/\epsilon_{\mathrm{tri}}^{J/\psi}$ as a function of p_{T} for different y^* bins with total uncertainties for left: pPb, right: Pbp.

Table 33: Trigger efficiencies J/ψ in pPb, in bins of p_{T} and y^* for the tight selection. The uncertainties are the total ones.

p_{T} bin	y^* bin	ϵ_{tri}
$0 < p_{\mathrm{T}} < 1$	$1.50 < y^* < 2.50$	0.730 ± 0.043
$0 < p_{\mathrm{T}} < 1$	$2.50 < y^* < 3.25$	0.806 ± 0.026
$0 < p_{\mathrm{T}} < 1$	$3.25 < y^* < 4.00$	0.854 ± 0.018
$1 < p_{\mathrm{T}} < 2$	$1.50 < y^* < 2.50$	0.790 ± 0.038
$1 < p_{\mathrm{T}} < 2$	$2.50 < y^* < 3.25$	0.831 ± 0.028
$1 < p_{\mathrm{T}} < 2$	$3.25 < y^* < 4.00$	0.865 ± 0.018
$2 < p_{\mathrm{T}} < 3$	$1.50 < y^* < 2.50$	0.823 ± 0.039
$2 < p_{\mathrm{T}} < 3$	$2.50 < y^* < 3.25$	0.850 ± 0.028
$2 < p_{\mathrm{T}} < 3$	$3.25 < y^* < 4.00$	0.873 ± 0.019
$3 < p_{\mathrm{T}} < 4$	$1.50 < y^* < 2.50$	0.849 ± 0.032
$3 < p_{\mathrm{T}} < 4$	$2.50 < y^* < 3.25$	0.874 ± 0.025
$3 < p_{\mathrm{T}} < 4$	$3.25 < y^* < 4.00$	0.877 ± 0.018
$4 < p_{\mathrm{T}} < 5$	$1.50 < y^* < 2.50$	0.870 ± 0.027
$4 < p_{\mathrm{T}} < 5$	$2.50 < y^* < 3.25$	0.883 ± 0.022
$4 < p_{\mathrm{T}} < 5$	$3.25 < y^* < 4.00$	0.890 ± 0.018
$5 < p_{\mathrm{T}} < 6$	$1.50 < y^* < 2.50$	0.878 ± 0.024
$5 < p_{\mathrm{T}} < 6$	$2.50 < y^* < 3.25$	0.893 ± 0.021
$5 < p_{\mathrm{T}} < 6$	$3.25 < y^* < 4.00$	0.897 ± 0.019
$6 < p_{\mathrm{T}} < 7$	$1.50 < y^* < 2.50$	0.882 ± 0.024
$6 < p_{\mathrm{T}} < 7$	$2.50 < y^* < 3.25$	0.900 ± 0.022
$6 < p_{\mathrm{T}} < 7$	$3.25 < y^* < 4.00$	0.899 ± 0.019
$7 < p_{\mathrm{T}} < 8$	$1.50 < y^* < 2.50$	0.889 ± 0.022
$7 < p_{\mathrm{T}} < 8$	$2.50 < y^* < 3.25$	0.894 ± 0.022
$7 < p_{\mathrm{T}} < 8$	$3.25 < y^* < 4.00$	0.899 ± 0.020
$8 < p_{\mathrm{T}} < 10$	$1.50 < y^* < 2.50$	0.893 ± 0.022
$8 < p_{\mathrm{T}} < 10$	$2.50 < y^* < 3.25$	0.896 ± 0.022
$8 < p_{\mathrm{T}} < 10$	$3.25 < y^* < 4.00$	0.904 ± 0.020
$10 < p_{\mathrm{T}} < 14$	$1.50 < y^* < 2.50$	0.894 ± 0.019
$10 < p_{\mathrm{T}} < 14$	$2.50 < y^* < 3.25$	0.896 ± 0.019
$10 < p_{\mathrm{T}} < 14$	$3.25 < y^* < 4.00$	0.925 ± 0.020

Table 34: Trigger efficiencies J/ψ in Pbp, in bins of p_{T} and y^* for the tight selection. The uncertainties are the total ones.

p_{T} bin	y^* bin	ϵ_{tri}
$0 < p_{\mathrm{T}} < 1$	$-3.25 < y^* < -2.50$	0.744 ± 0.047
$0 < p_{\mathrm{T}} < 1$	$-4.00 < y^* < -3.25$	0.794 ± 0.040
$0 < p_{\mathrm{T}} < 1$	$-5.00 < y^* < -4.00$	0.844 ± 0.019
$1 < p_{\mathrm{T}} < 2$	$-3.25 < y^* < -2.50$	0.782 ± 0.047
$1 < p_{\mathrm{T}} < 2$	$-4.00 < y^* < -3.25$	0.829 ± 0.039
$1 < p_{\mathrm{T}} < 2$	$-5.00 < y^* < -4.00$	0.850 ± 0.020
$2 < p_{\mathrm{T}} < 3$	$-3.25 < y^* < -2.50$	0.815 ± 0.041
$2 < p_{\mathrm{T}} < 3$	$-4.00 < y^* < -3.25$	0.852 ± 0.035
$2 < p_{\mathrm{T}} < 3$	$-5.00 < y^* < -4.00$	0.864 ± 0.019
$3 < p_{\mathrm{T}} < 4$	$-3.25 < y^* < -2.50$	0.852 ± 0.033
$3 < p_{\mathrm{T}} < 4$	$-4.00 < y^* < -3.25$	0.872 ± 0.028
$3 < p_{\mathrm{T}} < 4$	$-5.00 < y^* < -4.00$	0.877 ± 0.019
$4 < p_{\mathrm{T}} < 5$	$-3.25 < y^* < -2.50$	0.870 ± 0.026
$4 < p_{\mathrm{T}} < 5$	$-4.00 < y^* < -3.25$	0.879 ± 0.026
$4 < p_{\mathrm{T}} < 5$	$-5.00 < y^* < -4.00$	0.889 ± 0.019
$5 < p_{\mathrm{T}} < 6$	$-3.25 < y^* < -2.50$	0.884 ± 0.024
$5 < p_{\mathrm{T}} < 6$	$-4.00 < y^* < -3.25$	0.895 ± 0.023
$5 < p_{\mathrm{T}} < 6$	$-5.00 < y^* < -4.00$	0.892 ± 0.019
$6 < p_{\mathrm{T}} < 7$	$-3.25 < y^* < -2.50$	0.887 ± 0.023
$6 < p_{\mathrm{T}} < 7$	$-4.00 < y^* < -3.25$	0.884 ± 0.021
$6 < p_{\mathrm{T}} < 7$	$-5.00 < y^* < -4.00$	0.880 ± 0.020
$7 < p_{\mathrm{T}} < 8$	$-3.25 < y^* < -2.50$	0.902 ± 0.024
$7 < p_{\mathrm{T}} < 8$	$-4.00 < y^* < -3.25$	0.896 ± 0.023
$7 < p_{\mathrm{T}} < 8$	$-5.00 < y^* < -4.00$	0.894 ± 0.022
$8 < p_{\mathrm{T}} < 10$	$-3.25 < y^* < -2.50$	0.882 ± 0.022
$8 < p_{\mathrm{T}} < 10$	$-4.00 < y^* < -3.25$	0.894 ± 0.021
$8 < p_{\mathrm{T}} < 10$	$-5.00 < y^* < -4.00$	0.912 ± 0.023
$10 < p_{\mathrm{T}} < 14$	$-3.25 < y^* < -2.50$	0.896 ± 0.022
$10 < p_{\mathrm{T}} < 14$	$-4.00 < y^* < -3.25$	0.887 ± 0.023
$10 < p_{\mathrm{T}} < 14$	$-5.00 < y^* < -4.00$	0.900 ± 0.026

Table 35: Trigger efficiencies $\psi(2S)$ in pPb, in bins of p_T and y^* for the tight selection. The uncertainties are the total ones.

p_T bin	y^* bin	ϵ_{tri}
$0 < p_T < 1$	$1.50 < y^* < 2.50$	0.800 ± 0.038
$0 < p_T < 1$	$2.50 < y^* < 3.25$	0.842 ± 0.026
$0 < p_T < 1$	$3.25 < y^* < 4.00$	0.866 ± 0.018
$1 < p_T < 2$	$1.50 < y^* < 2.50$	0.823 ± 0.035
$1 < p_T < 2$	$2.50 < y^* < 3.25$	0.856 ± 0.026
$1 < p_T < 2$	$3.25 < y^* < 4.00$	0.875 ± 0.018
$2 < p_T < 3$	$1.50 < y^* < 2.50$	0.845 ± 0.032
$2 < p_T < 3$	$2.50 < y^* < 3.25$	0.863 ± 0.024
$2 < p_T < 3$	$3.25 < y^* < 4.00$	0.878 ± 0.018
$3 < p_T < 4$	$1.50 < y^* < 2.50$	0.864 ± 0.027
$3 < p_T < 4$	$2.50 < y^* < 3.25$	0.879 ± 0.023
$3 < p_T < 4$	$3.25 < y^* < 4.00$	0.887 ± 0.018
$4 < p_T < 5$	$1.50 < y^* < 2.50$	0.874 ± 0.025
$4 < p_T < 5$	$2.50 < y^* < 3.25$	0.886 ± 0.023
$4 < p_T < 5$	$3.25 < y^* < 4.00$	0.891 ± 0.018
$5 < p_T < 6$	$1.50 < y^* < 2.50$	0.879 ± 0.022
$5 < p_T < 6$	$2.50 < y^* < 3.25$	0.895 ± 0.021
$5 < p_T < 6$	$3.25 < y^* < 4.00$	0.895 ± 0.020
$6 < p_T < 7$	$1.50 < y^* < 2.50$	0.887 ± 0.023
$6 < p_T < 7$	$2.50 < y^* < 3.25$	0.895 ± 0.023
$6 < p_T < 7$	$3.25 < y^* < 4.00$	0.903 ± 0.019
$7 < p_T < 8$	$1.50 < y^* < 2.50$	0.900 ± 0.022
$7 < p_T < 8$	$2.50 < y^* < 3.25$	0.886 ± 0.021
$7 < p_T < 8$	$3.25 < y^* < 4.00$	0.893 ± 0.020
$8 < p_T < 10$	$1.50 < y^* < 2.50$	0.895 ± 0.020
$8 < p_T < 10$	$2.50 < y^* < 3.25$	0.903 ± 0.021
$8 < p_T < 10$	$3.25 < y^* < 4.00$	0.909 ± 0.020
$10 < p_T < 14$	$1.50 < y^* < 2.50$	0.889 ± 0.019
$10 < p_T < 14$	$2.50 < y^* < 3.25$	0.905 ± 0.020
$10 < p_T < 14$	$3.25 < y^* < 4.00$	0.901 ± 0.021

Table 36: Trigger efficiencies $\psi(2S)$ in Pbp, in bins of p_T and y^* for the tight selection. The uncertainties are the total ones.

p_T bin	y^* bin	ϵ_{tri}
$0 < p_T < 1$	$-3.25 < y^* < -2.50$	0.793 ± 0.043
$0 < p_T < 1$	$-4.00 < y^* < -3.25$	0.832 ± 0.035
$0 < p_T < 1$	$-5.00 < y^* < -4.00$	0.865 ± 0.020
$1 < p_T < 2$	$-3.25 < y^* < -2.50$	0.818 ± 0.039
$1 < p_T < 2$	$-4.00 < y^* < -3.25$	0.849 ± 0.033
$1 < p_T < 2$	$-5.00 < y^* < -4.00$	0.870 ± 0.019
$2 < p_T < 3$	$-3.25 < y^* < -2.50$	0.841 ± 0.033
$2 < p_T < 3$	$-4.00 < y^* < -3.25$	0.859 ± 0.028
$2 < p_T < 3$	$-5.00 < y^* < -4.00$	0.875 ± 0.019
$3 < p_T < 4$	$-3.25 < y^* < -2.50$	0.863 ± 0.029
$3 < p_T < 4$	$-4.00 < y^* < -3.25$	0.875 ± 0.025
$3 < p_T < 4$	$-5.00 < y^* < -4.00$	0.886 ± 0.019
$4 < p_T < 5$	$-3.25 < y^* < -2.50$	0.872 ± 0.026
$4 < p_T < 5$	$-4.00 < y^* < -3.25$	0.884 ± 0.023
$4 < p_T < 5$	$-5.00 < y^* < -4.00$	0.890 ± 0.019
$5 < p_T < 6$	$-3.25 < y^* < -2.50$	0.878 ± 0.023
$5 < p_T < 6$	$-4.00 < y^* < -3.25$	0.889 ± 0.021
$5 < p_T < 6$	$-5.00 < y^* < -4.00$	0.898 ± 0.019
$6 < p_T < 7$	$-3.25 < y^* < -2.50$	0.884 ± 0.023
$6 < p_T < 7$	$-4.00 < y^* < -3.25$	0.895 ± 0.020
$6 < p_T < 7$	$-5.00 < y^* < -4.00$	0.899 ± 0.020
$7 < p_T < 8$	$-3.25 < y^* < -2.50$	0.901 ± 0.022
$7 < p_T < 8$	$-4.00 < y^* < -3.25$	0.884 ± 0.021
$7 < p_T < 8$	$-5.00 < y^* < -4.00$	0.898 ± 0.020
$8 < p_T < 10$	$-3.25 < y^* < -2.50$	0.898 ± 0.020
$8 < p_T < 10$	$-4.00 < y^* < -3.25$	0.897 ± 0.019
$8 < p_T < 10$	$-5.00 < y^* < -4.00$	0.910 ± 0.020
$10 < p_T < 14$	$-3.25 < y^* < -2.50$	0.885 ± 0.020
$10 < p_T < 14$	$-4.00 < y^* < -3.25$	0.906 ± 0.020
$10 < p_T < 14$	$-5.00 < y^* < -4.00$	0.896 ± 0.020

Table 37: Trigger efficiencies J/ψ in pPb, in bins of p_{T} and y^* for the loose selection. The uncertainties are the statistical ones.

p_{T} bin	y^* bin	$\epsilon_{\mathrm{Loose\ tri}}$
$0 < p_{\mathrm{T}} < 1$	$1.50 < y^* < 2.50$	0.722 ± 0.003
$0 < p_{\mathrm{T}} < 1$	$2.50 < y^* < 3.25$	0.799 ± 0.002
$0 < p_{\mathrm{T}} < 1$	$3.25 < y^* < 4.00$	0.848 ± 0.003
$1 < p_{\mathrm{T}} < 2$	$1.50 < y^* < 2.50$	0.782 ± 0.002
$1 < p_{\mathrm{T}} < 2$	$2.50 < y^* < 3.25$	0.826 ± 0.002
$1 < p_{\mathrm{T}} < 2$	$3.25 < y^* < 4.00$	0.859 ± 0.002
$2 < p_{\mathrm{T}} < 3$	$1.50 < y^* < 2.50$	0.818 ± 0.002
$2 < p_{\mathrm{T}} < 3$	$2.50 < y^* < 3.25$	0.845 ± 0.002
$2 < p_{\mathrm{T}} < 3$	$3.25 < y^* < 4.00$	0.869 ± 0.002
$3 < p_{\mathrm{T}} < 4$	$1.50 < y^* < 2.50$	0.845 ± 0.002
$3 < p_{\mathrm{T}} < 4$	$2.50 < y^* < 3.25$	0.870 ± 0.002
$3 < p_{\mathrm{T}} < 4$	$3.25 < y^* < 4.00$	0.874 ± 0.003
$4 < p_{\mathrm{T}} < 5$	$1.50 < y^* < 2.50$	0.866 ± 0.003
$4 < p_{\mathrm{T}} < 5$	$2.50 < y^* < 3.25$	0.881 ± 0.002
$4 < p_{\mathrm{T}} < 5$	$3.25 < y^* < 4.00$	0.887 ± 0.003
$5 < p_{\mathrm{T}} < 6$	$1.50 < y^* < 2.50$	0.875 ± 0.003
$5 < p_{\mathrm{T}} < 6$	$2.50 < y^* < 3.25$	0.890 ± 0.003
$5 < p_{\mathrm{T}} < 6$	$3.25 < y^* < 4.00$	0.894 ± 0.004
$6 < p_{\mathrm{T}} < 7$	$1.50 < y^* < 2.50$	0.880 ± 0.004
$6 < p_{\mathrm{T}} < 7$	$2.50 < y^* < 3.25$	0.898 ± 0.004
$6 < p_{\mathrm{T}} < 7$	$3.25 < y^* < 4.00$	0.898 ± 0.005
$7 < p_{\mathrm{T}} < 8$	$1.50 < y^* < 2.50$	0.887 ± 0.005
$7 < p_{\mathrm{T}} < 8$	$2.50 < y^* < 3.25$	0.894 ± 0.005
$7 < p_{\mathrm{T}} < 8$	$3.25 < y^* < 4.00$	0.899 ± 0.006
$8 < p_{\mathrm{T}} < 10$	$1.50 < y^* < 2.50$	0.891 ± 0.005
$8 < p_{\mathrm{T}} < 10$	$2.50 < y^* < 3.25$	0.894 ± 0.005
$8 < p_{\mathrm{T}} < 10$	$3.25 < y^* < 4.00$	0.901 ± 0.007
$10 < p_{\mathrm{T}} < 14$	$1.50 < y^* < 2.50$	0.893 ± 0.006
$10 < p_{\mathrm{T}} < 14$	$2.50 < y^* < 3.25$	0.894 ± 0.007
$10 < p_{\mathrm{T}} < 14$	$3.25 < y^* < 4.00$	0.925 ± 0.008

Table 38: Trigger efficiencies J/ψ in Pbp, in bins of $p_{\rm T}$ and y^{*} for the loose selection. The uncertainties are only the statistical ones.

$p_{\rm T}$ bin	y^{*} bin	$\epsilon_{\rm Loose\ tri}$
$0 < p_{\rm T} < 1$	$-3.25 < y^{*} < -2.50$	0.737 ± 0.005
$0 < p_{\rm T} < 1$	$-4.00 < y^{*} < -3.25$	0.785 ± 0.003
$0 < p_{\rm T} < 1$	$-5.00 < y^{*} < -4.00$	0.836 ± 0.004
$1 < p_{\rm T} < 2$	$-3.25 < y^{*} < -2.50$	0.775 ± 0.003
$1 < p_{\rm T} < 2$	$-4.00 < y^{*} < -3.25$	0.821 ± 0.002
$1 < p_{\rm T} < 2$	$-5.00 < y^{*} < -4.00$	0.845 ± 0.002
$2 < p_{\rm T} < 3$	$-3.25 < y^{*} < -2.50$	0.810 ± 0.003
$2 < p_{\rm T} < 3$	$-4.00 < y^{*} < -3.25$	0.848 ± 0.002
$2 < p_{\rm T} < 3$	$-5.00 < y^{*} < -4.00$	0.858 ± 0.002
$3 < p_{\rm T} < 4$	$-3.25 < y^{*} < -2.50$	0.847 ± 0.003
$3 < p_{\rm T} < 4$	$-4.00 < y^{*} < -3.25$	0.867 ± 0.002
$3 < p_{\rm T} < 4$	$-5.00 < y^{*} < -4.00$	0.873 ± 0.003
$4 < p_{\rm T} < 5$	$-3.25 < y^{*} < -2.50$	0.865 ± 0.004
$4 < p_{\rm T} < 5$	$-4.00 < y^{*} < -3.25$	0.874 ± 0.003
$4 < p_{\rm T} < 5$	$-5.00 < y^{*} < -4.00$	0.887 ± 0.004
$5 < p_{\rm T} < 6$	$-3.25 < y^{*} < -2.50$	0.880 ± 0.005
$5 < p_{\rm T} < 6$	$-4.00 < y^{*} < -3.25$	0.892 ± 0.004
$5 < p_{\rm T} < 6$	$-5.00 < y^{*} < -4.00$	0.890 ± 0.005
$6 < p_{\rm T} < 7$	$-3.25 < y^{*} < -2.50$	0.883 ± 0.006
$6 < p_{\rm T} < 7$	$-4.00 < y^{*} < -3.25$	0.881 ± 0.006
$6 < p_{\rm T} < 7$	$-5.00 < y^{*} < -4.00$	0.878 ± 0.008
$7 < p_{\rm T} < 8$	$-3.25 < y^{*} < -2.50$	0.898 ± 0.008
$7 < p_{\rm T} < 8$	$-4.00 < y^{*} < -3.25$	0.893 ± 0.008
$7 < p_{\rm T} < 8$	$-5.00 < y^{*} < -4.00$	0.887 ± 0.011
$8 < p_{\rm T} < 10$	$-3.25 < y^{*} < -2.50$	0.880 ± 0.009
$8 < p_{\rm T} < 10$	$-4.00 < y^{*} < -3.25$	0.892 ± 0.009
$8 < p_{\rm T} < 10$	$-5.00 < y^{*} < -4.00$	0.907 ± 0.012
$10 < p_{\rm T} < 14$	$-3.25 < y^{*} < -2.50$	0.896 ± 0.012
$10 < p_{\rm T} < 14$	$-4.00 < y^{*} < -3.25$	0.884 ± 0.014
$10 < p_{\rm T} < 14$	$-5.00 < y^{*} < -4.00$	0.897 ± 0.019

Table 39: $\psi(2S)$ over J/ψ trigger efficiency (with tight PID selection) ratios in pPb, in bins of $p_{\rm T}$ and y^* with total uncertainties.

$p_{\rm T}$ bin	y^* bin	$\epsilon_{\rm tri}^{\psi(2S)}/\epsilon_{\rm tri}^{J/\psi}$
$0 < p_{\rm T} < 1$	$1.50 < y^* < 2.50$	1.097 ± 0.014
$0 < p_{\rm T} < 1$	$2.50 < y^* < 3.25$	1.044 ± 0.008
$0 < p_{\rm T} < 1$	$3.25 < y^* < 4.00$	1.014 ± 0.009
$1 < p_{\rm T} < 2$	$1.50 < y^* < 2.50$	1.042 ± 0.008
$1 < p_{\rm T} < 2$	$2.50 < y^* < 3.25$	1.030 ± 0.006
$1 < p_{\rm T} < 2$	$3.25 < y^* < 4.00$	1.012 ± 0.006
$2 < p_{\rm T} < 3$	$1.50 < y^* < 2.50$	1.026 ± 0.011
$2 < p_{\rm T} < 3$	$2.50 < y^* < 3.25$	1.015 ± 0.008
$2 < p_{\rm T} < 3$	$3.25 < y^* < 4.00$	1.006 ± 0.006
$3 < p_{\rm T} < 4$	$1.50 < y^* < 2.50$	1.017 ± 0.008
$3 < p_{\rm T} < 4$	$2.50 < y^* < 3.25$	1.007 ± 0.006
$3 < p_{\rm T} < 4$	$3.25 < y^* < 4.00$	1.011 ± 0.007
$4 < p_{\rm T} < 5$	$1.50 < y^* < 2.50$	1.005 ± 0.006
$4 < p_{\rm T} < 5$	$2.50 < y^* < 3.25$	1.003 ± 0.005
$4 < p_{\rm T} < 5$	$3.25 < y^* < 4.00$	1.001 ± 0.007
$5 < p_{\rm T} < 6$	$1.50 < y^* < 2.50$	1.002 ± 0.007
$5 < p_{\rm T} < 6$	$2.50 < y^* < 3.25$	1.002 ± 0.006
$5 < p_{\rm T} < 6$	$3.25 < y^* < 4.00$	0.997 ± 0.008
$6 < p_{\rm T} < 7$	$1.50 < y^* < 2.50$	1.005 ± 0.008
$6 < p_{\rm T} < 7$	$2.50 < y^* < 3.25$	0.995 ± 0.008
$6 < p_{\rm T} < 7$	$3.25 < y^* < 4.00$	1.004 ± 0.011
$7 < p_{\rm T} < 8$	$1.50 < y^* < 2.50$	1.012 ± 0.010
$7 < p_{\rm T} < 8$	$2.50 < y^* < 3.25$	0.990 ± 0.010
$7 < p_{\rm T} < 8$	$3.25 < y^* < 4.00$	0.993 ± 0.014
$8 < p_{\rm T} < 10$	$1.50 < y^* < 2.50$	1.002 ± 0.010
$8 < p_{\rm T} < 10$	$2.50 < y^* < 3.25$	1.007 ± 0.010
$8 < p_{\rm T} < 10$	$3.25 < y^* < 4.00$	1.005 ± 0.013
$10 < p_{\rm T} < 14$	$1.50 < y^* < 2.50$	0.994 ± 0.011
$10 < p_{\rm T} < 14$	$2.50 < y^* < 3.25$	1.010 ± 0.012
$10 < p_{\rm T} < 14$	$3.25 < y^* < 4.00$	0.974 ± 0.015

Table 40: $\psi(2S)$ over J/ψ trigger efficiency (with tight PID selection) ratios in Pbp, in bins of p_{T} and y^* with total uncertainties.

p_{T} bin	y^* bin	$\epsilon_{\mathrm{tri}}^{\psi(2S)}/\epsilon_{\mathrm{tri}}^{J/\psi}$
$0 < p_{\mathrm{T}} < 1$	$-3.25 < y^* < -2.50$	1.066 ± 0.015
$0 < p_{\mathrm{T}} < 1$	$-4.00 < y^* < -3.25$	1.048 ± 0.011
$0 < p_{\mathrm{T}} < 1$	$-5.00 < y^* < -4.00$	1.024 ± 0.010
$1 < p_{\mathrm{T}} < 2$	$-3.25 < y^* < -2.50$	1.047 ± 0.014
$1 < p_{\mathrm{T}} < 2$	$-4.00 < y^* < -3.25$	1.024 ± 0.010
$1 < p_{\mathrm{T}} < 2$	$-5.00 < y^* < -4.00$	1.024 ± 0.007
$2 < p_{\mathrm{T}} < 3$	$-3.25 < y^* < -2.50$	1.031 ± 0.013
$2 < p_{\mathrm{T}} < 3$	$-4.00 < y^* < -3.25$	1.008 ± 0.010
$2 < p_{\mathrm{T}} < 3$	$-5.00 < y^* < -4.00$	1.014 ± 0.006
$3 < p_{\mathrm{T}} < 4$	$-3.25 < y^* < -2.50$	1.012 ± 0.008
$3 < p_{\mathrm{T}} < 4$	$-4.00 < y^* < -3.25$	1.003 ± 0.006
$3 < p_{\mathrm{T}} < 4$	$-5.00 < y^* < -4.00$	1.010 ± 0.006
$4 < p_{\mathrm{T}} < 5$	$-3.25 < y^* < -2.50$	1.002 ± 0.008
$4 < p_{\mathrm{T}} < 5$	$-4.00 < y^* < -3.25$	1.006 ± 0.007
$4 < p_{\mathrm{T}} < 5$	$-5.00 < y^* < -4.00$	1.000 ± 0.007
$5 < p_{\mathrm{T}} < 6$	$-3.25 < y^* < -2.50$	0.994 ± 0.009
$5 < p_{\mathrm{T}} < 6$	$-4.00 < y^* < -3.25$	0.993 ± 0.007
$5 < p_{\mathrm{T}} < 6$	$-5.00 < y^* < -4.00$	1.007 ± 0.009
$6 < p_{\mathrm{T}} < 7$	$-3.25 < y^* < -2.50$	0.996 ± 0.011
$6 < p_{\mathrm{T}} < 7$	$-4.00 < y^* < -3.25$	1.013 ± 0.010
$6 < p_{\mathrm{T}} < 7$	$-5.00 < y^* < -4.00$	1.021 ± 0.013
$7 < p_{\mathrm{T}} < 8$	$-3.25 < y^* < -2.50$	1.000 ± 0.013
$7 < p_{\mathrm{T}} < 8$	$-4.00 < y^* < -3.25$	0.986 ± 0.013
$7 < p_{\mathrm{T}} < 8$	$-5.00 < y^* < -4.00$	1.004 ± 0.016
$8 < p_{\mathrm{T}} < 10$	$-3.25 < y^* < -2.50$	1.018 ± 0.014
$8 < p_{\mathrm{T}} < 10$	$-4.00 < y^* < -3.25$	1.003 ± 0.013
$8 < p_{\mathrm{T}} < 10$	$-5.00 < y^* < -4.00$	0.997 ± 0.017
$10 < p_{\mathrm{T}} < 14$	$-3.25 < y^* < -2.50$	0.988 ± 0.017
$10 < p_{\mathrm{T}} < 14$	$-4.00 < y^* < -3.25$	1.022 ± 0.018
$10 < p_{\mathrm{T}} < 14$	$-5.00 < y^* < -4.00$	0.996 ± 0.024

6.6 Total efficiencies

The total efficiency, equal to the product of all efficiencies mentioned above, is given in Fig. 36 for J/ψ the tight selection, in Fig. 37 for J/ψ the loose selection and in Fig. 38 for $\psi(2S)$ tight selection. The errors are the statistical errors from the simulation statistics and the systematic uncertainties affecting the efficiencies and detailed in the following section, added quadratically. The numerical results are given in Tables 41 (tight pPb), 42 (tight Pbp), 43 (loose pPb) and 44 (loose Pbp) and in Tables 45 ($\psi(2S)$ pPb) and 46 ($\psi(2S)$ Pbp).

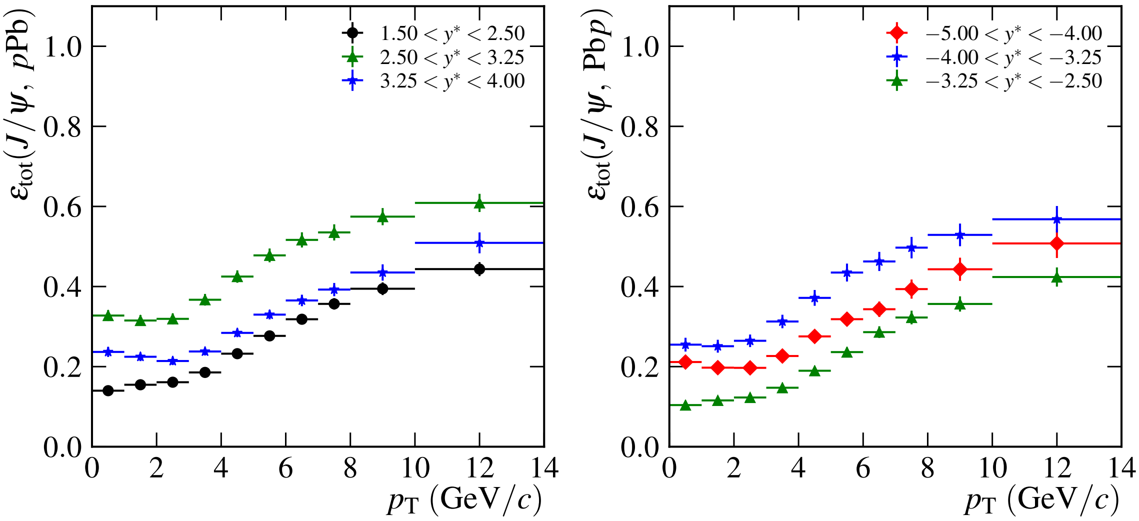

Figure 36: Total efficiency $\epsilon_{\rm tot}$ as a function of $p_{\rm T}$ in different y^* bins for left: J/ψ tight selection in pPb, right: J/ψ tight selection in Pbp. The displayed uncertainty corresponds to the total uncertainty.

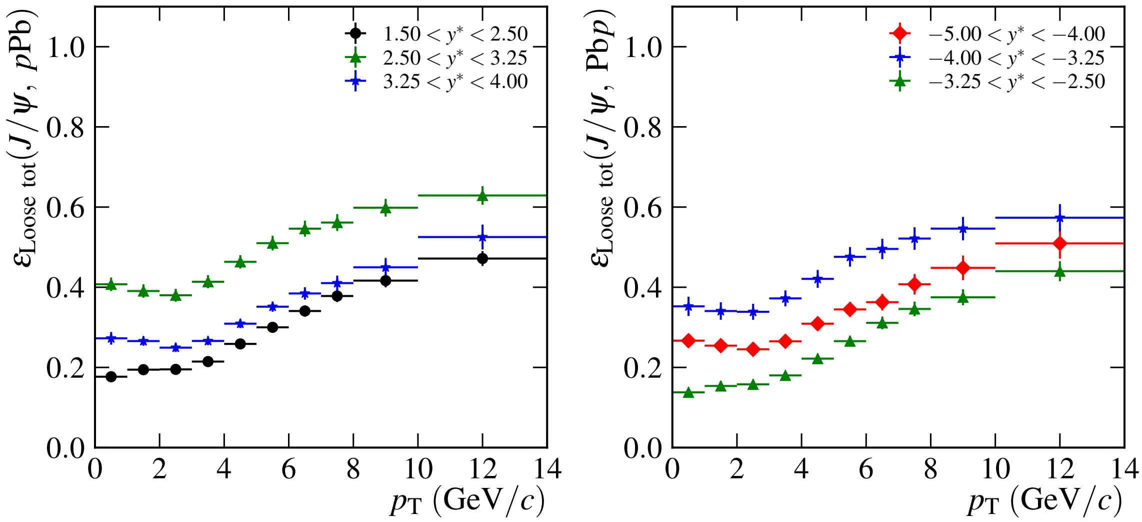

Figure 37: Total efficiency ϵ_{tot} as a function of p_{T} in different y^* bins for left: J/ψ loose selection in pPb, right: J/ψ loose selection in Pbp. The displayed uncertainty corresponds to the total uncertainty.

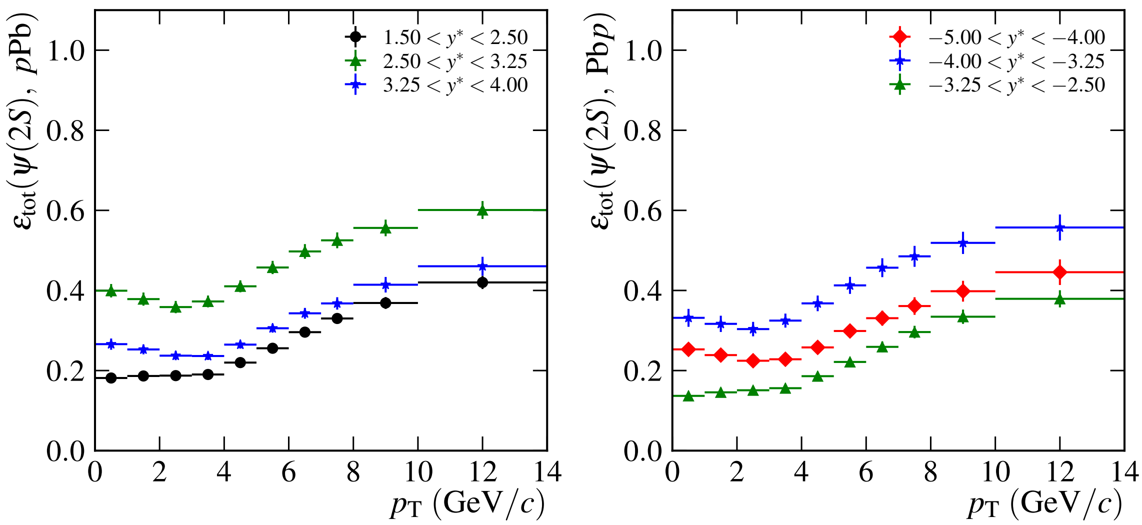

Figure 38: Total efficiency ϵ_{tot} as a function of p_{T} in different y^* bins for left: $\psi(2S)$ tight selection in pPb, right: $\psi(2S)$ tight selection in Pbp. The displayed uncertainty corresponds to the total uncertainty.

Table 41: Total efficiencies J/ψ in pPb, in bins of p_{T} and y^* for the tight selection with total uncertainties.

p_{T} bin	y^* bin	ϵ_{tot}
$0 < p_{\mathrm{T}} < 1$	$1.50 < y^* < 2.50$	0.140 ± 0.010
$0 < p_{\mathrm{T}} < 1$	$2.50 < y^* < 3.25$	0.328 ± 0.014
$0 < p_{\mathrm{T}} < 1$	$3.25 < y^* < 4.00$	0.237 ± 0.013
$1 < p_{\mathrm{T}} < 2$	$1.50 < y^* < 2.50$	0.155 ± 0.009
$1 < p_{\mathrm{T}} < 2$	$2.50 < y^* < 3.25$	0.315 ± 0.014
$1 < p_{\mathrm{T}} < 2$	$3.25 < y^* < 4.00$	0.225 ± 0.011
$2 < p_{\mathrm{T}} < 3$	$1.50 < y^* < 2.50$	0.161 ± 0.009
$2 < p_{\mathrm{T}} < 3$	$2.50 < y^* < 3.25$	0.319 ± 0.014
$2 < p_{\mathrm{T}} < 3$	$3.25 < y^* < 4.00$	0.214 ± 0.010
$3 < p_{\mathrm{T}} < 4$	$1.50 < y^* < 2.50$	0.186 ± 0.009
$3 < p_{\mathrm{T}} < 4$	$2.50 < y^* < 3.25$	0.367 ± 0.015
$3 < p_{\mathrm{T}} < 4$	$3.25 < y^* < 4.00$	0.238 ± 0.010
$4 < p_{\mathrm{T}} < 5$	$1.50 < y^* < 2.50$	0.232 ± 0.010
$4 < p_{\mathrm{T}} < 5$	$2.50 < y^* < 3.25$	0.425 ± 0.016
$4 < p_{\mathrm{T}} < 5$	$3.25 < y^* < 4.00$	0.284 ± 0.011
$5 < p_{\mathrm{T}} < 6$	$1.50 < y^* < 2.50$	0.277 ± 0.011
$5 < p_{\mathrm{T}} < 6$	$2.50 < y^* < 3.25$	0.478 ± 0.017
$5 < p_{\mathrm{T}} < 6$	$3.25 < y^* < 4.00$	0.330 ± 0.012
$6 < p_{\mathrm{T}} < 7$	$1.50 < y^* < 2.50$	0.318 ± 0.013
$6 < p_{\mathrm{T}} < 7$	$2.50 < y^* < 3.25$	0.516 ± 0.019
$6 < p_{\mathrm{T}} < 7$	$3.25 < y^* < 4.00$	0.365 ± 0.014
$7 < p_{\mathrm{T}} < 8$	$1.50 < y^* < 2.50$	0.357 ± 0.014
$7 < p_{\mathrm{T}} < 8$	$2.50 < y^* < 3.25$	0.535 ± 0.020
$7 < p_{\mathrm{T}} < 8$	$3.25 < y^* < 4.00$	0.392 ± 0.017
$8 < p_{\mathrm{T}} < 10$	$1.50 < y^* < 2.50$	0.394 ± 0.016
$8 < p_{\mathrm{T}} < 10$	$2.50 < y^* < 3.25$	0.575 ± 0.021
$8 < p_{\mathrm{T}} < 10$	$3.25 < y^* < 4.00$	0.435 ± 0.020
$10 < p_{\mathrm{T}} < 14$	$1.50 < y^* < 2.50$	0.444 ± 0.017
$10 < p_{\mathrm{T}} < 14$	$2.50 < y^* < 3.25$	0.609 ± 0.023
$10 < p_{\mathrm{T}} < 14$	$3.25 < y^* < 4.00$	0.509 ± 0.026

Table 42: Total efficiencies J/ψ in Pbp, in bins of p_{T} and y^* for the tight selection with total uncertainties.

p_{T} bin	y^* bin	ϵ_{tot}
$0 < p_{\mathrm{T}} < 1$	$-3.25 < y^* < -2.50$	0.104 ± 0.009
$0 < p_{\mathrm{T}} < 1$	$-4.00 < y^* < -3.25$	0.255 ± 0.017
$0 < p_{\mathrm{T}} < 1$	$-5.00 < y^* < -4.00$	0.211 ± 0.014
$1 < p_{\mathrm{T}} < 2$	$-3.25 < y^* < -2.50$	0.116 ± 0.009
$1 < p_{\mathrm{T}} < 2$	$-4.00 < y^* < -3.25$	0.251 ± 0.016
$1 < p_{\mathrm{T}} < 2$	$-5.00 < y^* < -4.00$	0.197 ± 0.012
$2 < p_{\mathrm{T}} < 3$	$-3.25 < y^* < -2.50$	0.123 ± 0.008
$2 < p_{\mathrm{T}} < 3$	$-4.00 < y^* < -3.25$	0.265 ± 0.016
$2 < p_{\mathrm{T}} < 3$	$-5.00 < y^* < -4.00$	0.197 ± 0.012
$3 < p_{\mathrm{T}} < 4$	$-3.25 < y^* < -2.50$	0.147 ± 0.009
$3 < p_{\mathrm{T}} < 4$	$-4.00 < y^* < -3.25$	0.313 ± 0.017
$3 < p_{\mathrm{T}} < 4$	$-5.00 < y^* < -4.00$	0.227 ± 0.013
$4 < p_{\mathrm{T}} < 5$	$-3.25 < y^* < -2.50$	0.190 ± 0.010
$4 < p_{\mathrm{T}} < 5$	$-4.00 < y^* < -3.25$	0.372 ± 0.020
$4 < p_{\mathrm{T}} < 5$	$-5.00 < y^* < -4.00$	0.275 ± 0.015
$5 < p_{\mathrm{T}} < 6$	$-3.25 < y^* < -2.50$	0.236 ± 0.012
$5 < p_{\mathrm{T}} < 6$	$-4.00 < y^* < -3.25$	0.435 ± 0.022
$5 < p_{\mathrm{T}} < 6$	$-5.00 < y^* < -4.00$	0.318 ± 0.017
$6 < p_{\mathrm{T}} < 7$	$-3.25 < y^* < -2.50$	0.286 ± 0.015
$6 < p_{\mathrm{T}} < 7$	$-4.00 < y^* < -3.25$	0.463 ± 0.024
$6 < p_{\mathrm{T}} < 7$	$-5.00 < y^* < -4.00$	0.343 ± 0.019
$7 < p_{\mathrm{T}} < 8$	$-3.25 < y^* < -2.50$	0.323 ± 0.017
$7 < p_{\mathrm{T}} < 8$	$-4.00 < y^* < -3.25$	0.497 ± 0.027
$7 < p_{\mathrm{T}} < 8$	$-5.00 < y^* < -4.00$	0.394 ± 0.024
$8 < p_{\mathrm{T}} < 10$	$-3.25 < y^* < -2.50$	0.356 ± 0.019
$8 < p_{\mathrm{T}} < 10$	$-4.00 < y^* < -3.25$	0.529 ± 0.028
$8 < p_{\mathrm{T}} < 10$	$-5.00 < y^* < -4.00$	0.443 ± 0.029
$10 < p_{\mathrm{T}} < 14$	$-3.25 < y^* < -2.50$	0.424 ± 0.024
$10 < p_{\mathrm{T}} < 14$	$-4.00 < y^* < -3.25$	0.568 ± 0.033
$10 < p_{\mathrm{T}} < 14$	$-5.00 < y^* < -4.00$	0.508 ± 0.036

Table 43: Total efficiencies J/ψ in pPb, in bins of p_{T} and y^* for the loose selection with total uncertainties.

p_{T} bin	y^* bin	$\epsilon_{\text{Loose tot}}$
$0 < p_{\mathrm{T}} < 1$	$1.50 < y^* < 2.50$	0.177 ± 0.012
$0 < p_{\mathrm{T}} < 1$	$2.50 < y^* < 3.25$	0.407 ± 0.017
$0 < p_{\mathrm{T}} < 1$	$3.25 < y^* < 4.00$	0.273 ± 0.016
$1 < p_{\mathrm{T}} < 2$	$1.50 < y^* < 2.50$	0.194 ± 0.011
$1 < p_{\mathrm{T}} < 2$	$2.50 < y^* < 3.25$	0.391 ± 0.017
$1 < p_{\mathrm{T}} < 2$	$3.25 < y^* < 4.00$	0.266 ± 0.012
$2 < p_{\mathrm{T}} < 3$	$1.50 < y^* < 2.50$	0.195 ± 0.011
$2 < p_{\mathrm{T}} < 3$	$2.50 < y^* < 3.25$	0.380 ± 0.016
$2 < p_{\mathrm{T}} < 3$	$3.25 < y^* < 4.00$	0.249 ± 0.011
$3 < p_{\mathrm{T}} < 4$	$1.50 < y^* < 2.50$	0.215 ± 0.010
$3 < p_{\mathrm{T}} < 4$	$2.50 < y^* < 3.25$	0.414 ± 0.016
$3 < p_{\mathrm{T}} < 4$	$3.25 < y^* < 4.00$	0.266 ± 0.010
$4 < p_{\mathrm{T}} < 5$	$1.50 < y^* < 2.50$	0.259 ± 0.011
$4 < p_{\mathrm{T}} < 5$	$2.50 < y^* < 3.25$	0.463 ± 0.017
$4 < p_{\mathrm{T}} < 5$	$3.25 < y^* < 4.00$	0.309 ± 0.011
$5 < p_{\mathrm{T}} < 6$	$1.50 < y^* < 2.50$	0.300 ± 0.012
$5 < p_{\mathrm{T}} < 6$	$2.50 < y^* < 3.25$	0.510 ± 0.018
$5 < p_{\mathrm{T}} < 6$	$3.25 < y^* < 4.00$	0.351 ± 0.013
$6 < p_{\mathrm{T}} < 7$	$1.50 < y^* < 2.50$	0.341 ± 0.014
$6 < p_{\mathrm{T}} < 7$	$2.50 < y^* < 3.25$	0.546 ± 0.020
$6 < p_{\mathrm{T}} < 7$	$3.25 < y^* < 4.00$	0.384 ± 0.016
$7 < p_{\mathrm{T}} < 8$	$1.50 < y^* < 2.50$	0.378 ± 0.015
$7 < p_{\mathrm{T}} < 8$	$2.50 < y^* < 3.25$	0.561 ± 0.021
$7 < p_{\mathrm{T}} < 8$	$3.25 < y^* < 4.00$	0.410 ± 0.019
$8 < p_{\mathrm{T}} < 10$	$1.50 < y^* < 2.50$	0.417 ± 0.017
$8 < p_{\mathrm{T}} < 10$	$2.50 < y^* < 3.25$	0.598 ± 0.022
$8 < p_{\mathrm{T}} < 10$	$3.25 < y^* < 4.00$	0.450 ± 0.023
$10 < p_{\mathrm{T}} < 14$	$1.50 < y^* < 2.50$	0.472 ± 0.018
$10 < p_{\mathrm{T}} < 14$	$2.50 < y^* < 3.25$	0.629 ± 0.023
$10 < p_{\mathrm{T}} < 14$	$3.25 < y^* < 4.00$	0.525 ± 0.031

Table 44: Total efficiencies J/ψ in Pbp, in bins of p_{T} and y^* for the loose selection with total uncertainties.

p_{T} bin	y^* bin	$\epsilon_{\text{Loose tot}}$
$0 < p_{\mathrm{T}} < 1$	$-3.25 < y^* < -2.50$	0.138 ± 0.011
$0 < p_{\mathrm{T}} < 1$	$-4.00 < y^* < -3.25$	0.352 ± 0.024
$0 < p_{\mathrm{T}} < 1$	$-5.00 < y^* < -4.00$	0.267 ± 0.016
$1 < p_{\mathrm{T}} < 2$	$-3.25 < y^* < -2.50$	0.154 ± 0.012
$1 < p_{\mathrm{T}} < 2$	$-4.00 < y^* < -3.25$	0.341 ± 0.022
$1 < p_{\mathrm{T}} < 2$	$-5.00 < y^* < -4.00$	0.254 ± 0.014
$2 < p_{\mathrm{T}} < 3$	$-3.25 < y^* < -2.50$	0.158 ± 0.011
$2 < p_{\mathrm{T}} < 3$	$-4.00 < y^* < -3.25$	0.339 ± 0.020
$2 < p_{\mathrm{T}} < 3$	$-5.00 < y^* < -4.00$	0.245 ± 0.013
$3 < p_{\mathrm{T}} < 4$	$-3.25 < y^* < -2.50$	0.180 ± 0.010
$3 < p_{\mathrm{T}} < 4$	$-4.00 < y^* < -3.25$	0.372 ± 0.020
$3 < p_{\mathrm{T}} < 4$	$-5.00 < y^* < -4.00$	0.265 ± 0.014
$4 < p_{\mathrm{T}} < 5$	$-3.25 < y^* < -2.50$	0.222 ± 0.012
$4 < p_{\mathrm{T}} < 5$	$-4.00 < y^* < -3.25$	0.421 ± 0.022
$4 < p_{\mathrm{T}} < 5$	$-5.00 < y^* < -4.00$	0.309 ± 0.016
$5 < p_{\mathrm{T}} < 6$	$-3.25 < y^* < -2.50$	0.266 ± 0.013
$5 < p_{\mathrm{T}} < 6$	$-4.00 < y^* < -3.25$	0.476 ± 0.024
$5 < p_{\mathrm{T}} < 6$	$-5.00 < y^* < -4.00$	0.345 ± 0.018
$6 < p_{\mathrm{T}} < 7$	$-3.25 < y^* < -2.50$	0.311 ± 0.016
$6 < p_{\mathrm{T}} < 7$	$-4.00 < y^* < -3.25$	0.496 ± 0.025
$6 < p_{\mathrm{T}} < 7$	$-5.00 < y^* < -4.00$	0.363 ± 0.021
$7 < p_{\mathrm{T}} < 8$	$-3.25 < y^* < -2.50$	0.346 ± 0.018
$7 < p_{\mathrm{T}} < 8$	$-4.00 < y^* < -3.25$	0.521 ± 0.028
$7 < p_{\mathrm{T}} < 8$	$-5.00 < y^* < -4.00$	0.407 ± 0.026
$8 < p_{\mathrm{T}} < 10$	$-3.25 < y^* < -2.50$	0.375 ± 0.020
$8 < p_{\mathrm{T}} < 10$	$-4.00 < y^* < -3.25$	0.546 ± 0.029
$8 < p_{\mathrm{T}} < 10$	$-5.00 < y^* < -4.00$	0.448 ± 0.031
$10 < p_{\mathrm{T}} < 14$	$-3.25 < y^* < -2.50$	0.440 ± 0.025
$10 < p_{\mathrm{T}} < 14$	$-4.00 < y^* < -3.25$	0.573 ± 0.034
$10 < p_{\mathrm{T}} < 14$	$-5.00 < y^* < -4.00$	0.509 ± 0.038

Table 45: Total efficiencies $\psi(2S)$ in pPb, in bins of p_{T} and y^* for the tight selection with total uncertainties.

p_{T} bin	y^* bin	ϵ_{tot}
$0 < p_{\mathrm{T}} < 1$	$1.50 < y^* < 2.50$	0.181 ± 0.013
$0 < p_{\mathrm{T}} < 1$	$2.50 < y^* < 3.25$	0.399 ± 0.017
$0 < p_{\mathrm{T}} < 1$	$3.25 < y^* < 4.00$	0.266 ± 0.014
$1 < p_{\mathrm{T}} < 2$	$1.50 < y^* < 2.50$	0.186 ± 0.011
$1 < p_{\mathrm{T}} < 2$	$2.50 < y^* < 3.25$	0.378 ± 0.016
$1 < p_{\mathrm{T}} < 2$	$3.25 < y^* < 4.00$	0.253 ± 0.012
$2 < p_{\mathrm{T}} < 3$	$1.50 < y^* < 2.50$	0.187 ± 0.011
$2 < p_{\mathrm{T}} < 3$	$2.50 < y^* < 3.25$	0.359 ± 0.015
$2 < p_{\mathrm{T}} < 3$	$3.25 < y^* < 4.00$	0.237 ± 0.011
$3 < p_{\mathrm{T}} < 4$	$1.50 < y^* < 2.50$	0.190 ± 0.009
$3 < p_{\mathrm{T}} < 4$	$2.50 < y^* < 3.25$	0.373 ± 0.015
$3 < p_{\mathrm{T}} < 4$	$3.25 < y^* < 4.00$	0.236 ± 0.010
$4 < p_{\mathrm{T}} < 5$	$1.50 < y^* < 2.50$	0.220 ± 0.009
$4 < p_{\mathrm{T}} < 5$	$2.50 < y^* < 3.25$	0.410 ± 0.015
$4 < p_{\mathrm{T}} < 5$	$3.25 < y^* < 4.00$	0.265 ± 0.010
$5 < p_{\mathrm{T}} < 6$	$1.50 < y^* < 2.50$	0.256 ± 0.010
$5 < p_{\mathrm{T}} < 6$	$2.50 < y^* < 3.25$	0.457 ± 0.016
$5 < p_{\mathrm{T}} < 6$	$3.25 < y^* < 4.00$	0.306 ± 0.011
$6 < p_{\mathrm{T}} < 7$	$1.50 < y^* < 2.50$	0.296 ± 0.012
$6 < p_{\mathrm{T}} < 7$	$2.50 < y^* < 3.25$	0.497 ± 0.018
$6 < p_{\mathrm{T}} < 7$	$3.25 < y^* < 4.00$	0.343 ± 0.013
$7 < p_{\mathrm{T}} < 8$	$1.50 < y^* < 2.50$	0.330 ± 0.013
$7 < p_{\mathrm{T}} < 8$	$2.50 < y^* < 3.25$	0.525 ± 0.020
$7 < p_{\mathrm{T}} < 8$	$3.25 < y^* < 4.00$	0.368 ± 0.015
$8 < p_{\mathrm{T}} < 10$	$1.50 < y^* < 2.50$	0.369 ± 0.015
$8 < p_{\mathrm{T}} < 10$	$2.50 < y^* < 3.25$	0.556 ± 0.021
$8 < p_{\mathrm{T}} < 10$	$3.25 < y^* < 4.00$	0.414 ± 0.019
$10 < p_{\mathrm{T}} < 14$	$1.50 < y^* < 2.50$	0.420 ± 0.017
$10 < p_{\mathrm{T}} < 14$	$2.50 < y^* < 3.25$	0.601 ± 0.022
$10 < p_{\mathrm{T}} < 14$	$3.25 < y^* < 4.00$	0.460 ± 0.024

Table 46: Total efficiencies $\psi(2S)$ in Pbp, in bins of p_{T} and y^* for the tight selection with total uncertainties.

p_{T} bin	y^* bin	ϵ_{tot}
$0 < p_{\mathrm{T}} < 1$	$-3.25 < y^* < -2.50$	0.137 ± 0.011
$0 < p_{\mathrm{T}} < 1$	$-4.00 < y^* < -3.25$	0.332 ± 0.022
$0 < p_{\mathrm{T}} < 1$	$-5.00 < y^* < -4.00$	0.253 ± 0.016
$1 < p_{\mathrm{T}} < 2$	$-3.25 < y^* < -2.50$	0.146 ± 0.011
$1 < p_{\mathrm{T}} < 2$	$-4.00 < y^* < -3.25$	0.317 ± 0.020
$1 < p_{\mathrm{T}} < 2$	$-5.00 < y^* < -4.00$	0.239 ± 0.015
$2 < p_{\mathrm{T}} < 3$	$-3.25 < y^* < -2.50$	0.151 ± 0.010
$2 < p_{\mathrm{T}} < 3$	$-4.00 < y^* < -3.25$	0.304 ± 0.018
$2 < p_{\mathrm{T}} < 3$	$-5.00 < y^* < -4.00$	0.224 ± 0.013
$3 < p_{\mathrm{T}} < 4$	$-3.25 < y^* < -2.50$	0.156 ± 0.009
$3 < p_{\mathrm{T}} < 4$	$-4.00 < y^* < -3.25$	0.325 ± 0.017
$3 < p_{\mathrm{T}} < 4$	$-5.00 < y^* < -4.00$	0.228 ± 0.013
$4 < p_{\mathrm{T}} < 5$	$-3.25 < y^* < -2.50$	0.186 ± 0.010
$4 < p_{\mathrm{T}} < 5$	$-4.00 < y^* < -3.25$	0.368 ± 0.020
$4 < p_{\mathrm{T}} < 5$	$-5.00 < y^* < -4.00$	0.258 ± 0.014
$5 < p_{\mathrm{T}} < 6$	$-3.25 < y^* < -2.50$	0.221 ± 0.011
$5 < p_{\mathrm{T}} < 6$	$-4.00 < y^* < -3.25$	0.413 ± 0.021
$5 < p_{\mathrm{T}} < 6$	$-5.00 < y^* < -4.00$	0.299 ± 0.016
$6 < p_{\mathrm{T}} < 7$	$-3.25 < y^* < -2.50$	0.259 ± 0.013
$6 < p_{\mathrm{T}} < 7$	$-4.00 < y^* < -3.25$	0.457 ± 0.024
$6 < p_{\mathrm{T}} < 7$	$-5.00 < y^* < -4.00$	0.331 ± 0.019
$7 < p_{\mathrm{T}} < 8$	$-3.25 < y^* < -2.50$	0.296 ± 0.016
$7 < p_{\mathrm{T}} < 8$	$-4.00 < y^* < -3.25$	0.485 ± 0.026
$7 < p_{\mathrm{T}} < 8$	$-5.00 < y^* < -4.00$	0.361 ± 0.022
$8 < p_{\mathrm{T}} < 10$	$-3.25 < y^* < -2.50$	0.334 ± 0.018
$8 < p_{\mathrm{T}} < 10$	$-4.00 < y^* < -3.25$	0.519 ± 0.028
$8 < p_{\mathrm{T}} < 10$	$-5.00 < y^* < -4.00$	0.398 ± 0.026
$10 < p_{\mathrm{T}} < 14$	$-3.25 < y^* < -2.50$	0.379 ± 0.021
$10 < p_{\mathrm{T}} < 14$	$-4.00 < y^* < -3.25$	0.557 ± 0.032
$10 < p_{\mathrm{T}} < 14$	$-5.00 < y^* < -4.00$	0.446 ± 0.032

6.7 Total efficiency ratios

The ratios of the total efficiency between the J/ψ and the $\psi(2S)$ for the tight PID selections are needed to determine the cross-section ratio. They are shown in Fig. 39. The errors are the statistical uncertainties from the simulation statistics and the systematic uncertainties affecting the efficiencies and detailed in the following section, added quadratically. The numerical results are given in Tables 47 and 48.

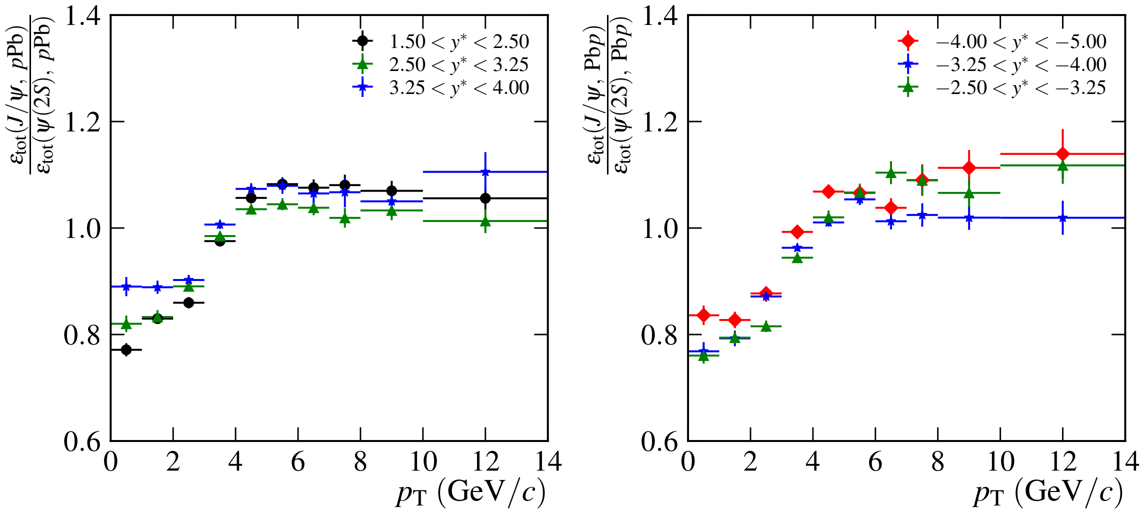

Figure 39: Total efficiency $\epsilon_{\rm tot}^{J/\psi}/\epsilon_{\rm tot}^{\psi(2S)}$ ratio as a function of $p_{\rm T}$ in different y^* bins for left: tight selection in pPb, right: tight selection in Pbp. The displayed uncertainty corresponds to the total uncertainty.

Table 47: $\psi(2S)$ over J/ψ total efficiency ratios in pPb, in bins of p_{T} and y^* for the tight selection with total uncertainties.

p_{T} bin	y^* bin	$\epsilon_{\mathrm{tot}}^{J/\psi}/\epsilon_{\mathrm{tot}}^{\psi(2S)}$
$0 < p_{\mathrm{T}} < 1$	$1.50 < y^* < 2.50$	0.771 ± 0.012
$0 < p_{\mathrm{T}} < 1$	$2.50 < y^* < 3.25$	0.820 ± 0.016
$0 < p_{\mathrm{T}} < 1$	$3.25 < y^* < 4.00$	0.890 ± 0.018
$1 < p_{\mathrm{T}} < 2$	$1.50 < y^* < 2.50$	0.830 ± 0.007
$1 < p_{\mathrm{T}} < 2$	$2.50 < y^* < 3.25$	0.833 ± 0.013
$1 < p_{\mathrm{T}} < 2$	$3.25 < y^* < 4.00$	0.889 ± 0.012
$2 < p_{\mathrm{T}} < 3$	$1.50 < y^* < 2.50$	0.860 ± 0.011
$2 < p_{\mathrm{T}} < 3$	$2.50 < y^* < 3.25$	0.890 ± 0.009
$2 < p_{\mathrm{T}} < 3$	$3.25 < y^* < 4.00$	0.902 ± 0.009
$3 < p_{\mathrm{T}} < 4$	$1.50 < y^* < 2.50$	0.975 ± 0.010
$3 < p_{\mathrm{T}} < 4$	$2.50 < y^* < 3.25$	0.985 ± 0.007
$3 < p_{\mathrm{T}} < 4$	$3.25 < y^* < 4.00$	1.006 ± 0.008
$4 < p_{\mathrm{T}} < 5$	$1.50 < y^* < 2.50$	1.057 ± 0.010
$4 < p_{\mathrm{T}} < 5$	$2.50 < y^* < 3.25$	1.035 ± 0.009
$4 < p_{\mathrm{T}} < 5$	$3.25 < y^* < 4.00$	1.073 ± 0.011
$5 < p_{\mathrm{T}} < 6$	$1.50 < y^* < 2.50$	1.082 ± 0.013
$5 < p_{\mathrm{T}} < 6$	$2.50 < y^* < 3.25$	1.045 ± 0.011
$5 < p_{\mathrm{T}} < 6$	$3.25 < y^* < 4.00$	1.079 ± 0.015
$6 < p_{\mathrm{T}} < 7$	$1.50 < y^* < 2.50$	1.076 ± 0.016
$6 < p_{\mathrm{T}} < 7$	$2.50 < y^* < 3.25$	1.038 ± 0.014
$6 < p_{\mathrm{T}} < 7$	$3.25 < y^* < 4.00$	1.065 ± 0.021
$7 < p_{\mathrm{T}} < 8$	$1.50 < y^* < 2.50$	1.081 ± 0.020
$7 < p_{\mathrm{T}} < 8$	$2.50 < y^* < 3.25$	1.019 ± 0.018
$7 < p_{\mathrm{T}} < 8$	$3.25 < y^* < 4.00$	1.067 ± 0.028
$8 < p_{\mathrm{T}} < 10$	$1.50 < y^* < 2.50$	1.070 ± 0.019
$8 < p_{\mathrm{T}} < 10$	$2.50 < y^* < 3.25$	1.033 ± 0.018
$8 < p_{\mathrm{T}} < 10$	$3.25 < y^* < 4.00$	1.050 ± 0.028
$10 < p_{\mathrm{T}} < 14$	$1.50 < y^* < 2.50$	1.056 ± 0.022
$10 < p_{\mathrm{T}} < 14$	$2.50 < y^* < 3.25$	1.013 ± 0.023
$10 < p_{\mathrm{T}} < 14$	$3.25 < y^* < 4.00$	1.105 ± 0.037

Table 48: $\psi(2S)$ over J/ψ total efficiency ratios in Pbp, in bins of p_{T} and y^{*} for the tight selection. The uncertainties are only the statistical ones.

p_{T} bin	y^{*} bin	$\epsilon_{\mathrm{tot}}^{J/\psi}/\epsilon_{\mathrm{tot}}^{\psi(2S)}$
$0 < p_{\mathrm{T}} < 1$	$2.32 < y^{*} < 1.57$	0.760 ± 0.015
$0 < p_{\mathrm{T}} < 1$	$3.07 < y^{*} < 2.32$	0.768 ± 0.017
$0 < p_{\mathrm{T}} < 1$	$4.07 < y^{*} < 3.07$	0.836 ± 0.018
$1 < p_{\mathrm{T}} < 2$	$2.32 < y^{*} < 1.57$	0.794 ± 0.012
$1 < p_{\mathrm{T}} < 2$	$3.07 < y^{*} < 2.32$	0.793 ± 0.015
$1 < p_{\mathrm{T}} < 2$	$4.07 < y^{*} < 3.07$	0.827 ± 0.015
$2 < p_{\mathrm{T}} < 3$	$2.32 < y^{*} < 1.57$	0.815 ± 0.011
$2 < p_{\mathrm{T}} < 3$	$3.07 < y^{*} < 2.32$	0.871 ± 0.010
$2 < p_{\mathrm{T}} < 3$	$4.07 < y^{*} < 3.07$	0.877 ± 0.009
$3 < p_{\mathrm{T}} < 4$	$2.32 < y^{*} < 1.57$	0.944 ± 0.010
$3 < p_{\mathrm{T}} < 4$	$3.07 < y^{*} < 2.32$	0.963 ± 0.007
$3 < p_{\mathrm{T}} < 4$	$4.07 < y^{*} < 3.07$	0.993 ± 0.008
$4 < p_{\mathrm{T}} < 5$	$2.32 < y^{*} < 1.57$	1.020 ± 0.013
$4 < p_{\mathrm{T}} < 5$	$3.07 < y^{*} < 2.32$	1.011 ± 0.008
$4 < p_{\mathrm{T}} < 5$	$4.07 < y^{*} < 3.07$	1.068 ± 0.010
$5 < p_{\mathrm{T}} < 6$	$2.32 < y^{*} < 1.57$	1.067 ± 0.017
$5 < p_{\mathrm{T}} < 6$	$3.07 < y^{*} < 2.32$	1.054 ± 0.011
$5 < p_{\mathrm{T}} < 6$	$4.07 < y^{*} < 3.07$	1.066 ± 0.013
$6 < p_{\mathrm{T}} < 7$	$2.32 < y^{*} < 1.57$	1.104 ± 0.022
$6 < p_{\mathrm{T}} < 7$	$3.07 < y^{*} < 2.32$	1.013 ± 0.015
$6 < p_{\mathrm{T}} < 7$	$4.07 < y^{*} < 3.07$	1.038 ± 0.018
$7 < p_{\mathrm{T}} < 8$	$2.32 < y^{*} < 1.57$	1.090 ± 0.028
$7 < p_{\mathrm{T}} < 8$	$3.07 < y^{*} < 2.32$	1.025 ± 0.022
$7 < p_{\mathrm{T}} < 8$	$4.07 < y^{*} < 3.07$	1.090 ± 0.030
$8 < p_{\mathrm{T}} < 10$	$2.32 < y^{*} < 1.57$	1.066 ± 0.027
$8 < p_{\mathrm{T}} < 10$	$3.07 < y^{*} < 2.32$	1.020 ± 0.023
$8 < p_{\mathrm{T}} < 10$	$4.07 < y^{*} < 3.07$	1.113 ± 0.034
$10 < p_{\mathrm{T}} < 14$	$2.32 < y^{*} < 1.57$	1.118 ± 0.035
$10 < p_{\mathrm{T}} < 14$	$3.07 < y^{*} < 2.32$	1.019 ± 0.032
$10 < p_{\mathrm{T}} < 14$	$4.07 < y^{*} < 3.07$	1.139 ± 0.047

7 Systematic uncertainties

The systematic uncertainties affecting the various quantities measured in the analysis are reported in this section. Some uncertainties are correlated between bins. The correlation of these uncertainties with the *pp* reference cross-section is also detailed. A large systematic uncertainty is due to the unknown polarisation of the J/ψ and $\psi(2S)$ mesons at production. In this analysis, this effect is ignored, assuming they are produced un-polarised. This is justified by the fact that the polarisation measured in *pp* collisions at similar energies is small. Note that this is not true for J/ψ from b decays which have a large polarisation in the decay of the b hadrons, but this polarisation is largely diluted when measuring it with respect to the detector axis and has an negligible effect on the efficiencies.

7.1 Monte Carlo statistics

This uncertainty is the statistical error on the individual efficiencies, due to the finite size of the simulation samples. This uncertainty is uncorrelated between bins and measurements. It was computed for the total efficiency. The uncertainty varies from 0.03% (0.03%) to 1.7% (2.0%) in *p*Pb for J/ψ ($\psi(2S)$) and from 0.04% (0.03%) to 4.0% (1.7%) in Pb*p* for J/ψ ($\psi(2S)$).

7.2 Signal extraction

The choice of the fit model for the mass and t_z distributions affects the number of events. The uncertainty associated with the choice of the signal mass function is estimated using a different function, namely the sum of a Gaussian function and a Crystal Ball function instead of the single Crystal Ball function used in the nominal fit. Figure 40 shows the distribution of the ratios of the number of events obtained for the nominal and alternate fit models. An uncertainty equal to the RMS of the distribution, 2.2%, is then used, associated with the mass fit model. This uncertainty is correlated between bins and between *p*Pb and Pb*p*.

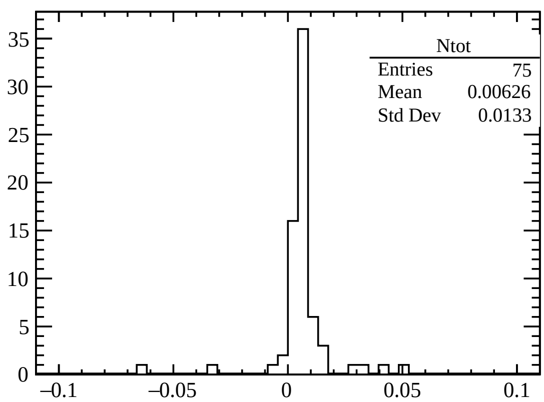

Figure 40: Ratio of number of signal events obtained with the nominal fit (single Crystal Ball function) and the alternate fit (Crystal Ball plus Gaussian functions).

7.3 Particle multiplicity

Since the tracking and the PID efficiencies depend on the detector occupancy, different distributions of particle multiplicities in signal J/ψ or $\psi(2S)$ events could lead to a systematic bias in the determination of the $\psi(2S)$ cross-section and of the ratio with respect to the J/ψ production cross-section, since the data-driven corrections use J/ψ events as a calibration candle. In order to control this effect, the inclusive raw yield ratio between $\psi(2S)$ and J/ψ is extracted in the three different rapidity bins considered in this analysis in both collision systems as function of the number of SPD hits and of VELO clusters.

Figure 41 shows the ratios in pPb collisions and Fig.42 shows the corresponding ratio in Pbp collisions. Within the statistical limitation of the $\psi(2S)$ sample, no significant deviation can be found in the multiplicity range, where the efficiency start to drop significantly. Hence we do not assign any systematic uncertainty due to these differences.

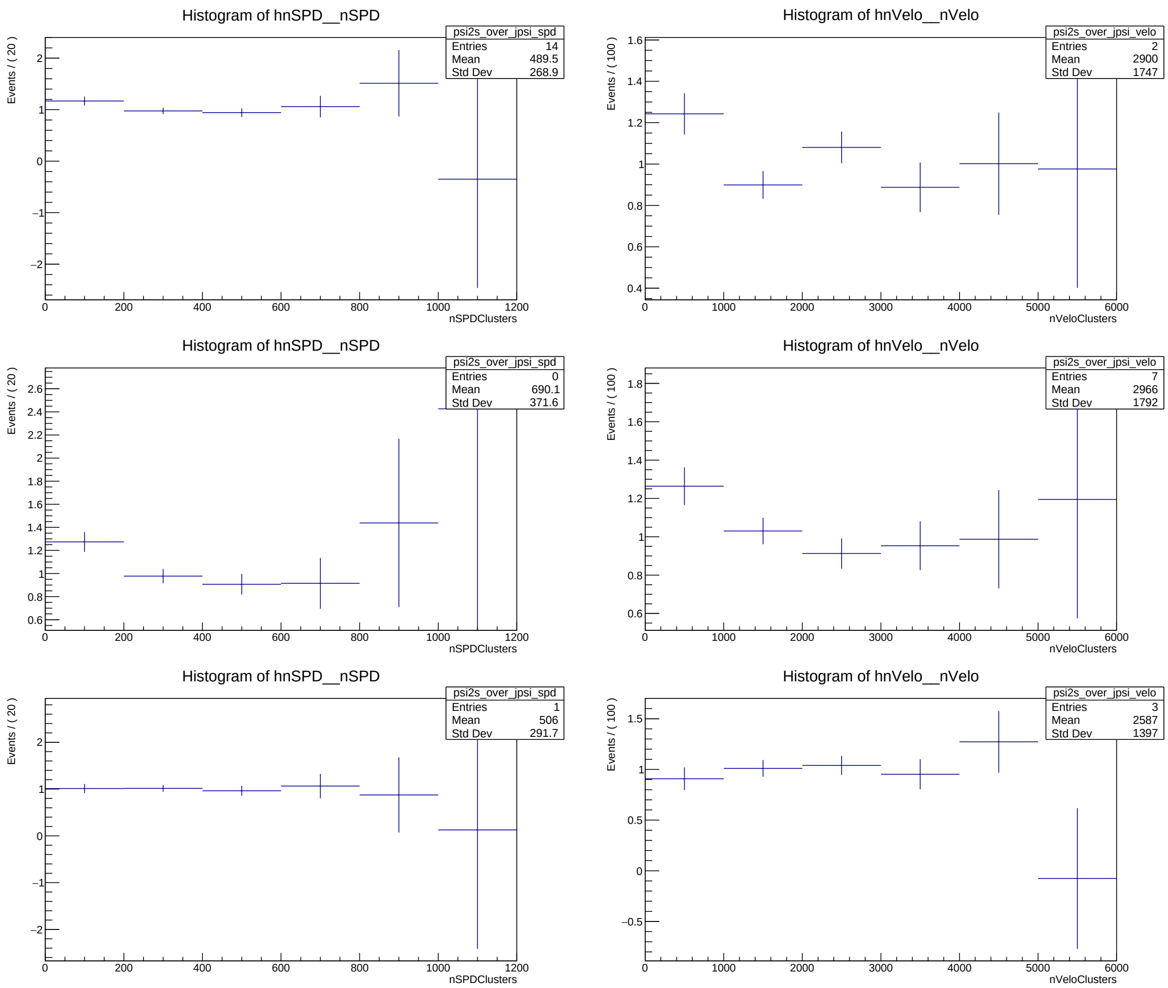

Figure 41: Ratio of raw yields of $\psi(2S)$ and J/ψ in the rapidity bins in the LHCb frame from top to bottom: $1.5 < y^* < 2.5$, $2.5 < y^* < 3.25$ and $3.25 < y^* < 4.0$ in pPb collisions as a function of the number of SPD hits (right) and of the number of VELO clusters. All distributions are divided by their respective integral for normalisation before the different species are divided by each other.

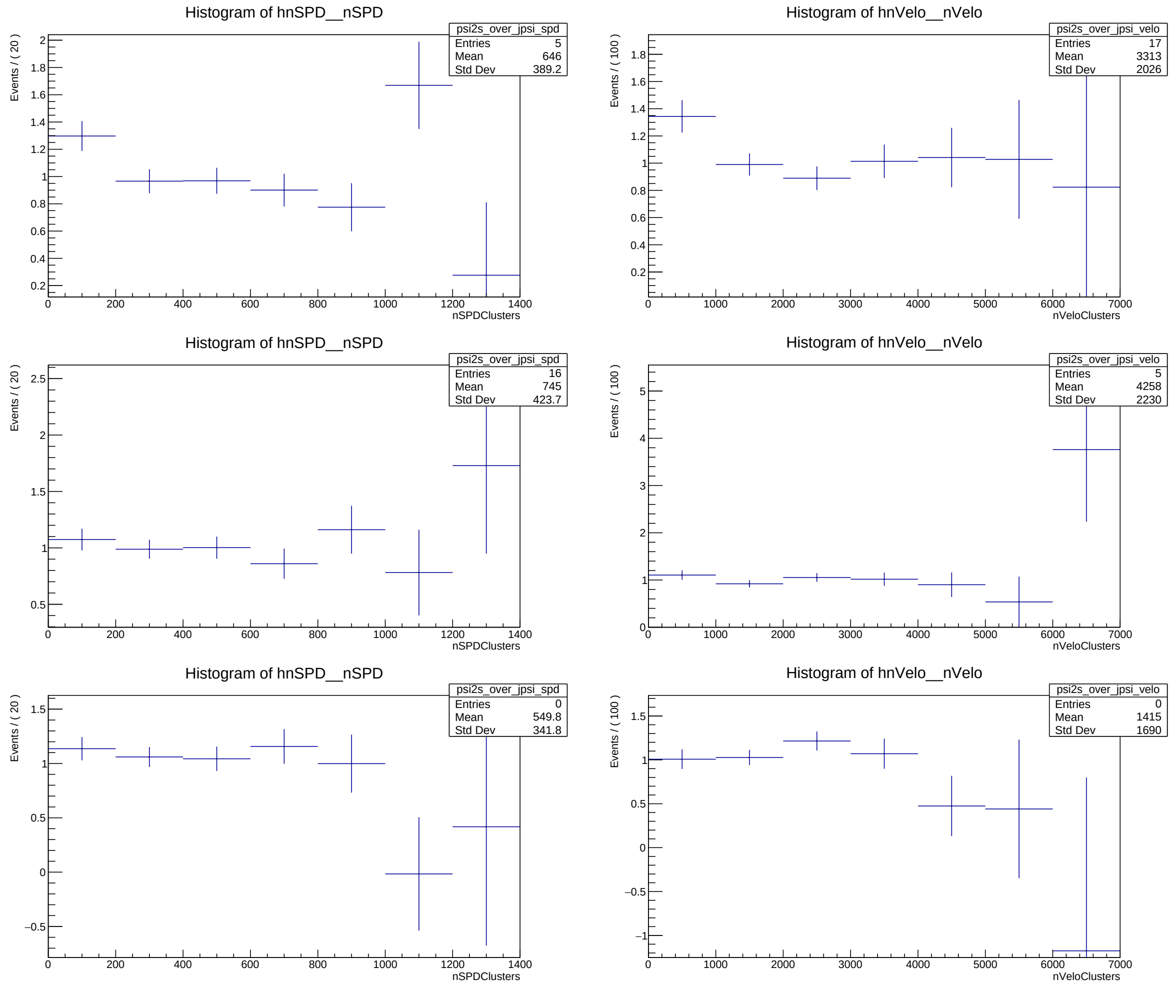

Figure 42: Ratio of raw yields of $\psi(2S)$ and J/ψ normalized to their respective total integrals before division in the rapidity bins in the LHCb frame from top to bottom: $-3.25 < y^* < -2.5$, $-4 < y^* < -3.25$ and $-5 < y^* < -4$ in Pbp collisions as a function of the number of SPD hits (right) and of the number of VELO clusters. All distributions are divided by their respective integral for normalisation before the difference species are divided by each other.

7.4 Bin to bin migration

Due to finite resolution of the p_{T} and y measurements, events can be counted in a wrong bin. However, the resolutions are small compared to the bin widths used for this measurement. Figure 43 shows the comparison of true and reconstructed values of p_{T} and y (in two example bins) of the Monte Carlo candidates and the bin to bin migration effect is estimated to be less than 1% and, therefore, neglected.

7.5 Tracking efficiency

The tracking efficiency correction tables have uncertainties coming from three sources: the statistics of the calibration sample, the signal extraction uncertainty and the offline selection uncertainty. First, the uncertainty on cross-sections are discussed; the cancellation of the involved efficiencies in the $\psi(2S)$ to J/ψ cross-section ratio is explained afterwards. The signal extraction systematic uncertainty for the tracking efficiency, described in

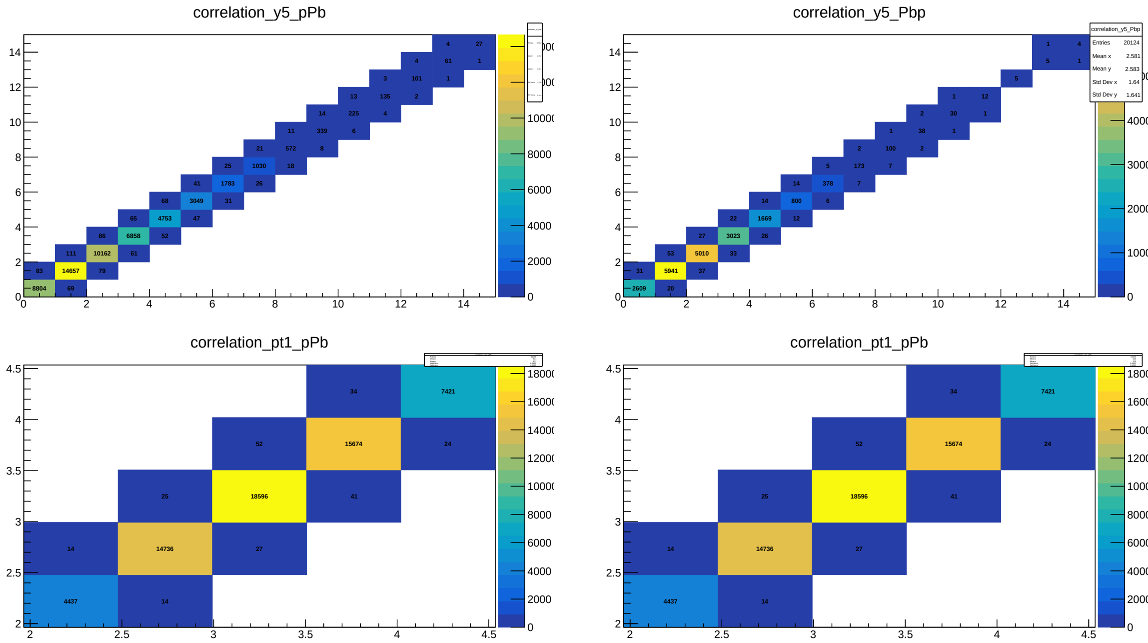

Figure 43: Effect of bin to bin migration in the simulation. *y-axis*: generator-level values, *x-axis*: reconstructed values. The top plots show the bin to bin migration effect for p_{T} (for the most forward rapidity bin), while the bottom plots show the effect on the rapidity (for the bin $0 < p_{\mathrm{T}} < 1\,\mathrm{GeV}/c$). Left: pPb, right: Pbp.

Sect. 6.2, largely cancels in the efficiency calculation. However for bins where the signal purity is small, especially in the "pre-matched" sample, the signal yield is found to be dependent on the mass window in the fit (essentially because of the background shape). For the high purity bins, the effect is much smaller than the statistical uncertainty. The variation of the efficiency in the different mass windows in each bin is considered as systematic uncertainty, as shown in Fig. 44.

The effect of the additional offline selections is checked with the pPb sample. The tracking efficiency in both data and simulation is calculated again without these cuts. It is found that for the simulation the efficiency changes by less than 0.1%, while for data the variation of the efficiency is of order of few percents as shown in Fig. 45. The variation of the efficiency in each bin is considered as a systematic uncertainty per track, correlated in all bins, and is supposed to be identical for the forward and the backward samples. The total uncertainty from these three effects, obtained adding them in quadrature, varies from 2.0% (1.7%) to 3.0% (3.5%) for pPb and from 4.0% (4.0%) to 5.6% (5.5%) for Pbp for J/ψ ($\psi(2S)$).

The long method has an uncertainty of 0.8% per track, as suggested by the tracking group [56]. The tracking uncertainties are correlated between bins.

For the cross-section ratio between $\psi(2S)$ and J/ψ, the *method* uncertainty fully cancels. For the estimation of the correlation of the uncertaintes in the tracking efficiency tables, the following procedure is employed:

- A Gaussian random number is generated for each bin of the look-up table separately according to the bin uncertainty.

- For a given "randomised" look-up table, the tracking efficiency of the $\psi(2S)$ and

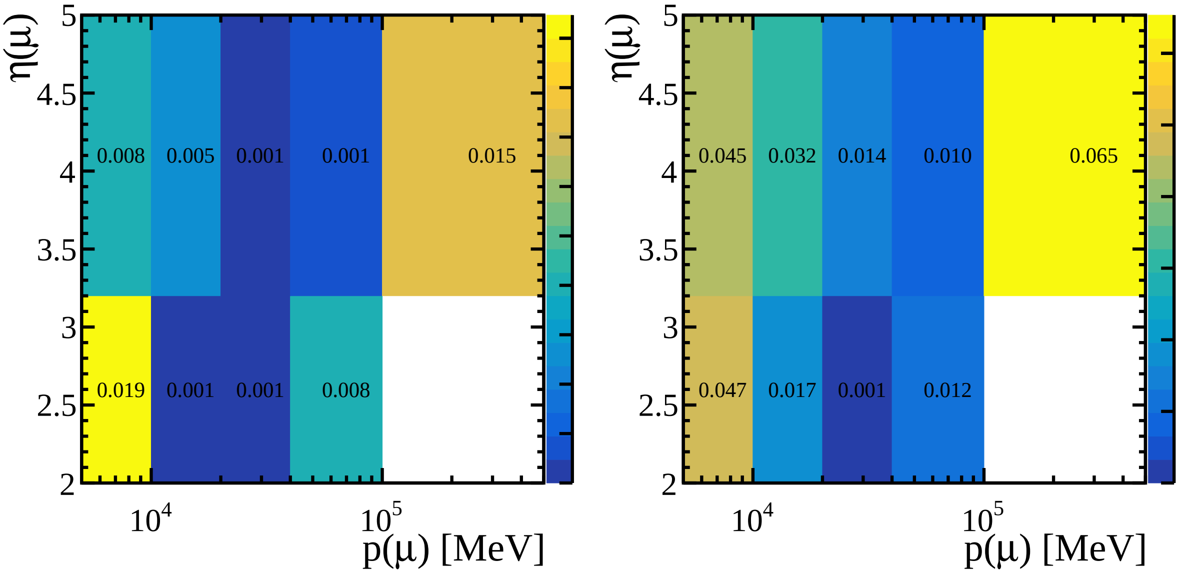

Figure 44: Relative systematic uncertainty due to signal extraction for the tracking efficiency computation. Left: pPb, right: Pbp.

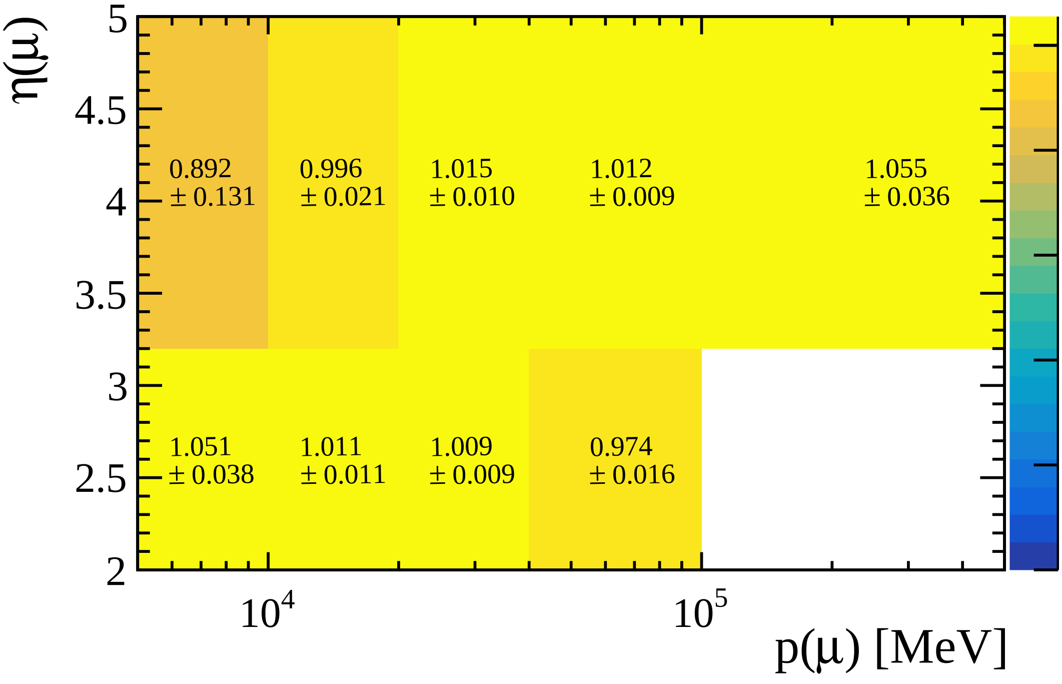

Figure 45: Ratio of probe track matching efficiency with and without additional offline selections in the pPb sample.

J/ψ is evaluated in the kinematic bins of the analysis. The ratio of the tracking efficiency is formed after looping over all simulation candidates of $\psi(2S)$ and J/ψ and for the given look-up table.

- The process is repeated 1000 times. Each time, the efficiency is extracted.

- As estimate of the uncertainty in the efficiency, the root mean square of the efficiency ratio distribution over all 1000 trials is determined.

The extracted numbers range between 0.0 and 0.1 %. They are negligibly small at large pair-rapidity and large pair-p_T where the kinematic difference between the J/ψ and ψ(2S) is smallest and where the tracks are ending in the same kinematic bins for both species. These uncertainties are attached on the ratios of reconstruction efficiencies between J/ψ and $\psi(2S)$.

7.6 Selection efficiency

7.6.1 Global event cut

The large NoBias sample gives a reliable way to compute directly on data the efficiency of the global event cut on the number of VELO clusters. The precision on the efficiency is equal to 0.1% given the large sample collected of NoBias triggered events. This uncertainty can be neglected for the final result.

7.6.2 Primary vertex reconstruction efficiency

The primary vertex reconstruction efficiency is taken from *pp* simulations where it is equal to 100%. Given the larger particle multiplicity in *p*Pb collisions with respect to *pp* collisions, we assume that the PV finding is also fully efficient for this analysis.

7.6.3 Other selection requirements

The efficiency for the selection cut on the track χ^2 lower than 3 is cross-checked comparing the distributions of this variable between data and simulation. In Monte Carlo, candidates are required to be truth matched, while for data the signal shape is obtained subtracting the combinatorial background with the sPlot technique. In Fig. 46 (right) it is possible to see that, although the shape of the distribution is not perfectly reproduced in simulation, the chosen cut is fully efficient (less than 0.1% of candidates fall above the cut). The track ghost probability distribution is shown in Fig. 46 (left). In this case, the value chosen for the cut corresponds to the default cut applied at the reconstruction level (< 0.4).

7.7 PID efficiency

The PID efficiency uncertainty has the following sources:

1. The uncertainty induced by the finite statistics of the calibration sample in *pp* data,

2. The uncertainty due to the binning choice of the correction tables for the muons,

3. The uncertainty due to the usage of sWeights to derive the correction tables, equal to 0.1% [57].

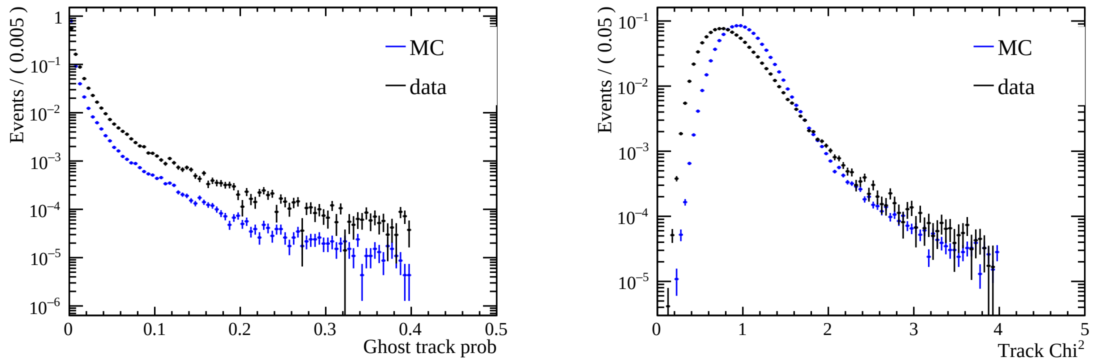

Figure 46: Comparison between pPb simulation (blue) and data (black): the track ghost probability distribution is shown on the left and the track χ^2 distribution on the right.

First, we discuss the uncertainty on the absolute cross-section measurements. The uncertainty due to the binning choice is determined by changing the binning schemes for the calibration tables, for the variables: p, η and SPD multiplicity. The PID efficiencies are recomputed with these new tables and the largest deviation between all different cases is chosen as systematic uncertainty. The relative uncertainty due to the choice of calibration table binning varies from being negligible to 4.1%, 4.1%, 2.5% and 3.0% for the J/ψ tight selection in pPb, for the J/ψ tight selection in Pbp, the $\psi(2S)$ selection in pPb and $\psi(2S)$ selection in Pbp, respectively, depending on the analysis bin. The total uncertainty due to the PID, obtained adding in quadrature the different sources, varies from 0.4% (0.4%) to 4.3% (2.8%) for pPb tight J/ψ ($\psi(2S)$) and from 0.8% (0.7%) to 4.4% (3.1%) for Pbp for tight J/ψ ($\psi(2S)$).

The uncertainties on the cross-section ratios related to the statistical uncertainty of the tables are extracted in the same way as for the tracking efficiency. The uncertainty is always below the sensitivity of the method. We hence assume that this uncertainty fully cancels with respect to other uncertainty sources. In addition, the variation of the granularity of the correction tables as function of p and η enters the uncertainty on the efficiency ratio. The efficiency at the di-muon level is determined for every variation separately and the variation is taken as systematic uncertainty. This uncertainty ranges between being negligible and 1.7% (2.0%) in pPb (Pbp) and is the only significant contribution to the systematic uncertainty on the efficiency ratio.

As a cross check, the J/ψ cross-section is compared between the tight and the loose selections. The ratios are reported in Fig. 47 for the prompt component. Apart from a possible deviation in the lowest p_{T}-bin and all rapidities, the ratio is compatible with unity for pPb collisions. The ratio for Pbp shows a systematic difference with respect to unity. This is attributed to the effect of the particle multiplicity on the PID efficiency, not completely corrected by the weighting of the pp calibration tables.

7.8 Trigger efficiency

The systematic uncertainties on the absolute value of the trigger efficiencies are determined in the same way as explained in the analysis note of the J/ψ production in pPb and Pbp

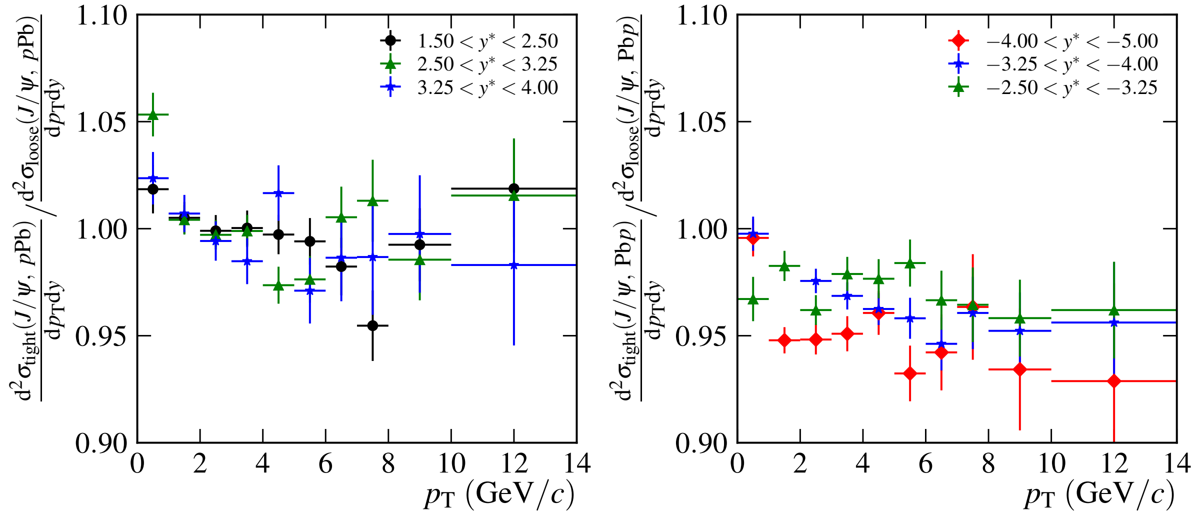

Figure 47: Cross-section ratio for prompt J/ψ with the tight and loose PID selections in (left) pPb and (right) Pbp. Systematic uncertainties are assumed correlated and statistic uncertainties uncorrelated.

with the loose selection [33]. For the uncertainty determination on the cross-section ratio, the HLT1 and the L0 steps are considered separately. The HLT1 trigger efficiency ratio is found to be consistent with unity in simulations within statistical uncertainties, between the J/ψ and the $\psi(2S)$ in all kinematic bins. There is no uncertainty considered for this efficiency step.

The uncertainty on the L0 efficiency ratio $\epsilon_{\text{tri,J}/\psi}/\epsilon_{\text{tri},\psi(2\text{S})}$ that enters as uncertainty of the cross-section ratio between J/ψ and $\psi(2S)$ is determined in the following way:

- Via a tag-and-probe method using the J/ψ samples in simulation and in data, efficiency maps are determined for single μ^+ or μ^- in two dimensions (η and p_{T}). The maps are shown in Fig. 48 and 49 for pPb and Pbp.

- The simulation candidates of $\psi(2S)$ and J/ψ after all selections are filtered with these L0-trigger efficiency maps in order to derive four pair-level L0 trigger efficiencies in the kinematic bins of the analysis. The L0-trigger efficiencies derived in this way are shown in Fig. 50 for J/ψ and in Fig. 51 for $\psi(2S)$.

- Finally, the double ratio $\frac{\epsilon_{\text{tri,J}/\psi,\text{data}-\text{map}}/\epsilon_{\text{tri},\psi(2\text{S}),\text{data}-\text{map}}}{\epsilon_{\text{tri,J}/\psi,\text{simu}-\text{map}}/\epsilon_{\text{tri},\psi(2\text{S}),\text{simu}-\text{map}}}$ maps are extracted. This ratio is shown in Fig. 52.

In Fig. 48 and 49, a large discrepancy is observed at low η and p_{T}, at the edge of the single track acceptance. It was verified that this single track trigger efficiency discrepancy has a negligible impact on the di-muon efficiency that uses a logical `OR` to obtain the trigger efficiency. This was verified by using the positive charge track map artificially for both μ^+ and μ^- and comparing the outcome on the di-muon efficiency.

As additional cross-checks, the single track efficiency maps are also extracted based on the $\psi(2S)$ simulation instead of the J/ψ simulation. They are shown for the pPb configuration in Fig. 53. The derived di-muon efficiencies are found to be very similar that those from the J/ψ tables that can be seen in Fig. 54. The simple simulation to data

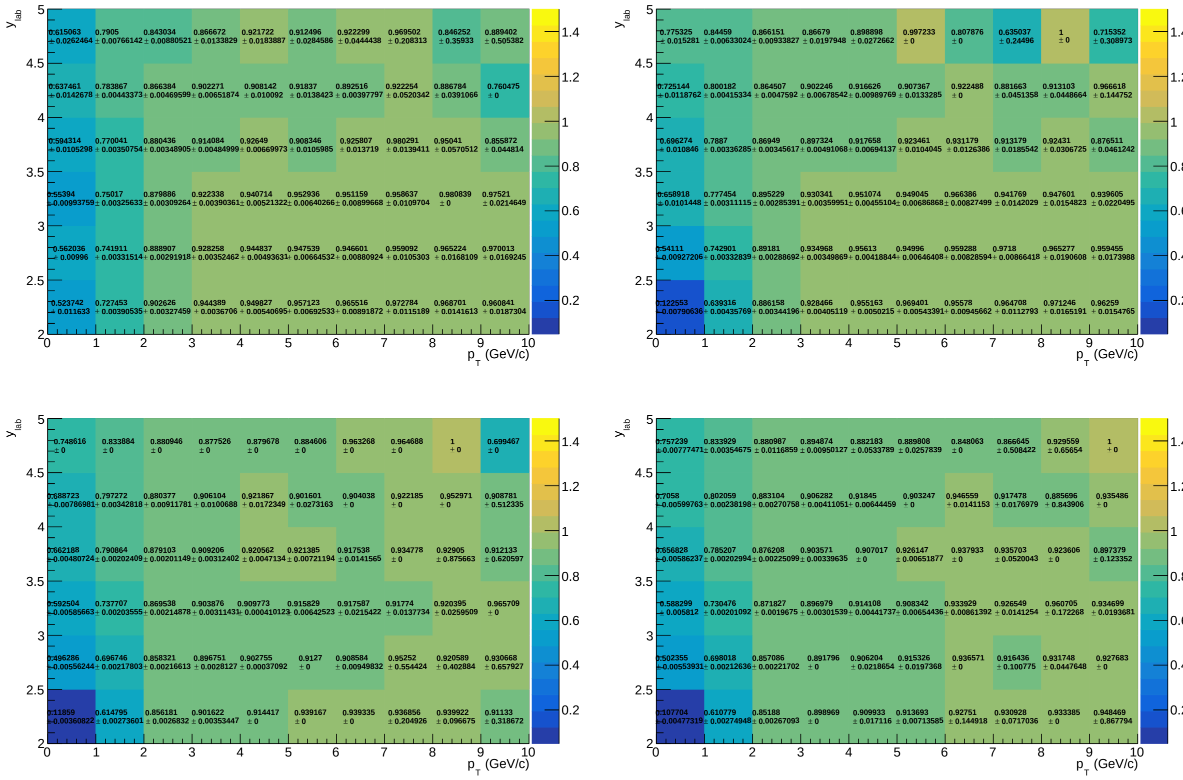

Figure 48: The upper row shows the single track trigger efficiency maps for data for μ^- (left) and μ^+ (right) in the pPb collision system. The lower row shows the single track trigger efficiency map from the same tag and probe method used in data and applied here on simulation for μ^- (left) and μ^+ (right) in the pPb collision system. The vertical axis represents the track η, the horizonal axis the track p_{T}.

efficiency ratio shows significant differences with respect to unity as found for the J/ψ cross-section measurement in pPb at 8.2 TeV. The double ratio discrepancies from unity are found to be very close to the statistical uncertainties. For the final uncertainty, the deviation from unity was taken as uncertainty, when exceeding one standard deviation of the statistical uncertainty and the statistical uncertainty, when the deviation from unity was found to be smaller than the latter. In lack of statistics for the efficiency maps via the tag-and-probe method, the uncertainty for the last investigated bin from 10 to 14 GeV/c was set to 0 considering that the systematic uncertainty is negligible compared to the statistical uncertainty and the track-level kinematic differences are the smallest between the J/ψ and the $\psi(2S)$. Tables 49 and 50 summarise the considered trigger uncertainties affecting the cross-section ratio.

7.9 Luminosity

The luminosity is determined using the same procedure than for the 2013 pPb run [58]. Only van der Meer scans were used for this determination. The relative uncertainties on the pPb luminosity is 2.6% and the one on the Pbp luminosity is 2.5%, correlated amongst bins.

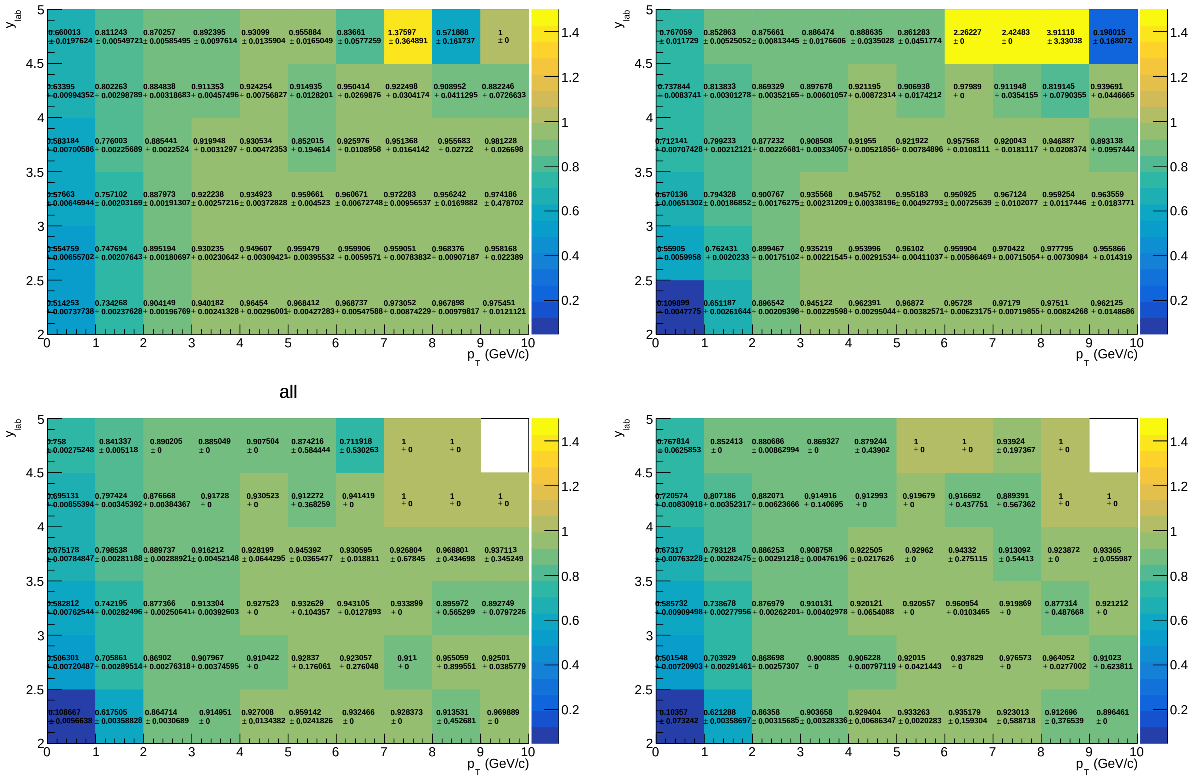

Figure 49: The upper row shows the single track trigger efficiency maps for data for μ^- (left) and μ^+ (right) in the Pbp collision system. The lower row shows the single track trigger efficiency map from the same tag and probe method used in data and applied here on simulation for μ^- (left) and μ^+ (right) in the Pbp collision system. The vertical axis represents the track η, the horizonal axis the track p_{T}.

7.10 Summary

Table 51 summarizes all systematic uncertainties affecting the measurements presented in this note for the cross-section ratio. The correlated systematic uncertainties are assumed to be uncorrelated with the similar ones for pp.

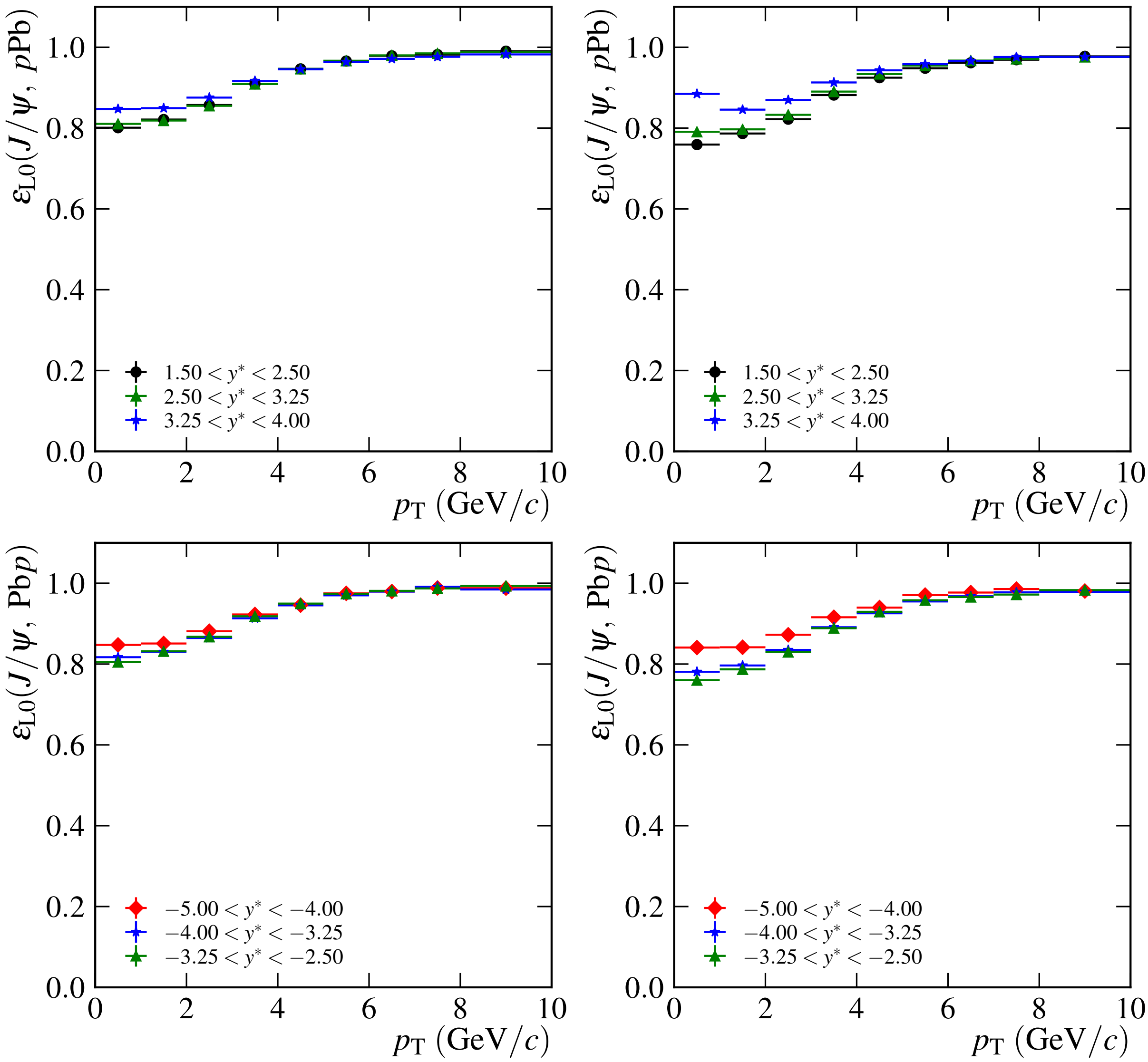

Figure 50: L0 trigger efficiencies, based on the tag-and-probe method, for J/ψ kinematic variables. Top left: pPb based on the data single muon trigger efficiency map. Top right: pPb based on the simulation single muon trigger efficiency map. Bottom left: Pbp based on the data single muon trigger efficiency map. Bottom right: Pbp based on simulation trigger efficiency map.

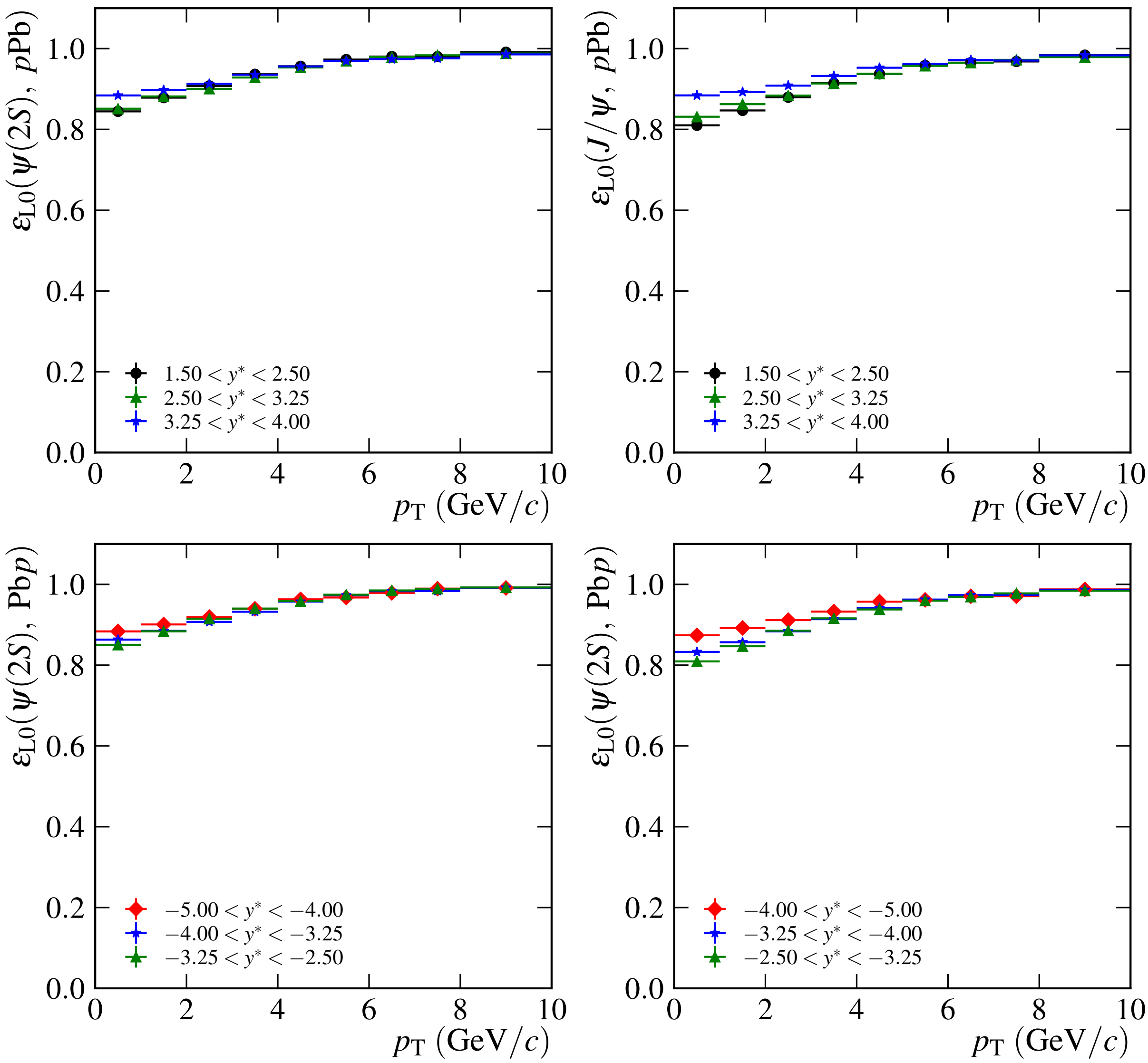

Figure 51: L0 trigger efficiencies, based on the tag-and-probe method, for $\psi(2S)$ kinematic variables. Top left: pPb based on the data single muon trigger efficiency map. Top right: pPb based on the simulation single muon trigger efficiency map. Bottom left: Pbp based on the data single muon trigger efficiency map. Bottom right: Pbp based on simulation trigger efficiency map.

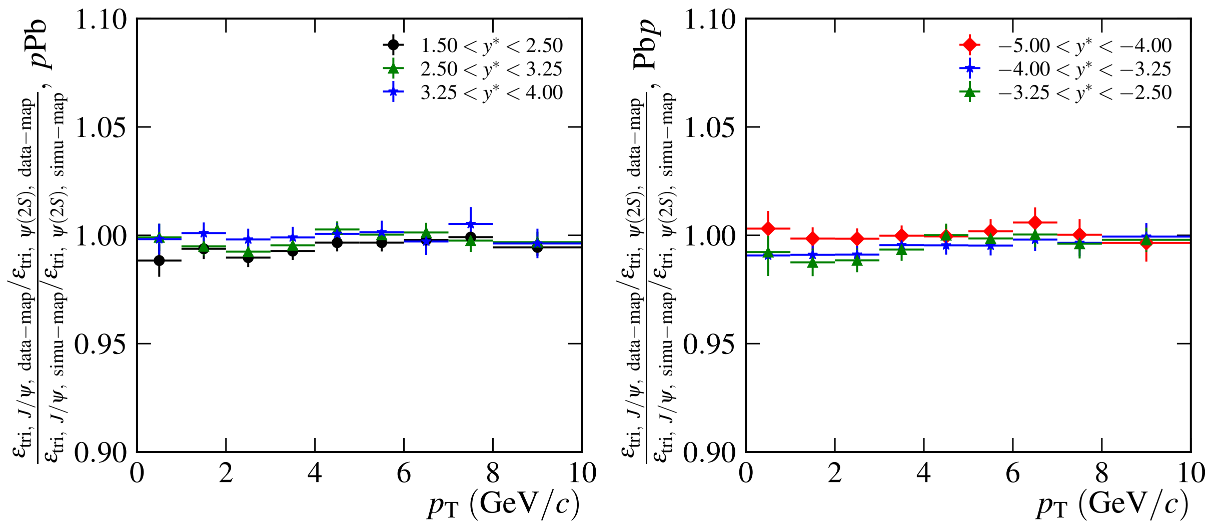

Figure 52: Trigger efficiency double ratio between $\psi(2S)$ and J/ψ data and simulation in pPb (left) and in Pbp (right).

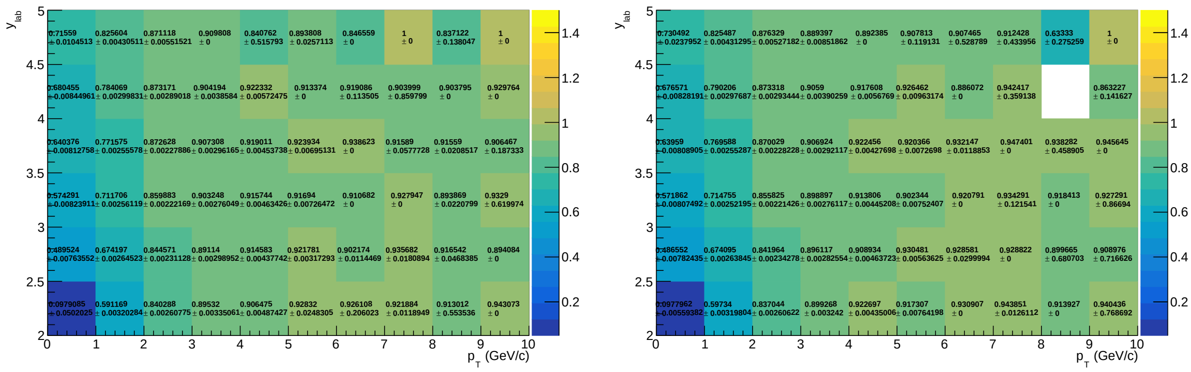

Figure 53: L0 trigger efficiency as function of the track η (vertical axis) and p_{T} (horizontal axis) for μ^- (left) and μ^+ (right) in the $\psi(2S)$ simulation for pPb.

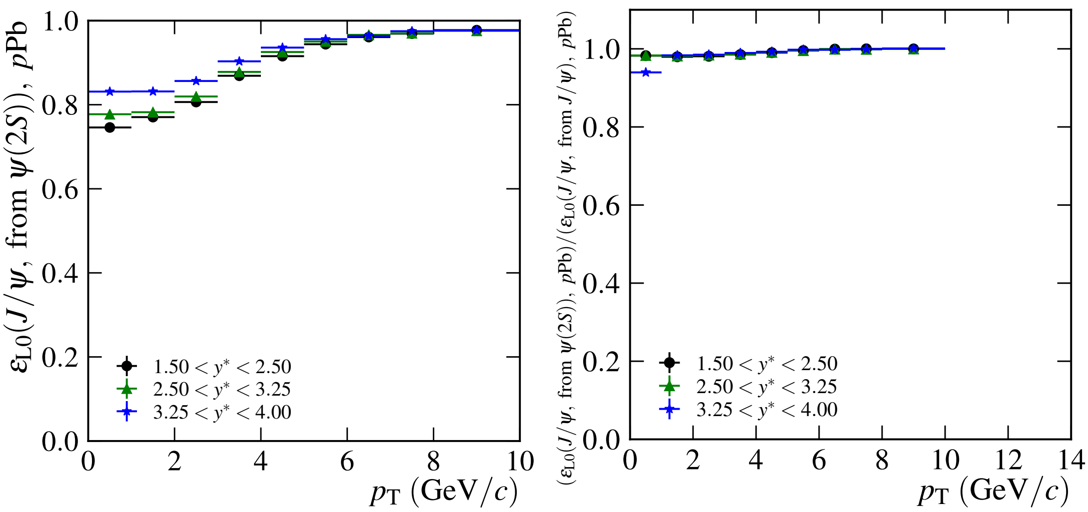

Figure 54: L0 trigger efficiency based on tables from $\psi(2S)$ simulations for J/ψ kinematics in pPb on the left. The ratio with respect to the efficiency extracted from the J/ψ simulation, as shown in 50 top right, is on the right.

Table 49: Trigger systematic uncertainties on the cross-section ration for pPb.

$y^*_{\rm min} < y < y^*_{\rm max}$	$p_{\rm T}^{\rm min} < p_{\rm T} < p_{\rm T}^{\rm max}$ (GeV/c)	relative uncertainty
$1.50 < y < 2.50$	$0 < p_{\rm T} < 1$	0.0120
$2.50 < y < 3.25$	$0 < p_{\rm T} < 1$	0.0063
$3.25 < y < 4.00$	$0 < p_{\rm T} < 1$	0.0071
$1.50 < y < 2.50$	$1 < p_{\rm T} < 2$	0.0062
$2.50 < y < 3.25$	$1 < p_{\rm T} < 2$	0.0051
$3.25 < y < 4.00$	$1 < p_{\rm T} < 2$	0.0049
$1.50 < y < 2.50$	$2 < p_{\rm T} < 3$	0.0103
$2.50 < y < 3.25$	$2 < p_{\rm T} < 3$	0.0076
$3.25 < y < 4.00$	$2 < p_{\rm T} < 3$	0.0049
$1.50 < y < 2.50$	$3 < p_{\rm T} < 4$	0.0073
$2.50 < y < 3.25$	$3 < p_{\rm T} < 4$	0.0046
$3.25 < y < 4.00$	$3 < p_{\rm T} < 4$	0.0049
$1.50 < y < 2.50$	$4 < p_{\rm T} < 5$	0.0040
$2.50 < y < 3.25$	$4 < p_{\rm T} < 5$	0.0037
$3.25 < y < 4.00$	$4 < p_{\rm T} < 5$	0.0049
$1.50 < y < 2.50$	$5 < p_{\rm T} < 6$	0.0040
$2.50 < y < 3.25$	$5 < p_{\rm T} < 6$	0.0039
$3.25 < y < 4.00$	$5 < p_{\rm T} < 6$	0.0053
$1.50 < y < 2.50$	$6 < p_{\rm T} < 7$	0.0044
$2.50 < y < 3.25$	$6 < p_{\rm T} < 7$	0.0044
$3.25 < y < 4.00$	$6 < p_{\rm T} < 7$	0.0062
$1.50 < y < 2.50$	$7 < p_{\rm T} < 8$	0.0054
$2.50 < y < 3.25$	$7 < p_{\rm T} < 8$	0.0053
$3.25 < y < 4.00$	$7 < p_{\rm T} < 8$	0.0078
$1.50 < y < 2.50$	$8 < p_{\rm T} < 10$	0.0056
$2.50 < y < 3.25$	$8 < p_{\rm T} < 10$	0.0048
$3.25 < y < 4.00$	$8 < p_{\rm T} < 10$	0.0068
$1.50 < y < 2.50$	$10 < p_{\rm T} < 14$	< 0.0001
$2.50 < y < 3.25$	$10 < p_{\rm T} < 14$	< 0.0001
$3.25 < y < 4.00$	$10 < p_{\rm T} < 14$	< 0.0001

Table 50: Trigger systematic uncertainties on the cross-section ration for Pbp.

$y^*_{\min} < y < y^*_{\max}$	$p_{\mathrm{T}}^{\min} < p_{\mathrm{T}} < p_{\mathrm{T}}^{\max}$ (GeV/c)	relative uncertainty
$-3.25 < y < -2.50$	$0 < p_{\mathrm{T}} < 1$	0.0111
$-4.00 < y < -3.25$	$0 < p_{\mathrm{T}} < 1$	0.0093
$-5.00 < y < -4.00$	$0 < p_{\mathrm{T}} < 1$	0.0081
$-3.25 < y < -2.50$	$1 < p_{\mathrm{T}} < 2$	0.0125
$-4.00 < y < -3.25$	$1 < p_{\mathrm{T}} < 2$	0.0090
$-5.00 < y < -4.00$	$1 < p_{\mathrm{T}} < 2$	0.0052
$-3.25 < y < -2.50$	$2 < p_{\mathrm{T}} < 3$	0.0116
$-4.00 < y < -3.25$	$2 < p_{\mathrm{T}} < 3$	0.0089
$-5.00 < y < -4.00$	$2 < p_{\mathrm{T}} < 3$	0.0048
$-3.25 < y < -2.50$	$3 < p_{\mathrm{T}} < 4$	0.0066
$-4.00 < y < -3.25$	$3 < p_{\mathrm{T}} < 4$	0.0045
$-5.00 < y < -4.00$	$3 < p_{\mathrm{T}} < 4$	0.0047
$-3.25 < y < -2.50$	$4 < p_{\mathrm{T}} < 5$	0.0053
$-4.00 < y < -3.25$	$4 < p_{\mathrm{T}} < 5$	0.0046
$-5.00 < y < -4.00$	$4 < p_{\mathrm{T}} < 5$	0.0051
$-3.25 < y < -2.50$	$5 < p_{\mathrm{T}} < 6$	0.0053
$-4.00 < y < -3.25$	$5 < p_{\mathrm{T}} < 6$	0.0048
$-5.00 < y < -4.00$	$5 < p_{\mathrm{T}} < 6$	0.0056
$-3.25 < y < -2.50$	$6 < p_{\mathrm{T}} < 7$	0.0059
$-4.00 < y < -3.25$	$6 < p_{\mathrm{T}} < 7$	0.0052
$-5.00 < y < -4.00$	$6 < p_{\mathrm{T}} < 7$	0.0070
$-3.25 < y < -2.50$	$7 < p_{\mathrm{T}} < 8$	0.0068
$-4.00 < y < -3.25$	$7 < p_{\mathrm{T}} < 8$	0.0062
$-5.00 < y < -4.00$	$7 < p_{\mathrm{T}} < 8$	0.0072
$-3.25 < y < -2.50$	$8 < p_{\mathrm{T}} < 10$	0.0056
$-4.00 < y < -3.25$	$8 < p_{\mathrm{T}} < 10$	0.0063
$-5.00 < y < -4.00$	$8 < p_{\mathrm{T}} < 10$	0.0087
$-3.25 < y < -2.50$	$10 < p_{\mathrm{T}} < 14$	< 0.0001
$-4.00 < y < -3.25$	$10 < p_{\mathrm{T}} < 14$	< 0.0001
$-5.00 < y < -4.00$	$10 < p_{\mathrm{T}} < 14$	< 0.0001

Table 51: Summary of systematic uncertainties on the $\psi(2S)$ to J/ψ cross-section ratio.

Source	pPb	Pbp	Comment
L0	$0\% - 1.1\%$	$0\% - 1.1\%$	correlated
HLT	negligible	negligible	
Tracking correction table	0–0.1%	0–0.1%	correlated
PID	$0 - 1.7\%$	$0 - 2.0\%$	correlated
Monte Carlo statistics	$0.3\% - 3.2\%$	$0.4\% - 4.0\%$	uncorrelated
Signal extraction	2.2%	2.2%	correlated
$\frac{\mathcal{B}(J/\psi\to\mu^+\mu^-)}{\mathcal{B}(\psi(2S)\to\mu^+\mu^-)}$ (assuming lepton universality)	2.2%	2.2%	correlated

8 Results

From the number of signal candidates, the efficiencies, the luminosities ($\mathcal{L}_{int} = 13.6 \pm 0.3\,\mathrm{nb}^{-1}$ (pPb) and $\mathcal{L}_{int} = 20.8 \pm 0.5\,\mathrm{nb}^{-1}$(Pb$p$)) and the efficiency ratios, the absolute cross-sections of J/ψ and $\psi(2S)$ cross-sections and the cross-section ratios of $\psi(2S)$ over J/ψ can be computed in the binning scheme defined for the analysis, for prompt production and production from b-decays. From them, and from the pp reference cross-sections, nuclear modification factors are extracted. Finally, forward to backward ratios are also measured.

8.1 $\psi(2S)$ to J/ψ cross-section ratios

The prompt production cross-section ratios, $\frac{\sigma_{\psi(2S)}}{\sigma_{J/\psi}}$, are shown in Fig. 55 as a function of p_{T} in the three rapidity bins of the analysis for pPb and Pbp. The numerical values are tabulated in Table 90 and 91. The production cross-section ratios for the production from b-hadrons are shown in Fig. 56 as a function of p_{T} in the three rapidity bins of the analysis for pPb. The numerical values are tabulated in Table 92 and in 93.

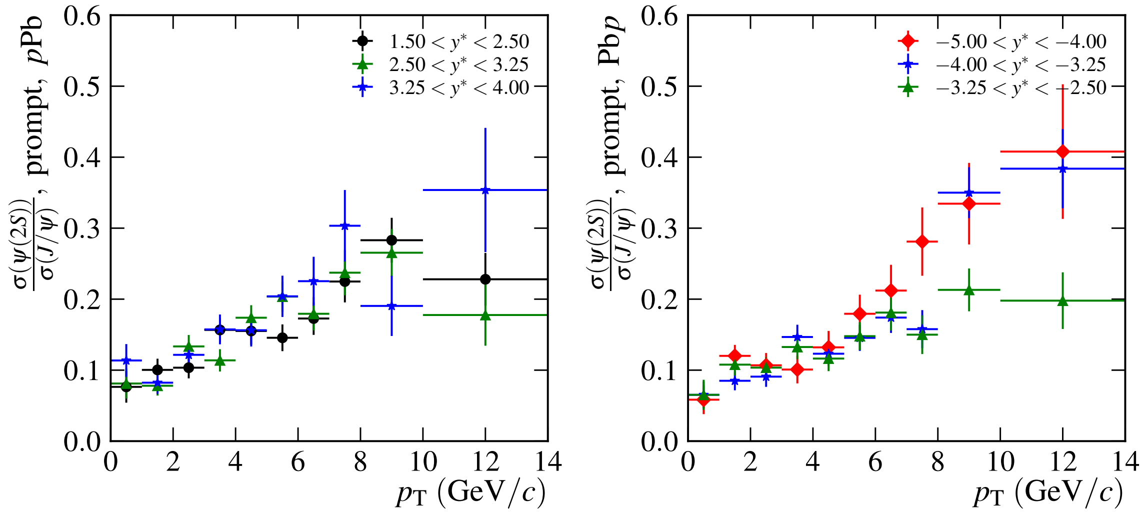

Figure 55: Ratio of prompt $\psi(2S)$ over prompt J/ψ production cross-section in pPb (left) and Pbp (right), as a function of p_{T} for the different rapidity bins. Horizontal error bars are the bin widths, vertical error bars the total uncertainties.

The prompt production cross-section ratios as a function of p_{T} and integrated as function of rapidity y^* are shown in Fig. 57. The corresponding figures for the case of production from b-hadron decays are shown in Fig. 58.

The production cross-section ratios are also extracted as a function of rapidity integrated over p_{T} in the range $0 - 14\,\mathrm{GeV}/c$. The cross-section ratios as a function of rapidity are shown in Fig. 59. The values integrated over the full considered p_T and y^* range in pPb and Pbp are tabulated in Table 102 (103) for prompt (from-b) production.

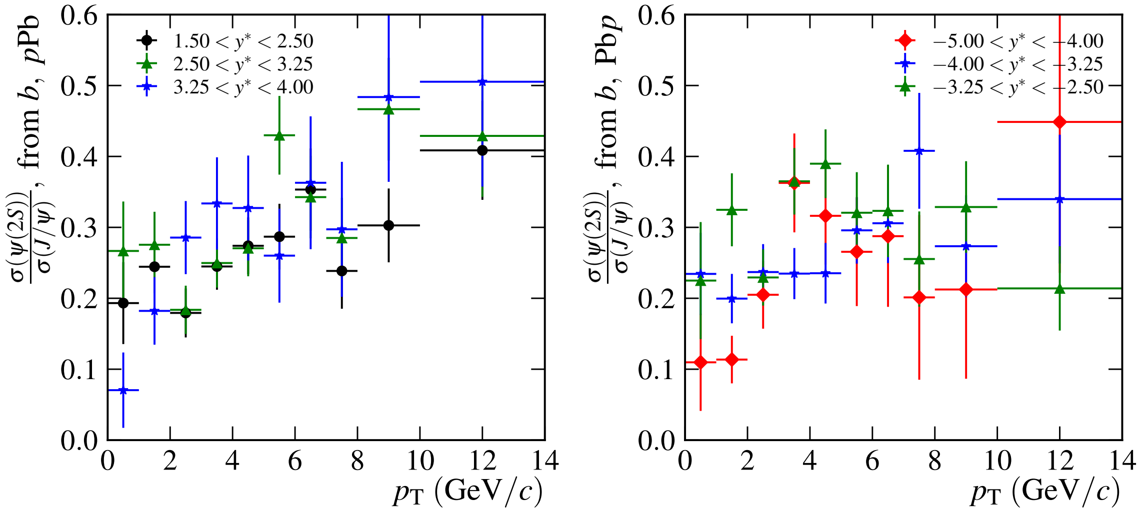

Figure 56: Ratio of $\psi(2S)$-from-b over J/ψ-from-b production cross-section in pPb (left) and Pbp (right), as a function of p_{T} for the different rapidity bins. Horizontal error bars are the bin widths, vertical error bars the total uncertainties.

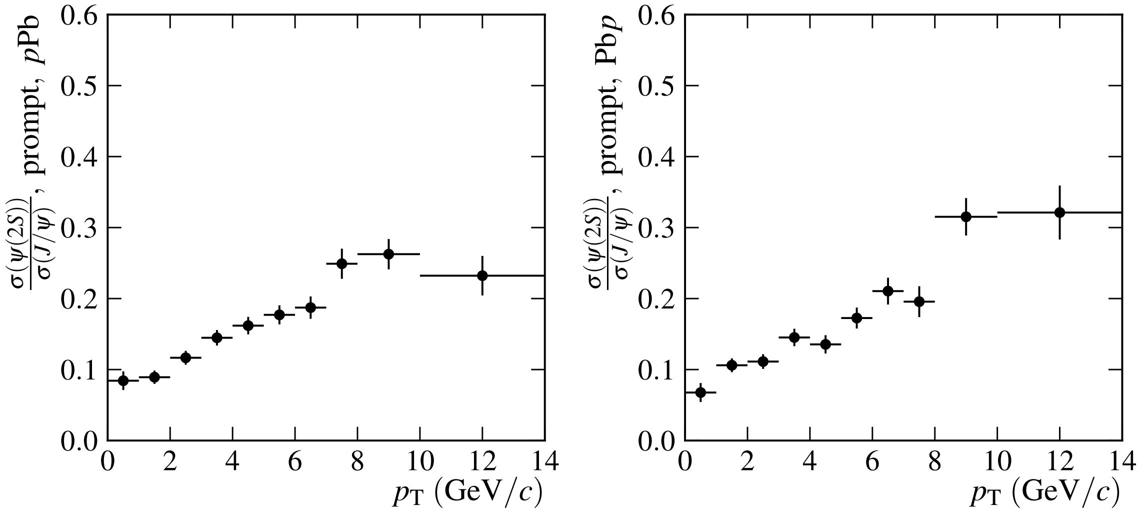

Figure 57: Ratio of prompt $\psi(2S)$ to J/ψ production cross-section in pPb (left) and Pbp (right), as a function of p_{T} integrated over rapidity. Horizontal error bars are the bin widths, vertical error bars the total uncertainties.

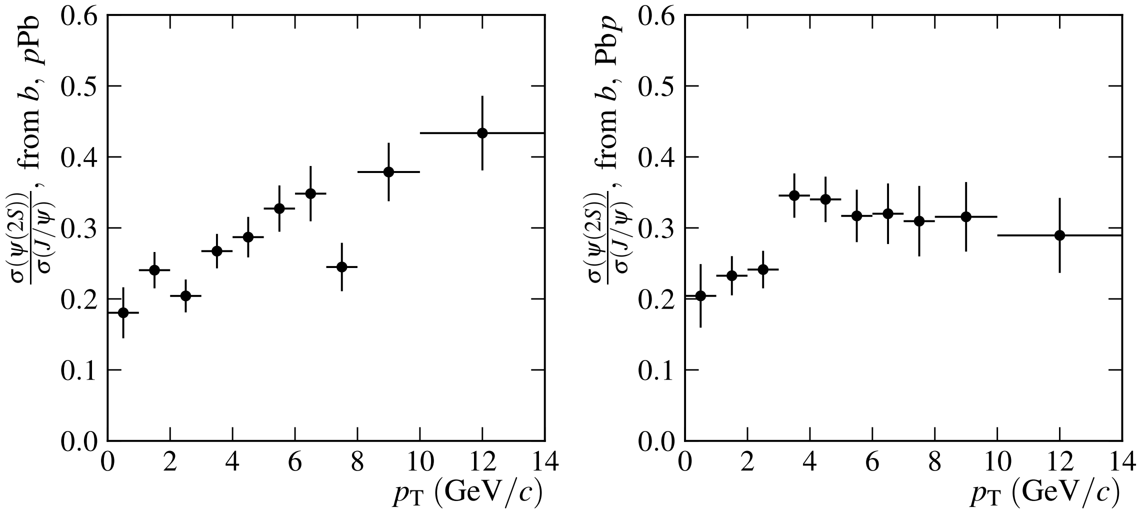

Figure 58: Ratio of $\psi(2S)$ to J/ψ production cross-section in b-hadron decays, in pPb (left) and Pbp (right), as a function of p_{T} integrated over rapidity. Horizontal error bars are the bin widths, vertical error bars the total uncertainties.

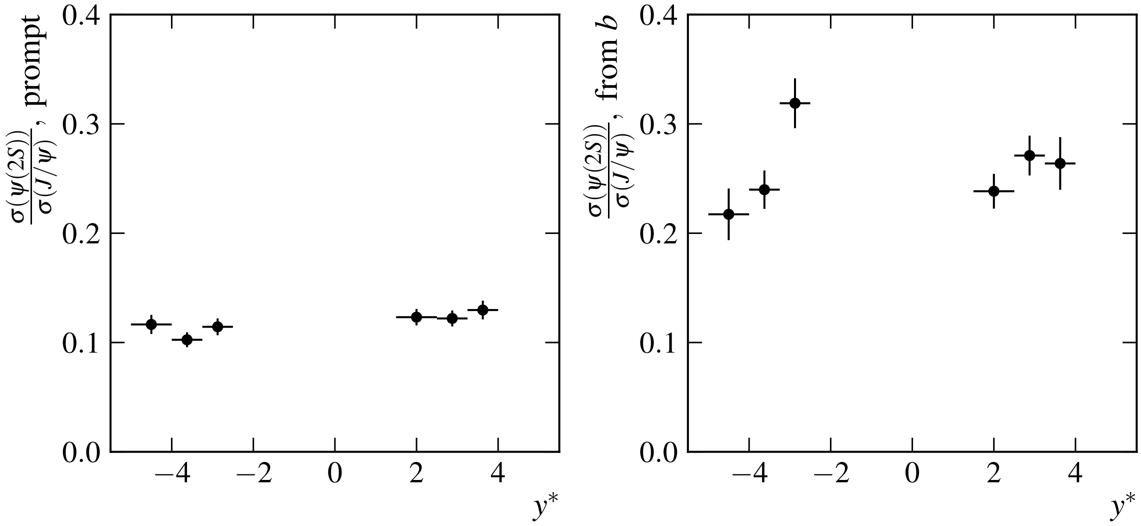

Figure 59: Ratio of prompt $\psi(2S)$ to J/ψ (left) and in b-hadron decays (right) production cross-section, as a function of rapidity integrated over p_{T}. Horizontal error bars are the bin widths, vertical error bars the total uncertainties.

8.2 J/ψ cross-sections

The absolute prompt J/ψ production cross-section for the binning used for this analysis and for the loose selection, is shown in Fig. 60, as a function of p_{T} for different rapidity bins. The numerical results are in Tables 66, 67. The absolute J/ψ-from-b production cross-section is shown in Fig. 61, as a function of p_{T} for different rapidity bins. The numerical results are in Tables 68, 69.

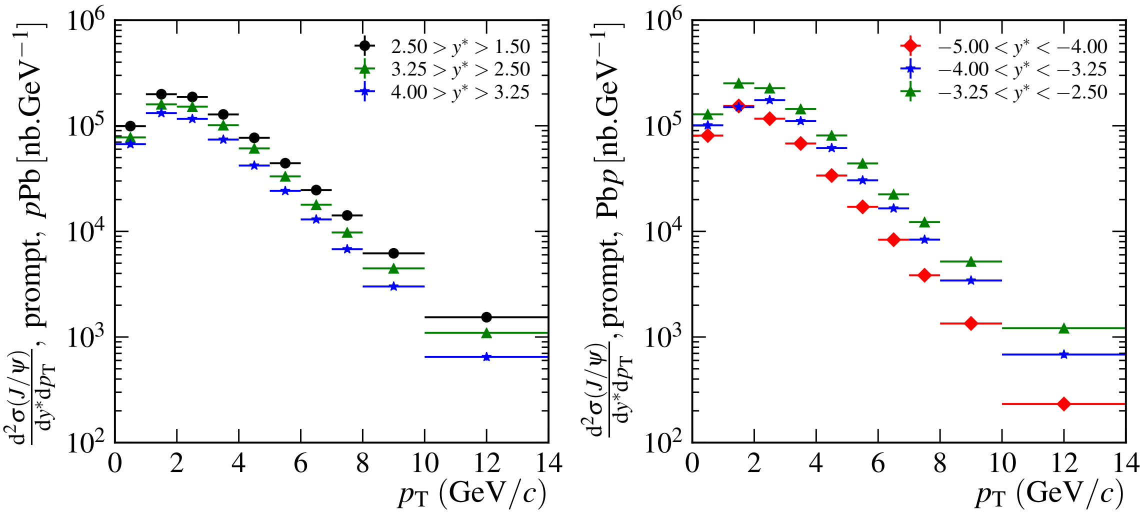

Figure 60: Prompt J/ψ absolute production cross-section in pPb (left) and Pbp (right), as a function of p_{T} for the different rapidity bins. Horizontal error bars are the bin widths, vertical error bars the total uncertainties.

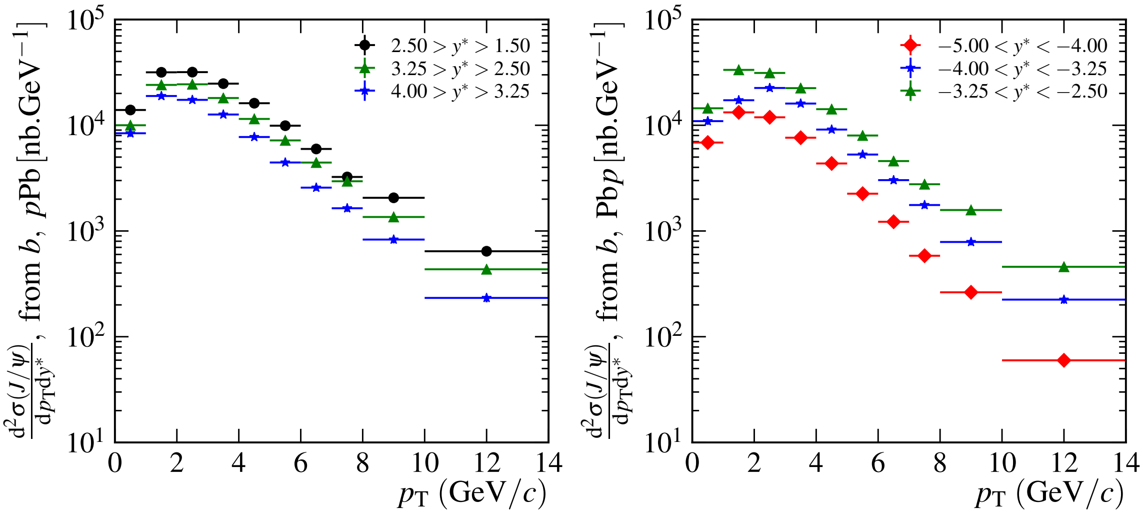

Figure 61: J/ψ-from-b absolute production cross-section in pPb (left) and Pbp (right), as a function of p_{T} for the different rapidity bins. Horizontal error bars are the bin widths, vertical error bars the total uncertainties.

The absolute cross-sections, integrated over p_{T} in the range $0 < p_{\mathrm{T}} < 14\,\mathrm{GeV}/c$, as a function of y^* are shown in Fig. 62, for prompt J/ψ and J/ψ-from-b. The numerical values are shown in Table 74(76) for prompt J/ψ in pPb (Pbp) and in Table 75 (77) for J/ψ-from-b in pPb (Pbp). The cross-sections, integrated over y^* in the analysis bins, as a function of p_{T} are shown in Fig. 63. The numerical values can be found in Table 70 (71) for prompt J/ψ in pPb (Pbp) and in Table 72 (73) for J/ψ-from-b in pPb (Pbp). The integrated cross-sections are compared with the cross-sections published in Ref. [33], *i.e.* with the loose J/ψ selection and a finer binning.

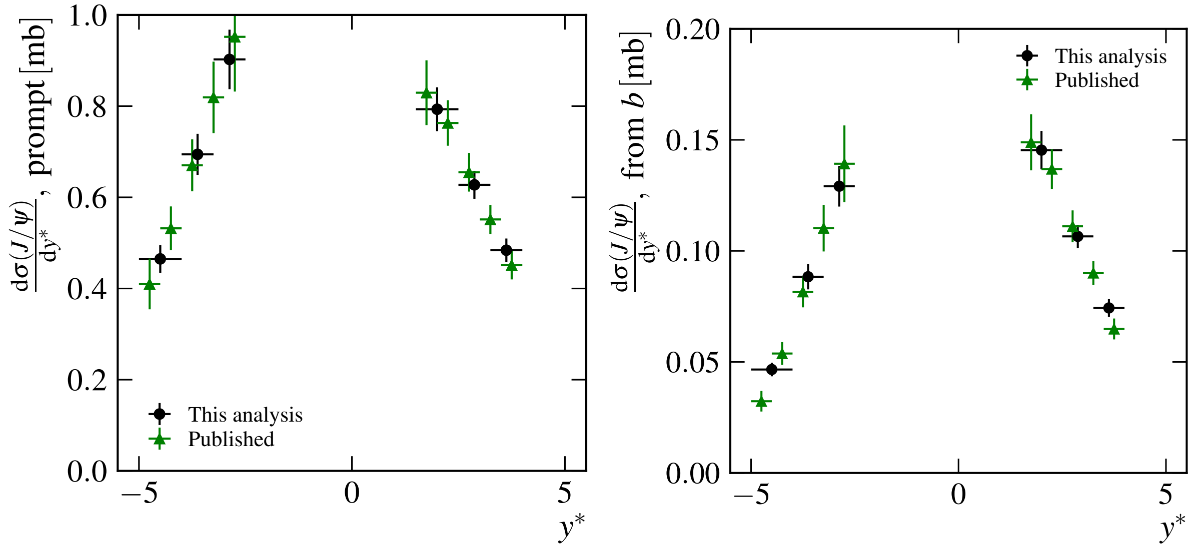

Figure 62: Absolute production cross-section, integrated over p_{T} in the range $0 < p_{\mathrm{T}} < 14\,\mathrm{GeV}/c$, as a function of y^* for (left) prompt J/ψ and (right) J/ψ from b. Horizontal error bars are the bin widths, vertical error bars the total uncertainties. The black dots are the cross-section measured with the tight J/ψ selection of this analysis and the green triangles are the cross-section published in Ref. [33] with the loose selection.

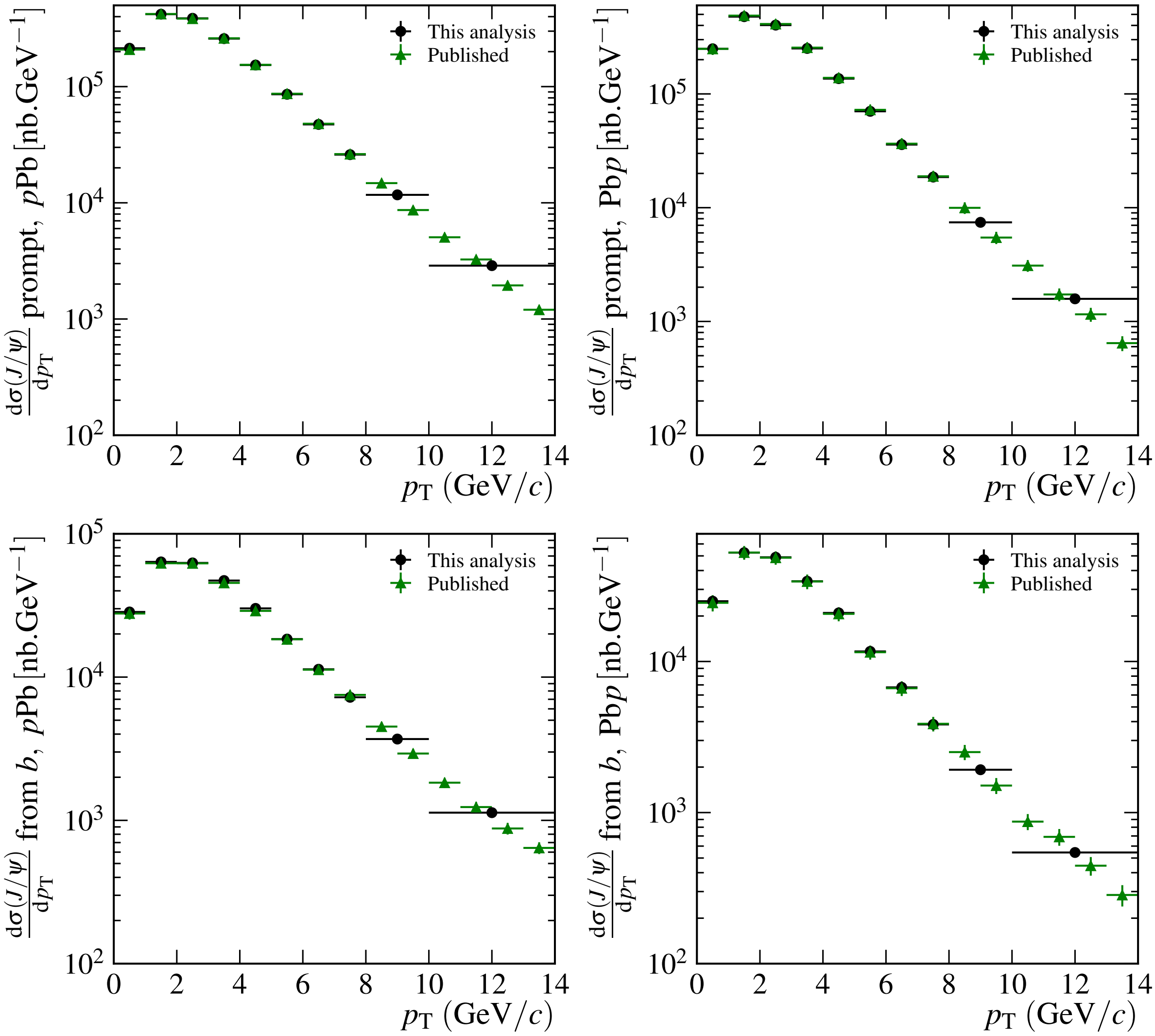

Figure 63: Absolute production cross-section, integrated over y^* in the analysis range, as a function of p_T for (top left) prompt J/ψ in pPb, (top right) prompt J/ψ from b in Pbp, (bottom left) J/ψ from b in pPb and (bottom right) J/ψ from b in Pbp. Horizontal error bars are the bin widths, vertical error bars the total uncertainties. The black dots are the cross-section measured with the tight J/ψ selection of this analysis and the green triangles are the cross-section published in Ref. [33] with the loose selection.

8.3 $\psi(2S)$ cross sections

The absolute prompt $\psi(2S)$ production cross-section is shown in Fig. 64, as a function of p_{T} for different rapidity bins, for pPb and Pbp. The numerical results are in Tables 78 and 79. The absolute $\psi(2S)$-from-b production cross-sections is shown in Fig. 65, as a function of p_{T} for different rapidity bins, for pPb and Pbp. The numerical results are in Tables 80 and 81.

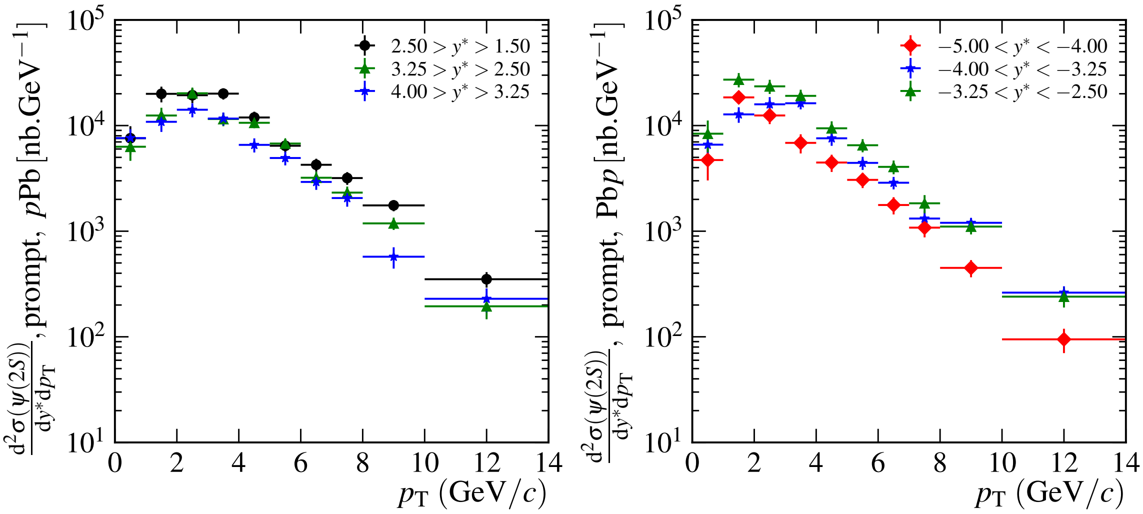

Figure 64: Prompt $\psi(2S)$ absolute production cross-section in pPb (left) and Pbp (right), as a function of p_{T} for the different rapidity bins. Horizontal error bars are the bin widths, vertical error bars the total uncertainties.

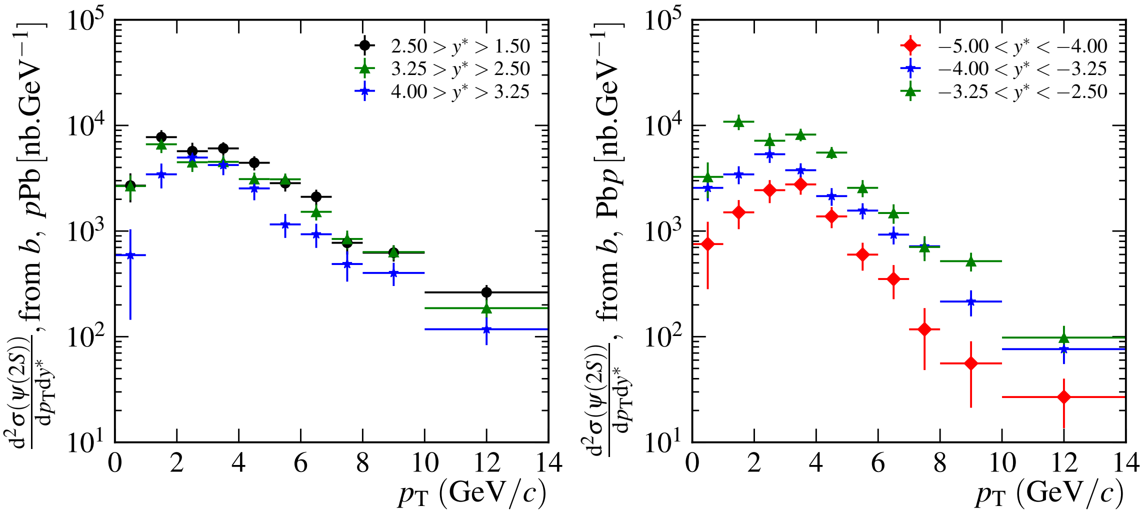

Figure 65: $\psi(2S)$ from b absolute production cross-section in pPb (left) and Pbp (right), as a function of p_{T} for the different rapidity bins. Horizontal error bars are the bin widths, vertical error bars the total uncertainties.

The absolute cross-sections, integrated over p_{T} in the range $0 < p_{\mathrm{T}} < 14\,\mathrm{GeV}/c$, as a function of y^* are shown in Fig. 66, for prompt $\psi(2S)$ and $\psi(2S)$ from b. The cross-sections, integrated over y^* in the analysis bins, as a function of p_{T} are shown in Fig. 67. The numerical values are listed in Tab. 82 (83) for prompt $\psi(2S)$ pPb (Pbp) and in Tab. 84 (85) for pPb (Pbp).

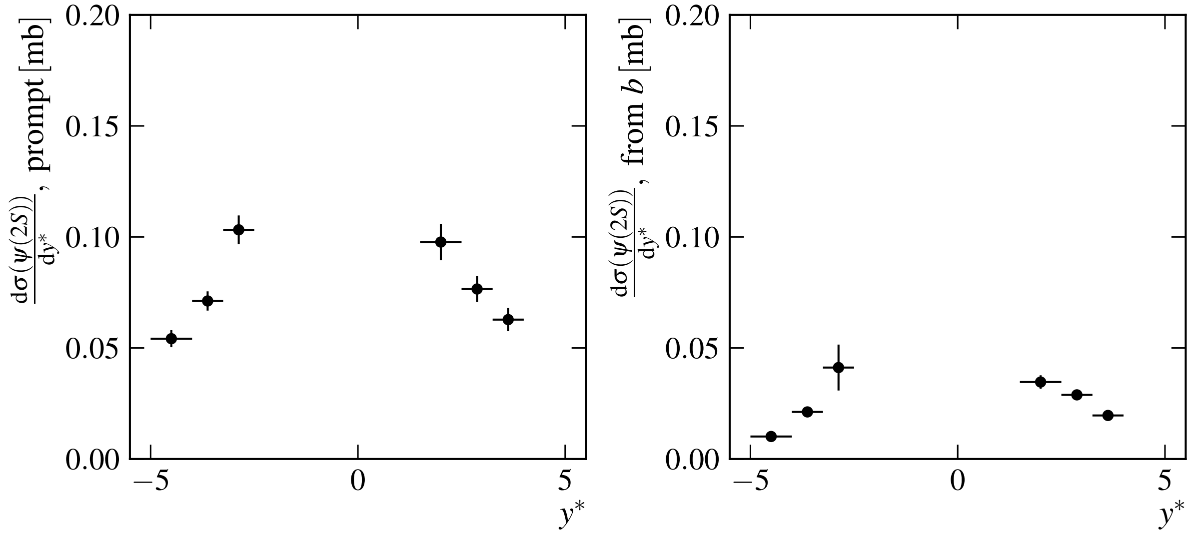

Figure 66: Absolute production cross-section, integrated over p_{T} in the range $0 < p_{\mathrm{T}} < 14\,\mathrm{GeV}/c$, as a function of y^* for left: prompt $\psi(2S)$, right: $\psi(2S)$-from-b. Horizontal error bars are the bin widths, vertical error bars the total uncertainties.

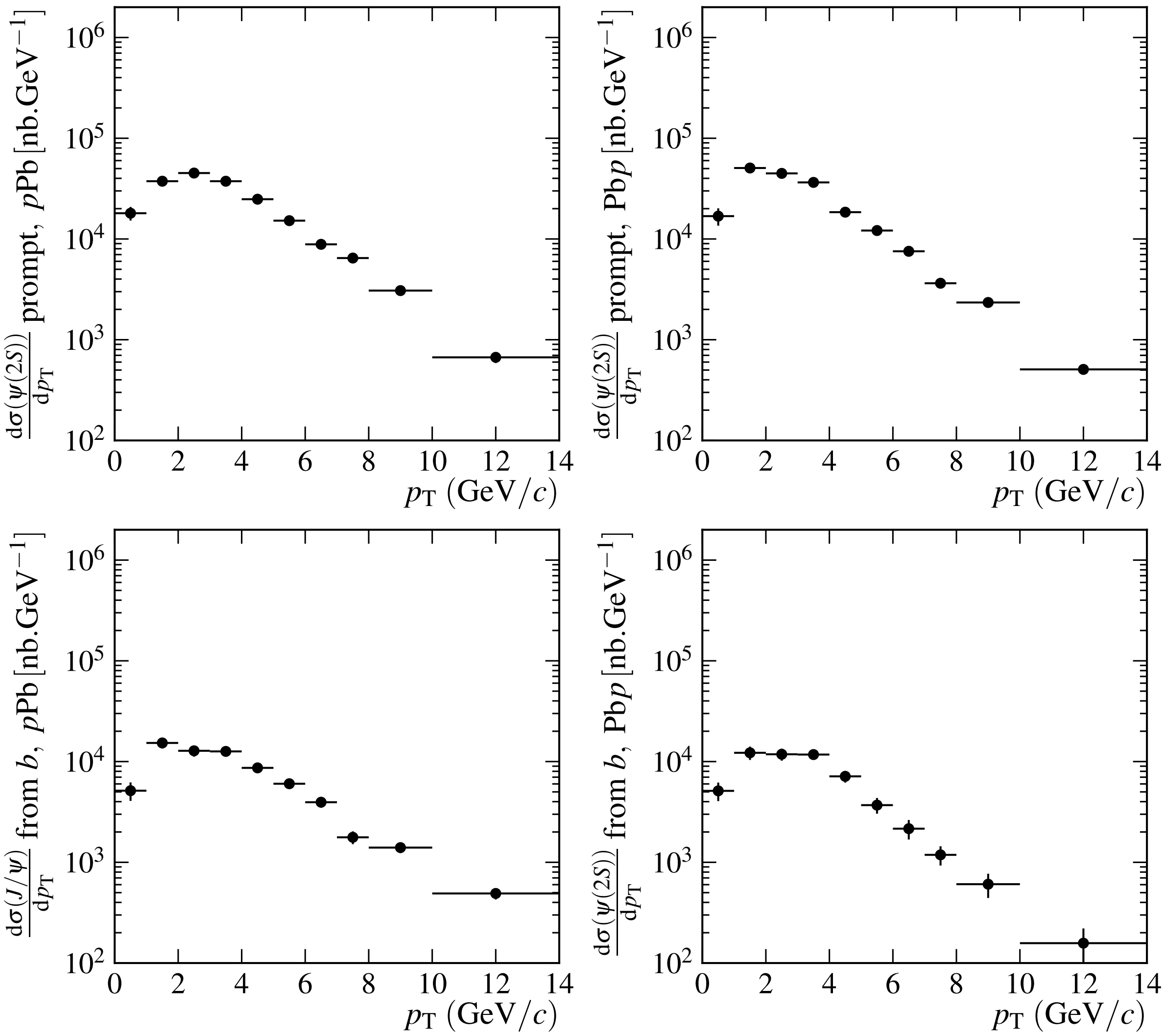

Figure 67: Absolute production cross-section, integrated over y^* in the analysis range, as a function of p_T for top left: prompt $\psi(2S)$ in pPb, top right: prompt $\psi(2S)$ in Pbp, bottom left: $\psi(2S)$-from-b in pPb, bottom right: $\psi(2S)$-from-b in Pbp. Horizontal error bars are the bin widths, vertical error bars the total uncertainties.

9 $\psi(2S)$ to J/ψ double cross-section ratios between pPb/Pbp and pp

We discuss several phenomenological approaches in comparison with the experimental data. These comparisons use the cross-section double ratio since the uncertainties cancel out to a large extent on experimental and model sides. The nuclear modification factor and the cross-sections for $\psi(2S)$ can be interpreted along the same lines. However, the discriminative power is weaker due to the larger uncertainties.

The double ratios

$$\left[\frac{\sigma(\psi(2S))}{\sigma(J/\psi)}\right]_{p\mathrm{Pb},\mathrm{Pb}p} \Big/ \left[\frac{\sigma(\psi(2S))}{\sigma(J/\psi)}\right]_{pp} \tag{22}$$

as a function of p_{T} integrated over y^* for prompt and from-b production are shown in Fig. 68. The corresponding ratios as function of rapidity and integrated over p_{T} are shown in Fig. 70. The fully integrated (over p_{T} and y^*) ratio obtained in this analysis and the similar measurement at $\sqrt{s_{NN}}$ =5 TeV (Run 1 data) are shown in Fig. 72. The results obtained at 8.16 TeV are more precise than those at 5 TeV. Both measurements are consistent within the uncertainties.

The double ratio shows indications of a sizeable relative suppression of the excited $\psi(2S)$ compared to the J/ψ. The results obtained with Run 1 data by ALICE and LHCb and at lower energy by Phenix have triggered discussions in the heavy-ion phenomenology community seeking for an explanation of the relative additional suppression of the $\psi(2S)$ compared to the J/ψ. The interest is driven by the fact that the phenomenon is naively not explained with the phenomenological modelling used for the J/ψ. All the main predictions and main effects assume that the nuclear suppression of the quarkonium state is induced at a time scale that is shorter than the hadronisation time scale. The mechanisms hence apply universally to the J/ψ and $\psi(2S)$ states. Due to the proximity of J/ψ and $\psi(2S)$ masses, the nuclear effects are hence for all practical purposes the same. These considerations apply to all main classes of modification models applied to J/ψ production (nPDFs [24, 59, 60], standard CGC framework [25, 26], coherent energy loss [21])

However, a good understanding of this phenomenon is crucial for the interpretation of measurements in heavy-ion collisions (e.g. PbPb) aiming to describe the deconfined medium produced in such systems. As a matter of fact, the previously mentioned models predict different behaviors of the $\psi(2S)$ to J/ψ cross-section ratio in the presence of deconfined phase. Therefore, the measurement of this production ratio in pPb collisions, where usually a large deconfined system is not expected to be created, would provide important inputs to the models in order to anticipate the charmonium behavior in heavy-ion collisions.

The relative modification of $\psi(2S)$ compared to the J/ψ in pPb collisions could be caused by interactions at late stages that do not obey simple QCD factorisation. At the moment, there are different models exploiting this idea:

- The Comover model by Elena Ferreiro [39]: according to the observed final state particle density, it assumes an interaction cross-section between the quarkonium and the "comoving" particles. This cross-section depends on the assumed size of the quarkonium state (larger cross-section for the $\psi(2S)$ excited state than for the J/ψ ground state). This model does not account for the nature of the so-called comovers.

- The CGC model by Ma et al. [41]: this model considers the gluon density around the quarkonium state, assuming a given p_T of these gluons that are expected to act on the quarkonium state. This action of the gluons can be responsible for kicking the quarkonium state out of the binding. Therefore, the less binded $\psi(2S)$ state will be much more affected (dissociated) than the J/ψ state. The gluons p_T kick, of the order of the MeV, is treated as a parameter of the model to describe the data.

Fig. 69 shows the comparison with the factorisation breaking calculation by soft gluons within a CGC approach [41] as a function of p_{T} in the pPb configuration. Fig. 71 shows the comparison of the prompt double ratio results with the comover model by Elena Ferreiro [39] as well as the comparison with the factorisation breaking calculation by soft gluons within a CGC approach [41]. With appropriate parameter choices that also describe RHIC data at lower collision energy, the models are able to describe the data reasonably well. Due to the feed-down of $\psi(2S)$ into the J/ψ, the difference in nuclear modification between the two states also implies a small effect on the J/ψ affecting the usage of J/ψ for the extraction of nuclear parton distribution functions or the comparison with color glass condensate calculations. However, given the small contribution of the $\psi(2S)$ to the inclusive prompt J/ψ production, in the range of 10-20%, and the rather small additional observed suppression of 30%, these effects are typically below the size of the overall J/ψ data uncertainties on absolute cross-section or on the nuclear modification factor level.

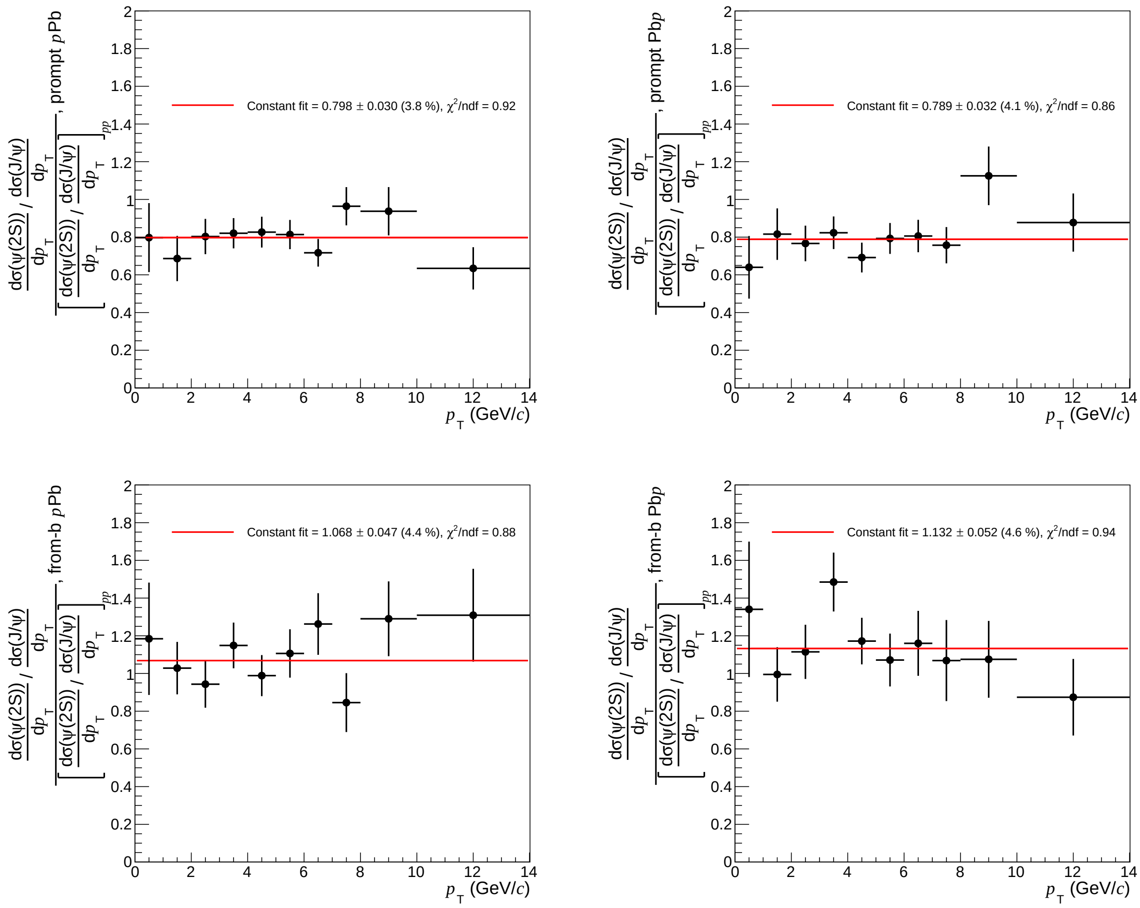

Figure 68: Cross-section double ratios $[\psi(2S)/J/\psi]_{p\mathrm{Pb}/\mathrm{Pb}p}\,/\,[\psi(2S)/J/\psi]_{pp}$ as function of p_{T}, top left: prompt in pPb, top right: prompt in Pbp, bottom left: from-b in pPb, bottom right: from-b in Pbp.

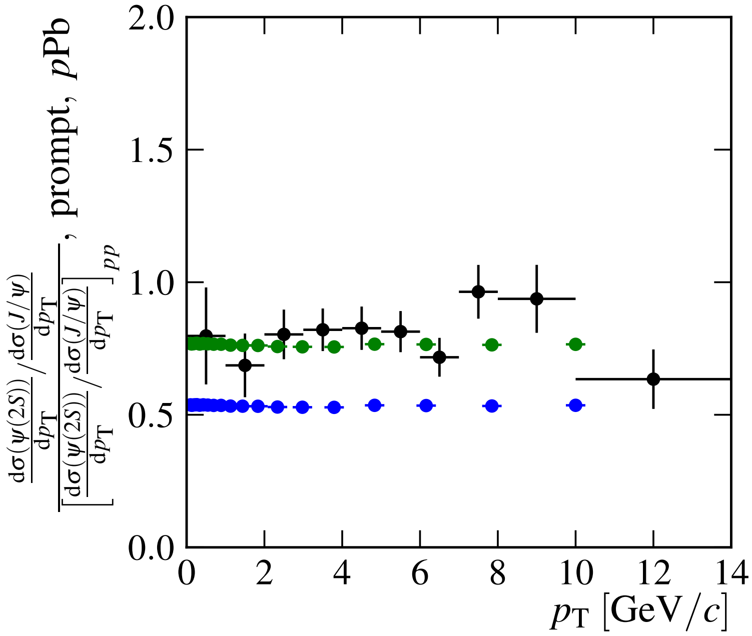

Figure 69: Prompt cross-section double ratios $(\psi(2S)/J/\psi)_{p\text{Pb}/\text{Pb}p}/(\psi(2S)/J/\psi)_{pp}$ as function of y^* compared with two incarnations of the CGC soft gluon interaction model for $\Lambda = 10$ MeV (green) and for $\Lambda = 20$ MeV (blue).

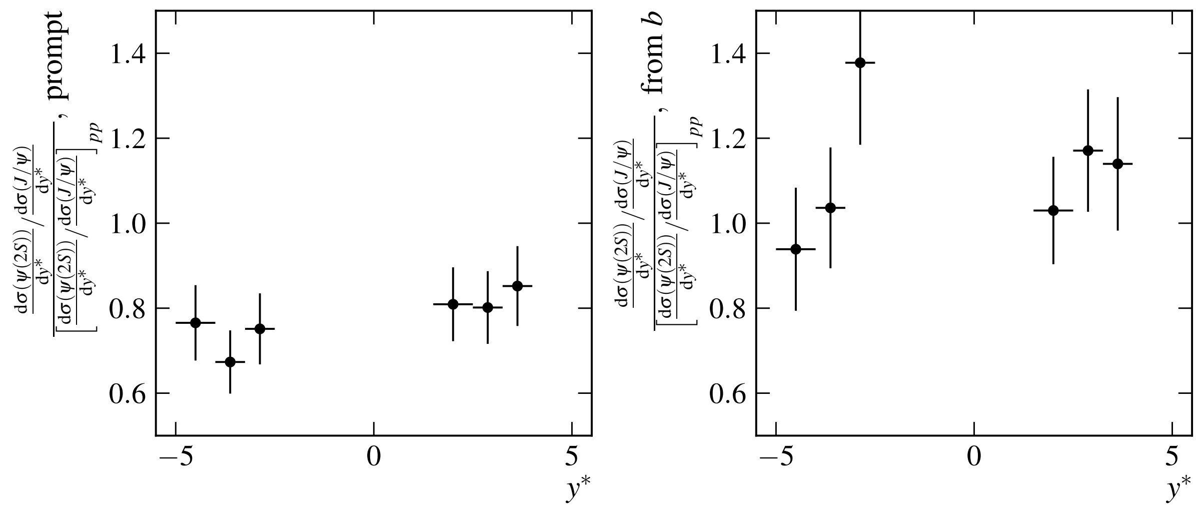

Figure 70: Cross-section double ratios $(\psi(2S)/J/\psi)_{p\text{Pb}/\text{Pb}p}/(\psi(2S)/J/\psi)_{pp}$ as function of y^*, left: prompt, right: from-b.

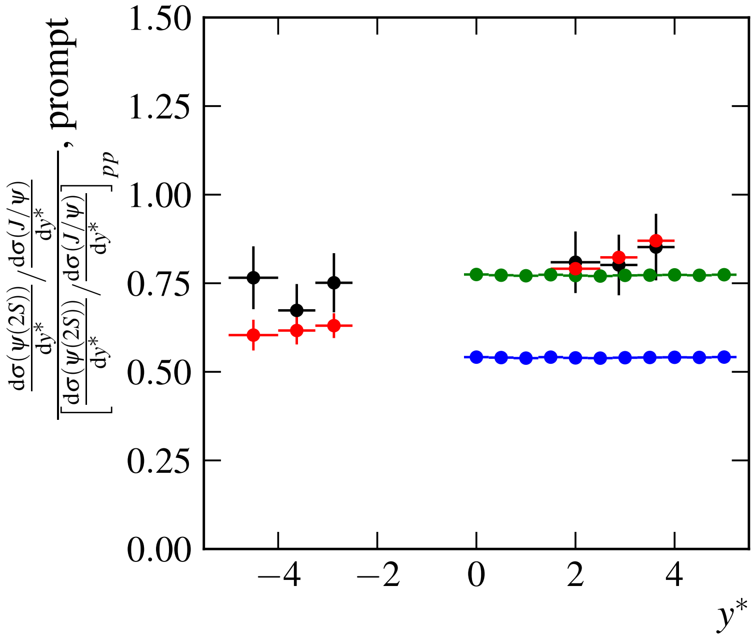

Figure 71: Prompt cross-section double ratios $(\psi(2S)/J/\psi)_{p\mathrm{Pb}/\mathrm{Pb}p}/(\psi(2S)/J/\psi)_{pp}$ as function of y^* compared with the comover model (red) and two incarnations of the CGC soft gluon interaction model for $\Lambda = 10$ MeV (green) and for $\Lambda = 20$ MeV (blue).

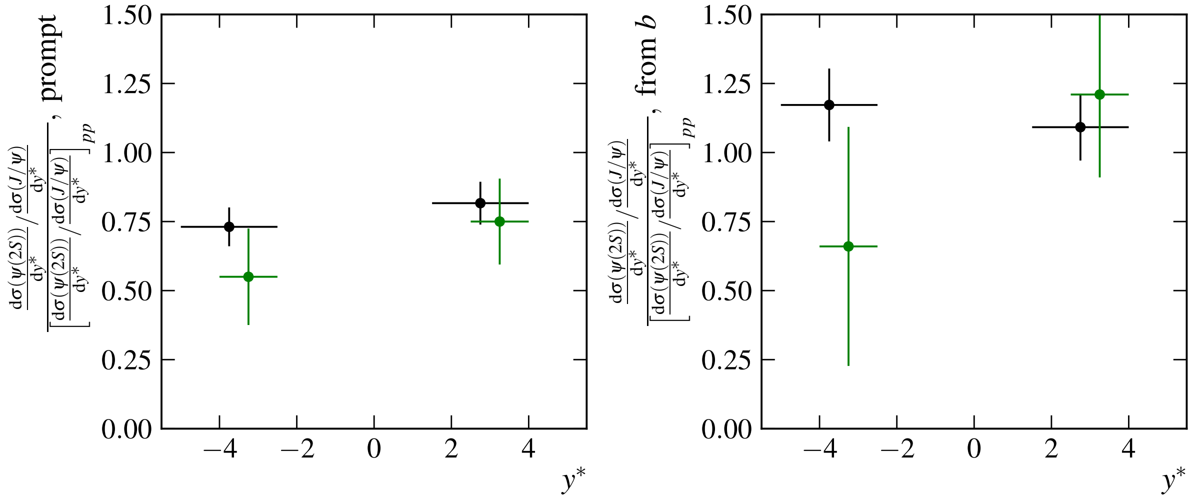

Figure 72: Cross-section double ratios $(\psi(2S)/J/\psi)_{p\mathrm{Pb}/\mathrm{Pb}p}/(\psi(2S)/J/\psi)_{pp}$ integrated over y^* and p_T, left: prompt, right: from-b. The result at 5 TeV is shown in green colour.

9.1 J/ψ nuclear modification factors

The J/ψ nuclear modification factor in the $\psi(2S)$ analysis bins, integrated over y^* as a function of p_{T} are shown in Fig. 73. The numerical values are listed in Tab. 109 (110) for prompt J/ψ pPb (Pbp) and in Tab. 111 (112) for J/ψ-from-b pPb (Pbp). The observed suppression for prompt-J/ψ can be accounted for by different mechanisms: nPDF as e.g. in [24,59,60], CGC calculations [25,26] as well as coherent energy loss [21]. The J/ψ-from-b nuclear modification factor can be accounted for by nPDF [24, 59, 60]. For b-production scales are thought to be too large to provide a useful description in the CGC framework[2]. The coherent energy loss calculation should in principle also apply for beauty production at forward rapidity and give qualitiatively similar but weaker kinematic dependences as for prompt production. However, the calculation has not been yet published. A detailed discussion of the prompt J/ψ and J/ψ-from-b production can be found in the LHCb publication [33].

9.2 $\psi(2S)$ nuclear modification factors

The $\psi(2S)$ nuclear modification factors integrated over y^* as a function of p_{T} are shown in Fig. 74. The numerical values are listed in Tab. 113 (114) for prompt $\psi(2S)$ in pPb (Pbp) and in Tab. 115 (116) for $\psi(2S)$-from-b in pPb (Pbp). Since the nuclear modification of $\psi(2S)$ can be reconstructed from the nuclear modification factor of J/ψ and the double ratio, there is no surprise in the observed patterns: the kinematic dependences for the prompt case are similar as for the J/ψ-case, however with an additional suppression. The $\psi(2S)$-from-b nuclear modification factor is overall consistent with the corresponding J/ψ measurement with notably larger uncertainties due to the smaller available statistics and the worse signal to background ratio.

9.3 $\psi(2S)$ forward to backward ratio

The $\psi(2S)$ forward to backward ratio for prompt and from-b production integrated over y^* (p_{T}) as a function of p_{T} (y^*) are shown in Fig. 75. The numerical values are listed in Tab. 117 (119) for prompt $\psi(2S)$ and in Tab. 118 (120) for $\psi(2S)$-from-b. The forward to backward ratio can provide slightly smaller systematic uncertainties than the nuclear modification factor, however, it can be only extracted in the overlap region of the kinematics, which reduce the available units in rapidity to 1.5. A comparison with calculations could be done but given the different kinematic regimes of backward and forward rapidity, it is difficult to provide a good account for the cancellation of uncertainties. Furthermore, the main effect that is observed, the additional suppression of $\psi(2S)$ w.r.t. J/ψ, is hidden in these plots.

10 Conclusion

The measurement of $\psi(2S)$ by LHCb with 2016 pPb and Pbp is presented and is compared with J/ψ production in the same collision system as well as with the productions in pp collisions. In agreement with the Run 1 findings, the double ratio

[2] The saturation scale at forward rapidity at the LHC might be as large as 3 GeV, for beauty production at 10 GeV for low-p_{T}, CGC is hence not in its optimal range of applicability.

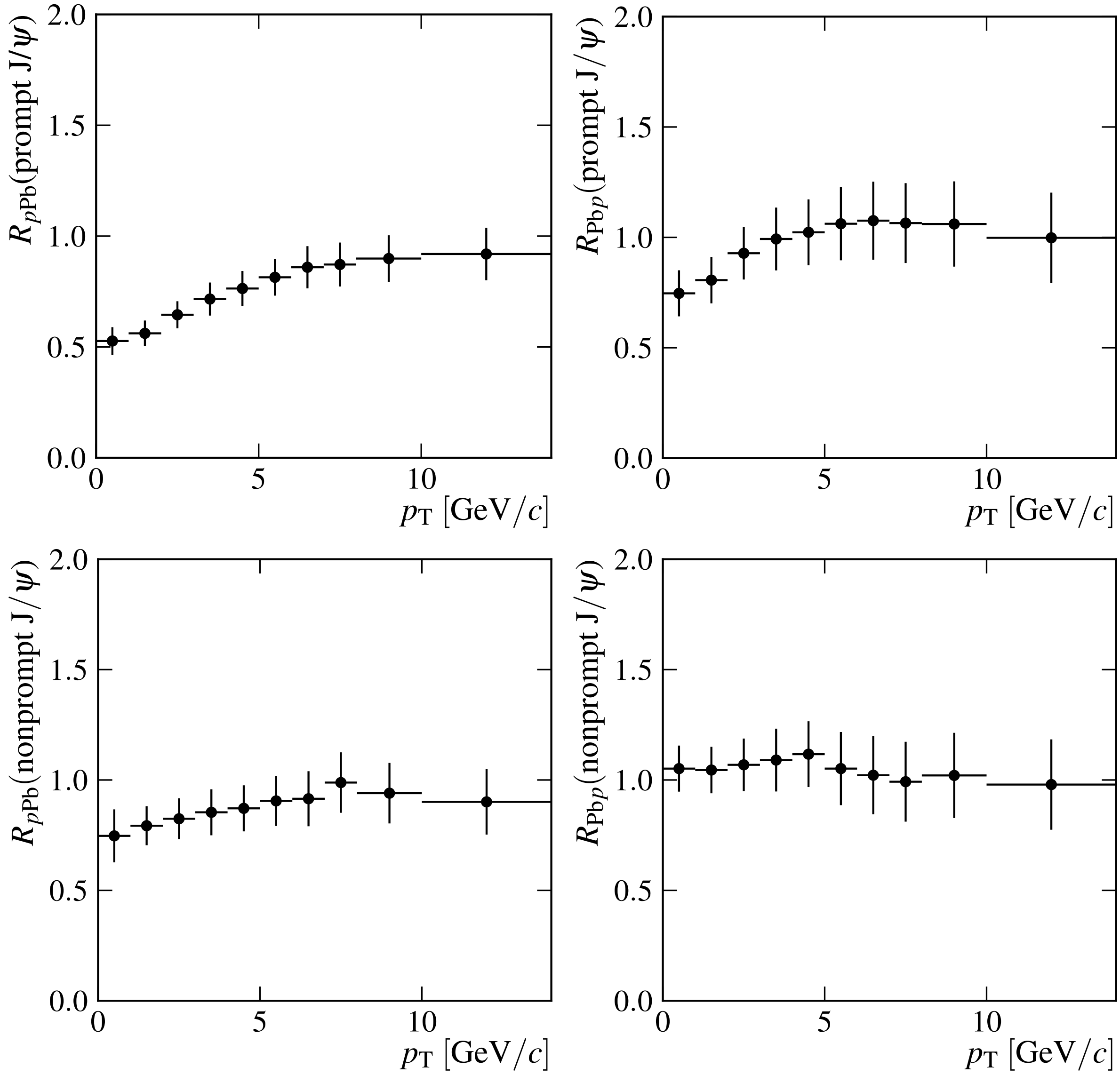

Figure 73: Nuclear modification factor for J/ψ as function of p_{T} and integrated over y^*, top left: prompt in pPb, top right: prompt in Pbp, bottom left: from-b in pPb, bottom right: from-b in Pbp.

$[\sigma(\psi(2S))/\sigma(J/\psi)]_{pPb/Pbp} \, / \, [\sigma(\psi(2S))/\sigma(J/\psi)]_{pp}$ is below unity indicating factorisation breaking w.r.t. the final state. These findings are supported by the corresponding measurements of the nuclear modification factor which however feature larger systematic uncertainties. This additional suppression is compatible with each other at forward and at backward rapidity and amounts to approximately 30% in the double ratio integrated over p_{T}. With increasing p_{T}, the suppression tends to be smaller although large statistical uncertainties at high-p_{T} prevent from firm statements. The observed behaviour can be described by models invoking late stage interaction preferentially destroying $\psi(2S)$ compared to J/ψ due to larger interaction cross-sections or closeness to the open charm boundary of the excited state. These findings are important to correct the extraction of nuclear parton distribution functions from J/ψ data and as a precise constraint on factorisation

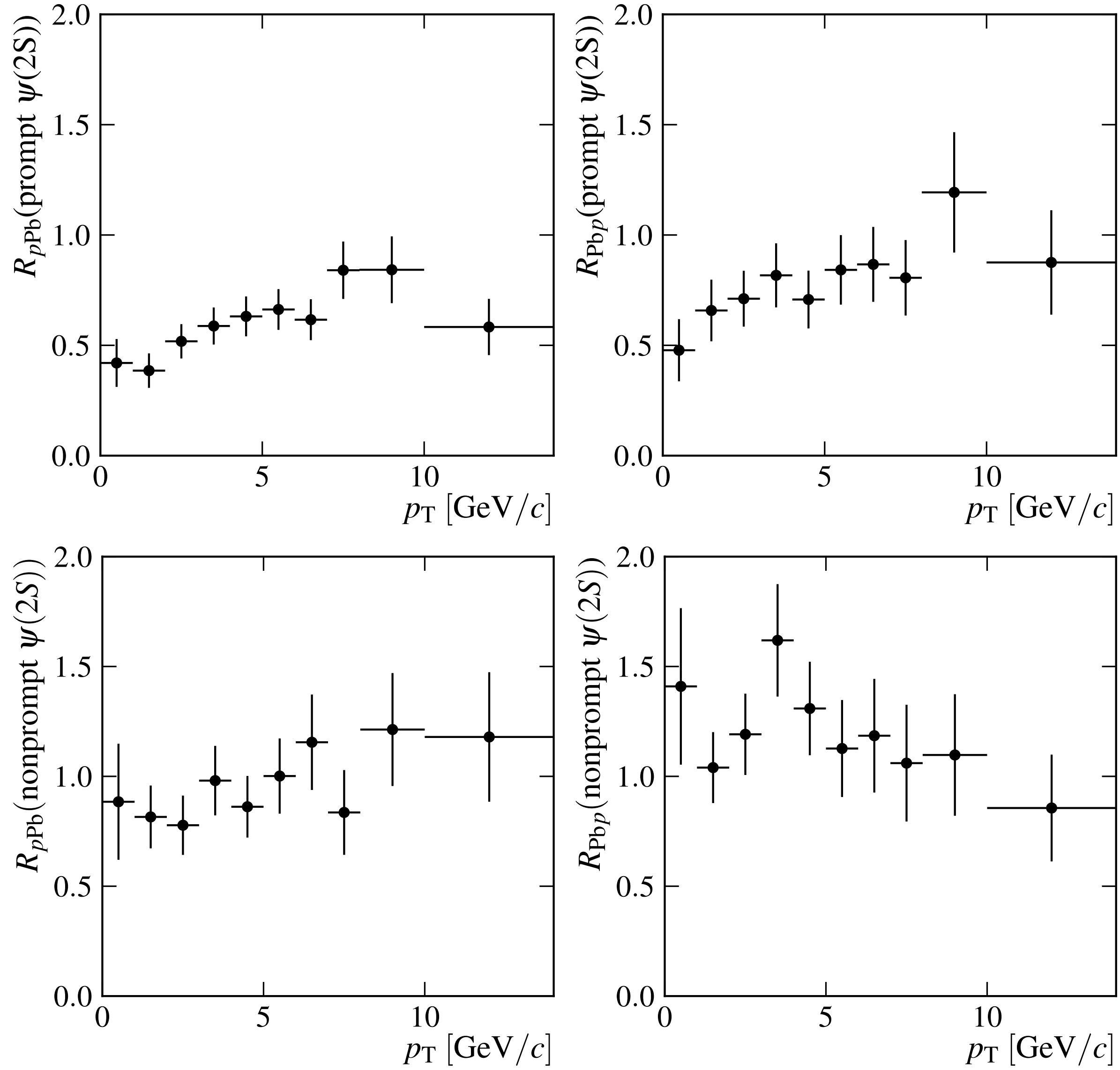

Figure 74: Nuclear modification factor for $\psi(2S)$ as function of p_{T} and integrated over y^*, top left: prompt in pPb, top right: prompt in Pbp, bottom left: from-b in pPb, bottom right: from-b in Pbp.

breaking with respect to the final state in nuclear collisions as a basic knowledge for ion-ion collisions, where quarkonia are a key measurement in view of deconfinement. The future will show whether the traditional "factorisation" between effects in pPb/Pbp collisions and larger systems like PbPb is becoming obsolete in the field of quarkonium and whether a quantitative understanding of the different effects in proton-nucleus collisions will be a prerequisite for quarkonium in larger systems as a probe of deconfinement.

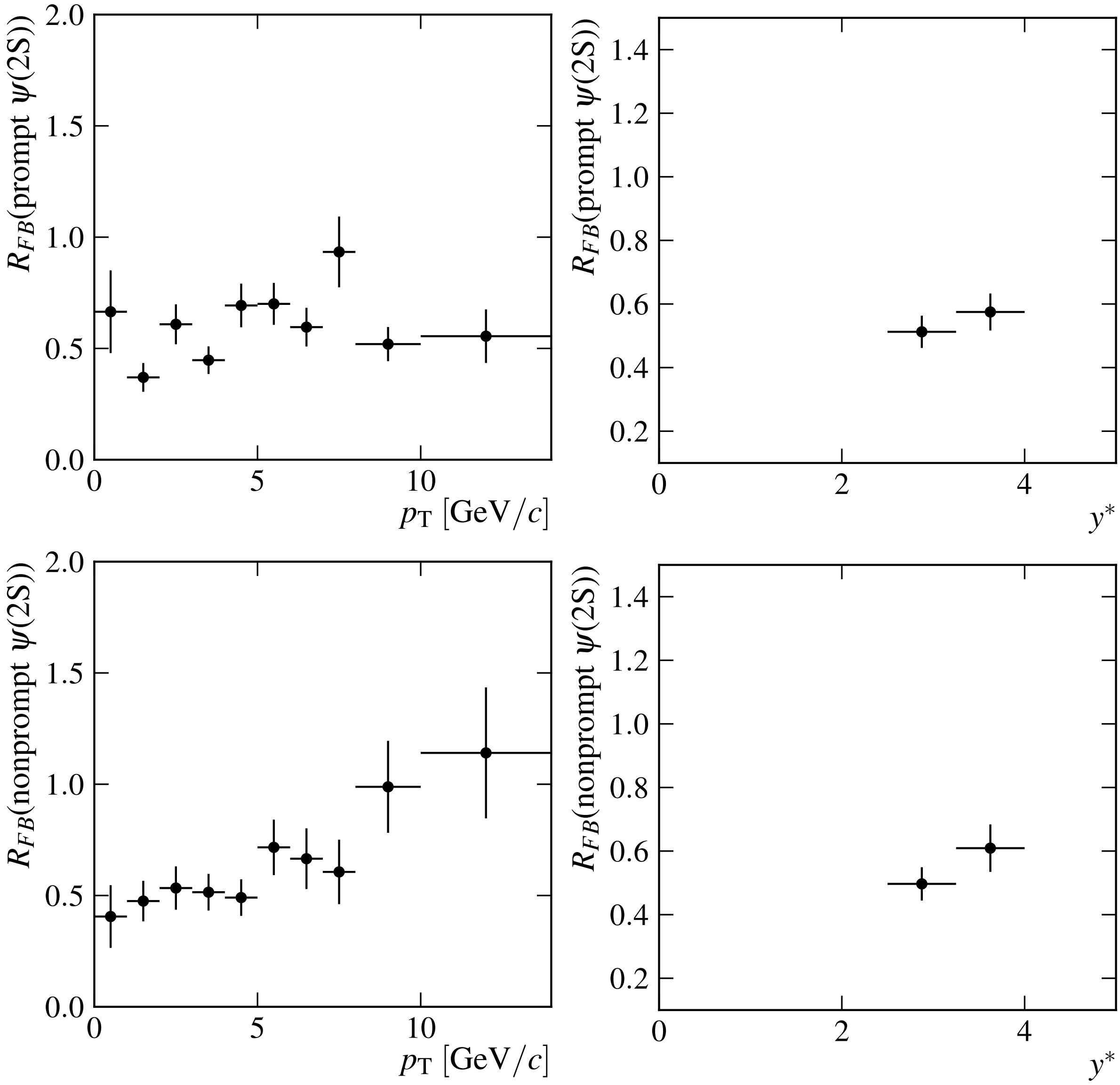

Figure 75: Forward-to-backward ratios as function of p_{T} (y^*) and integrated over y^* (p_{T}), top left: prompt $\psi(2S)$ as function of p_{T}, top right: prompt $\psi(2S)$ as function of y^*, bottom left: $\psi(2S)$ from-b as function of p_{T}, bottom right: $\psi(2S)$ from-b as function of y^*.

Appendices

A Mass and t_z fit results

A.1 Event yields for $\psi(2S)$ and J/ψ in pPb

Table 52: Fit results for $\psi(2S)$ in pPb, in bins of p_{T} and y^*. The uncertainties are statistical only.

y^* bin	p_{T} bin	N_{prompt}	N_{b}
$1.50< y^* <2.50$	$0 < p_{\mathrm{T}} <1000$	149.9 ± 43.4	54.1 ± 16.0
$2.50< y^* <3.25$	$0 < p_{\mathrm{T}} <1000$	213.1 ± 55.0	89.7 ± 23.1
$3.25< y^* <4.00$	$0 < p_{\mathrm{T}} <1000$	166.0 ± 33.4	12.4 ± 9.3
$1.50< y^* <2.50$	$1000 < p_{\mathrm{T}} <2000$	414.5 ± 62.3	118.2 ± 22.2
$2.50< y^* <3.25$	$1000 < p_{\mathrm{T}} <2000$	379.9 ± 66.3	200.6 ± 33.2
$3.25< y^* <4.00$	$1000 < p_{\mathrm{T}} <2000$	221.7 ± 42.0	68.6 ± 17.7
$1.50< y^* <2.50$	$2000 < p_{\mathrm{T}} <3000$	388.2 ± 55.5	115.5 ± 21.9
$2.50< y^* <3.25$	$2000 < p_{\mathrm{T}} <3000$	580.2 ± 68.5	124.7 ± 22.8
$3.25< y^* <4.00$	$2000 < p_{\mathrm{T}} <3000$	267.2 ± 37.7	93.0 ± 16.4
$1.50< y^* <2.50$	$3000 < p_{\mathrm{T}} <4000$	408.5 ± 43.1	122.5 ± 16.0
$2.50< y^* <3.25$	$3000 < p_{\mathrm{T}} <4000$	344.4 ± 46.8	133.8 ± 18.1
$3.25< y^* <4.00$	$3000 < p_{\mathrm{T}} <4000$	217.5 ± 28.5	77.5 ± 14.8
$1.50< y^* <2.50$	$4000 < p_{\mathrm{T}} <5000$	279.6 ± 34.1	103.8 ± 14.8
$2.50< y^* <3.25$	$4000 < p_{\mathrm{T}} <5000$	340.6 ± 33.5	104.5 ± 14.9
$3.25< y^* <4.00$	$4000 < p_{\mathrm{T}} <5000$	141.8 ± 20.4	48.6 ± 10.8
$1.50< y^* <2.50$	$5000 < p_{\mathrm{T}} <6000$	175.1 ± 22.2	75.8 ± 12.0
$2.50< y^* <3.25$	$5000 < p_{\mathrm{T}} <6000$	242.3 ± 24.5	113.9 ± 14.1
$3.25< y^* <4.00$	$5000 < p_{\mathrm{T}} <6000$	117.4 ± 16.4	28.4 ± 7.1
$1.50< y^* <2.50$	$6000 < p_{\mathrm{T}} <7000$	133.2 ± 17.2	69.2 ± 11.0
$2.50< y^* <3.25$	$6000 < p_{\mathrm{T}} <7000$	128.7 ± 16.4	59.0 ± 9.7
$3.25< y^* <4.00$	$6000 < p_{\mathrm{T}} <7000$	80.7 ± 11.9	25.3 ± 6.4
$1.50< y^* <2.50$	$7000 < p_{\mathrm{T}} <8000$	112.3 ± 13.9	33.1 ± 7.4
$2.50< y^* <3.25$	$7000 < p_{\mathrm{T}} <8000$	102.5 ± 13.2	31.9 ± 6.8
$3.25< y^* <4.00$	$7000 < p_{\mathrm{T}} <8000$	64.6 ± 10.4	14.4 ± 5.5
$1.50< y^* <2.50$	$8000 < p_{\mathrm{T}} <10000$	137.7 ± 14.7	44.8 ± 8.0
$2.50< y^* <3.25$	$8000 < p_{\mathrm{T}} <10000$	105.5 ± 12.8	61.6 ± 8.7
$3.25< y^* <4.00$	$8000 < p_{\mathrm{T}} <10000$	40.1 ± 8.2	26.5 ± 6.3
$1.50< y^* <2.50$	$10000< p_{\mathrm{T}} <14000$	64.3 ± 10.1	46.8 ± 7.7
$2.50< y^* <3.25$	$10000< p_{\mathrm{T}} <14000$	38.1 ± 9.1	35.2 ± 6.8
$3.25< y^* <4.00$	$10000< p_{\mathrm{T}} <14000$	33.3 ± 8.0	17.6 ± 5.0

Table 53: Fit results for J/ψ in pPb, in bins of p_{T} and y^{*}. The uncertainties are statistical only.

y^{*} bin	p_{T} bin	N_{prompt}	N_{b}
1.50< y^{*} <2.50	0 < p_{T} <1000	14179.8 ± 162.043	1993.68 ± 62.1642
2.50< y^{*} <3.25	0 < p_{T} <1000	19182.3 ± 194.82	2470.5 ± 72.3968
3.25< y^{*} <4.00	0 < p_{T} <1000	11077.8 ± 134.567	1388.6 ± 52.4832
1.50< y^{*} <2.50	1000 < p_{T} <2000	31279 ± 231.808	4981.04 ± 94.3599
2.50< y^{*} <3.25	1000 < p_{T} <2000	37808.6 ± 257.779	5702.67 ± 102.184
3.25< y^{*} <4.00	1000 < p_{T} <2000	21243.4 ± 180.087	3047.06 ± 74.5795
1.50< y^{*} <2.50	2000 < p_{T} <3000	29550.8 ± 217.293	5017.74 ± 89.8346
2.50< y^{*} <3.25	2000 < p_{T} <3000	34922.5 ± 239.672	5624.65 ± 96.2833
3.25< y^{*} <4.00	2000 < p_{T} <3000	17558.5 ± 157.424	2628.5 ± 65.7148
1.50< y^{*} <2.50	3000 < p_{T} <4000	22221.1 ± 178.771	4295.12 ± 78.7789
2.50< y^{*} <3.25	3000 < p_{T} <4000	25416.6 ± 189.227	4541.74 ± 82.5957
3.25< y^{*} <4.00	3000 < p_{T} <4000	11937.7 ± 125.107	2038.59 ± 55.3763
1.50< y^{*} <2.50	4000 < p_{T} <5000	16076.4 ± 144.46	3379.65 ± 68.5015
2.50< y^{*} <3.25	4000 < p_{T} <5000	17169.5 ± 147.463	3225.36 ± 67.4781
3.25< y^{*} <4.00	4000 < p_{T} <5000	7877.54 ± 98.8029	1451.25 ± 45.7333
1.50< y^{*} <2.50	5000 < p_{T} <6000	10728.5 ± 110.362	2402.79 ± 54.1257
2.50< y^{*} <3.25	5000 < p_{T} <6000	10267.3 ± 107.091	2224.58 ± 52.1374
3.25< y^{*} <4.00	5000 < p_{T} <6000	5151.23 ± 74.849	947.416 ± 34.3458
1.50< y^{*} <2.50	6000 < p_{T} <7000	6780.7 ± 86.5854	1644.18 ± 44.5672
2.50< y^{*} <3.25	6000 < p_{T} <7000	5918.3 ± 80.3895	1469.89 ± 41.6285
3.25< y^{*} <4.00	6000 < p_{T} <7000	3027.89 ± 57.2117	599.471 ± 27.4059
1.50< y^{*} <2.50	7000 < p_{T} <8000	4329.84 ± 67.1874	991.764 ± 37.7606
2.50< y^{*} <3.25	7000 < p_{T} <8000	3326.39 ± 59.9663	1005.43 ± 34.1992
3.25< y^{*} <4.00	7000 < p_{T} <8000	1689.28 ± 42.7306	408.162 ± 22.3848
1.50< y^{*} <2.50	8000 < p_{T} <10000	4176.92 ± 69.1494	1387.73 ± 41.1309
2.50< y^{*} <3.25	8000 < p_{T} <10000	3242.15 ± 60.3044	984.302 ± 35.2725
3.25< y^{*} <4.00	8000 < p_{T} <10000	1641.44 ± 44.1732	452.541 ± 24.2045
1.50< y^{*} <2.50	10000< p_{T} <14000	2347.9 ± 51.4547	981.051 ± 34.6094
2.50< y^{*} <3.25	10000< p_{T} <14000	1670.08 ± 42.9224	662.562 ± 28.644
3.25< y^{*} <4.00	10000< p_{T} <14000	825.09 ± 30.8163	296.56 ± 18.8709

A.2 Event yields for $\psi(2S)$ and J/ψ in Pbp

Table 54: Fit results for $\psi(2S)$ in Pbp, in bins of p_{T} and y^*. The uncertainties are statistical only.

y^* bin	p_{T} bin	N_{prompt}	N_{b}
$-3.25< y^* <-2.50$	$0 < p_{\mathrm{T}} <1000$	134.5 ± 43.6	53.2 ± 19.3
$-4.00< y^* <-3.25$	$0 < p_{\mathrm{T}} <1000$	251.7 ± 72.3	92.8 ± 22.6
$-5.00< y^* <-4.00$	$0 < p_{\mathrm{T}} <1000$	183.2 ± 63.6	28.3 ± 17.6
$-3.25< y^* <-2.50$	$1000 < p_{\mathrm{T}} <2000$	458.8 ± 64.4	170.3 ± 26.3
$-4.00< y^* <-3.25$	$1000 < p_{\mathrm{T}} <2000$	612.3 ± 95.0	163.8 ± 28.1
$-5.00< y^* <-4.00$	$1000 < p_{\mathrm{T}} <2000$	639.0 ± 80.0	53.9 ± 15.8
$-3.25< y^* <-2.50$	$2000 < p_{\mathrm{T}} <3000$	398.5 ± 55.4	121.1 ± 20.6
$-4.00< y^* <-3.25$	$2000 < p_{\mathrm{T}} <3000$	567.2 ± 88.5	177.2 ± 29.0
$-5.00< y^* <-4.00$	$2000 < p_{\mathrm{T}} <3000$	423.4 ± 67.5	81.9 ± 18.9
$-3.25< y^* <-2.50$	$3000 < p_{\mathrm{T}} <4000$	347.7 ± 44.5	143.8 ± 17.8
$-4.00< y^* <-3.25$	$3000 < p_{\mathrm{T}} <4000$	615.9 ± 70.9	133.9 ± 20.2
$-5.00< y^* <-4.00$	$3000 < p_{\mathrm{T}} <4000$	240.9 ± 46.2	95.6 ± 18.0
$-3.25< y^* <-2.50$	$4000 < p_{\mathrm{T}} <5000$	203.5 ± 30.5	120.6 ± 14.4
$-4.00< y^* <-3.25$	$4000 < p_{\mathrm{T}} <5000$	322.3 ± 43.8	89.9 ± 16.0
$-5.00< y^* <-4.00$	$4000 < p_{\mathrm{T}} <5000$	180.8 ± 31.3	53.2 ± 11.3
$-3.25< y^* <-2.50$	$5000 < p_{\mathrm{T}} <6000$	172.2 ± 22.4	63.6 ± 11.1
$-4.00< y^* <-3.25$	$5000 < p_{\mathrm{T}} <6000$	217.7 ± 27.0	78.5 ± 12.1
$-5.00< y^* <-4.00$	$5000 < p_{\mathrm{T}} <6000$	138.3 ± 20.3	28.8 ± 8.2
$-3.25< y^* <-2.50$	$6000 < p_{\mathrm{T}} <7000$	128.6 ± 17.5	46.3 ± 9.1
$-4.00< y^* <-3.25$	$6000 < p_{\mathrm{T}} <7000$	149.3 ± 18.0	50.8 ± 9.1
$-5.00< y^* <-4.00$	$6000 < p_{\mathrm{T}} <7000$	88.2 ± 14.8	18.0 ± 6.2
$-3.25< y^* <-2.50$	$7000 < p_{\mathrm{T}} <8000$	65.1 ± 11.6	25.1 ± 6.5
$-4.00< y^* <-3.25$	$7000 < p_{\mathrm{T}} <8000$	76.0 ± 12.6	41.9 ± 8.1
$-5.00< y^* <-4.00$	$7000 < p_{\mathrm{T}} <8000$	63.0 ± 10.4	6.7 ± 3.8
$-3.25< y^* <-2.50$	$8000 < p_{\mathrm{T}} <10000$	86.9 ± 11.9	40.4 ± 7.7
$-4.00< y^* <-3.25$	$8000 < p_{\mathrm{T}} <10000$	144.1 ± 13.8	25.1 ± 6.5
$-5.00< y^* <-4.00$	$8000 < p_{\mathrm{T}} <10000$	58.2 ± 9.6	7.4 ± 4.3
$-3.25< y^* <-2.50$	$10000< p_{\mathrm{T}} <14000$	45.6 ± 9.0	18.6 ± 5.1
$-4.00< y^* <-3.25$	$10000< p_{\mathrm{T}} <14000$	69.2 ± 9.5	19.9 ± 5.2
$-5.00< y^* <-4.00$	$10000< p_{\mathrm{T}} <14000$	26.5 ± 6.0	7.5 ± 3.5

Table 55: Fit results for J/ψ in Pbp, in bins of p_{T} and y^*. The uncertainties are statistical only.

y^* bin	p_{T} bin	N_{prompt}	N_{b}
$-3.25< y^* <-2.50$	$0 < p_{\mathrm{T}} <1000$	16474.5 ± 179.88	1857.52 ± 62.404
$-4.00< y^* <-3.25$	$0 < p_{\mathrm{T}} <1000$	33144.8 ± 283.41	3586.35 ± 97.9107
$-5.00< y^* <-4.00$	$0 < p_{\mathrm{T}} <1000$	26729.0 ± 266.491	2270.97 ± 85.4338
$-3.25< y^* <-2.50$	$1000 < p_{\mathrm{T}} <2000$	36106.6 ± 259.146	4775.34 ± 95.1781
$-4.00< y^* <-3.25$	$1000 < p_{\mathrm{T}} <2000$	47579.5 ± 366.721	5465.95 ± 105.923
$-5.00< y^* <-4.00$	$1000 < p_{\mathrm{T}} <2000$	48544.8 ± 333.899	4177.39 ± 103.511
$-3.25< y^* <-2.50$	$2000 < p_{\mathrm{T}} <3000$	33349.2 ± 234.353	4586.79 ± 86.3895
$-4.00< y^* <-3.25$	$2000 < p_{\mathrm{T}} <3000$	55142.0 ± 332.592	7098.97 ± 113.933
$-5.00< y^* <-4.00$	$2000 < p_{\mathrm{T}} <3000$	35480.8 ± 271.644	3618.53 ± 86.1842
$-3.25< y^* <-2.50$	$3000 < p_{\mathrm{T}} <4000$	24145.6 ± 190.721	3761.97 ± 74.6854
$-4.00< y^* <-3.25$	$3000 < p_{\mathrm{T}} <4000$	38394.3 ± 253.604	5556.06 ± 94.7441
$-5.00< y^* <-4.00$	$3000 < p_{\mathrm{T}} <4000$	22354.9 ± 197.039	2507.06 ± 66.4951
$-3.25< y^* <-2.50$	$4000 < p_{\mathrm{T}} <5000$	16727.1 ± 150.179	2930.58 ± 63.6475
$-4.00< y^* <-3.25$	$4000 < p_{\mathrm{T}} <5000$	24093.6 ± 182.382	3565.61 ± 72.1213
$-5.00< y^* <-4.00$	$4000 < p_{\mathrm{T}} <5000$	12961.3 ± 136.603	1668.23 ± 51.6894
$-3.25< y^* <-2.50$	$5000 < p_{\mathrm{T}} <6000$	10879.9 ± 116.544	1976.43 ± 51.3186
$-4.00< y^* <-3.25$	$5000 < p_{\mathrm{T}} <6000$	13489.9 ± 129.436	2339.48 ± 56.1097
$-5.00< y^* <-4.00$	$5000 < p_{\mathrm{T}} <6000$	7295.37 ± 97.8403	963.625 ± 37.2006
$-3.25< y^* <-2.50$	$6000 < p_{\mathrm{T}} <7000$	6495.8 ± 88.6369	1327.05 ± 41.2538
$-4.00< y^* <-3.25$	$6000 < p_{\mathrm{T}} <7000$	7616.76 ± 94.9643	1395.55 ± 43.1961
$-5.00< y^* <-4.00$	$6000 < p_{\mathrm{T}} <7000$	3754.03 ± 68.5087	550.061 ± 27.6471
$-3.25< y^* <-2.50$	$7000 < p_{\mathrm{T}} <8000$	3940.87 ± 67.8396	890.361 ± 33.9795
$-4.00< y^* <-3.25$	$7000 < p_{\mathrm{T}} <8000$	4052.44 ± 68.5056	853.869 ± 33.3436
$-5.00< y^* <-4.00$	$7000 < p_{\mathrm{T}} <8000$	1942.35 ± 48.7258	294.723 ± 20.512
$-3.25< y^* <-2.50$	$8000 < p_{\mathrm{T}} <10000$	3620.09 ± 64.6558	1101.36 ± 37.3727
$-4.00< y^* <-3.25$	$8000 < p_{\mathrm{T}} <10000$	3485.95 ± 63.0132	799.948 ± 31.5356
$-5.00< y^* <-4.00$	$8000 < p_{\mathrm{T}} <10000$	1494.06 ± 43.4877	292.566 ± 20.1739
$-3.25< y^* <-2.50$	$10000< p_{\mathrm{T}} <14000$	1986.4 ± 47.7066	750.667 ± 29.9725
$-4.00< y^* <-3.25$	$10000< p_{\mathrm{T}} <14000$	1456.83 ± 41.1146	478.735 ± 24.7583
$-5.00< y^* <-4.00$	$10000< p_{\mathrm{T}} <14000$	586.518 ± 27.9558	151.112 ± 14.2827

B Cross section double ratios

Table 56: The cross section ratio prompt $\psi(2S)$ / prompt J/ψ in pPb over the same ratio in pp collisions, in bins of p_{T} integrated over $1.5 < y^* < 4.0$. The first uncertainty is statistical, the second systematic.

p_{T} bin	$(\sigma_{\psi(2S),pPb}/\sigma_{J/\psi,pPb})/\sigma_{\psi(2S),pp}/\sigma_{J/\psi,pp}$
$0.000 < p_{\mathrm{T}} < 1000.000$	$0.797 \pm 0.123 \pm 0.135$
$1000.000 < p_{\mathrm{T}} < 2000.000$	$0.686 \pm 0.070 \pm 0.097$
$2000.000 < p_{\mathrm{T}} < 3000.000$	$0.803 \pm 0.065 \pm 0.068$
$3000.000 < p_{\mathrm{T}} < 4000.000$	$0.821 \pm 0.059 \pm 0.054$
$4000.000 < p_{\mathrm{T}} < 5000.000$	$0.826 \pm 0.060 \pm 0.055$
$5000.000 < p_{\mathrm{T}} < 6000.000$	$0.814 \pm 0.059 \pm 0.050$
$6000.000 < p_{\mathrm{T}} < 7000.000$	$0.717 \pm 0.058 \pm 0.044$
$7000.000 < p_{\mathrm{T}} < 8000.000$	$0.964 \pm 0.079 \pm 0.063$
$8000.000 < p_{\mathrm{T}} < 10000.000$	$0.937 \pm 0.089 \pm 0.092$
$10000.000 < p_{\mathrm{T}} < 14000.000$	$0.634 \pm 0.083 \pm 0.075$

Table 57: The cross section ratio prompt $\psi(2S)$ / prompt J/ψ in Pbp over the same ratio in pp collisions, in bins of p_{T} integrated over $-5.0 < y^* < -2.5$. The first uncertainty is statistical, the second systematic.

p_{T} bin	$(\sigma_{\psi(2S),Pbp}/\sigma_{J/\psi,Pbp})/\sigma_{\psi(2S),pp}/\sigma_{J/\psi,pp}$
$0.000 < p_{\mathrm{T}} < 1000.000$	$0.640 \pm 0.126 \pm 0.108$
$1000.000 < p_{\mathrm{T}} < 2000.000$	$0.816 \pm 0.072 \pm 0.116$
$2000.000 < p_{\mathrm{T}} < 3000.000$	$0.766 \pm 0.069 \pm 0.064$
$3000.000 < p_{\mathrm{T}} < 4000.000$	$0.823 \pm 0.068 \pm 0.054$
$4000.000 < p_{\mathrm{T}} < 5000.000$	$0.692 \pm 0.064 \pm 0.046$
$5000.000 < p_{\mathrm{T}} < 6000.000$	$0.793 \pm 0.066 \pm 0.049$
$6000.000 < p_{\mathrm{T}} < 7000.000$	$0.806 \pm 0.070 \pm 0.050$
$7000.000 < p_{\mathrm{T}} < 8000.000$	$0.757 \pm 0.082 \pm 0.050$
$8000.000 < p_{\mathrm{T}} < 10000.000$	$1.125 \pm 0.108 \pm 0.112$
$10000.000 < p_{\mathrm{T}} < 14000.000$	$0.877 \pm 0.112 \pm 0.106$

Table 58: The cross section for $\psi(2S)$-from-b $/J/\psi$-from-b in pPb over the same ratio in pp collisions, in bins of p_{T} integrated over $1.5 < y^{*} < 4.0$. The first uncertainty is statistical, the second systematic.

p_{T} bin	$(\sigma_{\psi(2S),pPb}/\sigma_{J/\psi,pPb})/\sigma_{\psi(2S),pp}/\sigma_{J/\psi,pp}$	
0.000 $< p_{\mathrm{T}} <$1000.000	1.184 $\pm$	0.253 $\pm$ 0.158
1000.000 $< p_{\mathrm{T}} <$2000.000	1.028 $\pm$	0.109 $\pm$ 0.086
2000.000 $< p_{\mathrm{T}} <$3000.000	0.943 $\pm$	0.106 $\pm$ 0.067
3000.000 $< p_{\mathrm{T}} <$4000.000	1.149 $\pm$	0.102 $\pm$ 0.065
4000.000 $< p_{\mathrm{T}} <$5000.000	0.989 $\pm$	0.097 $\pm$ 0.050
5000.000 $< p_{\mathrm{T}} <$6000.000	1.106 $\pm$	0.110 $\pm$ 0.066
6000.000 $< p_{\mathrm{T}} <$7000.000	1.263 $\pm$	0.141 $\pm$ 0.083
7000.000 $< p_{\mathrm{T}} <$8000.000	0.846 $\pm$	0.129 $\pm$ 0.088
8000.000 $< p_{\mathrm{T}} <$10000.000	1.290 $\pm$	0.161 $\pm$ 0.115
10000.000$< p_{\mathrm{T}} <$14000.000	1.309 $\pm$	0.179 $\pm$ 0.169

Table 59: The cross section ratio $\psi(2S)$-from-b $/J/\psi$-from-b in Pbp over the same ratio in pp collisions, in bins of p_{T} integrated over $-5.0 < y^{*} < -2.5$. The first uncertainty is statistical, the second systematic.

p_{T} bin	$(\sigma_{\psi(2S),Pbp}/\sigma_{J/\psi,Pbp})/\sigma_{\psi(2S),pp}/\sigma_{J/\psi,pp}$	
0.000 $< p_{\mathrm{T}} <$1000.000	1.340 $\pm$	0.311 $\pm$ 0.006
1000.000 $< p_{\mathrm{T}} <$2000.000	0.995 $\pm$	0.117 $\pm$ 0.006
2000.000 $< p_{\mathrm{T}} <$3000.000	1.115 $\pm$	0.121 $\pm$ 0.006
3000.000 $< p_{\mathrm{T}} <$4000.000	1.485 $\pm$	0.132 $\pm$ 0.008
4000.000 $< p_{\mathrm{T}} <$5000.000	1.172 $\pm$	0.108 $\pm$ 0.008
5000.000 $< p_{\mathrm{T}} <$6000.000	1.071 $\pm$	0.125 $\pm$ 0.007
6000.000 $< p_{\mathrm{T}} <$7000.000	1.160 $\pm$	0.154 $\pm$ 0.008
7000.000 $< p_{\mathrm{T}} <$8000.000	1.069 $\pm$	0.184 $\pm$ 0.009
8000.000 $< p_{\mathrm{T}} <$10000.000	1.075 $\pm$	0.179 $\pm$ 0.009
10000.000$< p_{\mathrm{T}} <$14000.000	0.874 $\pm$	0.168 $\pm$ 0.010

Table 60: Prompt cross section ratio $\psi(2S)$ $/J/\psi$ in pPb over the same ratio in pp, in bins of y^{*} integrated over $0 < p_{\mathrm{T}} < 14.0$ GeV/c. the first uncertainty is statistical, the second systematic.

y^{*} bin	$(\sigma_{\psi(2S),pPb}/\sigma_{J/\psi,pPb})/\sigma_{\psi(2S),pp}/\sigma_{J/\psi,pp}$	
1.500$< y^{*} <$2.500	0.809 $\pm$	0.046 $\pm$ 0.074
2.500$< y^{*} <$3.250	0.802 $\pm$	0.044 $\pm$ 0.073
3.250$< y^{*} <$4.000	0.852 $\pm$	0.053 $\pm$ 0.078

Table 61: The cross section ratio $\psi(2S)$-from-b / J/ψ-from-b in pPb over the same ratio in pp, in bins of y^* integrated over $0 < p_{\mathrm{T}} < 14.0$ GeV/c. the first uncertainty is statistical, the second systematic.

y^* bin	$(\sigma_{\psi(2S),pPb}/\sigma_{J/\psi,pPb})/\sigma_{\psi(2S),pp}/\sigma_{J/\psi,pp}$
1.500< y^* <2.500	$1.030 \pm 0.077 \pm 0.100$
2.500< y^* <3.250	$1.171 \pm 0.088 \pm 0.114$
3.250< y^* <4.000	$1.140 \pm 0.111 \pm 0.111$

Table 62: The cross section ratio prompt $\psi(2S)$ / prompt J/ψ in Pbp over the same ratio in pp, in bins of y^* integrated over $0 < p_{\mathrm{T}} < 14$ GeV/c. the first uncertainty is statistical, the second systematic.

y^* bin	$(\sigma_{\psi(2S),Pbp}/\sigma_{J/\psi,Pbp})/\sigma_{\psi(2S),pp}/\sigma_{J/\psi,pp}$
-2.500> y^* >-3.250	$0.751 \pm 0.048 \pm 0.069$
-3.250> y^* >-4.000	$0.673 \pm 0.041 \pm 0.062$
-4.000> y^* >-5.000	$0.766 \pm 0.055 \pm 0.070$

Table 63: The cross section ratio $\psi(2S)$-from-b / J/ψ-from-b in Pbp over the same ratio in pp, in bins of y^* integrated over $0 < p_{\mathrm{T}} < 14$ GeV/c. the first uncertainty is statistical, the second systematic.

y^* bin	$(\sigma_{\psi(2S),Pbp}/\sigma_{J/\psi,Pbp})/\sigma_{\psi(2S),pp}/\sigma_{J/\psi,pp}$
-2.500> y^* >-3.250	$1.378 \pm 0.109 \pm 0.008$
-3.250> y^* >-4.000	$1.036 \pm 0.083 \pm 0.006$
-4.000> y^* >-5.000	$0.939 \pm 0.107 \pm 0.005$

Table 64: The cross section ratio prompt $\psi(2S)$ / prompt J/ψ in pPb/Pbp over the same ratio in pp, integrated over $0 < p_{\mathrm{T}} < 14$ GeV/c and the indicated y^*-ranges. the first uncertainty is statistical, the second systematic.

y^* bin	$(\sigma_{\psi(2S),pPb/Pbp}/\sigma_{J/\psi}, pPb/Pbp)/\sigma_{\psi(2S),pp}/\sigma_{J/\psi,pp}$
1.500 > y^* >4.000	$0.817 \pm 0.029 \pm 0.072$
-2.500> y^* >-5.000	$0.731 \pm 0.028 \pm 0.064$

Table 65: The cross section ratio $\psi(2S)$-from-b $/J/\psi$-from-b in pPb/Pbp over the same ratio in pp, integrated over $0 < p_{\mathrm{T}} < 14$ GeV/c and the indicated y^*-ranges. the first uncertainty is statistical, the second systematic.

y^* bin	$(\sigma_{\psi(2S),pPb/Pbp}/\sigma_{J/\psi}, pPb/Pbp)/\sigma_{\psi(2S),pp}/\sigma_{J/\psi,pp}$
1.500 > y^* >4.000	$1.092 \pm 0.063 \pm 0.103$
-2.500> y^* >-5.000	$1.172 \pm 0.072 \pm 0.111$

C Cross sections

C.1 J/ψ cross sections

Table 66: Total prompt cross section for J/ψ in pPb, in bins of p_{T} and y^*. The first uncertainty is statistical, the second systematic.

p_{T} bin	y^* bin	$d\sigma/dy^*dp_{\mathrm{T}}$ [nb/(GeV/c)]
$0 < p_{\mathrm{T}} < 1$	$1.50 < y^* < 2.50$	$99186.200 \pm 1133.470 \pm 7347.820$
$0 < p_{\mathrm{T}} < 1$	$2.50 < y^* < 3.25$	$77643.500 \pm 788.566 \pm 3847.310$
$0 < p_{\mathrm{T}} < 1$	$3.25 < y^* < 4.00$	$67011.200 \pm 814.015 \pm 4270.710$
$1 < p_{\mathrm{T}} < 2$	$1.50 < y^* < 2.50$	$198994.000 \pm 1474.740 \pm 12865.900$
$1 < p_{\mathrm{T}} < 2$	$2.50 < y^* < 3.25$	$159631.000 \pm 1088.370 \pm 8083.630$
$1 < p_{\mathrm{T}} < 2$	$3.25 < y^* < 4.00$	$131833.000 \pm 1117.590 \pm 6732.030$
$2 < p_{\mathrm{T}} < 3$	$1.50 < y^* < 2.50$	$187328.000 \pm 1377.460 \pm 11699.100$
$2 < p_{\mathrm{T}} < 3$	$2.50 < y^* < 3.25$	$151551.000 \pm 1040.090 \pm 7604.250$
$2 < p_{\mathrm{T}} < 3$	$3.25 < y^* < 4.00$	$116134.000 \pm 1041.220 \pm 5968.680$
$3 < p_{\mathrm{T}} < 4$	$1.50 < y^* < 2.50$	$128063.000 \pm 1030.280 \pm 7050.590$
$3 < p_{\mathrm{T}} < 4$	$2.50 < y^* < 3.25$	$101317.000 \pm 754.309 \pm 4821.340$
$3 < p_{\mathrm{T}} < 4$	$3.25 < y^* < 4.00$	$74003.800 \pm 775.560 \pm 3489.180$
$4 < p_{\mathrm{T}} < 5$	$1.50 < y^* < 2.50$	$76878.300 \pm 690.816 \pm 3921.070$
$4 < p_{\mathrm{T}} < 5$	$2.50 < y^* < 3.25$	$61094.900 \pm 524.723 \pm 2751.580$
$4 < p_{\mathrm{T}} < 5$	$3.25 < y^* < 4.00$	$42023.200 \pm 527.070 \pm 1880.620$
$5 < p_{\mathrm{T}} < 6$	$1.50 < y^* < 2.50$	$44225.200 \pm 454.936 \pm 2172.130$
$5 < p_{\mathrm{T}} < 6$	$2.50 < y^* < 3.25$	$33195.300 \pm 346.237 \pm 1482.180$
$5 < p_{\mathrm{T}} < 6$	$3.25 < y^* < 4.00$	$24167.300 \pm 351.158 \pm 1079.230$
$6 < p_{\mathrm{T}} < 7$	$1.50 < y^* < 2.50$	$24614.600 \pm 314.313 \pm 1204.000$
$6 < p_{\mathrm{T}} < 7$	$2.50 < y^* < 3.25$	$17869.200 \pm 242.721 \pm 808.319$
$6 < p_{\mathrm{T}} < 7$	$3.25 < y^* < 4.00$	$12985.600 \pm 245.361 \pm 629.814$
$7 < p_{\mathrm{T}} < 8$	$1.50 < y^* < 2.50$	$14162.200 \pm 219.760 \pm 680.569$
$7 < p_{\mathrm{T}} < 8$	$2.50 < y^* < 3.25$	$9770.240 \pm 176.132 \pm 449.716$
$7 < p_{\mathrm{T}} < 8$	$3.25 < y^* < 4.00$	$6788.380 \pm 171.713 \pm 359.433$
$8 < p_{\mathrm{T}} < 10$	$1.50 < y^* < 2.50$	$6200.590 \pm 102.651 \pm 298.488$
$8 < p_{\mathrm{T}} < 10$	$2.50 < y^* < 3.25$	$4467.420 \pm 83.095 \pm 204.106$
$8 < p_{\mathrm{T}} < 10$	$3.25 < y^* < 4.00$	$3009.460 \pm 80.988 \pm 176.159$
$10 < p_{\mathrm{T}} < 14$	$1.50 < y^* < 2.50$	$1539.140 \pm 33.731 \pm 72.864$
$10 < p_{\mathrm{T}} < 14$	$2.50 < y^* < 3.25$	$1094.650 \pm 28.134 \pm 49.896$
$10 < p_{\mathrm{T}} < 14$	$3.25 < y^* < 4.00$	$647.571 \pm 24.186 \pm 42.041$

Table 67: Total prompt cross section for J/ψ in Pbp, in bins of p_{T} and y^*. The first uncertainty is statistical, the second systematic.

p_{T} bin	y^* bin	$d\sigma/dy^*dp_{\mathrm{T}}$ [nb/(GeV/c)]
$0 < p_{\mathrm{T}} < 1$	$-2.50 > y^* > -3.25$	$128420.000 \pm 1402.180 \pm 10920.400$
$0 < p_{\mathrm{T}} < 1$	$-3.25 > y^* > -4.00$	$101106.000 \pm 864.523 \pm 7334.360$
$0 < p_{\mathrm{T}} < 1$	$-4.00 > y^* > -5.00$	$80792.700 \pm 805.512 \pm 5358.450$
$1 < p_{\mathrm{T}} < 2$	$-2.50 > y^* > -3.25$	$252516.000 \pm 1812.370 \pm 20569.100$
$1 < p_{\mathrm{T}} < 2$	$-3.25 > y^* > -4.00$	$150120.000 \pm 1157.060 \pm 10314.900$
$1 < p_{\mathrm{T}} < 2$	$-4.00 > y^* > -5.00$	$153904.000 \pm 1058.570 \pm 9208.460$
$2 < p_{\mathrm{T}} < 3$	$-2.50 > y^* > -3.25$	$227109.000 \pm 1595.950 \pm 16207.600$
$2 < p_{\mathrm{T}} < 3$	$-3.25 > y^* > -4.00$	$174964.000 \pm 1055.300 \pm 11239.800$
$2 < p_{\mathrm{T}} < 3$	$-4.00 > y^* > -5.00$	$116647.000 \pm 893.062 \pm 6902.400$
$3 < p_{\mathrm{T}} < 4$	$-2.50 > y^* > -3.25$	$144127.000 \pm 1138.430 \pm 9123.050$
$3 < p_{\mathrm{T}} < 4$	$-3.25 > y^* > -4.00$	$110880.000 \pm 732.389 \pm 6556.910$
$3 < p_{\mathrm{T}} < 4$	$-4.00 > y^* > -5.00$	$67986.600 \pm 599.242 \pm 3927.940$
$4 < p_{\mathrm{T}} < 5$	$-2.50 > y^* > -3.25$	$81011.100 \pm 727.333 \pm 4683.340$
$4 < p_{\mathrm{T}} < 5$	$-3.25 > y^* > -4.00$	$61527.700 \pm 465.748 \pm 3604.770$
$4 < p_{\mathrm{T}} < 5$	$-4.00 > y^* > -5.00$	$33811.600 \pm 356.350 \pm 1947.380$
$5 < p_{\mathrm{T}} < 6$	$-2.50 > y^* > -3.25$	$44040.000 \pm 471.751 \pm 2488.160$
$5 < p_{\mathrm{T}} < 6$	$-3.25 > y^* > -4.00$	$30470.300 \pm 292.363 \pm 1739.620$
$5 < p_{\mathrm{T}} < 6$	$-4.00 > y^* > -5.00$	$17061.600 \pm 228.818 \pm 1010.010$
$6 < p_{\mathrm{T}} < 7$	$-2.50 > y^* > -3.25$	$22441.500 \pm 306.221 \pm 1283.810$
$6 < p_{\mathrm{T}} < 7$	$-3.25 > y^* > -4.00$	$16519.500 \pm 205.962 \pm 944.719$
$6 < p_{\mathrm{T}} < 7$	$-4.00 > y^* > -5.00$	$8341.930 \pm 152.235 \pm 518.160$
$7 < p_{\mathrm{T}} < 8$	$-2.50 > y^* > -3.25$	$12249.200 \pm 210.862 \pm 718.389$
$7 < p_{\mathrm{T}} < 8$	$-3.25 > y^* > -4.00$	$8352.800 \pm 141.202 \pm 497.418$
$7 < p_{\mathrm{T}} < 8$	$-4.00 > y^* > -5.00$	$3843.600 \pm 96.421 \pm 260.081$
$8 < p_{\mathrm{T}} < 10$	$-2.50 > y^* > -3.25$	$5188.390 \pm 92.666 \pm 306.396$
$8 < p_{\mathrm{T}} < 10$	$-3.25 > y^* > -4.00$	$3429.610 \pm 61.995 \pm 203.365$
$8 < p_{\mathrm{T}} < 10$	$-4.00 > y^* > -5.00$	$1343.360 \pm 39.101 \pm 98.117$
$10 < p_{\mathrm{T}} < 14$	$-2.50 > y^* > -3.25$	$1212.890 \pm 29.129 \pm 75.451$
$10 < p_{\mathrm{T}} < 14$	$-3.25 > y^* > -4.00$	$682.612 \pm 19.265 \pm 43.994$
$10 < p_{\mathrm{T}} < 14$	$-4.00 > y^* > -5.00$	$232.066 \pm 11.061 \pm 18.323$

Table 68: Total J/ψ-from-b cross section in pPb, in bins of p_{T} and y^{*}. The first uncertainty is statistical, the second systematic.

p_{T} bin	y^{*} bin	$d\sigma/dy^{*}dp_{\mathrm{T}}$ [nb/(GeV/c)]
$0 < p_{\mathrm{T}} < 1$	$1.50 < y^{*} < 2.50$	$13945.600 \pm 434.832 \pm 1033.100$
$0 < p_{\mathrm{T}} < 1$	$2.50 < y^{*} < 3.25$	$9999.760 \pm 293.038 \pm 495.498$
$0 < p_{\mathrm{T}} < 1$	$3.25 < y^{*} < 4.00$	$8399.840 \pm 317.478 \pm 535.332$
$1 < p_{\mathrm{T}} < 2$	$1.50 < y^{*} < 2.50$	$31688.900 \pm 600.309 \pm 2048.840$
$1 < p_{\mathrm{T}} < 2$	$2.50 < y^{*} < 3.25$	$24077.200 \pm 431.430 \pm 1219.250$
$1 < p_{\mathrm{T}} < 2$	$3.25 < y^{*} < 4.00$	$18909.500 \pm 462.827 \pm 965.612$
$2 < p_{\mathrm{T}} < 3$	$1.50 < y^{*} < 2.50$	$31808.300 \pm 569.477 \pm 1986.510$
$2 < p_{\mathrm{T}} < 3$	$2.50 < y^{*} < 3.25$	$24408.900 \pm 417.834 \pm 1224.750$
$2 < p_{\mathrm{T}} < 3$	$3.25 < y^{*} < 4.00$	$17385.200 \pm 434.645 \pm 893.509$
$3 < p_{\mathrm{T}} < 4$	$1.50 < y^{*} < 2.50$	$24753.300 \pm 454.013 \pm 1362.810$
$3 < p_{\mathrm{T}} < 4$	$2.50 < y^{*} < 3.25$	$18104.600 \pm 329.248 \pm 861.534$
$3 < p_{\mathrm{T}} < 4$	$3.25 < y^{*} < 4.00$	$12637.600 \pm 343.287 \pm 595.844$
$4 < p_{\mathrm{T}} < 5$	$1.50 < y^{*} < 2.50$	$16161.700 \pm 327.578 \pm 824.305$
$4 < p_{\mathrm{T}} < 5$	$2.50 < y^{*} < 3.25$	$11476.900 \pm 240.110 \pm 516.895$
$4 < p_{\mathrm{T}} < 5$	$3.25 < y^{*} < 4.00$	$7741.790 \pm 243.967 \pm 346.460$
$5 < p_{\mathrm{T}} < 6$	$1.50 < y^{*} < 2.50$	$9904.810 \pm 223.118 \pm 486.478$
$5 < p_{\mathrm{T}} < 6$	$2.50 < y^{*} < 3.25$	$7192.300 \pm 168.566 \pm 321.139$
$5 < p_{\mathrm{T}} < 6$	$3.25 < y^{*} < 4.00$	$4444.850 \pm 161.135 \pm 198.493$
$6 < p_{\mathrm{T}} < 7$	$1.50 < y^{*} < 2.50$	$5968.530 \pm 161.783 \pm 291.946$
$6 < p_{\mathrm{T}} < 7$	$2.50 < y^{*} < 3.25$	$4438.050 \pm 125.689 \pm 200.757$
$6 < p_{\mathrm{T}} < 7$	$3.25 < y^{*} < 4.00$	$2570.920 \pm 117.534 \pm 124.692$
$7 < p_{\mathrm{T}} < 8$	$1.50 < y^{*} < 2.50$	$3243.910 \pm 123.509 \pm 155.887$
$7 < p_{\mathrm{T}} < 8$	$2.50 < y^{*} < 3.25$	$2953.140 \pm 100.450 \pm 135.930$
$7 < p_{\mathrm{T}} < 8$	$3.25 < y^{*} < 4.00$	$1640.200 \pm 89.954 \pm 86.846$
$8 < p_{\mathrm{T}} < 10$	$1.50 < y^{*} < 2.50$	$2060.070 \pm 61.058 \pm 99.169$
$8 < p_{\mathrm{T}} < 10$	$2.50 < y^{*} < 3.25$	$1356.290 \pm 48.603 \pm 61.966$
$8 < p_{\mathrm{T}} < 10$	$3.25 < y^{*} < 4.00$	$829.701 \pm 44.377 \pm 48.566$
$10 < p_{\mathrm{T}} < 14$	$1.50 < y^{*} < 2.50$	$643.118 \pm 22.688 \pm 30.445$
$10 < p_{\mathrm{T}} < 14$	$2.50 < y^{*} < 3.25$	$434.277 \pm 18.775 \pm 19.795$
$10 < p_{\mathrm{T}} < 14$	$3.25 < y^{*} < 4.00$	$232.755 \pm 14.811 \pm 15.111$

Table 69: Total J/ψ-from-b cross section in Pbp, in bins of p_{T} and y^*. The first uncertainty is statistical, the second systematic.

p_{T} bin	y^* bin	$d\sigma/dy^*dp_{\mathrm{T}}$ [nb/(GeV/c)]
$0 < p_{\mathrm{T}} < 1$	$-2.50 > y^* > -3.25$	$14479.500 \pm 486.444 \pm 1231.290$
$0 < p_{\mathrm{T}} < 1$	$-3.25 > y^* > -4.00$	$10939.900 \pm 298.670 \pm 793.596$
$0 < p_{\mathrm{T}} < 1$	$-4.00 > y^* > -5.00$	$6864.370 \pm 258.237 \pm 455.269$
$1 < p_{\mathrm{T}} < 2$	$-2.50 > y^* > -3.25$	$33396.900 \pm 665.640 \pm 2720.400$
$1 < p_{\mathrm{T}} < 2$	$-3.25 > y^* > -4.00$	$17245.800 \pm 334.202 \pm 1184.980$
$1 < p_{\mathrm{T}} < 2$	$-4.00 > y^* > -5.00$	$13243.800 \pm 328.165 \pm 792.408$
$2 < p_{\mathrm{T}} < 3$	$-2.50 > y^* > -3.25$	$31236.200 \pm 588.316 \pm 2229.160$
$2 < p_{\mathrm{T}} < 3$	$-3.25 > y^* > -4.00$	$22524.800 \pm 361.506 \pm 1447.010$
$2 < p_{\mathrm{T}} < 3$	$-4.00 > y^* > -5.00$	$11896.300 \pm 283.341 \pm 703.945$
$3 < p_{\mathrm{T}} < 4$	$-2.50 > y^* > -3.25$	$22455.600 \pm 445.804 \pm 1421.400$
$3 < p_{\mathrm{T}} < 4$	$-3.25 > y^* > -4.00$	$16045.500 \pm 273.614 \pm 948.854$
$3 < p_{\mathrm{T}} < 4$	$-4.00 > y^* > -5.00$	$7624.560 \pm 202.227 \pm 440.511$
$4 < p_{\mathrm{T}} < 5$	$-2.50 > y^* > -3.25$	$14193.100 \pm 308.252 \pm 820.520$
$4 < p_{\mathrm{T}} < 5$	$-3.25 > y^* > -4.00$	$9105.480 \pm 184.176 \pm 533.469$
$4 < p_{\mathrm{T}} < 5$	$-4.00 > y^* > -5.00$	$4351.840 \pm 134.840 \pm 250.645$
$5 < p_{\mathrm{T}} < 6$	$-2.50 > y^* > -3.25$	$8000.260 \pm 207.729 \pm 451.996$
$5 < p_{\mathrm{T}} < 6$	$-3.25 > y^* > -4.00$	$5284.290 \pm 126.738 \pm 301.692$
$5 < p_{\mathrm{T}} < 6$	$-4.00 > y^* > -5.00$	$2253.620 \pm 87.001 \pm 133.410$
$6 < p_{\mathrm{T}} < 7$	$-2.50 > y^* > -3.25$	$4584.660 \pm 142.523 \pm 262.275$
$6 < p_{\mathrm{T}} < 7$	$-3.25 > y^* > -4.00$	$3026.710 \pm 93.685 \pm 173.092$
$6 < p_{\mathrm{T}} < 7$	$-4.00 > y^* > -5.00$	$1222.310 \pm 61.435 \pm 75.924$
$7 < p_{\mathrm{T}} < 8$	$-2.50 > y^* > -3.25$	$2767.460 \pm 105.616 \pm 162.306$
$7 < p_{\mathrm{T}} < 8$	$-3.25 > y^* > -4.00$	$1759.980 \pm 68.727 \pm 104.808$
$7 < p_{\mathrm{T}} < 8$	$-4.00 > y^* > -5.00$	$583.210 \pm 40.590 \pm 39.464$
$8 < p_{\mathrm{T}} < 10$	$-2.50 > y^* > -3.25$	$1578.490 \pm 53.563 \pm 93.216$
$8 < p_{\mathrm{T}} < 10$	$-3.25 > y^* > -4.00$	$787.019 \pm 31.026 \pm 46.668$
$8 < p_{\mathrm{T}} < 10$	$-4.00 > y^* > -5.00$	$263.055 \pm 18.139 \pm 19.213$
$10 < p_{\mathrm{T}} < 14$	$-2.50 > y^* > -3.25$	$458.354 \pm 18.301 \pm 28.513$
$10 < p_{\mathrm{T}} < 14$	$-3.25 > y^* > -4.00$	$224.316 \pm 11.601 \pm 14.457$
$10 < p_{\mathrm{T}} < 14$	$-4.00 > y^* > -5.00$	$59.790 \pm 5.651 \pm 4.721$

Table 70: Total prompt cross section for J/ψ in pPb, in bins of p_{T} integrated over $1.5 < y^{*} < 4.0$. The first uncertainty is statistical, the second systematic.

p_{T} bin	$d\sigma/dp_{\mathrm{T}}$ [nb/(GeV/c)]
$0 < p_{\mathrm{T}} < 1$	$213795.000 \pm 1393.630 \pm 13661.700$
$1 < p_{\mathrm{T}} < 2$	$419795.000 \pm 1883.770 \pm 24634.500$
$2 < p_{\mathrm{T}} < 3$	$387076.000 \pm 1763.650 \pm 22074.000$
$3 < p_{\mathrm{T}} < 4$	$258666.000 \pm 1322.580 \pm 13332.400$
$4 < p_{\mathrm{T}} < 5$	$153321.000 \pm 898.785 \pm 7339.450$
$5 < p_{\mathrm{T}} < 6$	$85870.500 \pm 611.983 \pm 3987.570$
$6 < p_{\mathrm{T}} < 7$	$47259.400 \pm 424.857 \pm 2215.550$
$7 < p_{\mathrm{T}} < 8$	$25967.600 \pm 299.902 \pm 1212.810$
$8 < p_{\mathrm{T}} < 10$	$11707.600 \pm 135.483 \pm 556.293$
$10 < p_{\mathrm{T}} < 14$	$2879.060 \pm 44.054 \pm 135.022$

Table 71: Total prompt cross section for J/ψ in Pbp, in bins of p_{T} integrated over $-5.0 < y^{*} < -2.5$. The first uncertainty is statistical, the second systematic.

p_{T} bin	$d\sigma/dp_{\mathrm{T}}$ [nb/(GeV/c)]
$0 < p_{\mathrm{T}} < 1$	$249244.000 \pm 1344.800 \pm 18997.100$
$1 < p_{\mathrm{T}} < 2$	$477550.000 \pm 1815.730 \pm 35215.000$
$2 < p_{\mathrm{T}} < 3$	$402481.000 \pm 1609.650 \pm 27102.700$
$3 < p_{\mathrm{T}} < 4$	$251006.000 \pm 1147.200 \pm 15375.300$
$4 < p_{\mathrm{T}} < 5$	$136232.000 \pm 733.349 \pm 7897.890$
$5 < p_{\mathrm{T}} < 6$	$70303.700 \pm 473.343 \pm 3978.310$
$6 < p_{\mathrm{T}} < 7$	$35851.700 \pm 310.922 \pm 2035.990$
$7 < p_{\mathrm{T}} < 8$	$18581.400 \pm 209.971 \pm 1070.950$
$8 < p_{\mathrm{T}} < 10$	$7433.170 \pm 90.182 \pm 430.336$
$10 < p_{\mathrm{T}} < 14$	$1580.140 \pm 26.425 \pm 93.016$

Table 72: Total J/ψ-from-b cross section in pPb, in bins of p_{T} integrated over $1.5 < y^{*} < 4.0$. The first uncertainty is statistical, the second systematic.

p_{T} bin	$d\sigma/dp_{\mathrm{T}}$ [nb/(GeV/c)]
$0 < p_{\mathrm{T}} < 1$	$28472.700 \pm 569.214 \pm 1837.850$
$1 < p_{\mathrm{T}} < 2$	$63646.500 \pm 808.088 \pm 3750.670$
$2 < p_{\mathrm{T}} < 3$	$62638.800 \pm 764.007 \pm 3589.620$
$3 < p_{\mathrm{T}} < 4$	$47189.300 \pm 597.259 \pm 2439.360$
$4 < p_{\mathrm{T}} < 5$	$30162.100 \pm 425.964 \pm 1448.820$
$5 < p_{\mathrm{T}} < 6$	$18417.100 \pm 301.315 \pm 856.338$
$6 < p_{\mathrm{T}} < 7$	$11338.000 \pm 221.447 \pm 532.159$
$7 < p_{\mathrm{T}} < 8$	$7229.380 \pm 167.752 \pm 337.290$
$8 < p_{\mathrm{T}} < 10$	$3694.550 \pm 79.915 \pm 175.050$
$10 < p_{\mathrm{T}} < 14$	$1131.720 \pm 29.383 \pm 52.983$

Table 73: Total J/ψ-from-b cross section in Pbp, in bins of p_{T} integrated over $-5.0 < y^{*} < -2.5$. The first uncertainty is statistical, the second systematic.

p_{T} bin	$d\sigma/dp_{\mathrm{T}}$ [nb/(GeV/c)]
$0 < p_{\mathrm{T}} < 1$	$25059.400 \pm 496.958 \pm 1932.570$
$1 < p_{\mathrm{T}} < 2$	$52518.900 \pm 674.929 \pm 3907.700$
$2 < p_{\mathrm{T}} < 3$	$48954.200 \pm 612.600 \pm 3314.760$
$3 < p_{\mathrm{T}} < 4$	$33964.700 \pm 451.371 \pm 2084.520$
$4 < p_{\mathrm{T}} < 5$	$20965.200 \pm 310.177 \pm 1213.150$
$5 < p_{\mathrm{T}} < 6$	$11656.900 \pm 206.364 \pm 658.732$
$6 < p_{\mathrm{T}} < 7$	$6740.840 \pm 145.180 \pm 381.662$
$7 < p_{\mathrm{T}} < 8$	$3831.060 \pm 102.644 \pm 219.440$
$8 < p_{\mathrm{T}} < 10$	$1921.030 \pm 49.545 \pm 110.375$
$10 < p_{\mathrm{T}} < 14$	$544.199 \pm 15.966 \pm 31.831$

Table 74: Total prompt cross section for J/ψ in pPb, in bins of y^{*} integrated over $0 < p_{\mathrm{T}} < 14.0$ GeV/c. The first uncertainty is statistical, the second systematic.

y^{*} bin	$d\sigma/dy^{*}$ [nb]
$1.500 < y^{*} < 2.500$	$793171.000 \pm 2698.500 \pm 47978.600$
$2.500 < y^{*} < 3.250$	$627400.000 \pm 1994.160 \pm 30586.500$
$3.250 < y^{*} < 4.000$	$483948.000 \pm 2060.830 \pm 25589.600$

Table 75: Total J/ψ-from-b cross section in pPb, in bins of y^* integrated over $0 < p_{\mathrm{T}} < 14.0$ GeV/c. The first uncertainty is statistical, the second systematic.

y^* bin	$d\sigma/dy^*$ [nb]
1.500< y^* <2.500	145378.000 ± 1205.850 ± 8575.030
2.500< y^* <3.250	106534.000 ± 858.627 ± 5148.090
3.250< y^* <4.000	74308.600 ± 881.852 ± 3890.720

Table 76: Total prompt cross section for J/ψ in Pbp, in bins of y^* integrated over $0 < p_{\mathrm{T}} < 14$ GeV/c. The first uncertainty is statistical, the second systematic.

y^* bin	$d\sigma/dy^*$ [nb]
-2.500> y^* >-3.250	902438.000 ± 3092.580 ± 65190.900
-3.250> y^* >-4.000	694270.000 ± 1919.300 ± 44970.300
-4.000> y^* >-5.000	464906.000 ± 1583.300 ± 30285.100

Table 77: Total J/ψ-from-b cross section in Pbp, in bins of y^* integrated over $0 < p_{\mathrm{T}} < 14$ GeV/c. The first uncertainty is statistical, the second systematic.

y^* bin	$d\sigma/dy^*$ [nb]
-2.500> y^* >-3.250	129129.000 ± 1235.510 ± 9082.800
-3.250> y^* >-4.000	88368.500 ± 729.010 ± 5650.710
-4.000> y^* >-5.000	46586.900 ± 555.179 ± 3010.470

C.2 $\psi(2S)$ cross sections

Table 78: Total prompt cross section for $\psi(2S)$ in pPb, in bins of p_{T} and y^*. The first uncertainty is statistical, the second systematic.

p_{T} bin	y^* bin	$d\sigma/dy^*dp_{\mathrm{T}}$ [nb/(GeV/c)]
$0 < p_{\mathrm{T}} < 1$	$1.50 < y^* < 2.50$	$7580.680 \pm 2196.170 \pm 596.000$
$0 < p_{\mathrm{T}} < 1$	$2.50 < y^* < 3.25$	$6301.820 \pm 1627.700 \pm 359.115$
$0 < p_{\mathrm{T}} < 1$	$3.25 < y^* < 4.00$	$7614.150 \pm 1528.190 \pm 533.259$
$1 < p_{\mathrm{T}} < 2$	$1.50 < y^* < 2.50$	$19969.700 \pm 3096.560 \pm 1368.300$
$1 < p_{\mathrm{T}} < 2$	$2.50 < y^* < 3.25$	$12451.700 \pm 2175.060 \pm 708.520$
$1 < p_{\mathrm{T}} < 2$	$3.25 < y^* < 4.00$	$10851.100 \pm 2056.740 \pm 617.053$
$2 < p_{\mathrm{T}} < 3$	$1.50 < y^* < 2.50$	$19379.700 \pm 2771.830 \pm 1297.950$
$2 < p_{\mathrm{T}} < 3$	$2.50 < y^* < 3.25$	$20219.800 \pm 2385.780 \pm 1117.380$
$2 < p_{\mathrm{T}} < 3$	$3.25 < y^* < 4.00$	$14115.900 \pm 1990.970 \pm 796.698$
$3 < p_{\mathrm{T}} < 4$	$1.50 < y^* < 2.50$	$20059.000 \pm 2118.160 \pm 1198.520$
$3 < p_{\mathrm{T}} < 4$	$2.50 < y^* < 3.25$	$11528.800 \pm 1567.080 \pm 604.319$
$3 < p_{\mathrm{T}} < 4$	$3.25 < y^* < 4.00$	$11647.100 \pm 1525.040 \pm 608.012$
$4 < p_{\mathrm{T}} < 5$	$1.50 < y^* < 2.50$	$11928.400 \pm 1453.920 \pm 667.637$
$4 < p_{\mathrm{T}} < 5$	$2.50 < y^* < 3.25$	$10620.000 \pm 1043.430 \pm 534.119$
$4 < p_{\mathrm{T}} < 5$	$3.25 < y^* < 4.00$	$6563.650 \pm 946.338 \pm 330.594$
$5 < p_{\mathrm{T}} < 6$	$1.50 < y^* < 2.50$	$6438.220 \pm 814.430 \pm 351.772$
$5 < p_{\mathrm{T}} < 6$	$2.50 < y^* < 3.25$	$6758.250 \pm 683.112 \pm 340.841$
$5 < p_{\mathrm{T}} < 6$	$3.25 < y^* < 4.00$	$4929.540 \pm 686.618 \pm 252.370$
$6 < p_{\mathrm{T}} < 7$	$1.50 < y^* < 2.50$	$4251.740 \pm 552.561 \pm 234.368$
$6 < p_{\mathrm{T}} < 7$	$2.50 < y^* < 3.25$	$3205.460 \pm 407.368 \pm 165.524$
$6 < p_{\mathrm{T}} < 7$	$3.25 < y^* < 4.00$	$2925.790 \pm 433.698 \pm 164.973$
$7 < p_{\mathrm{T}} < 8$	$1.50 < y^* < 2.50$	$3184.030 \pm 402.743 \pm 176.546$
$7 < p_{\mathrm{T}} < 8$	$2.50 < y^* < 3.25$	$2318.220 \pm 300.821 \pm 124.361$
$7 < p_{\mathrm{T}} < 8$	$3.25 < y^* < 4.00$	$2059.440 \pm 330.043 \pm 129.296$
$8 < p_{\mathrm{T}} < 10$	$1.50 < y^* < 2.50$	$1754.790 \pm 186.953 \pm 97.056$
$8 < p_{\mathrm{T}} < 10$	$2.50 < y^* < 3.25$	$1185.590 \pm 144.621 \pm 63.164$
$8 < p_{\mathrm{T}} < 10$	$3.25 < y^* < 4.00$	$573.173 \pm 124.985 \pm 38.715$
$10 < p_{\mathrm{T}} < 14$	$1.50 < y^* < 2.50$	$350.910 \pm 55.404 \pm 19.602$
$10 < p_{\mathrm{T}} < 14$	$2.50 < y^* < 3.25$	$194.453 \pm 46.681 \pm 10.674$
$10 < p_{\mathrm{T}} < 14$	$3.25 < y^* < 4.00$	$229.068 \pm 55.273 \pm 17.407$

Table 79: Total prompt cross section for $\psi(2S)$ in Pbp, in bins of p_{T} and y^*. The first uncertainty is statistical, the second systematic.

p_{T} bin	y^* bin	$d\sigma/dy^*dp_{\mathrm{T}}$ [nb/(GeV/c)]
$0 < p_{\mathrm{T}} < 1$	$-2.50 < y^* < -3.25$	$8375.740 \pm 2711.910 \pm 751.289$
$0 < p_{\mathrm{T}} < 1$	$-3.25 < y^* < -4.00$	$6593.200 \pm 1893.510 \pm 516.579$
$0 < p_{\mathrm{T}} < 1$	$-4.00 < y^* < -5.00$	$4715.710 \pm 1637.650 \pm 341.828$
$1 < p_{\mathrm{T}} < 2$	$-2.50 < y^* < -3.25$	$27206.900 \pm 3821.690 \pm 2318.410$
$1 < p_{\mathrm{T}} < 2$	$-3.25 < y^* < -4.00$	$12760.300 \pm 1979.460 \pm 943.367$
$1 < p_{\mathrm{T}} < 2$	$-4.00 < y^* < -5.00$	$18484.300 \pm 2313.360 \pm 1214.350$
$2 < p_{\mathrm{T}} < 3$	$-2.50 < y^* < -3.25$	$23514.500 \pm 3270.240 \pm 1772.920$
$2 < p_{\mathrm{T}} < 3$	$-3.25 < y^* < -4.00$	$15894.100 \pm 2479.660 \pm 1087.390$
$2 < p_{\mathrm{T}} < 3$	$-4.00 < y^* < -5.00$	$12462.300 \pm 1987.500 \pm 790.801$
$3 < p_{\mathrm{T}} < 4$	$-2.50 < y^* < -3.25$	$19104.800 \pm 2442.270 \pm 1287.970$
$3 < p_{\mathrm{T}} < 4$	$-3.25 < y^* < -4.00$	$16264.300 \pm 1872.160 \pm 1025.930$
$3 < p_{\mathrm{T}} < 4$	$-4.00 < y^* < -5.00$	$6856.470 \pm 1316.100 \pm 424.282$
$4 < p_{\mathrm{T}} < 5$	$-2.50 < y^* < -3.25$	$9422.590 \pm 1412.650 \pm 590.301$
$4 < p_{\mathrm{T}} < 5$	$-3.25 < y^* < -4.00$	$7575.530 \pm 1029.930 \pm 474.588$
$4 < p_{\mathrm{T}} < 5$	$-4.00 < y^* < -5.00$	$4466.870 \pm 772.827 \pm 276.522$
$5 < p_{\mathrm{T}} < 6$	$-2.50 < y^* < -3.25$	$6512.050 \pm 847.140 \pm 404.563$
$5 < p_{\mathrm{T}} < 6$	$-3.25 < y^* < -4.00$	$4432.110 \pm 548.762 \pm 273.106$
$5 < p_{\mathrm{T}} < 6$	$-4.00 < y^* < -5.00$	$3060.600 \pm 450.406 \pm 195.418$
$6 < p_{\mathrm{T}} < 7$	$-2.50 < y^* < -3.25$	$4063.320 \pm 552.049 \pm 260.485$
$6 < p_{\mathrm{T}} < 7$	$-3.25 < y^* < -4.00$	$2874.990 \pm 346.659 \pm 180.106$
$6 < p_{\mathrm{T}} < 7$	$-4.00 < y^* < -5.00$	$1769.280 \pm 296.536 \pm 119.760$
$7 < p_{\mathrm{T}} < 8$	$-2.50 < y^* < -3.25$	$1836.710 \pm 326.899 \pm 123.576$
$7 < p_{\mathrm{T}} < 8$	$-3.25 < y^* < -4.00$	$1317.470 \pm 218.968 \pm 87.877$
$7 < p_{\mathrm{T}} < 8$	$-4.00 < y^* < -5.00$	$1080.320 \pm 178.616 \pm 82.189$
$8 < p_{\mathrm{T}} < 10$	$-2.50 < y^* < -3.25$	$1105.440 \pm 151.021 \pm 74.500$
$8 < p_{\mathrm{T}} < 10$	$-3.25 < y^* < -4.00$	$1200.270 \pm 114.846 \pm 79.985$
$8 < p_{\mathrm{T}} < 10$	$-4.00 < y^* < -5.00$	$449.317 \pm 74.207 \pm 37.016$
$10 < p_{\mathrm{T}} < 14$	$-2.50 < y^* < -3.25$	$240.008 \pm 47.158 \pm 17.607$
$10 < p_{\mathrm{T}} < 14$	$-3.25 < y^* < -4.00$	$261.970 \pm 36.097 \pm 19.577$
$10 < p_{\mathrm{T}} < 14$	$-4.00 < y^* < -5.00$	$94.651 \pm 21.251 \pm 8.698$

Table 80: Total $\psi(2S)$-from-b cross section in pPb, in bins of p_{T} and y^{*}. The first uncertainty is statistical, the second systematic.

p_{T} bin	y^{*} bin	$d\sigma/dy^{*}dp_{\mathrm{T}}$ [nb/(GeV/c)]
$0 < p_{\mathrm{T}} < 1$	$1.50 < y^{*} < 2.50$	$2694.420 \pm 797.407 \pm 211.838$
$0 < p_{\mathrm{T}} < 1$	$2.50 < y^{*} < 3.25$	$2667.130 \pm 688.469 \pm 151.989$
$0 < p_{\mathrm{T}} < 1$	$3.25 < y^{*} < 4.00$	$591.692 \pm 445.333 \pm 41.439$
$1 < p_{\mathrm{T}} < 2$	$1.50 < y^{*} < 2.50$	$7747.000 \pm 1157.050 \pm 530.815$
$1 < p_{\mathrm{T}} < 2$	$2.50 < y^{*} < 3.25$	$6632.870 \pm 1097.730 \pm 377.419$
$1 < p_{\mathrm{T}} < 2$	$3.25 < y^{*} < 4.00$	$3445.500 \pm 891.278 \pm 195.929$
$2 < p_{\mathrm{T}} < 3$	$1.50 < y^{*} < 2.50$	$5704.540 \pm 1083.630 \pm 382.061$
$2 < p_{\mathrm{T}} < 3$	$2.50 < y^{*} < 3.25$	$4484.130 \pm 820.153 \pm 247.800$
$2 < p_{\mathrm{T}} < 3$	$3.25 < y^{*} < 4.00$	$4964.840 \pm 878.049 \pm 280.214$
$3 < p_{\mathrm{T}} < 4$	$1.50 < y^{*} < 2.50$	$6060.470 \pm 789.171 \pm 362.110$
$3 < p_{\mathrm{T}} < 4$	$2.50 < y^{*} < 3.25$	$4520.920 \pm 612.983 \pm 236.979$
$3 < p_{\mathrm{T}} < 4$	$3.25 < y^{*} < 4.00$	$4217.360 \pm 807.205 \pm 220.157$
$4 < p_{\mathrm{T}} < 5$	$1.50 < y^{*} < 2.50$	$4428.290 \pm 630.946 \pm 247.853$
$4 < p_{\mathrm{T}} < 5$	$2.50 < y^{*} < 3.25$	$3104.570 \pm 442.319 \pm 156.141$
$4 < p_{\mathrm{T}} < 5$	$3.25 < y^{*} < 4.00$	$2533.680 \pm 562.704 \pm 127.615$
$5 < p_{\mathrm{T}} < 6$	$1.50 < y^{*} < 2.50$	$2841.250 \pm 448.556 \pm 155.240$
$5 < p_{\mathrm{T}} < 6$	$2.50 < y^{*} < 3.25$	$3091.490 \pm 383.795 \pm 155.914$
$5 < p_{\mathrm{T}} < 6$	$3.25 < y^{*} < 4.00$	$1156.230 \pm 289.422 \pm 59.194$
$6 < p_{\mathrm{T}} < 7$	$1.50 < y^{*} < 2.50$	$2108.660 \pm 336.382 \pm 116.235$
$6 < p_{\mathrm{T}} < 7$	$2.50 < y^{*} < 3.25$	$1520.630 \pm 250.611 \pm 78.523$
$6 < p_{\mathrm{T}} < 7$	$3.25 < y^{*} < 4.00$	$932.889 \pm 234.642 \pm 52.602$
$7 < p_{\mathrm{T}} < 8$	$1.50 < y^{*} < 2.50$	$773.839 \pm 169.507 \pm 42.907$
$7 < p_{\mathrm{T}} < 8$	$2.50 < y^{*} < 3.25$	$841.655 \pm 162.775 \pm 45.150$
$7 < p_{\mathrm{T}} < 8$	$3.25 < y^{*} < 4.00$	$487.505 \pm 152.437 \pm 30.607$
$8 < p_{\mathrm{T}} < 10$	$1.50 < y^{*} < 2.50$	$623.690 \pm 104.025 \pm 34.496$
$8 < p_{\mathrm{T}} < 10$	$2.50 < y^{*} < 3.25$	$632.883 \pm 93.837 \pm 33.718$
$8 < p_{\mathrm{T}} < 10$	$3.25 < y^{*} < 4.00$	$401.341 \pm 95.733 \pm 27.108$
$10 < p_{\mathrm{T}} < 14$	$1.50 < y^{*} < 2.50$	$262.745 \pm 43.060 \pm 14.677$
$10 < p_{\mathrm{T}} < 14$	$2.50 < y^{*} < 3.25$	$186.281 \pm 35.980 \pm 10.225$
$10 < p_{\mathrm{T}} < 14$	$3.25 < y^{*} < 4.00$	$117.614 \pm 33.249 \pm 8.938$

Table 81: Total $\psi(2S)$-from-b cross section in Pbp, in bins of p_{T} and y^*. The first uncertainty is statistical, the second systematic.

p_{T} bin	y^* bin	$d\sigma/dy^*dp_{\mathrm{T}}$ [nb/(GeV/c)]
$0 < p_{\mathrm{T}} < 1$	$-2.50 < y^* < -3.25$	$3257.430 \pm 1184.780 \pm 292.185$
$0 < p_{\mathrm{T}} < 1$	$-3.25 < y^* < -4.00$	$2563.960 \pm 624.496 \pm 200.887$
$0 < p_{\mathrm{T}} < 1$	$-4.00 < y^* < -5.00$	$753.113 \pm 469.020 \pm 54.591$
$1 < p_{\mathrm{T}} < 2$	$-2.50 < y^* < -3.25$	$10845.100 \pm 1677.100 \pm 924.156$
$1 < p_{\mathrm{T}} < 2$	$-3.25 < y^* < -4.00$	$3441.230 \pm 589.329 \pm 254.410$
$1 < p_{\mathrm{T}} < 2$	$-4.00 < y^* < -5.00$	$1504.290 \pm 440.722 \pm 98.826$
$2 < p_{\mathrm{T}} < 3$	$-2.50 < y^* < -3.25$	$7164.640 \pm 1217.220 \pm 540.191$
$2 < p_{\mathrm{T}} < 3$	$-3.25 < y^* < -4.00$	$5337.460 \pm 872.685 \pm 365.162$
$2 < p_{\mathrm{T}} < 3$	$-4.00 < y^* < -5.00$	$2438.240 \pm 562.395 \pm 154.720$
$3 < p_{\mathrm{T}} < 4$	$-2.50 < y^* < -3.25$	$8194.850 \pm 1016.700 \pm 552.465$
$3 < p_{\mathrm{T}} < 4$	$-3.25 < y^* < -4.00$	$3767.360 \pm 567.291 \pm 237.641$
$3 < p_{\mathrm{T}} < 4$	$-4.00 < y^* < -5.00$	$2765.140 \pm 521.695 \pm 171.108$
$4 < p_{\mathrm{T}} < 5$	$-2.50 < y^* < -3.25$	$5532.040 \pm 659.618 \pm 346.568$
$4 < p_{\mathrm{T}} < 5$	$-3.25 < y^* < -4.00$	$2142.460 \pm 382.368 \pm 134.220$
$4 < p_{\mathrm{T}} < 5$	$-4.00 < y^* < -5.00$	$1376.340 \pm 293.613 \pm 85.203$
$5 < p_{\mathrm{T}} < 6$	$-2.50 < y^* < -3.25$	$2564.950 \pm 446.297 \pm 159.348$
$5 < p_{\mathrm{T}} < 6$	$-3.25 < y^* < -4.00$	$1563.030 \pm 241.886 \pm 96.314$
$5 < p_{\mathrm{T}} < 6$	$-4.00 < y^* < -5.00$	$598.427 \pm 170.215 \pm 38.209$
$6 < p_{\mathrm{T}} < 7$	$-2.50 < y^* < -3.25$	$1481.850 \pm 291.403 \pm 94.996$
$6 < p_{\mathrm{T}} < 7$	$-3.25 < y^* < -4.00$	$925.499 \pm 165.591 \pm 57.979$
$6 < p_{\mathrm{T}} < 7$	$-4.00 < y^* < -5.00$	$351.506 \pm 120.011 \pm 23.793$
$7 < p_{\mathrm{T}} < 8$	$-2.50 < y^* < -3.25$	$706.675 \pm 181.984 \pm 47.546$
$7 < p_{\mathrm{T}} < 8$	$-3.25 < y^* < -4.00$	$717.906 \pm 139.044 \pm 47.885$
$7 < p_{\mathrm{T}} < 8$	$-4.00 < y^* < -5.00$	$117.371 \pm 67.065 \pm 8.929$
$8 < p_{\mathrm{T}} < 10$	$-2.50 < y^* < -3.25$	$518.782 \pm 98.806 \pm 34.963$
$8 < p_{\mathrm{T}} < 10$	$-3.25 < y^* < -4.00$	$215.169 \pm 55.368 \pm 14.339$
$8 < p_{\mathrm{T}} < 10$	$-4.00 < y^* < -5.00$	$55.872 \pm 32.792 \pm 4.603$
$10 < p_{\mathrm{T}} < 14$	$-2.50 < y^* < -3.25$	$98.057 \pm 26.714 \pm 7.193$
$10 < p_{\mathrm{T}} < 14$	$-3.25 < y^* < -4.00$	$76.226 \pm 19.745 \pm 5.696$
$10 < p_{\mathrm{T}} < 14$	$-4.00 < y^* < -5.00$	$26.824 \pm 12.392 \pm 2.465$

Table 82: Total prompt cross section for $\psi(2S)$ in pPb, in bins of p_{T} integrated over $1.5 < y^* < 4.0$. The first uncertainty is statistical, the second systematic.

p_{T} bin	$d\sigma/dp_{\mathrm{T}}$ [nb/(GeV/c)]
$0< p_{\mathrm{T}} <0$	$18017.700 \pm 2761.720 \pm 355.219$
$0< p_{\mathrm{T}} <0$	$37446.900 \pm 3824.830 \pm 959.613$
$0< p_{\mathrm{T}} <0$	$45131.400 \pm 3621.390 \pm 777.311$
$0< p_{\mathrm{T}} <0$	$37441.000 \pm 2678.840 \pm 703.077$
$0< p_{\mathrm{T}} <0$	$24816.100 \pm 1797.230 \pm 457.558$
$0< p_{\mathrm{T}} <0$	$15204.100 \pm 1091.320 \pm 312.473$
$0< p_{\mathrm{T}} <0$	$8850.170 \pm 710.262 \pm 209.699$
$0< p_{\mathrm{T}} <0$	$6467.280 \pm 523.810 \pm 95.862$
$0< p_{\mathrm{T}} <0$	$3073.860 \pm 235.591 \pm 77.208$
$0< p_{\mathrm{T}} <0$	$668.551 \pm 77.549 \pm 27.435$

Table 83: Total prompt cross section for $\psi(2S)$ in Pbp, in bins of p_{T} integrated over $-5.0 < y^* < -2.5$. The first uncertainty is statistical, the second systematic.

p_{T} bin	$d\sigma/dp_{\mathrm{T}}$ [nb/(GeV/c)]
$0 < p_{\mathrm{T}} <1$	$16857.400 \pm 3298.450 \pm 0.000$
$1 < p_{\mathrm{T}} <2$	$50640.400 \pm 4451.920 \pm 0.000$
$2 < p_{\mathrm{T}} <3$	$44781.800 \pm 4046.620 \pm 0.000$
$3 < p_{\mathrm{T}} <4$	$36445.300 \pm 2985.060 \pm 0.000$
$4 < p_{\mathrm{T}} <5$	$18454.400 \pm 1711.200 \pm 0.000$
$5 < p_{\mathrm{T}} <6$	$12131.600 \pm 1000.570 \pm 0.000$
$6 < p_{\mathrm{T}} <7$	$7546.520 \pm 649.475 \pm 0.000$
$7 < p_{\mathrm{T}} <8$	$3635.060 \pm 389.588 \pm 0.000$
$8 < p_{\mathrm{T}} <10$	$2342.630 \pm 182.548 \pm 0.000$
$10< p_{\mathrm{T}} <14$	$507.473 \pm 56.665 \pm 0.000$

Table 84: Total $\psi(2S)$-from-b cross section in pPb, in bins of p_{T} integrated over $1.5 < y^* < 4.0$. The first uncertainty is statistical, the second systematic.

p_{T} bin	$d\sigma/dp_{\mathrm{T}}$ [nb/(GeV/c)]
$0 < p_{\mathrm{T}} < 1$	$5138.540 \pm 1006.990 \pm 355.219$
$1 < p_{\mathrm{T}} < 2$	$15305.800 \pm 1569.530 \pm 959.613$
$2 < p_{\mathrm{T}} < 3$	$12791.300 \pm 1409.360 \pm 777.311$
$3 < p_{\mathrm{T}} < 4$	$12614.200 \pm 1095.750 \pm 703.077$
$4 < p_{\mathrm{T}} < 5$	$8656.980 \pm 828.403 \pm 457.558$
$5 < p_{\mathrm{T}} < 6$	$6027.040 \pm 575.478 \pm 312.473$
$6 < p_{\mathrm{T}} < 7$	$3948.800 \pm 423.616 \pm 209.699$
$7 < p_{\mathrm{T}} < 8$	$1770.710 \pm 238.133 \pm 95.862$
$8 < p_{\mathrm{T}} < 10$	$1399.360 \pm 144.670 \pm 77.208$
$10 < p_{\mathrm{T}} < 14$	$490.666 \pm 56.606 \pm 27.435$

Table 85: Total $\psi(2S)$-from-b cross section in Pbp, in bins of p_{T} integrated over $-5.0 < y^* < -2.5$. The first uncertainty is statistical, the second systematic.

p_{T} bin	$d\sigma/dp_{\mathrm{T}}$ [nb/(GeV/c)]
$0 < p_{\mathrm{T}} < 1$	$5119.150 \pm 1108.570 \pm 1004.730$
$1 < p_{\mathrm{T}} < 2$	$12219.100 \pm 1404.180 \pm 1934.800$
$2 < p_{\mathrm{T}} < 3$	$11814.800 \pm 1256.220 \pm 874.295$
$3 < p_{\mathrm{T}} < 4$	$11736.800 \pm 1017.170 \pm 1472.200$
$4 < p_{\mathrm{T}} < 5$	$7132.220 \pm 642.799 \pm 1253.450$
$5 < p_{\mathrm{T}} < 6$	$3694.410 \pm 417.042 \pm 598.837$
$6 < p_{\mathrm{T}} < 7$	$2157.010 \pm 278.553 \pm 372.815$
$7 < p_{\mathrm{T}} < 8$	$1185.810 \pm 184.395 \pm 208.825$
$8 < p_{\mathrm{T}} < 10$	$606.335 \pm 91.056 \pm 80.330$
$10 < p_{\mathrm{T}} < 14$	$157.536 \pm 27.826 \pm 15.133$

Table 86: Total prompt cross section for $\psi(2S)$ in pPb, in bins of y^* integrated over $0 < p_{\mathrm{T}} < 14.0$ GeV/c. The first uncertainty is statistical, the second systematic.

y^* bin	$d\sigma/dy^*$ [nb]
$1.500 < y^* < 2.500$	$97704.700 \pm 5478.600 \pm 6120.600$
$2.500 < y^* < 3.250$	$76553.000 \pm 4178.310 \pm 4099.960$
$3.250 < y^* < 4.000$	$62769.400 \pm 3825.010 \pm 3547.420$

Table 87: Total $\psi(2S)$-from-b cross section in pPb, in bins of y^* integrated over $0 < p_{\mathrm{T}} < 14.0$ GeV/c. The first uncertainty is statistical, the second systematic.

y^* bin	$d\sigma/dy^*$ [nb]
1.500< y^* <2.500	$34656.800 \pm 2141.450 \pm 2159.850$
2.500< y^* <3.250	$28874.300 \pm 1793.200 \pm 1546.980$
3.250< y^* <4.000	$19602.800 \pm 1717.060 \pm 1086.520$

Table 88: Total prompt cross section for $\psi(2S)$ in Pbp, in bins of y^* integrated over $0 < p_{\mathrm{T}} < 14$ GeV/c. The first uncertainty is statistical, the second systematic.

y^* bin	$d\sigma/dy^*$ [nb]
-2.500> y^* >-3.250	$103208.000 \pm 6470.750 \pm 0.000$
-3.250> y^* >-4.000	$71160.400 \pm 4331.390 \pm 0.000$
-4.000> y^* >-5.000	$54173.200 \pm 3829.490 \pm 0.000$

Table 89: Total $\psi(2S)$-from-b cross section in Pbp, in bins of y^* integrated over $0 < p_{\mathrm{T}} < 14$ GeV/c. The first uncertainty is statistical, the second systematic.

y^* bin	$d\sigma/dy^*$ [nb]
-2.500> y^* >-3.250	$41177.300 \pm 2744.890 \pm 9973.180$
-3.250> y^* >-4.000	$21194.100 \pm 1445.920 \pm 1683.070$
-4.000> y^* >-5.000	$10123.500 \pm 1069.350 \pm 663.388$

D Cross section ratios

Table 90: Prompt cross section ratio $\psi(2S)\ /J/\psi$ in pPb, in bins of p_{T} and y^{*}. The first uncertainty is statistical, the second systematic.

p_{T} bin	y^{*} bin	$\sigma_{\psi(2S)}/\sigma_{J/\psi}$
$0 < p_{\mathrm{T}} < 1$	$1.50 < y^{*} < 2.50$	$0.076 \pm 0.022 \pm 0.002$
$0 < p_{\mathrm{T}} < 1$	$2.50 < y^{*} < 3.25$	$0.081 \pm 0.021 \pm 0.002$
$0 < p_{\mathrm{T}} < 1$	$3.25 < y^{*} < 4.00$	$0.114 \pm 0.023 \pm 0.003$
$1 < p_{\mathrm{T}} < 2$	$1.50 < y^{*} < 2.50$	$0.100 \pm 0.016 \pm 0.002$
$1 < p_{\mathrm{T}} < 2$	$2.50 < y^{*} < 3.25$	$0.078 \pm 0.014 \pm 0.002$
$1 < p_{\mathrm{T}} < 2$	$3.25 < y^{*} < 4.00$	$0.082 \pm 0.016 \pm 0.002$
$2 < p_{\mathrm{T}} < 3$	$1.50 < y^{*} < 2.50$	$0.103 \pm 0.015 \pm 0.003$
$2 < p_{\mathrm{T}} < 3$	$2.50 < y^{*} < 3.25$	$0.133 \pm 0.016 \pm 0.003$
$2 < p_{\mathrm{T}} < 3$	$3.25 < y^{*} < 4.00$	$0.122 \pm 0.017 \pm 0.003$
$3 < p_{\mathrm{T}} < 4$	$1.50 < y^{*} < 2.50$	$0.157 \pm 0.017 \pm 0.004$
$3 < p_{\mathrm{T}} < 4$	$2.50 < y^{*} < 3.25$	$0.114 \pm 0.015 \pm 0.003$
$3 < p_{\mathrm{T}} < 4$	$3.25 < y^{*} < 4.00$	$0.157 \pm 0.021 \pm 0.004$
$4 < p_{\mathrm{T}} < 5$	$1.50 < y^{*} < 2.50$	$0.155 \pm 0.019 \pm 0.004$
$4 < p_{\mathrm{T}} < 5$	$2.50 < y^{*} < 3.25$	$0.174 \pm 0.017 \pm 0.004$
$4 < p_{\mathrm{T}} < 5$	$3.25 < y^{*} < 4.00$	$0.156 \pm 0.023 \pm 0.004$
$5 < p_{\mathrm{T}} < 6$	$1.50 < y^{*} < 2.50$	$0.146 \pm 0.018 \pm 0.004$
$5 < p_{\mathrm{T}} < 6$	$2.50 < y^{*} < 3.25$	$0.204 \pm 0.021 \pm 0.005$
$5 < p_{\mathrm{T}} < 6$	$3.25 < y^{*} < 4.00$	$0.204 \pm 0.029 \pm 0.005$
$6 < p_{\mathrm{T}} < 7$	$1.50 < y^{*} < 2.50$	$0.173 \pm 0.023 \pm 0.005$
$6 < p_{\mathrm{T}} < 7$	$2.50 < y^{*} < 3.25$	$0.179 \pm 0.023 \pm 0.005$
$6 < p_{\mathrm{T}} < 7$	$3.25 < y^{*} < 4.00$	$0.225 \pm 0.034 \pm 0.007$
$7 < p_{\mathrm{T}} < 8$	$1.50 < y^{*} < 2.50$	$0.225 \pm 0.029 \pm 0.006$
$7 < p_{\mathrm{T}} < 8$	$2.50 < y^{*} < 3.25$	$0.237 \pm 0.031 \pm 0.007$
$7 < p_{\mathrm{T}} < 8$	$3.25 < y^{*} < 4.00$	$0.303 \pm 0.049 \pm 0.011$
$8 < p_{\mathrm{T}} < 10$	$1.50 < y^{*} < 2.50$	$0.283 \pm 0.031 \pm 0.008$
$8 < p_{\mathrm{T}} < 10$	$2.50 < y^{*} < 3.25$	$0.265 \pm 0.033 \pm 0.008$
$8 < p_{\mathrm{T}} < 10$	$3.25 < y^{*} < 4.00$	$0.190 \pm 0.042 \pm 0.007$
$10 < p_{\mathrm{T}} < 14$	$1.50 < y^{*} < 2.50$	$0.228 \pm 0.036 \pm 0.007$
$10 < p_{\mathrm{T}} < 14$	$2.50 < y^{*} < 3.25$	$0.178 \pm 0.043 \pm 0.006$
$10 < p_{\mathrm{T}} < 14$	$3.25 < y^{*} < 4.00$	$0.354 \pm 0.086 \pm 0.014$

Table 91: Prompt cross section $\psi(2S)$ $/J/\psi$ in Pbp, in bins of p_{T} and y^{*}. The first uncertainty is statistical, the second systematic.

p_{T} bin	y^{*} bin	$\sigma_{\psi(2S)}/\sigma_{J/\psi}$
$0 < p_{\mathrm{T}} < 1$	$-2.50 > y^{*} > -3.25$	$0.065 \pm 0.021 \pm 0.002$
$0 < p_{\mathrm{T}} < 1$	$-3.25 > y^{*} > -4.00$	$0.065 \pm 0.019 \pm 0.002$
$0 < p_{\mathrm{T}} < 1$	$-4.00 > y^{*} > -5.00$	$0.058 \pm 0.020 \pm 0.002$
$1 < p_{\mathrm{T}} < 2$	$-2.50 > y^{*} > -3.25$	$0.108 \pm 0.015 \pm 0.003$
$1 < p_{\mathrm{T}} < 2$	$-3.25 > y^{*} > -4.00$	$0.085 \pm 0.013 \pm 0.002$
$1 < p_{\mathrm{T}} < 2$	$-4.00 > y^{*} > -5.00$	$0.120 \pm 0.015 \pm 0.003$
$2 < p_{\mathrm{T}} < 3$	$-2.50 > y^{*} > -3.25$	$0.104 \pm 0.014 \pm 0.003$
$2 < p_{\mathrm{T}} < 3$	$-3.25 > y^{*} > -4.00$	$0.091 \pm 0.014 \pm 0.002$
$2 < p_{\mathrm{T}} < 3$	$-4.00 > y^{*} > -5.00$	$0.107 \pm 0.017 \pm 0.003$
$3 < p_{\mathrm{T}} < 4$	$-2.50 > y^{*} > -3.25$	$0.133 \pm 0.017 \pm 0.003$
$3 < p_{\mathrm{T}} < 4$	$-3.25 > y^{*} > -4.00$	$0.147 \pm 0.017 \pm 0.003$
$3 < p_{\mathrm{T}} < 4$	$-4.00 > y^{*} > -5.00$	$0.101 \pm 0.019 \pm 0.002$
$4 < p_{\mathrm{T}} < 5$	$-2.50 > y^{*} > -3.25$	$0.116 \pm 0.017 \pm 0.003$
$4 < p_{\mathrm{T}} < 5$	$-3.25 > y^{*} > -4.00$	$0.123 \pm 0.017 \pm 0.003$
$4 < p_{\mathrm{T}} < 5$	$-4.00 > y^{*} > -5.00$	$0.132 \pm 0.023 \pm 0.003$
$5 < p_{\mathrm{T}} < 6$	$-2.50 > y^{*} > -3.25$	$0.148 \pm 0.019 \pm 0.004$
$5 < p_{\mathrm{T}} < 6$	$-3.25 > y^{*} > -4.00$	$0.145 \pm 0.018 \pm 0.004$
$5 < p_{\mathrm{T}} < 6$	$-4.00 > y^{*} > -5.00$	$0.179 \pm 0.027 \pm 0.005$
$6 < p_{\mathrm{T}} < 7$	$-2.50 > y^{*} > -3.25$	$0.181 \pm 0.025 \pm 0.005$
$6 < p_{\mathrm{T}} < 7$	$-3.25 > y^{*} > -4.00$	$0.174 \pm 0.021 \pm 0.005$
$6 < p_{\mathrm{T}} < 7$	$-4.00 > y^{*} > -5.00$	$0.212 \pm 0.036 \pm 0.006$
$7 < p_{\mathrm{T}} < 8$	$-2.50 > y^{*} > -3.25$	$0.150 \pm 0.027 \pm 0.005$
$7 < p_{\mathrm{T}} < 8$	$-3.25 > y^{*} > -4.00$	$0.158 \pm 0.026 \pm 0.005$
$7 < p_{\mathrm{T}} < 8$	$-4.00 > y^{*} > -5.00$	$0.281 \pm 0.047 \pm 0.010$
$8 < p_{\mathrm{T}} < 10$	$-2.50 > y^{*} > -3.25$	$0.213 \pm 0.029 \pm 0.007$
$8 < p_{\mathrm{T}} < 10$	$-3.25 > y^{*} > -4.00$	$0.350 \pm 0.034 \pm 0.011$
$8 < p_{\mathrm{T}} < 10$	$-4.00 > y^{*} > -5.00$	$0.334 \pm 0.056 \pm 0.013$
$10 < p_{\mathrm{T}} < 14$	$-2.50 > y^{*} > -3.25$	$0.198 \pm 0.039 \pm 0.008$
$10 < p_{\mathrm{T}} < 14$	$-3.25 > y^{*} > -4.00$	$0.384 \pm 0.054 \pm 0.015$
$10 < p_{\mathrm{T}} < 14$	$-4.00 > y^{*} > -5.00$	$0.408 \pm 0.093 \pm 0.019$

Table 92: cross section ratio of $\psi(2S)$-from-b $/J/\psi$-from-b in pPb, in bins of $p_{\rm T}$ and y^*. The first uncertainty is statistical, the second systematic.

$p_{\rm T}$ bin	y^* bin	$\sigma_{\psi(2S)}/\sigma_{J/\psi}$
$0 < p_{\rm T} < 1$	$1.50 < y^* < 2.50$	$0.193 \pm 0.058 \pm 0.005$
$0 < p_{\rm T} < 1$	$2.50 < y^* < 3.25$	$0.267 \pm 0.069 \pm 0.008$
$0 < p_{\rm T} < 1$	$3.25 < y^* < 4.00$	$0.070 \pm 0.053 \pm 0.002$
$1 < p_{\rm T} < 2$	$1.50 < y^* < 2.50$	$0.244 \pm 0.037 \pm 0.006$
$1 < p_{\rm T} < 2$	$2.50 < y^* < 3.25$	$0.275 \pm 0.046 \pm 0.007$
$1 < p_{\rm T} < 2$	$3.25 < y^* < 4.00$	$0.182 \pm 0.047 \pm 0.005$
$2 < p_{\rm T} < 3$	$1.50 < y^* < 2.50$	$0.179 \pm 0.034 \pm 0.005$
$2 < p_{\rm T} < 3$	$2.50 < y^* < 3.25$	$0.184 \pm 0.034 \pm 0.004$
$2 < p_{\rm T} < 3$	$3.25 < y^* < 4.00$	$0.286 \pm 0.051 \pm 0.007$
$3 < p_{\rm T} < 4$	$1.50 < y^* < 2.50$	$0.245 \pm 0.032 \pm 0.006$
$3 < p_{\rm T} < 4$	$2.50 < y^* < 3.25$	$0.250 \pm 0.034 \pm 0.006$
$3 < p_{\rm T} < 4$	$3.25 < y^* < 4.00$	$0.334 \pm 0.065 \pm 0.008$
$4 < p_{\rm T} < 5$	$1.50 < y^* < 2.50$	$0.274 \pm 0.039 \pm 0.007$
$4 < p_{\rm T} < 5$	$2.50 < y^* < 3.25$	$0.271 \pm 0.039 \pm 0.006$
$4 < p_{\rm T} < 5$	$3.25 < y^* < 4.00$	$0.327 \pm 0.074 \pm 0.008$
$5 < p_{\rm T} < 6$	$1.50 < y^* < 2.50$	$0.287 \pm 0.046 \pm 0.007$
$5 < p_{\rm T} < 6$	$2.50 < y^* < 3.25$	$0.430 \pm 0.054 \pm 0.011$
$5 < p_{\rm T} < 6$	$3.25 < y^* < 4.00$	$0.260 \pm 0.066 \pm 0.007$
$6 < p_{\rm T} < 7$	$1.50 < y^* < 2.50$	$0.353 \pm 0.057 \pm 0.009$
$6 < p_{\rm T} < 7$	$2.50 < y^* < 3.25$	$0.343 \pm 0.057 \pm 0.009$
$6 < p_{\rm T} < 7$	$3.25 < y^* < 4.00$	$0.363 \pm 0.093 \pm 0.011$
$7 < p_{\rm T} < 8$	$1.50 < y^* < 2.50$	$0.239 \pm 0.053 \pm 0.007$
$7 < p_{\rm T} < 8$	$2.50 < y^* < 3.25$	$0.285 \pm 0.056 \pm 0.008$
$7 < p_{\rm T} < 8$	$3.25 < y^* < 4.00$	$0.297 \pm 0.095 \pm 0.010$
$8 < p_{\rm T} < 10$	$1.50 < y^* < 2.50$	$0.303 \pm 0.051 \pm 0.009$
$8 < p_{\rm T} < 10$	$2.50 < y^* < 3.25$	$0.467 \pm 0.071 \pm 0.013$
$8 < p_{\rm T} < 10$	$3.25 < y^* < 4.00$	$0.484 \pm 0.118 \pm 0.017$
$10 < p_{\rm T} < 14$	$1.50 < y^* < 2.50$	$0.409 \pm 0.069 \pm 0.013$
$10 < p_{\rm T} < 14$	$2.50 < y^* < 3.25$	$0.429 \pm 0.085 \pm 0.014$
$10 < p_{\rm T} < 14$	$3.25 < y^* < 4.00$	$0.505 \pm 0.147 \pm 0.020$

Table 93: The cross section ratio $\psi(2S)$-from-b $/J/\psi$-from-b in Pbp, in bins of p_{T} and y^{*}. The first uncertainty is statistical, the second systematic.

p_{T} bin	y^{*} bin	$\sigma_{\psi(2S)}/\sigma_{J/\psi}$
$0 < p_{\mathrm{T}} < 1$	$-2.50 < y^{*} < -3.25$	$0.225 \pm 0.082 \pm 0.007$
$0 < p_{\mathrm{T}} < 1$	$-3.25 < y^{*} < -4.00$	$0.234 \pm 0.057 \pm 0.007$
$0 < p_{\mathrm{T}} < 1$	$-4.00 < y^{*} < -5.00$	$0.110 \pm 0.068 \pm 0.003$
$1 < p_{\mathrm{T}} < 2$	$-2.50 < y^{*} < -3.25$	$0.325 \pm 0.051 \pm 0.009$
$1 < p_{\mathrm{T}} < 2$	$-3.25 < y^{*} < -4.00$	$0.200 \pm 0.034 \pm 0.006$
$1 < p_{\mathrm{T}} < 2$	$-4.00 < y^{*} < -5.00$	$0.114 \pm 0.033 \pm 0.003$
$2 < p_{\mathrm{T}} < 3$	$-2.50 < y^{*} < -3.25$	$0.229 \pm 0.039 \pm 0.006$
$2 < p_{\mathrm{T}} < 3$	$-3.25 < y^{*} < -4.00$	$0.237 \pm 0.039 \pm 0.006$
$2 < p_{\mathrm{T}} < 3$	$-4.00 < y^{*} < -5.00$	$0.205 \pm 0.048 \pm 0.005$
$3 < p_{\mathrm{T}} < 4$	$-2.50 < y^{*} < -3.25$	$0.365 \pm 0.046 \pm 0.009$
$3 < p_{\mathrm{T}} < 4$	$-3.25 < y^{*} < -4.00$	$0.235 \pm 0.036 \pm 0.005$
$3 < p_{\mathrm{T}} < 4$	$-4.00 < y^{*} < -5.00$	$0.363 \pm 0.069 \pm 0.009$
$4 < p_{\mathrm{T}} < 5$	$-2.50 < y^{*} < -3.25$	$0.390 \pm 0.047 \pm 0.010$
$4 < p_{\mathrm{T}} < 5$	$-3.25 < y^{*} < -4.00$	$0.235 \pm 0.042 \pm 0.006$
$4 < p_{\mathrm{T}} < 5$	$-4.00 < y^{*} < -5.00$	$0.316 \pm 0.068 \pm 0.008$
$5 < p_{\mathrm{T}} < 6$	$-2.50 < y^{*} < -3.25$	$0.321 \pm 0.057 \pm 0.009$
$5 < p_{\mathrm{T}} < 6$	$-3.25 < y^{*} < -4.00$	$0.296 \pm 0.046 \pm 0.007$
$5 < p_{\mathrm{T}} < 6$	$-4.00 < y^{*} < -5.00$	$0.266 \pm 0.076 \pm 0.007$
$6 < p_{\mathrm{T}} < 7$	$-2.50 < y^{*} < -3.25$	$0.323 \pm 0.064 \pm 0.010$
$6 < p_{\mathrm{T}} < 7$	$-3.25 < y^{*} < -4.00$	$0.306 \pm 0.056 \pm 0.008$
$6 < p_{\mathrm{T}} < 7$	$-4.00 < y^{*} < -5.00$	$0.288 \pm 0.099 \pm 0.008$
$7 < p_{\mathrm{T}} < 8$	$-2.50 < y^{*} < -3.25$	$0.255 \pm 0.067 \pm 0.009$
$7 < p_{\mathrm{T}} < 8$	$-3.25 < y^{*} < -4.00$	$0.408 \pm 0.081 \pm 0.013$
$7 < p_{\mathrm{T}} < 8$	$-4.00 < y^{*} < -5.00$	$0.201 \pm 0.116 \pm 0.007$
$8 < p_{\mathrm{T}} < 10$	$-2.50 < y^{*} < -3.25$	$0.329 \pm 0.064 \pm 0.011$
$8 < p_{\mathrm{T}} < 10$	$-3.25 < y^{*} < -4.00$	$0.273 \pm 0.071 \pm 0.009$
$8 < p_{\mathrm{T}} < 10$	$-4.00 < y^{*} < -5.00$	$0.212 \pm 0.126 \pm 0.008$
$10 < p_{\mathrm{T}} < 14$	$-2.50 < y^{*} < -3.25$	$0.214 \pm 0.059 \pm 0.008$
$10 < p_{\mathrm{T}} < 14$	$-3.25 < y^{*} < -4.00$	$0.340 \pm 0.090 \pm 0.013$
$10 < p_{\mathrm{T}} < 14$	$-4.00 < y^{*} < -5.00$	$0.449 \pm 0.212 \pm 0.021$

Table 94: Prompt cross section ratio $\psi(2S)$ $/J/\psi$ in pPb, in bins of p_{T} integrated over $1.5 < y^* < 4.0$. The first uncertainty is statistical, the second systematic.

p_{T} bin	$\sigma_{\psi(2S)}/\sigma_{J/\psi}$
$0 < p_{\mathrm{T}} < 1$	$0.084 \pm 0.013 \pm 0.002$
$1 < p_{\mathrm{T}} < 2$	$0.089 \pm 0.009 \pm 0.002$
$2 < p_{\mathrm{T}} < 3$	$0.117 \pm 0.009 \pm 0.003$
$3 < p_{\mathrm{T}} < 4$	$0.145 \pm 0.010 \pm 0.003$
$4 < p_{\mathrm{T}} < 5$	$0.162 \pm 0.012 \pm 0.004$
$5 < p_{\mathrm{T}} < 6$	$0.177 \pm 0.013 \pm 0.004$
$6 < p_{\mathrm{T}} < 7$	$0.187 \pm 0.015 \pm 0.004$
$7 < p_{\mathrm{T}} < 8$	$0.249 \pm 0.020 \pm 0.006$
$8 < p_{\mathrm{T}} < 10$	$0.263 \pm 0.020 \pm 0.006$
$10 < p_{\mathrm{T}} < 14$	$0.232 \pm 0.027 \pm 0.006$

Table 95: Prompt cross section ratio $\psi(2S)$ $/J/\psi$ in Pbp, in bins of p_{T} integrated over $-5.0 < y^* < -2.5$. The first uncertainty is statistical, the second systematic.

p_{T} bin	$\sigma_{\psi(2S)}/\sigma_{J/\psi}$
$0 < p_{\mathrm{T}} < 1$	$0.068 \pm 0.013 \pm 0.002$
$1 < p_{\mathrm{T}} < 2$	$0.106 \pm 0.009 \pm 0.003$
$2 < p_{\mathrm{T}} < 3$	$0.111 \pm 0.010 \pm 0.002$
$3 < p_{\mathrm{T}} < 4$	$0.145 \pm 0.012 \pm 0.003$
$4 < p_{\mathrm{T}} < 5$	$0.135 \pm 0.013 \pm 0.003$
$5 < p_{\mathrm{T}} < 6$	$0.173 \pm 0.014 \pm 0.004$
$6 < p_{\mathrm{T}} < 7$	$0.210 \pm 0.018 \pm 0.005$
$7 < p_{\mathrm{T}} < 8$	$0.196 \pm 0.021 \pm 0.005$
$8 < p_{\mathrm{T}} < 10$	$0.315 \pm 0.025 \pm 0.009$
$10 < p_{\mathrm{T}} < 14$	$0.321 \pm 0.036 \pm 0.011$

Table 96: The cross section ratio for $\psi(2S)$-from-b / J/ψ-from-b in pPb, in bins of p_{T} integrated over $1.5 < y^* < 4.0$. The first uncertainty is statistical, the second systematic.

p_{T} bin	$\sigma_{\psi(2S)}/\sigma_{J/\psi}$
$0 < p_{\mathrm{T}} < 1$	$0.180 \pm 0.036 \pm 0.005$
$1 < p_{\mathrm{T}} < 2$	$0.240 \pm 0.025 \pm 0.006$
$2 < p_{\mathrm{T}} < 3$	$0.204 \pm 0.023 \pm 0.005$
$3 < p_{\mathrm{T}} < 4$	$0.267 \pm 0.023 \pm 0.006$
$4 < p_{\mathrm{T}} < 5$	$0.287 \pm 0.028 \pm 0.007$
$5 < p_{\mathrm{T}} < 6$	$0.327 \pm 0.032 \pm 0.008$
$6 < p_{\mathrm{T}} < 7$	$0.348 \pm 0.038 \pm 0.009$
$7 < p_{\mathrm{T}} < 8$	$0.245 \pm 0.033 \pm 0.007$
$8 < p_{\mathrm{T}} < 10$	$0.379 \pm 0.040 \pm 0.010$
$10 < p_{\mathrm{T}} < 14$	$0.434 \pm 0.051 \pm 0.011$

Table 97: The cross section ratio $\psi(2S)$-from-b / J/ψ-from-b in Pbp, in bins of p_{T} integrated over $-5.0 < y^* < -2.5$. The first uncertainty is statistical, the second systematic.

p_{T} bin	$\sigma_{\psi(2S)}/\sigma_{J/\psi}$
$0 < p_{\mathrm{T}} < 1000$	$0.204 \pm 0.044 \pm 0.006$
$1000 < p_{\mathrm{T}} < 2000$	$0.233 \pm 0.027 \pm 0.006$
$2000 < p_{\mathrm{T}} < 3000$	$0.241 \pm 0.026 \pm 0.006$
$3000 < p_{\mathrm{T}} < 4000$	$0.346 \pm 0.030 \pm 0.008$
$4000 < p_{\mathrm{T}} < 5000$	$0.340 \pm 0.031 \pm 0.008$
$5000 < p_{\mathrm{T}} < 6000$	$0.317 \pm 0.036 \pm 0.007$
$6000 < p_{\mathrm{T}} < 7000$	$0.320 \pm 0.042 \pm 0.008$
$7000 < p_{\mathrm{T}} < 8000$	$0.310 \pm 0.049 \pm 0.009$
$8000 < p_{\mathrm{T}} < 10000$	$0.316 \pm 0.048 \pm 0.009$
$10000 < p_{\mathrm{T}} < 14000$	$0.289 \pm 0.052 \pm 0.010$

Table 98: The cross section ratio prompt $\psi(2S)$ / prompt J/ψ in pPb, in bins of y^* integrated over $0 < p_{\mathrm{T}} < 14.0$ GeV/c. The first uncertainty is statistical, the second systematic.

y^* bin	$\sigma_{\psi(2S)}/\sigma_{J/\psi}$
$1.500 < y^* < 2.500$	$0.123 \pm 0.007 \pm 0.003$
$2.500 < y^* < 3.250$	$0.122 \pm 0.007 \pm 0.003$
$3.250 < y^* < 4.000$	$0.130 \pm 0.008 \pm 0.003$

Table 99: The cross section ratio $\psi(2S)$-from-b $/J/\psi$-from-b in pPb, in bins of y^* integrated over $0 < p_{\rm T} < 14.0$ GeV/c. The first uncertainty is statistical, the second systematic.

y^* bin	$\sigma_{\psi(2S)}/\sigma_{J/\psi}$
1.500< y^* <2.500	$0.238 \pm 0.015 \pm 0.006$
2.500< y^* <3.250	$0.271 \pm 0.017 \pm 0.007$
3.250< y^* <4.000	$0.264 \pm 0.023 \pm 0.006$

Table 100: The cross section ratio prompt $\psi(2S)$ / prompt J/ψ in Pbp, in bins of y^* integrated over $0 < p_{\rm T} < 14$ GeV/c. The first uncertainty is statistical, the second systematic.

y^* bin	$\sigma_{\psi(2S)}/\sigma_{J/\psi}$
-2.500> y^* >-3.250	$0.114 \pm 0.007 \pm 0.003$
-3.250> y^* >-4.000	$0.102 \pm 0.006 \pm 0.003$
-4.000> y^* >-5.000	$0.117 \pm 0.008 \pm 0.003$

Table 101: The cross section ratio $\psi(2S)$-from-b $/J/\psi$-from-b in Pbp, in bins of y^* integrated over $0 < p_{\rm T} < 14$ GeV/c. The first uncertainty is statistical, the second systematic.

y^* bin	$\sigma_{\psi(2S)}/\sigma_{J/\psi}$
-2.500> y^* >-3.250	$0.319 \pm 0.021 \pm 0.008$
-3.250> y^* >-4.000	$0.240 \pm 0.016 \pm 0.006$
-4.000> y^* >-5.000	$0.217 \pm 0.023 \pm 0.005$

Table 102: The cross section ratio prompt $\psi(2S)$ / prompt J/ψ in pPb/Pbp, integrated over $0 < p_{\rm T} < 14$ GeV/c in the indicated y^*-ranges. The first uncertainty is statistical, the second systematic.

y^* bin	$\sigma_{\psi(2S)}/\sigma_{J/\psi}$
1.500 > y^* >4.000	$0.124 \pm 0.004 \pm 0.000$
-2.500> y^* >-5.000	$0.111 \pm 0.004 \pm 0.000$

Table 103: The cross section ratio $\psi(2S)$-from-b $/J/\psi$-from-b in Pbp, integrated over $0 < p_{\rm T} <$ 14 GeV/c in the indicated y^*-ranges. The first uncertainty is statistical, the second systematic.

y^* bin	$\sigma_{\psi(2S)}/\sigma_{J/\psi}$
1.500 > y^* >4.000	$0.253 \pm 0.010 \pm 0.000$
-2.500> y^* >-5.000	$0.271 \pm 0.012 \pm 0.001$

E Cross-section extrapolation for J/ψ and $\psi(2S)$ at 8.16 TeV

The center-of-mass energy of the proton-lead colliding system in this analysis is $\sqrt{s_{\rm NN}} = 8.16\,\text{TeV}$ per nucleon-nucleon pair. We need the cross-sections at the same energy in proton-proton collisions to study nuclear modification factors. The J/ψ cross-section has been measured in pp collisions at 2.76 TeV [61], 5 TeV [62], 7 TeV [63, 64], 8 TeV [65] and 13 TeV [66], while for $\psi(2S)$ the cross-section measurement has only been published for 7 TeV and 13 TeV [67]. Here we determine the J/ψ and $\psi(2S)$ cross-sections at $\sqrt{s} = 8.16\,\text{TeV}$ using the extrapolation and interpolation methods described in the note [68] and the publication [38]. The J/ψ cross-section is determined using interpolations from measurements at other energies, while the $\psi(2S)$ cross-section is scaled from the measurement at 7 TeV assuming that the cross-section ratio $\sigma(J/\psi)/\sigma(\psi(2S))$ is the same at 7 TeV and 8.16 TeV.

E.1 Cross-section interpolation for J/ψ

We make the interpolation for the J/ψ cross-section in bins of $p_{\rm T}$ and y, and also as a function of $p_{\rm T}$ integrated over y, or as a function of y integrated over $p_{\rm T}$. Because of this, the measurements at 2.76 TeV are not considered in the interpolation as only $p_{\rm T}$ differential results integrated over the y range $2 < y < 4.5$ were published. Since the 8 TeV point is close to the interpolated energy, the result is dominated by the 8 TeV measurements. It is also noted that in the J/ψ polarization measurement analysis, the J/ψ cross-section at 7 TeV was updated with updated tracking corrections, luminosity value, etc... for $p_{\rm T} > 2\,\text{GeV}/c$. For this reason, for the J/ψ cross-section at 7 TeV, we use the values in Ref [61] for $p_{\rm T} < 2\,\text{GeV}/c$ and in Ref [64] for $p_{\rm T} > 2\,\text{GeV}/c$.

In principle the single differential cross-section at 8.16 TeV can be integrated from the interpolated double differential cross-section. However to reduce the extrapolation uncertainties, single differential interpolations are performed independently. First, the J/ψ cross-section integrated over y or $p_{\rm T}$ are taken from the published results; where if the integrated results are not available in the published papers, the integration is done separating the correlated and uncorrelated uncertainties. The single differential integration is obtained over the range $p_{\rm T} < 14\,\text{GeV}$ for $p_{\rm T}$ as a function of y, and in the range $2.5 < y < 4.0$ (common range for Fwd, Bwd and pp) for y as a function of $p_{\rm T}$.

The measurements at 7, 8 and 13 TeV are fitted with an analytical function, and the interpolated results including uncertainties at 8.16 TeV are given by the function. This procedure is performed for each bin independently. In the note [68], three functions were used: a linear function, $1 + p_0 \times \sqrt{s}$; a power law function, $\sqrt{s}^{p_0}$ and an exponential function $1 - \exp^{-p_0 \times \sqrt{s}}$. However it is found in this analysis that the exponential fit does not work well, especially in the high $p_{\rm T}$ or y bins. The exponential function probes a saturation of cross-section at higher energies, which could be true for total cross-section but not true for small high $p_{\rm T}$ or high-rapidity bins, for which the increase of colliding energy produces a harder spectrum that favors this region. In the end, to be consistent in all kinematic region, we only consider linear and power law function, while the latter is theoretically preferred, the former one is a first order approximation.

The correlated systematic uncertainties between measurements at different energies are considered in this way: for the measurements at 7, 8 and 13 TeV, we subtract a common amount as $\sigma_c = \sqrt{\rho} \times min(\sigma_7, \sigma_8, \sigma_{13})$ that is supposed to contribute to the correlation ρ, and the interpolation is made using the remaining uncertainties that are supposed to be uncorrelated. Then the common correlated uncertainty is added back in quadrature to the interpolated result. The exact correlation coefficient of the systematic uncertainty in fact is very difficult to calculate precisely, while in the default case the correlation among all measurements is assumed to be 50%, following discussions in the paper [66]. We also considered doing the interpolation using only statistical uncertainties, and found similar numbers for central values and uncertainties, which is because the interpolated results are significantly dominated by the measurements at 8 TeV, which is the closest point. We consider the difference between the two interpolation function as a systematic uncertainty, which is in the end much smaller than other systematic uncertainties. In Fig. 76, an example of the interpolation fit is given (the exponential interpolation is also depicted as a comparison). In Tables 104 and 105, the interpolated double differential cross-sections are given, while in Table 106 and 107, the results of the interpolated single differential cross-section are listed.

Since the cross-section at 8.16 TeV is determined by this method only for bins in the range $2 < y < 4.5$, a further extrapolation is needed to get the cross-section in the rapidity bins $1.5 < y < 2$ and $4.5 < y < 5$. In this case, the extrapolation uses Gaussian functions, 2nd order polynomial or 4th order polynomial, all centered at $y = 0$, following strategies described in the note [68]. Only statistical uncertainties are considered in the fit, and the systematic uncertainties are added back. The systematic uncertainty is studied in the follwing way: an alternative fit is performed with each point augmented by its uncertainty. The difference between the new extrapolated result and the one considering only the statistical uncertainty is taken as systematic uncertainty. The average of the integration over the rapidity range ($1.5 < y < 2$ or $4.5 < y < 5$) of the fits with three different functions is taken as the nominal value. Half of the maximum difference between the three fits is taken as an additional systematic uncertainty due to fit model. The extrapolation fit is shown in Fig. 77, and the results are given in Table 107. It should be noted that the interpolation is only done for rapidity integrated over p_{T}. As a crosscheck, we compare the extrapolated value at $y = 0$ to the ALICE measurement [69]. The result from the ALICE Collaboration in the range $p_{\mathrm{T}} > 0\,\mathrm{GeV}/c$, $|y| < 0.9$ is $10.6 \pm 1.9\,\mu\mathrm{b}$, while the extrapolated value is $11.6 \pm 1.8\,\mu\mathrm{b}$.

As said earlier, as the energy 8.16 TeV is close to the 8 TeV energy of the *pp* measurements, the interpolated results are expected to very close to those measured at 8 TeV. In Fig. 78, the interpolated results are compared to 8 TeV measurements, from which it can be seen that the cross-sections are very close to each other.

E.2 Cross-section determination for $\psi(2S)$ at 8.16 TeV

Since this analysis measures the $\psi(2S)$ cross-section by normalizing it to the J/ψ cross-section, we only need to determine their ratios in *pp* collisions as well, while the absolute cross-section for $\psi(2S)$ production in *pp* collisions is not needed. The cross-section ratio in *pp* at 7 TeV has been published in the analysis [67], up to the constant factor of the $\psi \to \mu^+\mu^-$ branching fractions, for both prompt and from-b contributions. We assume that the ratio of p_{T} differential cross-section between $\psi(2S)$ and J/ψ production at 8.16 TeV in *pp* collisions is the same as at 7 TeV. The ratios are shown in Tab. 108 for prompt and

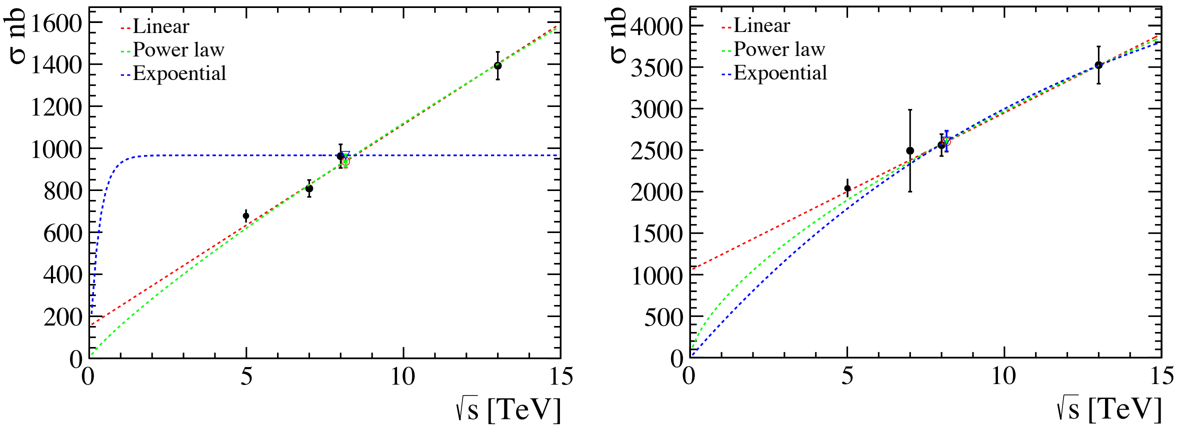

Figure 76: Cross-section interpolation in one (left) p_{T} bin ($3 < p_{\mathrm{T}} < 4\,\mathrm{GeV}/c$) and (right) y bin ($2.0 < y < 2.5$), for prompt J/ψ, as examples. The interpolation is made using only uncorrelated uncertainty. The measurements at each energy and the interpolated results are shown with total uncertainties.

Table 104: Interpolated cross-section at 8.16 TeV in different p_{T} and y bins for prompt J/ψ. The first uncertainty is statistical, the second is the total systematic uncertainty including those from LHCb measurements (propagated from fit) and the difference between the two models.

y bin	$[1.5-2.0]$	$[2-2.5]$	$[2.5-3]$	$[3-3.5]$	$[3.5-4]$	$[4-4.5]$	$[4.5-5]$
$[0-1]$	$873.7 \pm 8.2 \pm 77.0$	$743.9 \pm 25.2 \pm 57.6$	$781.3 \pm 8.4 \pm 54.7$	$734.9 \pm 5.4 \pm 49.9$	$667.3 \pm 4.7 \pm 45.2$	$559.4 \pm 4.7 \pm 39.0$	$462.4 \pm 7.1 \pm 54.4$
$[1-2]$	$1678.0 \pm 9.3 \pm 152.0$	$1476.6 \pm 19.6 \pm 104.0$	$1489.5 \pm 8.9 \pm 99.9$	$1375.0 \pm 6.4 \pm 91.9$	$1204.8 \pm 6.4 \pm 82.3$	$981.0 \pm 6.6 \pm 67.1$	$765.3 \pm 9.2 \pm 124.0$
$[2-3]$	$1369.6 \pm 7.4 \pm 139.6$	$1244.7 \pm 13.6 \pm 87.8$	$1183.6 \pm 7.2 \pm 67.9$	$1047.7 \pm 5.1 \pm 54.4$	$884.3 \pm 4.4 \pm 47.0$	$683.4 \pm 4.9 \pm 41.2$	$465.4 \pm 6.7 \pm 120.0$
$[3-4]$	$863.9 \pm 4.7 \pm 98.9$	$759.6 \pm 8.0 \pm 54.1$	$739.3 \pm 4.4 \pm 42.2$	$629.3 \pm 3.4 \pm 33.0$	$509.6 \pm 3.0 \pm 27.1$	$374.5 \pm 3.2 \pm 23.4$	$219.5 \pm 4.2 \pm 90.9$
$[4-5]$	$487.1 \pm 3.0 \pm 61.7$	$434.5 \pm 4.9 \pm 32.7$	$408.2 \pm 2.8 \pm 23.3$	$340.8 \pm 2.1 \pm 18.0$	$268.6 \pm 2.0 \pm 14.4$	$189.0 \pm 2.2 \pm 11.8$	$94.8 \pm 2.8 \pm 58.6$
$[5-6]$	$261.7 \pm 1.9 \pm 32.9$	$234.2 \pm 2.4 \pm 15.4$	$217.5 \pm 1.8 \pm 12.3$	$177.2 \pm 1.5 \pm 9.5$	$135.4 \pm 1.2 \pm 7.7$	$90.2 \pm 1.4 \pm 5.6$	$36.1 \pm 1.7 \pm 37.4$
$[6-7]$	$139.6 \pm 1.3 \pm 20.4$	$125.7 \pm 1.7 \pm 8.4$	$112.5 \pm 1.2 \pm 6.5$	$90.0 \pm 1.0 \pm 4.9$	$68.6 \pm 0.8 \pm 3.7$	$42.3 \pm 0.8 \pm 2.8$	$13.0 \pm 1.0 \pm 20.1$
$[7-8]$	$76.5 \pm 0.8 \pm 12.7$	$70.0 \pm 1.2 \pm 4.6$	$61.1 \pm 0.7 \pm 3.7$	$47.8 \pm 0.6 \pm 2.6$	$34.2 \pm 0.5 \pm 2.0$	$22.5 \pm 0.6 \pm 1.5$	$4.9 \pm 0.7 \pm 11.3$
$[8-9]$	$43.1 \pm 0.6 \pm 7.5$	$38.8 \pm 0.8 \pm 2.7$	$34.1 \pm 0.6 \pm 1.9$	$25.9 \pm 0.5 \pm 1.5$	$18.7 \pm 0.4 \pm 1.1$	$10.9 \pm 0.4 \pm 0.8$	$1.2 \pm 0.5 \pm 6.7$
$[9-10]$	$24.6 \pm 0.4 \pm 4.5$	$22.3 \pm 0.5 \pm 1.5$	$19.4 \pm 0.4 \pm 1.1$	$13.9 \pm 0.4 \pm 0.8$	$9.9 \pm 0.3 \pm 0.7$	$5.9 \pm 0.2 \pm 0.5$	$0.0 \pm 0.3 \pm 4.0$
$[10-11]$	$14.9 \pm 0.3 \pm 2.8$	$13.5 \pm 0.4 \pm 1.0$	$11.0 \pm 0.3 \pm 0.7$	$9.2 \pm 0.2 \pm 0.6$	$5.7 \pm 0.2 \pm 0.4$	$3.4 \pm 0.2 \pm 0.3$	$0.0 \pm 0.2 \pm 2.5$
$[11-12]$	$8.5 \pm 0.2 \pm 1.5$	$7.7 \pm 0.2 \pm 0.6$	$6.6 \pm 0.2 \pm 0.4$	$5.2 \pm 0.2 \pm 0.3$	$3.2 \pm 0.1 \pm 0.2$	$2.1 \pm 0.2 \pm 0.2$	$0.0 \pm 0.2 \pm 1.6$
$[12-13]$	$5.8 \pm 0.2 \pm 1.3$	$5.2 \pm 0.2 \pm 0.4$	$4.2 \pm 0.1 \pm 0.3$	$3.4 \pm 0.1 \pm 0.2$	$1.7 \pm 0.1 \pm 0.2$	$1.1 \pm 0.1 \pm 0.1$	$0.0 \pm 0.1 \pm 1.1$
$[13-14]$	$4.1 \pm 0.1 \pm 1.0$	$3.4 \pm 0.2 \pm 0.3$	$3.1 \pm 0.1 \pm 0.2$	$1.9 \pm 0.1 \pm 0.2$	$1.5 \pm 0.1 \pm 0.1$	$0.5 \pm 0.1 \pm 0.1$	$0.0 \pm 0.1 \pm 0.8$

from-b components respectively.

We also assume that the $\psi(2S)$ over J/ψ cross-section ratio integrated over p_{T} does not strongly depend of the rapidity (actually assuming that the ratio is the same in the $2 < y < 4.5$ and in the range covered by proton-lead data), which is almost true as the rapidity is mostly determined by the colliding energy (while for p_{T} distribution it is determined by particle production mechanism). This has been checked with data, and also measurements of cross-section ratios between $\Upsilon(nS)$ states by LHCb [70]. Thus the ratio as a function of rapidity (p_{T} integrated) is determined by dividing the total cross-section for $\psi(2S)$ and J/ψ to be $0.145 \pm 0.001(\mathrm{stat}) \pm 0.012(\mathrm{syst})$ for prompt and $0.286 \pm 0.012(\mathrm{stat}) \pm 0.025(\mathrm{syst})$ for the from-b component. The values are consistent with expectations from the measurements at 13 TeV [67], given the different fiducial p_{T} region.

Table 105: Interpolated cross-section at 8.16 TeV in different p_{T} and y bins for J/ψ-from-b. The first uncertainty is statistical, the second is the total systematic uncertainty including those from LHCb measurements (propagated from the fit) and the difference between the two models.

y bin	[1.5 − 2.0]	[2 − 2.5]	[2.5 − 3]	[3 − 3.5]	[3.5 − 4]	[4 − 4.5]	[4.5 − 5]
[0 − 1]	$96.4 \pm 3.1 \pm 19.2$	$76.4 \pm 8.6 \pm 10.2$	$74.0 \pm 3.0 \pm 7.0$	$63.7 \pm 1.7 \pm 4.7$	$47.2 \pm 1.2 \pm 3.2$	$28.8 \pm 1.3 \pm 2.3$	$9.9 \pm 1.9 \pm 12.1$
[1 − 2]	$195.8 \pm 2.8 \pm 27.8$	$166.6 \pm 4.4 \pm 12.2$	$159.3 \pm 2.7 \pm 9.1$	$136.4 \pm 2.0 \pm 7.7$	$97.5 \pm 1.7 \pm 5.4$	$65.5 \pm 1.7 \pm 4.5$	$25.6 \pm 2.2 \pm 26.1$
[2 − 3]	$192.2 \pm 2.3 \pm 32.7$	$166.6 \pm 3.5 \pm 11.4$	$153.1 \pm 2.2 \pm 8.4$	$125.5 \pm 1.5 \pm 7.5$	$88.2 \pm 1.3 \pm 5.6$	$55.8 \pm 1.2 \pm 4.0$	$14.9 \pm 1.6 \pm 26.3$
[3 − 4]	$137.5 \pm 1.6 \pm 25.5$	$119.2 \pm 2.7 \pm 8.0$	$108.6 \pm 1.4 \pm 6.6$	$86.5 \pm 1.3 \pm 4.6$	$60.1 \pm 0.9 \pm 3.9$	$36.7 \pm 0.7 \pm 2.8$	$6.7 \pm 1.0 \pm 19.2$
[4 − 5]	$87.0 \pm 1.0 \pm 16.4$	$76.7 \pm 1.7 \pm 4.8$	$67.2 \pm 0.8 \pm 4.1$	$52.3 \pm 0.7 \pm 2.9$	$36.5 \pm 0.6 \pm 2.5$	$20.7 \pm 0.6 \pm 1.8$	$1.2 \pm 0.8 \pm 13.8$
[5 − 6]	$53.6 \pm 0.8 \pm 10.9$	$48.0 \pm 1.1 \pm 3.1$	$41.6 \pm 0.7 \pm 2.6$	$31.6 \pm 0.6 \pm 2.1$	$20.2 \pm 0.4 \pm 1.4$	$11.9 \pm 0.4 \pm 0.9$	$0.0 \pm 0.6 \pm 8.9$
[6 − 7]	$32.6 \pm 0.6 \pm 7.2$	$29.8 \pm 0.6 \pm 2.0$	$25.8 \pm 0.7 \pm 1.7$	$18.4 \pm 0.4 \pm 1.2$	$11.7 \pm 0.3 \pm 1.0$	$6.7 \pm 0.3 \pm 0.6$	$0.0 \pm 0.4 \pm 5.5$
[7 − 8]	$20.5 \pm 0.4 \pm 4.7$	$18.9 \pm 0.5 \pm 1.3$	$15.0 \pm 0.3 \pm 1.0$	$11.4 \pm 0.3 \pm 0.7$	$7.3 \pm 0.2 \pm 0.6$	$3.8 \pm 0.2 \pm 0.3$	$0.0 \pm 0.2 \pm 3.5$
[8 − 9]	$13.3 \pm 0.3 \pm 3.5$	$11.7 \pm 0.4 \pm 0.8$	$10.2 \pm 0.3 \pm 0.7$	$6.7 \pm 0.2 \pm 0.5$	$4.2 \pm 0.2 \pm 0.3$	$2.2 \pm 0.1 \pm 0.2$	$0.0 \pm 0.2 \pm 2.2$
[9 − 10]	$8.7 \pm 0.2 \pm 2.1$	$7.9 \pm 0.3 \pm 0.5$	$6.3 \pm 0.2 \pm 0.4$	$4.5 \pm 0.2 \pm 0.4$	$2.6 \pm 0.1 \pm 0.3$	$1.2 \pm 0.1 \pm 0.2$	$0.0 \pm 0.2 \pm 1.8$
[10 − 11]	$5.7 \pm 0.2 \pm 1.6$	$5.3 \pm 0.2 \pm 0.4$	$4.0 \pm 0.1 \pm 0.3$	$2.9 \pm 0.1 \pm 0.3$	$1.5 \pm 0.1 \pm 0.2$	$0.8 \pm 0.1 \pm 0.1$	$0.0 \pm 0.1 \pm 1.0$
[11 − 12]	$4.2 \pm 0.1 \pm 1.1$	$3.9 \pm 0.1 \pm 0.2$	$2.8 \pm 0.1 \pm 0.2$	$1.8 \pm 0.1 \pm 0.2$	$1.0 \pm 0.1 \pm 0.1$	$0.4 \pm 0.1 \pm 0.1$	$0.0 \pm 0.1 \pm 1.0$
[12 − 13]	$2.9 \pm 0.1 \pm 0.9$	$2.5 \pm 0.1 \pm 0.2$	$2.1 \pm 0.1 \pm 0.2$	$1.3 \pm 0.1 \pm 0.1$	$0.7 \pm 0.1 \pm 0.1$	$0.3 \pm 0.0 \pm 0.1$	$0.0 \pm 0.1 \pm 0.6$
[13 − 14]	$2.0 \pm 0.1 \pm 0.7$	$1.7 \pm 0.1 \pm 0.2$	$1.4 \pm 0.1 \pm 0.1$	$0.9 \pm 0.1 \pm 0.1$	$0.4 \pm 0.1 \pm 0.1$	$0.2 \pm 0.0 \pm 0.0$	$0.0 \pm 0.0 \pm 0.4$

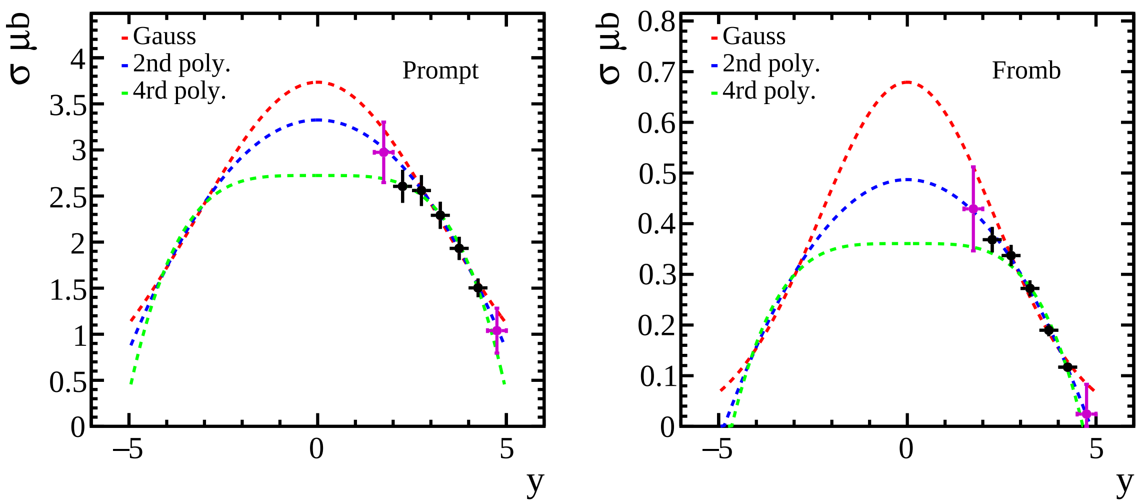

Figure 77: Extrapolation fit to determine the J/ψ cross-section in bins of $1.5 < y < 2$ and $4.5 < y < 5$ for (left) prompt J/ψ and (right) J/ψ-from-b.

Table 106: Interpolated cross-section at 8.16 TeV in different p_{T} bins for rapidity integrated over $2.5 < y < 4$. The first uncertainty is statistical, the second is the difference between the interpolation functions, and the third is the total uncertainty dominated by other LHCb measurements.

Prompt J/ψ	
$[0-1]$	$1094.3 \pm 5.6 \pm 2.3 \pm 74.5$
$[1-2]$	$2036.7 \pm 6.6 \pm 5.5 \pm 136.0$
$[2-3]$	$1559.1 \pm 5.0 \pm 8.8 \pm 84.4$
$[3-4]$	$940.7 \pm 3.2 \pm 3.6 \pm 51.0$
$[4-5]$	$509.9 \pm 2.0 \pm 1.2 \pm 27.7$
$[5-6]$	$265.5 \pm 1.3 \pm 0.4 \pm 14.6$
$[6-7]$	$135.8 \pm 0.9 \pm 0.5 \pm 7.4$
$[7-8]$	$71.7 \pm 0.6 \pm 0.4 \pm 4.0$
$[8-9]$	$39.4 \pm 0.4 \pm 0.4 \pm 2.2$
$[9-10]$	$21.7 \pm 0.3 \pm 0.4 \pm 1.2$
$[10-11]$	$13.0 \pm 0.2 \pm 0.2 \pm 0.8$
$[11-12]$	$7.5 \pm 0.2 \pm 0.2 \pm 0.5$
$[12-13]$	$4.7 \pm 0.1 \pm 0.1 \pm 0.3$
$[13-14]$	$2.9 \pm 0.1 \pm 0.1 \pm 0.2$
J/ψ-from-b	
$[0-1]$	$92.3 \pm 1.9 \pm 0.2 \pm 6.9$
$[1-2]$	$197.0 \pm 1.9 \pm 0.2 \pm 10.7$
$[2-3]$	$183.7 \pm 1.5 \pm 0.7 \pm 10.4$
$[3-4]$	$127.8 \pm 1.1 \pm 0.7 \pm 7.3$
$[4-5]$	$78.0 \pm 0.7 \pm 1.1 \pm 4.6$
$[5-6]$	$46.7 \pm 0.5 \pm 0.6 \pm 3.1$
$[6-7]$	$28.0 \pm 0.4 \pm 0.6 \pm 1.8$
$[7-8]$	$16.8 \pm 0.2 \pm 0.4 \pm 1.1$
$[8-9]$	$10.5 \pm 0.2 \pm 0.3 \pm 0.7$
$[9-10]$	$6.7 \pm 0.1 \pm 0.2 \pm 0.5$
$[10-11]$	$4.2 \pm 0.1 \pm 0.2 \pm 0.3$
$[11-12]$	$2.9 \pm 0.1 \pm 0.1 \pm 0.2$
$[12-13]$	$2.0 \pm 0.1 \pm 0.1 \pm 0.2$
$[13-14]$	$1.3 \pm 0.1 \pm 0.1 \pm 0.1$

Table 107: Interpolated cross-section at 8.16 TeV in different y bins for p_{T} integrated over $p_{\mathrm{T}} < 14\,\mathrm{GeV}/c$. The first uncertainty is statistical, the second is the difference between the interpolation functions, and the third is the total uncertainty dominated by other LHCb measurements.

Prompt J/ψ	
$[1.0-1.5]$	$2.974 \pm 0.009 \pm 0.267 \pm 0.328$
$[1.5-2.0]$	$2.605 \pm 0.021 \pm 0.000 \pm 0.179$
$[2.0-2.5]$	$2.559 \pm 0.008 \pm 0.000 \pm 0.167$
$[2.5-3.0]$	$2.291 \pm 0.005 \pm 0.000 \pm 0.147$
$[3.0-3.5]$	$1.932 \pm 0.005 \pm 0.000 \pm 0.126$
$[3.5-4.0]$	$1.503 \pm 0.005 \pm 0.000 \pm 0.101$
$[4.0-4.5]$	$1.039 \pm 0.007 \pm 0.233 \pm 0.244$
J/ψ-from-b	
$[1.0-1.5]$	$0.429 \pm 0.003 \pm 0.079 \pm 0.083$
$[1.5-2.0]$	$0.368 \pm 0.006 \pm 0.000 \pm 0.025$
$[2.0-2.5]$	$0.337 \pm 0.003 \pm 0.000 \pm 0.021$
$[2.5-3.0]$	$0.272 \pm 0.002 \pm 0.000 \pm 0.016$
$[3.0-3.5]$	$0.190 \pm 0.002 \pm 0.000 \pm 0.012$
$[3.5-4.0]$	$0.117 \pm 0.001 \pm 0.000 \pm 0.009$
$[4.0-4.5]$	$0.024 \pm 0.002 \pm 0.059 \pm 0.059$

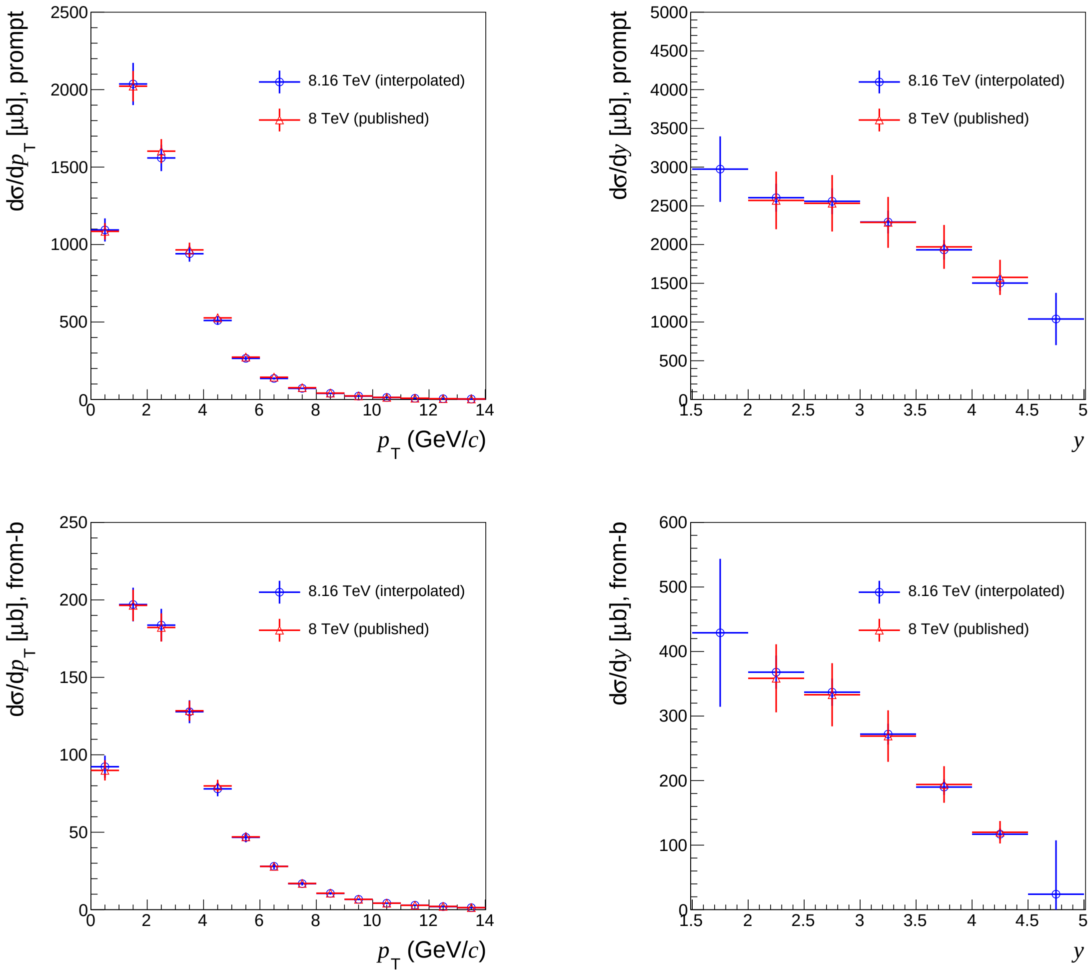

Figure 78: Interpolated single differential cross-section for J/ψ at 8.16 TeV, as a function of (left) p_{T} and (right) rapidity, compared with measurements at 8 TeV. The top two plots are for prompt J/ψ, while the bottom one are for J/ψ-from-b.

Table 108: Cross-section ratio between $\psi(2S)$ and J/ψ as a function of p_{T}

Prompt	Corrected values	Old values
$[0-1]$	0.0952 ± 0.0207	$0.1057 \pm 0.0021 \pm 0.0176$
$[1-2]$	0.1156 ± 0.0211	$0.1300 \pm 0.0009 \pm 0.0181$
$[2-3]$	0.1392 ± 0.0112	$0.1452 \pm 0.0007 \pm 0.0117$
$[3-4]$	0.1685 ± 0.0105	$0.1764 \pm 0.0008 \pm 0.0110$
$[4-5]$	0.1856 ± 0.0117	$0.1958 \pm 0.0010 \pm 0.0123$
$[5-6]$	0.2063 ± 0.0119	$0.2176 \pm 0.0014 \pm 0.0125$
$[6-7]$	0.2442 ± 0.0142	$0.2612 \pm 0.0022 \pm 0.0150$
$[7-8]$	0.2377 ± 0.0147	$0.2584 \pm 0.0027 \pm 0.0157$
$[8-10]$	0.2738 ± 0.0301	$0.2801 \pm 0.0154 \pm 0.0267$
$[10-14]$	0.3409 ± 0.0443	$0.3661 \pm 0.0217 \pm 0.0424$
Nonprompt	Corrected values	Old values
$[0-1]$	0.1760 ± 0.0566	$0.1524 \pm 0.0125 \pm 0.0199$
$[1-2]$	0.2700 ± 0.0539	$0.2338 \pm 0.0055 \pm 0.0188$
$[2-3]$	0.2512 ± 0.0392	$0.2165 \pm 0.0033 \pm 0.0144$
$[3-4]$	0.2678 ± 0.0455	$0.2327 \pm 0.0035 \pm 0.0120$
$[4-5]$	0.3294 ± 0.0458	$0.2903 \pm 0.0041 \pm 0.0132$
$[5-6]$	0.3325 ± 0.0479	$0.2958 \pm 0.0064 \pm 0.0163$
$[6-7]$	0.3133 ± 0.0468	$0.2759 \pm 0.0063 \pm 0.0169$
$[7-8]$	0.3268 ± 0.0479	$0.2897 \pm 0.0196 \pm 0.0292$
$[8-10]$	0.3273 ± 0.0510	$0.2936 \pm 0.0196 \pm 0.0252$
$[10-14]$	0.3452 ± 0.0655	$0.3312 \pm 0.0228 \pm 0.0419$

F Nuclear modification factors

Table 109: Nuclear modification factor of prompt J/ψ in bins of p_{T} integrated over $1.5 < y^* < 4.0$. the first uncertainty is statistical, the second systematic.

p_{T} bin	R_{pPb} (prompt J/ψ)	
$0.000 < p_{\mathrm{T}} < 1.000$	$0.527 \pm$	0.004 ± 0.062
$1.000 < p_{\mathrm{T}} < 2.000$	$0.561 \pm$	0.003 ± 0.058
$2.000 < p_{\mathrm{T}} < 3.000$	$0.645 \pm$	0.003 ± 0.061
$3.000 < p_{\mathrm{T}} < 4.000$	$0.716 \pm$	0.004 ± 0.074
$4.000 < p_{\mathrm{T}} < 5.000$	$0.764 \pm$	0.005 ± 0.079
$5.000 < p_{\mathrm{T}} < 6.000$	$0.814 \pm$	0.006 ± 0.082
$6.000 < p_{\mathrm{T}} < 7.000$	$0.859 \pm$	0.008 ± 0.095
$7.000 < p_{\mathrm{T}} < 8.000$	$0.872 \pm$	0.011 ± 0.099
$8.000 < p_{\mathrm{T}} < 10.000$	$0.899 \pm$	0.011 ± 0.104
$10.000 < p_{\mathrm{T}} < 14.000$	$0.919 \pm$	0.015 ± 0.117

Table 110: Nuclear modification factor of prompt J/ψ in bins of p_{T} integrated over $-5.0 < y^* < 2.5$. the first uncertainty is statistical, the second systematic.

p_{T} bin	R_{Pbp} (prompt J/ψ)	
$0.000 < p_{\mathrm{T}} < 1.000$	$0.746 \pm$	0.005 ± 0.104
$1.000 < p_{\mathrm{T}} < 2.000$	$0.806 \pm$	0.004 ± 0.105
$2.000 < p_{\mathrm{T}} < 3.000$	$0.928 \pm$	0.004 ± 0.119
$3.000 < p_{\mathrm{T}} < 4.000$	$0.993 \pm$	0.005 ± 0.142
$4.000 < p_{\mathrm{T}} < 5.000$	$1.023 \pm$	0.006 ± 0.149
$5.000 < p_{\mathrm{T}} < 6.000$	$1.062 \pm$	0.007 ± 0.165
$6.000 < p_{\mathrm{T}} < 7.000$	$1.076 \pm$	0.010 ± 0.176
$7.000 < p_{\mathrm{T}} < 8.000$	$1.065 \pm$	0.012 ± 0.180
$8.000 < p_{\mathrm{T}} < 10.000$	$1.061 \pm$	0.013 ± 0.193
$10.000 < p_{\mathrm{T}} < 14.000$	$0.998 \pm$	0.018 ± 0.204

Table 111: Nuclear modification factor of J/ψ-from-b in bins of p_{T} integrated over $1.5 < y^* < 4.0$. the first uncertainty is statistical, the second systematic.

p_{T} bin	R_{pPb} (nonprompt J/ψ)	
$0.000 < p_{\mathrm{T}} < 1.000$	$0.747 \pm$	0.017 ± 0.119
$1.000 < p_{\mathrm{T}} < 2.000$	$0.793 \pm$	0.011 ± 0.088
$2.000 < p_{\mathrm{T}} < 3.000$	$0.824 \pm$	0.011 ± 0.092
$3.000 < p_{\mathrm{T}} < 4.000$	$0.854 \pm$	0.012 ± 0.104
$4.000 < p_{\mathrm{T}} < 5.000$	$0.872 \pm$	0.013 ± 0.103
$5.000 < p_{\mathrm{T}} < 6.000$	$0.905 \pm$	0.016 ± 0.112
$6.000 < p_{\mathrm{T}} < 7.000$	$0.915 \pm$	0.019 ± 0.123
$7.000 < p_{\mathrm{T}} < 8.000$	$0.988 \pm$	0.024 ± 0.135
$8.000 < p_{\mathrm{T}} < 10.000$	$0.940 \pm$	0.021 ± 0.135
$10.000 < p_{\mathrm{T}} < 14.000$	$0.901 \pm$	0.024 ± 0.146

Table 112: Nuclear modification factor of J/ψ-from-b in bins of p_{T} integrated over $-5.0 < y^* < -2.5$. the first uncertainty is statistical, the second systematic.

p_{T} bin	R_{Pbp} (nonprompt J/ψ)	
$0.000 < p_{\mathrm{T}} < 1.000$	$1.052 \pm$	0.023 ± 0.191
$1.000 < p_{\mathrm{T}} < 2.000$	$1.045 \pm$	0.014 ± 0.159
$2.000 < p_{\mathrm{T}} < 3.000$	$1.069 \pm$	0.013 ± 0.167
$3.000 < p_{\mathrm{T}} < 4.000$	$1.090 \pm$	0.014 ± 0.183
$4.000 < p_{\mathrm{T}} < 5.000$	$1.117 \pm$	0.017 ± 0.198
$5.000 < p_{\mathrm{T}} < 6.000$	$1.052 \pm$	0.019 ± 0.195
$6.000 < p_{\mathrm{T}} < 7.000$	$1.022 \pm$	0.022 ± 0.201
$7.000 < p_{\mathrm{T}} < 8.000$	$0.992 \pm$	0.026 ± 0.198
$8.000 < p_{\mathrm{T}} < 10.000$	$1.021 \pm$	0.026 ± 0.223
$10.000 < p_{\mathrm{T}} < 14.000$	$0.979 \pm$	0.030 ± 0.250

Table 113: Nuclear modification factor of prompt $\psi(2S)$ in bins of p_{T} integrated over $1.5 < y^* < 4.0$. the first uncertainty is statistical, the second systematic.

p_{T} bin	R_{pPb} (prompt ψ(2S))	
$0.000 < p_{\mathrm{T}} < 1.000$	$0.420 \pm$	0.065 ± 0.087
$1.000 < p_{\mathrm{T}} < 2.000$	$0.385 \pm$	0.040 ± 0.068
$2.000 < p_{\mathrm{T}} < 3.000$	$0.518 \pm$	0.042 ± 0.066
$3.000 < p_{\mathrm{T}} < 4.000$	$0.588 \pm$	0.042 ± 0.072
$4.000 < p_{\mathrm{T}} < 5.000$	$0.631 \pm$	0.046 ± 0.078
$5.000 < p_{\mathrm{T}} < 6.000$	$0.662 \pm$	0.048 ± 0.079
$6.000 < p_{\mathrm{T}} < 7.000$	$0.616 \pm$	0.050 ± 0.078
$7.000 < p_{\mathrm{T}} < 8.000$	$0.840 \pm$	0.070 ± 0.110
$8.000 < p_{\mathrm{T}} < 10.000$	$0.842 \pm$	0.081 ± 0.128
$10.000 < p_{\mathrm{T}} < 14.000$	$0.583 \pm$	0.077 ± 0.102

Table 114: Nuclear modification factor of prompt $\psi(2S)$ in bins of p_{T} integrated over $-5.0 < y^* < 2.5$. the first uncertainty is statistical, the second systematic.

p_{T} bin	R_{Pbp} (prompt ψ(2S))	
$0.000 < p_{\mathrm{T}} < 1.000$	$0.478 \pm$	0.094 ± 0.182
$1.000 < p_{\mathrm{T}} < 2.000$	$0.658 \pm$	0.058 ± 0.143
$2.000 < p_{\mathrm{T}} < 3.000$	$0.711 \pm$	0.065 ± 0.126
$3.000 < p_{\mathrm{T}} < 4.000$	$0.817 \pm$	0.067 ± 0.152
$4.000 < p_{\mathrm{T}} < 5.000$	$0.708 \pm$	0.066 ± 0.130
$5.000 < p_{\mathrm{T}} < 6.000$	$0.842 \pm$	0.070 ± 0.149
$6.000 < p_{\mathrm{T}} < 7.000$	$0.867 \pm$	0.076 ± 0.162
$7.000 < p_{\mathrm{T}} < 8.000$	$0.806 \pm$	0.088 ± 0.156
$8.000 < p_{\mathrm{T}} < 10.000$	$1.193 \pm$	0.116 ± 0.245
$10.000 < p_{\mathrm{T}} < 14.000$	$0.876 \pm$	0.113 ± 0.208

Table 115: Nuclear modification factor of $\psi(2S)$-from-b in bins of $p_{\rm T}$ integrated over $1.5 < y^* < 4.0$. the first uncertainty is statistical, the second systematic.

$p_{\rm T}$ bin	R_{pPb} (nonprompt ψ(2S))	
$0.000 < p_{\rm T} < 1.000$	$0.884 \pm$	0.190 ± 0.184
$1.000 < p_{\rm T} < 2.000$	$0.815 \pm$	0.087 ± 0.113
$2.000 < p_{\rm T} < 3.000$	$0.778 \pm$	0.088 ± 0.103
$3.000 < p_{\rm T} < 4.000$	$0.981 \pm$	0.088 ± 0.131
$4.000 < p_{\rm T} < 5.000$	$0.862 \pm$	0.085 ± 0.111
$5.000 < p_{\rm T} < 6.000$	$1.001 \pm$	0.101 ± 0.138
$6.000 < p_{\rm T} < 7.000$	$1.155 \pm$	0.131 ± 0.173
$7.000 < p_{\rm T} < 8.000$	$0.836 \pm$	0.129 ± 0.144
$8.000 < p_{\rm T} < 10.000$	$1.213 \pm$	0.154 ± 0.206
$10.000 < p_{\rm T} < 14.000$	$1.179 \pm$	0.164 ± 0.245

Table 116: Nuclear modification factor of $\psi(2S)$-from-b in bins of $p_{\rm T}$ integrated over $-5.0 < y^* < -2.5$. the first uncertainty is statistical, the second systematic.

$p_{\rm T}$ bin	R_{Pbp} (nonprompt ψ(2S))	
$0.000 < p_{\rm T} < 1.000$	$1.409 \pm$	0.329 ± 0.256
$1.000 < p_{\rm T} < 2.000$	$1.040 \pm$	0.123 ± 0.158
$2.000 < p_{\rm T} < 3.000$	$1.191 \pm$	0.130 ± 0.186
$3.000 < p_{\rm T} < 4.000$	$1.619 \pm$	0.146 ± 0.271
$4.000 < p_{\rm T} < 5.000$	$1.309 \pm$	0.123 ± 0.232
$5.000 < p_{\rm T} < 6.000$	$1.127 \pm$	0.133 ± 0.210
$6.000 < p_{\rm T} < 7.000$	$1.185 \pm$	0.160 ± 0.233
$7.000 < p_{\rm T} < 8.000$	$1.060 \pm$	0.184 ± 0.212
$8.000 < p_{\rm T} < 10.000$	$1.097 \pm$	0.185 ± 0.240
$10.000 < p_{\rm T} < 14.000$	$0.856 \pm$	0.166 ± 0.219

G $\psi(2S)$ forward to backward ratios

Table 117: Prompt $\psi(2S)$ forward to backward ratio in bins of p_{T} integrated over $4.0 < y^{*} < 2.5$. the first uncertainty is statistical, the second systematic.

p_{T} bin	R_{FB}(prompt $\psi(2S)$)	
$0.000 > p_{\mathrm{T}} > 1.000$	$0.665\pm$	0.182 ± 0.037
$1.000 > p_{\mathrm{T}} > 2.000$	$0.370\pm$	0.061 ± 0.020
$2.000 > p_{\mathrm{T}} > 3.000$	$0.608\pm$	0.084 ± 0.032
$3.000 > p_{\mathrm{T}} > 4.000$	$0.447\pm$	0.057 ± 0.023
$4.000 > p_{\mathrm{T}} > 5.000$	$0.693\pm$	0.091 ± 0.036
$5.000 > p_{\mathrm{T}} > 6.000$	$0.700\pm$	0.087 ± 0.037
$6.000 > p_{\mathrm{T}} > 7.000$	$0.596\pm$	0.081 ± 0.032
$7.000 > p_{\mathrm{T}} > 8.000$	$0.934\pm$	0.150 ± 0.052
$8.000 > p_{\mathrm{T}} > 10.000$	$0.519\pm$	0.071 ± 0.029
$10.000 > p_{\mathrm{T}} > 14.000$	$0.555\pm$	0.116 ± 0.034

Table 118: The $\psi(2S)$-from-b forward to backward ratio in bins of p_{T} integrated over $4.0 < y^{*} < 2.5$. the first uncertainty is statistical, the second systematic.

p_{T} bin	R_{FB}($\psi(2S)$ from-b)	
$0.000 > p_{\mathrm{T}} > 1.000$	$0.406\pm$	0.139 ± 0.023
$1.000 > p_{\mathrm{T}} > 2.000$	$0.475\pm$	0.087 ± 0.026
$2.000 > p_{\mathrm{T}} > 3.000$	$0.534\pm$	0.093 ± 0.028
$3.000 > p_{\mathrm{T}} > 4.000$	$0.515\pm$	0.078 ± 0.027
$4.000 > p_{\mathrm{T}} > 5.000$	$0.491\pm$	0.078 ± 0.025
$5.000 > p_{\mathrm{T}} > 6.000$	$0.716\pm$	0.119 ± 0.037
$6.000 > p_{\mathrm{T}} > 7.000$	$0.665\pm$	0.132 ± 0.036
$7.000 > p_{\mathrm{T}} > 8.000$	$0.606\pm$	0.141 ± 0.034
$8.000 > p_{\mathrm{T}} > 10.000$	$0.988\pm$	0.199 ± 0.056
$10.000 > p_{\mathrm{T}} > 14.000$	$1.141\pm$	0.286 ± 0.069

Table 119: Prompt $\psi(2S)$ forward to backward ratio in bins of y^* integrated over $0 < p_{\rm T} <$ 14 GeV/c. the first uncertainty is statistical, the second systematic.

y^* bin	R_{FB}(prompt $\psi(2S)$)	
1.500> y^* >2.500	$0.000\pm$	0.000 ± 0.000
2.500> y^* >3.250	$0.513\pm$	0.043 ± 0.027
3.250> y^* >4.000	$0.575\pm$	0.050 ± 0.030

Table 120: The $\psi(2S)$-from-b forward to backward ratio in bins of y^* integrated over $0 < p_{\rm T} <$ 14 GeV/c. the first uncertainty is statistical, the second systematic.

$p_{\rm T}$ bin	$\mathrm{R}_{FB}(\psi(2S)$ from-b)	
0.000 $> p_{\rm T} >$1.000	$0.406\pm$	0.139 ± 0.023
1.000 $> p_{\rm T} >$2.000	$0.475\pm$	0.087 ± 0.026
2.000 $> p_{\rm T} >$3.000	$0.534\pm$	0.093 ± 0.028
3.000 $> p_{\rm T} >$4.000	$0.515\pm$	0.078 ± 0.027
4.000 $> p_{\rm T} >$5.000	$0.491\pm$	0.078 ± 0.025
5.000 $> p_{\rm T} >$6.000	$0.716\pm$	0.119 ± 0.037
6.000 $> p_{\rm T} >$7.000	$0.665\pm$	0.132 ± 0.036
7.000 $> p_{\rm T} >$8.000	$0.606\pm$	0.141 ± 0.034
8.000 $> p_{\rm T} >$10.000	$0.988\pm$	0.199 ± 0.056
10.000$> p_{\rm T} >$14.000	$1.141\pm$	0.286 ± 0.069

References

[1] T. Matsui and H. Satz, *J/ψ suppression by Quark-Gluon Plasma formation*, Phys. Lett. **B178** (1986) 416.

[2] A. Mocsy, P. Petreczky, and M. Strickland, *Quarkonia in the Quark Gluon Plasma*, Int. J. Mod. Phys. **A28** (2013) 1340012, `arXiv:1302.2180`.

[3] A. Andronic *et al.*, *Heavy-flavour and quarkonium production in the LHC era: from proton-proton to heavy-ion collisions*, Eur. Phys. J. **C76** (2016) 07, `arXiv:1506.03981`.

[4] ALICE collaboration, B. Abelev *et al.*, *J/ψ suppression at forward rapidity in Pb–Pb collisions at $\sqrt{s_{NN}}$=2.76 TeV*, Phys. Rev. Lett. **109** (2012) 072301, `arXiv:1202.1383`.

[5] ALICE collaboration, B. Abelev *et al.*, *Centrality, rapidity and transverse momentum dependence of J/ψ suppression in Pb-Pb collisions at $\sqrt{s_{NN}}$=2.76 TeV*, Phys. Lett. **B734** (2014) 314, `arXiv:1311.0214`.

[6] ALICE collaboration, J. Adam *et al.*, *Inclusive, prompt and non-prompt J/ψ production at mid-rapidity in Pb-Pb collisions at $\sqrt{s_{NN}} = 2.76$ TeV*, JHEP **07** (2015) 051, `arXiv:1504.07151`.

[7] ALICE collaboration, J. Adam *et al.*, *Differential studies of inclusive J/ψ and ψ(2S) production at forward rapidity in Pb-Pb collisions at $\sqrt{s_{NN}}$=2.76 TeV*, JHEP **05** (2016) 179, `arXiv:1506.08804`.

[8] ALICE collaboration, J. Adam *et al.*, *J/ψ suppression at forward rapidity in Pb-Pb collisions at $\sqrt{s_{NN}} = 5.02$ TeV*, Phys. Lett. **B766** (2017) 212, `arXiv:1606.08197`.

[9] R. L. Thews, M. Schroedter, and J. Rafelski, *Enhanced J/ψ production in deconfined quark matter*, Phys. Rev. **C63** (2001) 054905, `arXiv:hep-ph/0007323`.

[10] P. Braun-Munzinger and J. Stachel, *(Non)thermal aspects of charmonium production and a new look at J/ψ suppression*, Phys. Lett. **B490** (2000) 196, `arXiv:nucl-th/0007059`.

[11] NA50 collaboration, B. Alessandro *et al.*, *psi-prime production in Pb-Pb collisions at 158-GeV/nucleon*, Eur. Phys. J. **C49** (2007) 559, `arXiv:nucl-ex/0612013`.

[12] ALICE collaboration, B. Abelev *et al.*, *Upgrade of the ALICE experiment: Letter Of Intent*, J. Phys. **G41** (2014) 087001.

[13] CMS collaboration, V. Khachatryan *et al.*, *Measurement of J/ψ and $\psi(2S)$ prompt double-differential cross sections in pp collisions at $\sqrt{s}$=7 TeV*, Phys. Rev. Lett. **114** (2015) 191802, `arXiv:1502.04155`.

[14] M. Hirai, S. Kumano, and T.-H. Nagai, *Determination of nuclear parton distribution functions and their uncertainties in next-to-leading order*, Phys. Rev. **C76** (2007) 065207, `arXiv:0709.3038`.

[15] K. J. Eskola, H. Paukkunen, and C. A. Salgado, *EPS09: A new generation of NLO and LO nuclear parton distribution functions*, JHEP **04** (2009) 065, `arXiv:0902.4154`.

[16] D. de Florian, R. Sassot, P. Zurita, and M. Stratmann, *Global analysis of nuclear parton distributions*, Phys. Rev. **D85** (2012) 074028, `arXiv:1112.6324`.

[17] K. Kovarik *et al.*, *nCTEQ15 - Global analysis of nuclear parton distributions with uncertainties in the CTEQ framework*, Phys. Rev. **D93** (2016) 085037, `arXiv:1509.00792`.

[18] K. J. Eskola, P. Paakkinen, H. Paukkunen, and C. A. Salgado, *EPPS16: Nuclear parton distributions with LHC data*, `arXiv:1612.05741`.

[19] F. Gelis, E. Iancu, J. Jalilian-Marian, and R. Venugopalan, *The Color Glass Condensate*, Ann. Rev. Nucl. Part. Sci. **60** (2010) 463, `arXiv:1002.0333`.

[20] H. Fujii, F. Gelis, and R. Venugopalan, *Quark pair production in high energy pA collisions: General features*, Nucl. Phys. **A780** (2006) 146, `arXiv:hep-ph/0603099`.

[21] F. Arleo and S. Peigne, *Heavy-quarkonium suppression in p-A collisions from parton energy loss in cold QCD matter*, JHEP **03** (2013) 122, `arXiv:1212.0434`.

[22] R. Vogt, *Shadowing and absorption effects on J/ψ production in dA collisions*, Phys. Rev. **C71** (2005) 054902, `arXiv:hep-ph/0411378`.

[23] R. Vogt, *Cold nuclear matter effects on J/ψ and Υ production at the LHC*, Phys. Rev. **C81** (2010) 044903, `arXiv:1003.3497`.

[24] J.-P. Lansberg and H.-S. Shao, *Towards an automated tool to evaluate the impact of the nuclear modification of the gluon density on quarkonium, D and B meson production in proton-nucleus collisions*, Eur. Phys. J. **C77** (2017) 1, `arXiv:1610.05382`.

[25] Y.-Q. Ma, R. Venugopalan, and H.-F. Zhang, *J/ψ production and suppression in high energy proton-nucleus collisions*, Phys. Rev. **D92** (2015) 071901, `arXiv:1503.07772`.

[26] Ducloué, B. and Lappi, T. and Mäntysaari, H. , *Forward J/ψ production in proton-nucleus collisions at high energy*, Phys. Rev. **D91** (2015) 114005, `arXiv:1503.02789`.

[27] ALICE collaboration, B. Abelev *et al.*, *J/ψ production and nuclear effects in p-Pb collisions at $\sqrt{S_{NN}}$ = 5.02 TeV*, JHEP **02** (2014) 073, `arXiv:1308.6726`.

[28] LHCb collaboration, R. Aaij *et al.*, *Study of J/ψ production and cold nuclear matter effects in pPb collisions at $\sqrt{s_{NN}}$ =5 TeV*, JHEP **02** (2014) 072, `arXiv:1308.6729`.

[29] ALICE collaboration, J. Adam *et al.*, *Rapidity and transverse-momentum dependence of the inclusive J/ψ nuclear modification factor in p-Pb collisions at $\sqrt{s_{NN}}$ = 5.02 TeV*, JHEP **06** (2015) 055, `arXiv:1503.07179`.

[30] ALICE collaboration, J. Adam *et al.*, *Centrality dependence of inclusive J/ψ production in p-Pb collisions at $\sqrt{s_{NN}}$=5.02 TeV*, JHEP **11** (2015) 127, `arXiv:1506.08808`.

[31] ATLAS collaboration, G. Aad *et al.*, *Measurement of differential J/ψ production cross sections and forward-backward ratios in p + Pb collisions with the ATLAS detector*, Phys. Rev. **C92** (2015), no. 3 034904, `arXiv:1505.08141`.

[32] CMS collaboration, A. M. Sirunyan *et al.*, *Measurement of prompt and non prompt J/ψ production in pp and pPb collisions at $\sqrt{s_{NN}}$ = 5.02 TeV*, Eur. Phys. J. **C77** (2017) 269, `arXiv:1702.01462`.

[33] LHCb collaboration, R. Aaij *et al.*, *Prompt and nonprompt J/ψ production and nuclear modification in pPb collisions at $\sqrt{s_{NN}} = 8.16$ TeV*, Phys. Lett. **B774** (2017) 159, `arXiv:1706.07122`.

[34] PHENIX collaboration, A. Adare *et al.*, *Nuclear modification of $\psi(2S)$, χ_c, and J/ψ production in d+Au collisions at $\sqrt{s_{NN}}$=200 GeV*, Phys. Rev. Lett. **111** (2013), no. 20 202301, `arXiv:1305.5516`.

[35] PHENIX collaboration, A. Adare *et al.*, *Measurement of the relative yields of $\psi(2S)$ to $\psi(1S)$ mesons produced at forward and backward rapidity in p+p, p+Al, p+Au, and ^{3}He+Au collisions at $\sqrt{s_{NN}} = 200$ GeV*, Phys. Rev. **C95** (2017), no. 3 034904, `arXiv:1609.06550`.

[36] ALICE collaboration, B. B. Abelev *et al.*, *Suppression of $\psi(2S)$ production in p-Pb collisions at $\sqrt{s_{NN}}$ = 5.02 TeV*, JHEP **12** (2014) 073, `arXiv:1405.3796`.

[37] ALICE collaboration, J. Adam *et al.*, *Centrality dependence of $\psi(2S)$ suppression in p-Pb collisions at $\sqrt{s_{NN}}$ = 5.02 TeV*, JHEP **06** (2016) 050, `arXiv:1603.02816`.

[38] LHCb collaboration, R. Aaij *et al.*, *Study of $\psi(2S)$ production cross-sections and cold nuclear matter effects in pPb collisions at $\sqrt{s_{NN}}$ =5 TeV*, JHEP **03** (2016) 133, `arXiv:1601.07878`.

[39] E. G. Ferreiro, *Excited charmonium suppression in proton–nucleus collisions as a consequence of comovers*, Phys. Lett. **B749** (2015) 98, `arXiv:1411.0549`.

[40] X. Du and R. Rapp, *Sequential regeneration of charmonia in heavy-ion collisions*, Nucl. Phys. **A943** (2015) 147, `arXiv:1504.00670`.

[41] Y.-Q. Ma, R. Venugopalan, K. Watanabe, and H.-F. Zhang, *$\psi(2S)$ versus J/ψ suppression in proton-nucleus collisions from factorization violating soft color exchanges*, Phys. Rev. **C97** (2018) 014909, `arXiv:1707.07266`.

[42] Particle Data Group, C. Patrignani *et al.*, *Review of particle physics*, Chin. Phys. **C40** (2016) 100001.

[43] ALICE collaboration, S. Acharya *et al.*, *Energy dependence of forward-rapidity* J/ψ *and* ψ(2S) *production in pp collisions at the LHC*, Eur. Phys. J. **C77** (2017) 392, `arXiv:1702.00557`.

[44] Geant4 collaboration, S. Agostinelli *et al.*, *Geant4: A simulation toolkit*, Nucl. Instrum. Meth. **A506** (2003) 250.

[45] Geant4 collaboration, J. Allison *et al.*, *Geant4 developments and applications*, IEEE Trans. Nucl. Sci. **53** (2006) 270.

[46] I. Belyaev *et al.*, *Handling of the generation of primary events in Gauss, the LHCb simulation framework*, J. Phys. Conf. Ser. **331** (2011) 032047.

[47] T. Pierog *et al.*, *EPOS LHC: Test of collective hadronization with data measured at the CERN Large Hadron Collider*, Phys. Rev. **C92** (2015) 034906, `arXiv:1306.0121`.

[48] D. J. Lange, *The EvtGen particle decay simulation package*, Nucl. Instrum. Meth. **A462** (2001) 152.

[49] P. Golonka and Z. Was, *PHOTOS Monte Carlo: A precision tool for QED corrections in Z and W decays*, Eur. Phys. J. **C45** (2006) 97, `arXiv:hep-ph/0506026`.

[50] T. Sjöstrand, S. Mrenna, and P. Skands, *A brief introduction to PYTHIA 8.1*, Comput. Phys. Commun. **178** (2008) 852, `arXiv:0710.3820`.

[51] T. Head *et al.*, *Measurement of J/ψ production cross-section in pp collisions at* $\sqrt{s} = 13\,\mathrm{TeV}$, LHCb-ANA-2015-004.

[52] Y. Zhang, *Study of b-hadron production in pPb collisions at LHCb*, LHCb-ANA-2018-015.

[53] LHCb collaboration, R. Aaij *et al.*, *Measurement of forward J/ψ production cross-sections in pp collisions at $\sqrt{s} = 13$ TeV*, JHEP **10** (2015) 172, `arXiv:1509.00771`, [Erratum: JHEP05,063(2017)].

[54] J. Lefrancois, *Crystal ball fits*, link.

[55] Particle Data Group, C. Patrignani *et al.*, *Review of Particle Physics*, Chin. Phys. **C40** (2016), no. 10 100001.

[56] `https://twiki.cern.ch/twiki/bin/view/LHCb/LHCbTrackingEfficiencies`.

[57] L. Anderlini *et al.*, *The PIDCalib package*, Tech. Rep. LHCb-INT-2016-028. CERN-LHCb-INT-2016-028, CERN, Geneva, Jun, 2016.

[58] LHCb collaboration, R. Aaij *et al.*, *Precision luminosity measurements at LHCb*, JINST **9** (2014) P12005, `arXiv:1410.0149`.

[59] H.-S. Shao, *HELAC-Onia 2.0: an upgraded matrix-element and event generator for heavy quarkonium physics*, Comput. Phys. Commun. **198** (2016) 238, `arXiv:1507.03435`.

[60] H.-S. Shao, *HELAC-Onia: An automatic matrix element generator for heavy quarkonium physics*, Comput. Phys. Commun. **184** (2013) 2562, `arXiv:1212.5293`.

[61] LHCb collaboration, R. Aaij *et al.*, *Measurement of J/ψ production in pp collisions at $\sqrt{s} = 2.76$ TeV*, JHEP **02** (2013) 041, `arXiv:1212.1045`.

[62] LHCb collaboration, R. Aaij *et al.*, *Measurement of J/ψ production cross-sections in pp collisions at $\sqrt{s} = 5$ TeV*, JHEP **11** (2021) 181, `arXiv:2109.00220`.

[63] LHCb collaboration, R. Aaij *et al.*, *Measurement of J/ψ production in pp collisions at $\sqrt{s}$ =7 TeV*, Eur. Phys. J. **C71** (2011) 1645, arXiv:1103.0423.

[64] LHCb collaboration, R. Aaij *et al.*, *Measurement of J/ψ polarization in pp collisions at $\sqrt{s}$ =7 TeV*, Eur. Phys. J. **C73** (2013) 2631, arXiv:1307.6379.

[65] LHCb collaboration, R. Aaij *et al.*, *Production of J/ψ and Υ mesons in pp collisions at $\sqrt{s}$ =8 TeV*, JHEP **06** (2013) 064, arXiv:1304.6977.

[66] LHCb collaboration, R. Aaij *et al.*, *Measurement of forward J/ψ production cross-sections in pp collisions at $\sqrt{s}$ =13 TeV*, JHEP **10** (2015) 172, Erratum ibid. **05** (2017) 063, arXiv:1509.00771.

[67] LHCb collaboration, R. Aaij *et al.*, *Measurement of $\psi(2S)$ production cross-sections in proton-proton collisions at $\sqrt{s}$ =7 and 13 TeV*, Eur. Phys. J. **C80** (2020) 185, arXiv:1908.03099.

[68] ALICE and LHCb collaborations, *Reference pp cross-sections for J/ψ studies in proton-lead collisions at $\sqrt{s_{NN}} = 5.02$ TeV and comparisons between ALICE and LHCb results*, Dec, 2013. LHCb-CONF-2013-013, ALICE-PUBLIC-2013-002.

[69] ALICE Collaboration, B. Abelev *et al.*, *Measurement of prompt J/ψ and beauty hadron production cross sections at mid-rapidity in pp collisions at $\sqrt{s} = 7$ TeV*, JHEP **11** (2012) 065, arXiv:1205.5880.

[70] LHCb collaboration, R. Aaij *et al.*, *Forward production of Υ mesons in pp collisions at $\sqrt{s}$ =7 and 8 TeV*, JHEP **11** (2015) 103, arXiv:1509.02372.